# JOURNAL OF GEOPHYSICAL RESEARCH

*The continuation of*

RESTRIAL MAGNETISM AND ATMOSPHERIC ELECTRICITY
(1896-1948)

An International Quarterly

LUME 58 December, 1953 NUMBER 4


## CONTENTS




*(Contents concluded on outside back cover)*



*Address all correspondence to*

JOURNAL OF GEOPHYSICAL RESEARCH
5241 BROAD BRANCH ROAD, NORTHWEST
WASHINGTON 15, D.C., U.S.A.

THREE DOLLARS AND FIFTY CENTS A YEAR SINGLE NUMBERS, ONE DOLLAR

PRINTED BY
THE WILLIAM BYRD PRESS, INC.
P. O. Box 2-W—Sherwood Ave. and Durham St., Richmond 5, Virginia

# JOURNAL OF GEOPHYSICAL RESEARCH

*The continuation of*

Terrestrial Magnetism and Atmospheric Electricity

(1896-1948)

An International Quarterly

*Founded 1896 by* L. A. BAUER *Continued 1928-1948 by* J. A. FLEMING




*Fields of Interest*

Terrestrial Magnetism
Atmospheric Electricity
The Ionosphere
Solar and Terrestrial Relationships
Aurora, Night Sky, and Zodiacal Light
The Ozone Layer
Meteorology of Highest Atmospheric Levels
The Constitution and Physical States of the Upper Atmosphere
Special Investigations of the Earth's Crust and Interior, including experimental seismic waves, physics of the deep ocean and ocean bottom, physics in geology
And similar topics

This Journal serves the interests of investigators concerned with terrestrial magnetism and electricity, the upper atmosphere, the earth's crust and interior by presenting papers of new analysis and interpretation or new experimental or observational approach, and contributions to international collaboration. It is not in a position to print, primarily for archive purposes, extensive tables of data from observatories or surveys, the significance of which has not been analyzed.

Forward *manuscripts* to one of the Associate Editors, or to the editorial office of the Journal at 5241 Broad Branch Road, Northwest, Washington 15, D. C., U. S. A. It is preferred that manuscripts be submitted in English, but communications in French, German, Italian, or Spanish are also acceptable. A brief abstract, preferably in English, must accompany each manuscript. A *publication charge* of \$4 per page will be billed by the Editor to the institution which sponsors the work of any author; private individuals are not assessed page charges. Manuscripts from outside the United States are invited, and should not be withheld or delayed because of currency restrictions or other special difficulties relating to page charges. Costs of publication are roughly twice the total income from page charges and subscriptions, and are met by subsidies from the Carnegie Institution of Washington and international and private sources.

*Back issues* and *reprints* are handled by the Editorial Office, 5241 Broad Branch Road, N.W., Washington 15, D.C., U.S.A.

*Subscriptions* are handled by the Editorial Office, 5241 Broad Branch Road, N.W., Washington 15, D.C., U.S.A.


Entered as second-class matter at the Post Office at Richmond, Virginia, under the act of March 3, 1879.

Journal of

# GEOPHYSICAL RESEARCH

*The continuation of*

*Terrestrial Magnetism and Atmospheric Electricity*

VOLUME 58 DECEMBER, 1953 No. 4

## ON THE COUPLED WAVE EQUATIONS OF MAGNETO-IONIC THEORY*

BY JOHN M. KELSO

*Ionosphere Research Laboratory, The Pennsylvania State University, State College, Pennsylvania*

(Received March 10, 1953)

ABSTRACT

The propagation of a plane radio wave incident vertically on an inhomogeneous ionosphere varying in the vertical direction in the presence of the terrestrial magnetic field is characterized by a pair of coupled wave equations. These equations can be changed in appearance by choosing various different forms for the time factor, coordinate system, particle charge, and wave functions. In the recent literature, this has led to some unfortunate confusion, which the present work is intended to clarify. The wave equations and the basic defining relations are presented in such a way as to show explicitly the effects of some of the possible arbitrary choices noted above. A table comparing the present notation with that used by various other authors is given.

Försterling [see 1 of "References" at end of paper] showed that the propagation of a radio wave incident vertically on a horizontally stratified ionosphere is governed by a pair of simultaneous second-order differential equations which can be written in the form,

$$\left.\begin{aligned}\frac{d^2\Pi_A}{d\xi_3^2} + [k_0^2\epsilon_A + M^2]\Pi_A &= -2M\frac{d\Pi_B}{d\xi_3} - \Pi_B\frac{dM}{d\xi_3}\\ \frac{d^2\Pi_B}{d\xi_3^2} + [k_0^2\epsilon_B + M^2]\Pi_B &= -2M\frac{d\Pi_A}{d\xi_3} - \Pi_A\frac{dM}{d\xi_3}\end{aligned}\right\}\qquad(1)$$

*The research reported in this paper has been supported, in part, by the Geophysical Research Division of the Air Force Cambridge Research Center under Contract AF 19 (122)-44.

where the notation will be discussed below. These equations are here referred to as the "coupled wave equations."

These equations were also discussed by Rydbeck [2] and were later applied by him [3] in attacking the problem of the "triple splitting" of ionospheric echoes. Other applications of these equations, based on essentially the form given by Rydbeck, were made by Gibbons and Nertney [4], by Kelso, Nearhoof, Nertney, and Waynick [5],** and by Davids [6].

The coupled wave equations were derived by Saha, Banerjea, and Guha [7], but with a notation (this word is used here in a broad sense, to include choice of type of coordinate system, etc.) different from that used in Equation (1), which differs only slightly from that of Rydbeck. These authors state in a footnote that Rydbeck has erred in that he has the same sign for the right-hand members in both of Equations (1). Budden [8], in a study of limiting polarization, refers to the comment by Saha and his colleagues, and points out that the same criticism can be applied to Försterling's form of these equations. This criticism, if justified, would cast doubt on the validity of the applications mentioned above. For this reason, it is important to point out that all of these various forms for the coupled wave equations are compatible (aside from some obviously typographical errors which will be discussed below), as can be seen if one is careful to follow the changes of notation and definitions in transforming from one form to another.

Following the procedure given by Rydbeck [2], these equations have been re-derived in a slightly more general form than that given by any of the writers referred to above. Because the techniques of the derivation are quite standard, the present author will not trouble the reader with still another exhibition of the procedure, but will state for reference purposes the basic equations needed for comparison with earlier results. The purpose of the present work is to show explicitly a number of the effects of numerous arbitrary choices (of coordinate systems, time factor, wave functions, etc.) which can be made, and which lead to several apparently very different forms for the coupled equations. Following the presentation of the basic equations, we then show the changes of notation required to reduce Equation (1) to the forms given by (*a*) Försterling; (*b*) Rydbeck (which except for the time factor is also that of Gibbons and Nertney, of Kelso, Nearhoof, Nertney, and Waynick, and of Davids); (*c*) Saha, Banerjea, and Guha; (*d*) Budden.

We introduce four factors, $a$, $b$, $d$, $f$, which explicitly account for some of the arbitrary choices which can be made in the course of the derivation. First, we use a time factor $e^{ia\omega t}$, where $a$ may be either of $\pm 1$. The charge of the particles is written $b \mid e \mid$ where $b = \pm 1$, as desired. The dip angle of the earth's magnetic field is defined as the angle between the vertical axis of the coordinate system and the direction of the magnetic field, and is denoted by $\theta_p$. In order to show the effect of the reversal of the direction of the vertical axis, or of the direction of the earth's field, we introduce the cosine of the dip angle as $f \mid \cos \theta_p \mid$ where $f = 1$ if $\theta_p < 90°$, and where $f = -1$ if $\theta_p > 90°$.

Because of the lack of attention paid to this detail by some authors, one of the most confusing problems in comparing the results of two workers is the problem

**The portions of this paper [5] which concern the coupled wave equations were based on the paper by Gibbons and Nertney [4], although preceding it in date of publication.

of determining the exact choice of coördinate system made in each case. Here we use a right-handed coordinate system as a basis, but allow for a left-handed system by multiplying the vector product and curl operators, where they appear, by a factor $d$ which is $+1$ for a right-handed system and is $-1$ for a left-handed system. In both cases, the magnetic field is taken to lie in the $\xi_2\xi_3$-plane, while the angle $\theta_p$ is the angle between the $\xi_3$-axis and the direction of the earth's magnetic field. The properties of the ionized medium vary in the $\xi_3$-direction, but not in the $\xi_1$- and $\xi_2$-directions. Since even the terms "right-handed" and "left-handed" do not seem to be used consistently by all writers (see Brillouin, "Les Tenseurs en Méchanique et en Élasticité," New York, 1946, pp. 7 to 9), we note that the present right-handed system can, for most purposes, be taken to have the axes directed as follows: the $\xi_3$-axis vertical and directed upward, the $\xi_2$-axis horizontal and directed toward magnetic north, and the $\xi_1$-axis horizontal and directed toward magnetic east.

After an application of the equation of motion of a charge in the field of the incident wave, we find that it is useful to separate the field into two "modes," $(A)$ and $(B)$, for which,

$$\frac{E_2^{(A)}}{E_1^{(A)}} = q_A\,, \qquad \frac{E_2^{(B)}}{E_1^{(B)}} = q_B \qquad (2)$$

where $q_A$ and $q_B$ are the polarizations of the two modes, and where

$$\left.\begin{aligned} q_A &= jabdf[\delta + \sqrt{\delta^2 + 1}] \\ q_B &= jabdf[\delta - \sqrt{\delta^2 + 1}] \end{aligned}\right\} \qquad (3)$$

The quantity $\delta$ is defined by

$$\delta = \frac{\gamma_T^2}{2\,|\,\gamma_L\,|\left\{1 - X_0^2\left(1 - j\dfrac{a\nu}{\omega}\right)\right\}} \qquad (4)$$

The quantities $a$, $b$, $d$, $f$ are the factors introduced above, and

$$\left.\begin{aligned} &X_0^2 = \frac{\omega^2}{\omega_c^2}, \qquad \omega_c^2 = \frac{4\pi Ne^2}{m}, \qquad \omega_H = \frac{H\,|\,e\,|}{mc}, \qquad k_0^2 = \frac{\omega^2}{c^2} \\ &\gamma_T = X_0^2\,\frac{\omega_H}{\omega}\sin\theta_p, \qquad \gamma_L = f\,|\,\gamma_L\,| = fX_0^2\,\frac{\omega_H}{\omega}\,|\cos\theta_p\,| \end{aligned}\right\} \qquad (5)$$

In Maxwell's field equations, we introduce, in place of the fields $E_1^{(A)}$, etc., the following wave functions,

$$\left.\begin{aligned} \Pi_A &= \sqrt{1 - q_A^2}\,E_1^{(A)} = j\sqrt{1 - q_B^2}\,E_2^{(A)} \\ \Pi_B &= j\sqrt{1 - q_B^2}\,E_1^{(B)} = \sqrt{1 - q_A^2}\,E_2^{(B)} \end{aligned}\right\} \qquad (6)$$

We then obtain the coupled wave equations given in Equation (1), where $\epsilon_A$ and $\epsilon_B$ are the "dielectric constants" of the two modes, $(A)$ and $(B)$,

$$\left.\begin{aligned}\epsilon_A &= 1 - \frac{1}{X_0^2\left(1 - j\dfrac{a\nu}{\omega}\right) + \dfrac{\gamma_T^2}{\left[1 - X_0^2\left(1 - j\dfrac{a\nu}{\omega}\right)\right]} + jabdf\,|\,\gamma_L\,|\,q_A} \\ \epsilon_B &= 1 - \frac{1}{X_0^2\left(1 - j\dfrac{a\nu}{\omega}\right) + \dfrac{\gamma_T^2}{\left[1 - X_0^2\left(1 - j\dfrac{a\nu}{\omega}\right)\right]} + jabdf\,|\,\gamma_L\,|\,q_B}\end{aligned}\right\}\quad\ldots(7)$$

and $M$ is the "coupling factor," defined by

$$M = \frac{\dfrac{dq}{d\xi_3}}{1 - q^2}\quad\ldots(8)$$

where $q$ can be considered to be either one of the two values given in Equation (3), since the same value of $M$ results in either case.

From Equations (3), (4), and (8), we see that the effect of changing a single one of the factors, $b$, $d$, or $f$, is to change the sign of the polarization $q$ and the sign of the coupling factor $M$. This then changes the signs of both terms of the right-hand members of both of Equations (1). A change of the factor $a$ would have the same effect, but would also change the quantity $\delta$, as may be seen from Equation (4). It is also possible to define the polarizations in Equation (2) in terms of quantities which differ from the present ones by a factor of $j$ for both modes. This gives a negative sign in both equations in front of the term $M^2$, and introduces a factor of $j$ on both of the right-hand members of Equation (1).

It is further possible to use, in place of the functions denoted here by $\Pi_A$ and $\Pi_B$, quantities which differ from the definitions in Equation (6) by some combination of the factors, $+1$, $-1$, $+j$, $-j$. If the *same* change is made in the definition of *both* functions, the equations will have the same signs as Equations (1), provided that the factor $abdf$ is not also changed; and, if just one of the quantities differs by the factor $-1$, then the right-hand members of the two coupled equations will have the same sign, which will then be the opposite sign from that in Equation (1). However, if these functions are chosen in such a way that just *one* differs from Equations (6) by $\pm j$, then the right-hand members of the resulting equations will differ in sign, introducing an antisymmetry in the two equations. It appears that it is this last change which gave rise to the idea that the equations of Försterling and of Rydbeck were incorrect in the sense discussed at the beginning of this paper. As shown here, it is possible to have either symmetric equations, or antisymmetric equations, dependent upon the basic definitions.

It would now be possible to write down a large number of apparently different sets of coupled wave equations, but anyone who wishes to see the effect of any particular choice of definitions can do so readily from the equations above. Instead, we shall list in Table 1 the notations required to reduce Equations (1) to those given by four of the previously mentioned workers.

TABLE 1—*Comparison of notations*

| Present system | Försterling [1] | Rydbeck [2, 3] | Saha, Banerjea, and Guha [7] | Budden [8] |
|---|---|---|---|---|
| $a$ | $+1$ | $-1$ | $+1$ | $+1$ |
| $b$ | $-1$ | $-1$ | $+1$ | $-1$ |
| $d$ | $+1$ | $+1$ | $-1$ | $+1$ |
| $\xi_1$ | $x$ | $x$ | $y$ | Along 1-axis |
| $\xi_2$ | $y$ | $y$ | $x$ | Along 2-axis |
| $\xi_3$ | $z/k_0$ | $z$ | $z = u/k_0$ | Along 3-axis $= h$ |
| $f$ | $+1$ | $+1$ | $+1$ | $+1$ |
| $q_A$ | $jq^{(1)}$ | $\bar{u}_2$ | $-j\rho_2$ | $-R_0$ |
| $q_B$ | $jq^{(2)}$ | $\bar{u}_1$ | $-j\rho_1$ | $-R_e$ |
| $\Pi_A$ | $u^{(1)}$ | $j\Pi_2$ | $V$ | $\Pi_0$ |
| $\Pi_B$ | $u^{(2)}$ | $j\Pi_1$ | $-jW$ | $j\Pi_e$ |
| $k_0^2\epsilon_A$ | $k_0^2\epsilon^{(1)}(z)$ | $k_0^2\epsilon_2$ | $k_0^2q_0^2$ | $k^2\mu_0^2$ |
| $k_0^2\epsilon_B$ | $k_0^2\epsilon^{(2)}(z)$ | $k_0^2\epsilon_1$ | $k_0^2q_e^2$ | $k^2\mu_e^2$ |
| $M$ | $jk\dfrac{\frac{dq}{dz}}{1+q^2}$ | $\dfrac{\frac{du}{dz}}{1-u^2} = \psi$ | $-jk_0\dot{\varphi} = -\dfrac{jk_0\frac{d\rho}{du}}{1+\rho^2}$ | $-j\psi$ |
| $f$ | $-1$ | $-1$ | $-1$ | $-1$ |
| $q_A$ | $jq^{(2)}$ | $\bar{u}_1$ | $-j\rho_1$ | $-R_e$ |
| $q_B$ | $jq^{(1)}$ | $\bar{u}_2$ | $-j\rho_2$ | $-R_0$ |
| $\Pi_A$ | $u^{(2)}$ | $\Pi_1$ | $-jW$ | $\Pi_e$ |
| $\Pi_B$ | $u^{(1)}$ | $\Pi_2$ | $V$ | $j\Pi_0$ |
| $k_0^2\epsilon_A$ | $k_0^2\epsilon^{(2)}(z)$ | $k_0^2\epsilon_1$ | $k_0^2q_e^2$ | $k^2\mu_e^2$ |
| $k_0^2\epsilon_B$ | $k_0^2\epsilon^{(1)}(z)$ | $k_0^2\epsilon_2$ | $k_0^2q_0^2$ | $k^2\mu_0^2$ |
| $M$ | $jk_0\dfrac{\frac{dq}{dz}}{1+q^2}$ | $\dfrac{\frac{du}{dz}}{1-u^2} = \psi$ | $-jk_0\dot{\varphi} = -\dfrac{jk_0\frac{d\rho}{du}}{1+\rho^2}$ | $-j\psi$ |

Because none of these four workers explicitly chose $\theta_p \gtrless 90°$, we divide the Table into two parts, one for $f = +1$ and one for $f = -1$. The final equations in all cases have the same appearance independently of whether $\theta_p$ is acute or

obtuse, but the relationship to the present notation changes in the manner shown in the Table.

When an author has treated the symbol $e$ as a positive quantity, but introduced the charge into the equations of motion as that of a *negative* electron, we are required to use $b = -1$.

It should be noted that Försterling's Equations (22), (23), and (25) should have a negative sign in front of the left-hand members in all cases. As shown by the equations preceding and following these, this is a purely typographical error which does not affect the rest of the work. This error is *not* the supposed sign error which led to the preparation of this paper.

The 1950 paper by Rydbeck, which is listed as reference [3], is one of several by him on this subject. The coupled equations in this paper are correct, but in other papers on triple splitting he has a typographical error in that the term, which we here call $M^2$, has a negative sign. This, again, does not influence the work which follows it, and is *not* the "sign error" in question.

The present method of separating the fields into "characteristic modes" which results in Equation (1), or some equations closely related, is not the only method of considering the vertical incidence problem. However, any discussion of other methods of attack is outside of the scope of this work. Also, it is clear that all of the possible changes of notation have not been touched upon, but it is felt that the present discussion embraces all of the cases which are particularly likely to arise. For example, it seems unlikely that anyone would choose to define the polarizations for the two modes in such a way, that, say,

$$\frac{E_2^{(A)}}{E_1^{(A)}} = q_A \,, \qquad \frac{E_2^{(B)}}{E_1^{(B)}} = jq_B$$

although this would seem to be a possible choice. It is clearly impractical to attempt to consider all such possibilities, and we do not do so here.

The author wishes to acknowledge the active cooperation of Prof. J. J. Gibbons and Prof. N. Davids, both of whom were of great assistance in this work.

## *References*

[1] K. Försterling, Über die Ausbreitung elektromagnetischer Wellen in einem magnetisierten Medium bei senkrechter Inzidenz, Hochf. Tech. u. Elec. Akus., **59**, 10-22 (1942).

[2] O. E. H. Rydbeck, On the propagation of radio waves, Trans. Chalmers Univ. of Technology, Gothenburg, No. 34 (1944).

[3] O. E. H. Rydbeck, Magneto-ionic triple splitting of ionospheric waves, J. Appl. Phys., **21**, 1205-1214 (1950).

[4] J. J. Gibbons and R. J. Nertney, Wave solutions, including coupling, of ionospherically reflected long radio waves for a particular $E$-region model, J. Geophys. Res., **57**, 323-338 (1952).

[5] J. M. Kelso, H. J. Nearhoof, R. J. Nertney, and A. H. Waynick, The polarization of vertically incident long radio waves, Ann. Géophys., **7**, 215-244 (1951).

[6] N. Davids, Theoretical group heights of reflection of 150 kc/s radio waves vertically incident on the ionosphere, J. Atmos. Terr. Phys., **2**, 324-336 (1952).

[7] M. N. Saha, B. K. Banerjea, and U. C. Guha, Vertical propagation of electromagnetic waves in the ionosphere, Proc. Nat. Inst. Sci. India, **17**, 205-226 (1951).

[8] K. G. Budden, The theory of the limiting polarization of radio waves reflected from the ionosphere, Proc. R. Soc., **215**, 215-233 (1952).

JOURNAL OF GEOPHYSICAL RESEARCH VOLUME 58, No. 4 DECEMBER, 1953

# REAL AND COMPLEX WAVE POLARIZATION IN THE IONOSPHERE*

By JAMES C. W. SCOTT

*Defence Research Telecommunications Establishment (Radio Physics Laboratory), Defence Research Board, Ottawa, Canada*

(Received March 16, 1953)

ABSTRACT

The relation between the polarization ellipse in the wave front and the complex polarization at vertical incidence in a slowly-varying horizontally-stratified ionosphere is reviewed. Charts and a table are given showing the sense, orientation and eccentricity of the polarization ellipse under all conditions of plasma frequency, collisional frequency, wave frequency, and magnetic field intensity and direction.

## *Introduction*

Providing the properties of the medium are a sufficiently slowly-varying function of height, the complex refractive index and the polarization of radio waves normally incident on the ionosphere are determined by the Appleton-Hartree equation.

Waves are then propagated in two characteristic modes, the ordinary and the extraordinary, each mode, in general, being elliptically polarized. In each mode, the electromagnetic vectors rotate at the wave frequency in ellipses for which the ellipticity, orientation, and sense of rotation are determined by the parameters of the medium and the wave frequency.

These parameters are four, the plasma frequency, which depends on the electron density, the collisional frequency of electrons with the surrounding gas, and the intensity and direction of the magnetic field of the earth. At any point in the ionosphere, the polarization of each mode may be found as a function of these four constitutive quantities and the wave frequency. The polarization at a given point in the ionosphere is thus a function of five independent variables.

In the derivation of ray paths for plane waves vertically incident on a horizontally stratified ionosphere, contour charts of the complex polarization were prepared [see 1 of "References" at end of paper]. In these charts, the dependence of the complex polarization for ordinary and extraordinary modes was completely displayed as a function of all five independent variables.

Because these charts of the complex polarization involve so many variables, they require careful study to deduce the specific dependence of the complex polarization on any one characteristic of the medium. It is then necessary to interpret the complex polarization in terms of the ellipticity, orientation, and polarity of the real polarization ellipse. In this brief report, two simple charts are

*Research conducted under Defence Research Board Project No. D48-95-11-01.

derived which give the parameters of the real polarization ellipse for all values of the ionospheric variables.

*The complex polarization*

For the derivation of the complex polarization in the ionosphere, the reader is referred to the above-mentioned paper [1]. It is defined as the ratio of the components of the complex electric-field vector in the plane of the wave surface.

In Cartesian coordinates orientated as in Figure 1, waves are propagated along $x$ and the constant magnetic field of the earth is in the $xy$ plane. Then the complex polarization is defined by

$$Re^{i\phi} = \frac{E_z}{E_y} = -\frac{B_y}{B_z} = \frac{V_z}{V_y} \qquad (1)$$

In this equation, $E$, $B$, and $V$ are the complex vector electric and magnetic radiation fields and the electron velocity. $B$ is confined to the plane of the wave surface, but $E$ and $V$ also may have components, $E_x$ and $V_x$ in the direction of wave propagation.

At any point in the ionosphere, the electric field of each mode is of the form $E = Ae^{i(\alpha - \omega t)}$, where $A$ and $\alpha$ are real. Thus, $R = A_z/A_y$ and $\phi = \alpha_z - \alpha_y$ , so that $R$ is the amplitude ratio and $\phi$ the phase difference of the field components in the horizontal plane which determine the polarization ellipse.

*The sense of rotation of the field vectors*

The polarization ellipse is easily derived from the complex polarization. In Figure 1, the real electric field in the horizontal plane (the plane of the wave

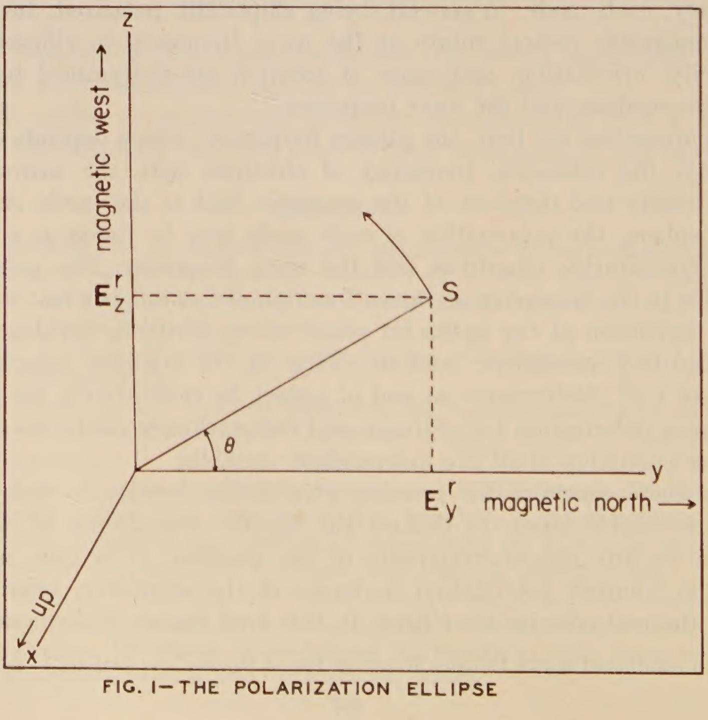


FIG. 1—THE POLARIZATION ELLIPSE

surface) is represented at time $t$ by the vector $S$, making angle $\theta$ with the positive $y$ axis. This vector has components $y = E_y^r$ and $z = E_z^r$, where the superscript indicates the real component of the complex field.

We have

$$E_y^r = A_y \cos(\alpha_y - \omega t)$$

$$E_z^r = A_z \cos(\alpha_z - \omega t)$$

Since we are not concerned with the size of the polarization ellipse but only with its ellipticity and orientation, we may put $A_y = 1$ and $\alpha_y = 0$. We then have $A_z = R$ and $\alpha_z = \phi$. Consequently, since $\tan\theta = E_z^r/E_y^r$, we obtain

$$\tan\theta = R(\cos\phi + \sin\phi \tan\omega t) \qquad (2)$$

Differentiating,

$$\sec^2\theta \frac{d\theta}{\omega\, dt} = R \sin\phi \sec^2 \omega t \qquad (3)$$

We conclude: the direction of rotation of the real electric vector is positive or negative as $\sin\phi$ is positive or negative. Thus, the direction of rotation is north to west when $\phi$ is in the first or second quadrant and north to east when $\phi$ is in the third or fourth quadrant.

Table 1 is a modification of a similar table which may be found in reference [1]. In the original table, the phase quadrants were incorrect, having been interchanged between northern and southern hemispheres. The table gives the direction of rotation of the field vectors under all conditions.

TABLE 1—*Vertical propagation, upgoing and downcoming waves*

| Mode | Term | Northern hemisphere | | Southern hemisphere | |
|---|---|---|---|---|---|
| .... | Plasma frequency | $\omega_0 < 1$ | $\omega_0 > 1$ | $\omega_0 < 1$ | $\omega_0 > 1$ |
| $o$ mode | Amplitude ratio | $R < 1$ | $R < 1$ | $R < 1$ | $R < 1$ |
| | Phase quadrant | $\phi$ in [2] | $\phi$ in [3] | $\phi$ in [4] | $\phi$ in [1] |
| | Rotation | N to W | N to E | N to E | N to W |
| $x$ mode | Amplitude ratio | $R > 1$ | $R > 1$ | $R > 1$ | $R > 1$ |
| | Phase quadrant | $\phi$ in [3] | $\phi$ in [2] | $\phi$ in [1] | $\phi$ in [4] |
| | Rotation | N to E | N to W | N to W | N to E |

*Note*: When $\omega_0 > 1$ and $M/g < 2$, the labels $o$ and $x$ must be interchanged. Under these conditions, the $o$ mode refers to the longitudinal ordinary mode commonly known as the $z$ mode. See the section below on "The polarization charts."

*The orientation of the polarization ellipse*

In polar coordinates, the equation of the ellipse is found to be

$$(1 - R^2)\sin^2\theta - 2R\cos\phi\sin\theta\cos\theta = \frac{R^2\sin^2\phi}{S^2} - R^2 \qquad (4)$$

Differentiating with respect to $\theta$ and putting $dS/d\theta = 0$, we obtain the angle, $\theta_0$, made by an axis of the ellipse with the positive $y$ coordinate.

$$\tan 2\theta_0 = \frac{2R\cos\phi}{1 - R^2} \quad \text{(5)}$$

To determine whether this angle, $\theta_0$, measures the deviation or tilt of the major axis or of the minor axis, we must differentiate again. Noting that $\theta_0$ defines the major axis when $d^2S/d\theta^2 < 0$, we find that this condition is obeyed when

$$\frac{1 - R^2}{\cos 2\theta_0} > 0 \quad \text{(6)}$$

If $\theta_M$ is the angle made by the major axis with the positive $y$ axis, we conclude,

$$\tan 2\theta_M = \frac{2R\cos\phi}{1 - R^2} \quad \text{(7)}$$

When

$$\left.\begin{array}{ll} R < 1, & |\theta_M| < \pi/4 \\ R > 1, & |\theta_M| > \pi/4 \end{array}\right\} \quad \text{(8)}$$

When

In particular, when $\phi = \pm\pi/2$, for $R < 1$, $\theta_M = 0$ and the major axis is north-south, and for $R > 1$, $\theta_M = \pi/2$ and the major axis is east-west.

If $R_0 e^{i\phi_0}$ is the polarization of the ordinary mode and $\theta_{MO}$ the tilt of the major axis of its ellipse, the corresponding polarization of the extraordinary mode is $R_0^{-1} e^{-i\phi_0}$ and the tilt of the major axis of its ellipse is given by $\theta_{MX}$, where

$$\tan 2\theta_{MX} = -\frac{2R_0\cos\phi_0}{1 - R_0^2} = -\tan 2\theta_{MO} \quad \text{(9)}$$

Consequently,

$$\theta_{MX} + \theta_{MO} = \pm\pi/2 \quad \text{(10)}$$

The solution $\theta_{MX} = -\theta_{MO}$ is not permitted because of (8). In the special case, $R = 1$, $\theta_{MX} = \theta_{MO} = \pm\pi/4$ for all values of $\phi$. In this case, the major axes of the ordinary and extraordinary modes coincide and are directed either to the northwest or to the northeast.

Measured from magnetic north, the deviations of the major axes of the ordinary and extraordinary modes are complementary. The major axes are both either in the northwest quadrant or the northeast quadrant. On examination of Table 1 in the light of equation (9), it will be found that in the northern hemisphere, the major axes of both modes are always in the northeastern quadrant, while in the southern hemisphere they are always in the northwestern quadrant.

The change in the orientation of the ellipse due to a change in $\phi$ is given by

$$\sec^2 2\theta_M \frac{d\theta_M}{d\phi} = -\frac{R}{1 - R^2}\sin\phi \quad \text{(11)}$$

Consequently, when

$$R < 1 \qquad \text{and} \qquad \sin \phi < 0$$

or

$$R > 1 \qquad \text{and} \qquad \sin \phi > 0$$

then

$$\frac{d\theta_M}{d\phi} > 0$$

Similarly, the change in the orientation of the ellipse due to a change in $R$ is given by

$$\sec^2 2\theta_M \frac{d\theta_M}{dR} = \frac{1 + R^2}{(1 - R^2)^2} \cos \phi \quad \text{.................. (12)}$$

Consequently,

$$\frac{d\theta_M}{dR} < \text{or} > 0 \qquad \text{as} \qquad \cos \phi < \text{or} > 0$$

*The eccentricity of the polarization ellipse*

The orientation of the ellipse was defined by $\theta_M$, which has been derived in equation (7) as a function of $R$ and $\phi$. Similarly, we can derive $\rho$, the ratio of the major to the minor axis of the real ellipse as a function of the complex polarization. The derivation is straightforward and need not be detailed. We find

$$\rho^2 = \frac{2(1 + R^2)}{(1 + R^2) - [(1 - R^2)^2 + (2R \cos \phi)^2]^{1/2}} - 1 \quad \text{.......... (13)}$$

Consequently, the tilt and eccentricity of the ellipse can both be expressed in terms of $R$ and $\phi$.

*The polarization charts*

Using equations (7) and (13), the amplitude $R$ and phase $\phi$ of the complex polarization were computed for integral values of the tilt and eccentricity of the ellipse. Contours of $\theta_M$ and $\rho$ were then drawn in the same coordinates used in reference [1].

These coordinates are $M/g$ and $M/(1 - \omega_0^2)$, where $M = h_T^2/|h_L|$ is a function of the magnetic field of the earth. The ionospheric variables are all normalized in terms of the angular wave frequency $\omega$ and have the following definitions:

$$\begin{aligned} \omega g &= \text{collisional frequency} \\ \omega\omega_0 &= \text{plasma frequency} \\ \omega h_T &= \text{transverse gyro-frequency} \\ \omega h_L &= \text{longitudinal gyro-frequency} \end{aligned}$$

Thus it is clear that the abscissa is a measure of the collisional frequency and the ordinate of the plasma frequency. The earth's field enters through $M$ as a scale factor.

To cover the wide range of the ionospheric variables, logarithmic coordinates are used in Figure 2. The solid contours give the axes ratio of the ellipse and the dashed contours the deviation of the major axis from magnetic north. At any

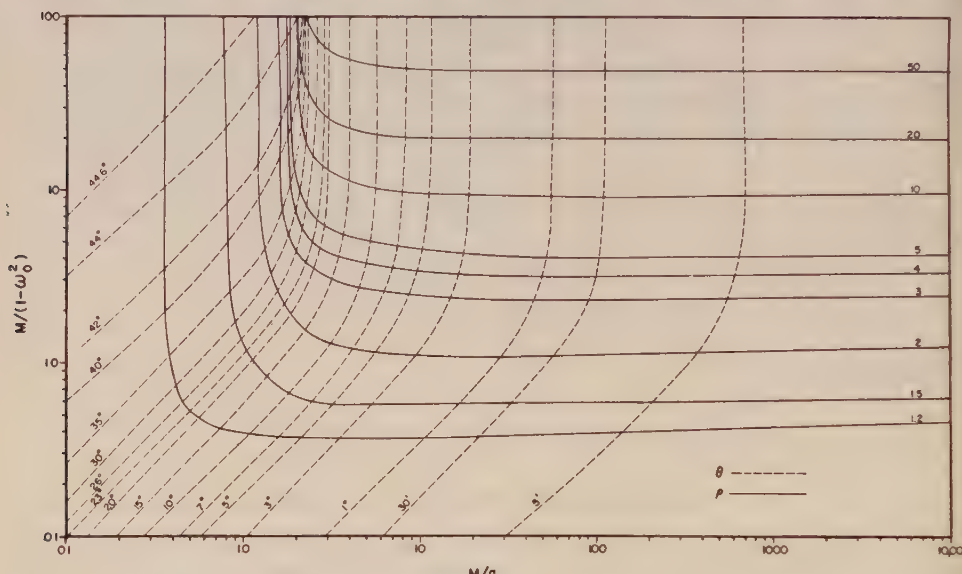


FIG. 2—THE POLARIZATION DESCRIBED BY CONTOURS OF TILT ANGLE, θ, AND AXIS RATIO, ρ, IN LOGARITHMIC COORDINATES

point in the ionosphere, the polarization ellipses for the ordinary and extraordinary modes are identical in shape, so that the values of $\rho$ hold for both modes. However, the orientations of the two ellipses are complimentary. The contours of $\theta_M$ have been labeled with the values for $R < 1$ and the subscript $M$ has been dropped. These (see Table 1) correspond to the ordinary mode, except in the reflection region of the longitudinal ($z$) mode. The tilt of the extraordinary mode ellipse is $\pi/2 - \theta$.

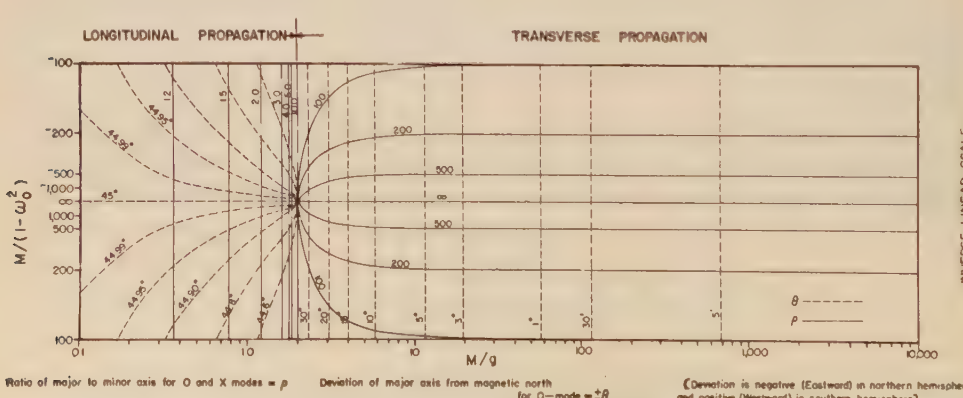


FIG. 3—THE POLARIZATION IN THE REGION OF ORDINARY MODE REFLECTION; THE ORDINATE SCALE IS INVERSE LINEAR

Figure 3 displays the polarization in the important region of ordinary mode reflection, $\omega_0 = 1$. In order to show conditions in this region, the logarithmic ordinate of Figure 2 has been replaced by an inverse linear scale. Figure 3 is therefore merely an extension of Figure 2 for values of $M/(1 - \omega_0^2)$ above 100 and through infinity into negative values.

The transition from transverse to longitudinal propagation as the collision frequency increases through $M/g = 2$ is clearly shown. When $M/g < 2$ and $M/(1 - \omega_0^2) < 0$, the ordinary mode becomes the longitudinal or $z$ mode. Under these conditions, the tilt of the $z$ mode ellipse is given by $\pi/2 - \theta$.

## *Summary*

The conclusions reached may be summarized as follows:

(1) Table 1 gives the sense of rotation of the field vectors in the polarization ellipse for $R < 1$ and $R > 1$. It reverses on passing through $\omega_0 = 1$ and on crossing the magnetic equator. $R < 1$ defines the ordinary mode except in the region $\omega_0 > 1$ and $M/g < 2$, where $R > 1$ for the $o$ mode and $R < 1$ for the $x$ mode.

(2) The direction of the major axis for $R < 1$ is

$$| \theta_M | < \pi/4 \qquad \text{and for} \qquad R > 1 \qquad \text{is} \qquad | \theta_M | > \pi/4.$$

(3) At any point in the ionosphere, the tilts of the ordinary and extraordinary mode ellipses are complementary, $\theta_{MO} + \theta_{MX} = \pm \pi/2$.

(4) For both modes, the major axis is in the northeastern quadrant in the northern hemisphere and in the northwestern quadrant in the southern hemisphere.

(5) The polarization of both modes at any point in the ionosphere is given in Figures 2 and 3 by $p$ and $\theta$ with due regard to the semi-quadrant of $\theta$.

## *Acknowledgments*

I wish to thank Mr. D. V. Dickson for his help in carrying out the computations and Dr. M. G. Morgan who kindly checked the manuscript for errors and moreover suggested the use of "north to west" and "north to east" instead of "right hand" and "left hand" to describe the sense of rotation of the field vectors.

## *References*

[1] J. C. W. Scott, Proc. Inst. Radio Eng., **38**, 1057 (1950).
[2] M. Taylor, Proc. Phys. Soc. (London), **45**, 245 (1933), and **46**, 408 (1934).
[3] V. A. Bailey, Phil. Mag., **18**, 516 (1934).
[4] G. Goubau, Hochf. Tech. u. Elec. Akus., **45**, 179 (1935).

JOURNAL OF GEOPHYSICAL RESEARCH VOLUME 58, No. 4 DECEMBER, 1953

# CORRELATION OF MAGNETIC, AURORAL, AND IONOSPHERIC VARIATIONS AT SASKATOON*

By J. H. MEEK

*Defence Research Telecommunications Establishment (Radio Physics Laboratory), Defence Research Board, Ottawa, Ontario, Canada*

(Received March 20, 1953)

ABSTRACT

An analysis has been made for the five-month period from December 1951 to April 1952 of the variations at Saskatoon of the horizontal component ($H$) of the earth's magnetic field, the position in the sky and intensity of auroral light, and of critical frequencies and heights of the ionospheric reflecting regions.

There is a relationship between the maximum elevation above the northern horizon of auroral light and the maximum amplitude of variation of $H$. Some types of sporadic $E$ reflecting layers appear more frequently during disturbances.

Detailed analysis of magnetically disturbed nights shows that magnetic bays and certain other phenomena are correlated. An increase in the intensity of aurora is related to the rate of decrease of $H$ in the bay. Radio wave absorption or weak reflections at levels below 100 km correspond to the periods when $H$ is of the order of 500 gammas or more from its normal value.

## INTRODUCTION

During periods when the earth's magnetic field is disturbed, causing an abnormal range of variation of its strength and direction, variations often are seen in other geophysical measurements such as occurrence of aurora and ionization and height of the reflecting and absorbing regions of the ionosphere.

It is of importance to study the relations between these measurements in an attempt to determine their cause or causes, and subsequently to find a system of predicting the amplitude and extent of each phenomenon. This may be done (1) by relating the variations of each type of measurement to observations of the phenomenon which is thought to cause the disturbance (in this instance, solar observations), or (2) by finding in one or other of the geophysical variations a pattern or sequence of events which can be used to estimate the course of a future disturbance after it is first detected. The present investigation is being made from the latter point of view.

Since it is necessary to compare the observations on undisturbed days with those on disturbed days, an observing site was chosen where the days are reason-

*The research reported here was performed at the University of Saskachewan under Defense Research Board Project D48-95-11-13.

ably well divided between disturbed and undisturbed periods. Saskatoon at 52°.1 north and 106°.6 west (60°.6 north, geomagnetic) is ideal from this point of view. Geomagnetic disturbance in Canada generally appears to spread out southward from the position of the normal auroral zone (65-68° north, geomagnetic latitude). Even minor disturbance effects are detected as far away from the zone as Saskatoon. Past work in this field has given statistical relations between southerly extension of auroral light and magnetic disturbance, and between abnormalities in ionospheric measurements and magnetic disturbance. Here we are interested primarily in comparing variations of the three types of observations, minute to minute, throughout each night.

## OBSERVATIONS

(*a*) *Magnetic*—Observations of variations of the $H$ component of the earth's magnetic field have been recorded continuously for a five-month period (149 days) between December 1951 and April 1952, inclusive.

The characteristics of magnetic bays at Saskatoon have been analysed for this period and a separate paper is being published on the subject. Magnetically disturbed nights may be thought of as variations due to a number of overlapping bays. Ionospheric and auroral characteristics are found to be related directly to the size and shape of these bays. The disturbances have been studied with this in mind.

(*b*) *Auroral*—Records of relative auroral light intensity along a narrow band (about $3^0$) of sky, from northern to southern horizon, along the geomagnetic meridian, are made regularly at Saskatoon and are available at ten-minute intervals on all clear (124) nights. During the five-month period aurora was recorded on 80 per cent of the clear nights.

Correlation of the presence of auroral light with magnetic variations during this period may be summarized as follows:

(1) Aurora was recorded low in the north on 30 per cent of the 28 clear and magnetically quiet nights. On three nights, aurora was seen to 60° elevation, and on only one night did it extend past the zenith. Magnetically quiet nights corresponded to nights of no aurora 79 per cent of the time, while nights of no aurora fell on magnetically quiet nights 68 per cent of the time.

(2) On nights with magnetic variations in $H$ from 50 to 200 gammas, about 85 per cent showed aurora low in the north and 75 per cent showed aurora up to 60° elevation. On only five out of 37 clear nights was no aurora recorded.

(3) On more disturbed nights (200 to 300 gammas variation in $H$), aurora was seen every night and at least to overhead on over half the nights.

(4) On the most disturbed nights (over 300 gammas variation in $H$), aurora extended at least to overhead every night.

If variations of $H$ up to 200 gammas at Saskatoon may be considered minor, then we can say that (*a*) absence of aurora always indicates absence of magnetic disturbance, and (*b*) presence of aurora to the south of the zenith indicates large magnetic disturbance 95 per cent of the time.

(c) *Ionospheric*—Ionospheric vertical incidence multifrequency (1-15 Mc/s) measurements were made at 20-second intervals, usually from 10 p.m. to 6 a.m., local time, on 77 of the 149 nights. The observations are similar to those obtained at other places of the same approximate geomagnetic latitude. Statistical correlation between ionospheric and magnetic variations have been reported by a number of writers, and the same statement may be made from an examination of the Saskatoon data.

The statistics of observations at Saskatoon on nights of different degrees of magnetic disturbance are shown in Figure 1. Occurrence of *F* region echoes de-

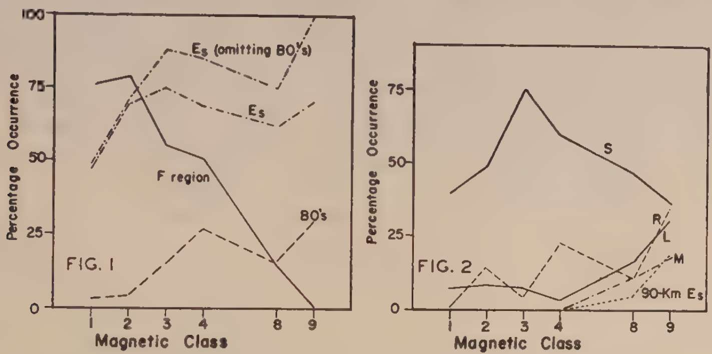


FIG. 1—IONOSPHERIC OBSERVATIONS
FIG. 2—OCCURRENCE OF Es COMPARED TO THE NUMBER OF TIMES WHEN ECHOES OF ANY TYPE WERE OBSERVED

creases with increasing magnetic disturbance, while the occurrence of *Es* and of blackouts increases. The increase in blackouts is probably the main reason for the absence of *F* region echoes. Figure 2 shows a breakdown of the various types of *Es* which have been described previously [see 1 of "References" at end of paper]. Several types of *Es* increase in occurrence with magnetic disturbance.

## AURORAL AND IONOSPHERIC VARIATION RELATED TO MAGNETIC DISTURBANCES AT SASKATOON

Detailed comparisons, minute to minute, of the variations of the three types of phenomena are very complex; however, the analysis of individual nights has resulted in useful information which is summarized as follows.

(a) *Undisturbed nights with fluctuations in H of less than* 50 *gammas*—The *F* region echoes are observed most of the night, but may be obscured occasionally by short periods of high absorption or by the presence of a blanketing *Es* of high reflection coefficient. The radio wave absorption is generally low, although it may increase during short periods of slight ionospheric disturbance.

Aurora, if it is present at all, is faint and low in the northern sky. Its presence does not necessarily coincide with the minor magnetic fluctuations or ionospheric variations which may occur.

(b) *Moderately disturbed nights with H variations up to* 300 *gammas, usually in the form of small magnetic bays*—The *F* region is present about half the night. During the remainder of the night, it is obscured either by formation of a low-level

*Es* or by increased radio wave absorption coincident with the larger bays. *Es* echoes are present most of the night. Weak aurora is present low in the north all night. It increases in intensity and elevation at times of magnetic bays.

(*c*) *Nights with a single large negative magnetic bay of over* 300 *gammas amplitude*—It is quite usual to have temporary partial recovery in *H* near the time of maximum deviation. The positive (first) phase usually associated with a large magnetic bay at temperate latitudes is seldom observed, although there is often a separate positive bay 3 to 10 hours before the negative bay.

The *F* region echoes disappear several hours before the main bay at the time when the minor magnetic fluctuations become significant. The echoes sometimes reappear for short intervals after this time and before the main decrease in *H* begins. *Es* echoes are very variable. They are accompanied by some spread echoes and a temporary increase of $fEs$ when a positive bay occurs. The $fEs$ becomes quite high about an hour before the main bay. At the time of the main decrease in *H*, the usual type of *Es* disappears, due either to a sharp increase in radio wave absorption or in some cases to the formation of a thin *E* layer at about 90 km virtual height. Recovery of the ionospheric layers is slow and it may be well into the morning before the regular layers reappear.

Faint aurora exists all night at most elevations in the north sky. When a positive bay is present in the evening before the main bay, the auroral light and normally the $fEs$ increase in intensity to some extent. Corresponding to the main drop in *H*, the aurora increases in intensity and extends past the zenith into the southern sky.

(*d*) *Very disturbed night with large and small bays often overlapping*—The magnetic field is below normal most of the night, since the individual bay does not often get a chance to recover before another has started.

*F* region traces are normally not observed on such nights, but may appear temporarily if the magnetic field does return to near normal. The *Es* echoes are present all night, except during the short intervals when there is a sharp decrease in *H*. During these intervals, no echoes are observed (except occasionally 90-km *Es*) as the low-level radio wave absorption is greatly increased.

The aurora extends at least to the zenith all night and becomes much brighter at times when the sharp deviation in magnetic field is observed.

## EXAMPLES OF PARTICULAR DISTURBANCES

The foregoing summary of disturbances is well illustrated by the observations on five particular nights, as shown in Figures 3 to 7, and described below. The following explanatory notes should be kept in mind when examining these Figures.

*H*—The trace has been redrawn from the magnetic record and some of the minor fluctuations are missing.

$fF2$—The trace has been thickened to indicate the range of the probable $f^oF2$ (or $f^xF2$) when spread echoes are present. Where two traces, upper and lower, are separated by a constant frequency (approximately 0.8 Mc/s), it may be assumed that they are the "$x$" and "$o$" components, respectively.

$f_{min}F$—The minimum frequency of reflection from the *F* region is included as a thin line wherever *F* region echoes are observed. Where it is not present, it may be assumed that the spread echoes exist down to the $f_{min}$ frequency.

*fEs*—The top frequency of each *Es* trace, regardless of height, is included. *R* type echoes may be distinguished by the double curve separated by approximately 0.8 Mc/s. $f_{min}Es$ is limited by interference from a local broadcast station (1.3 mc/s) up to 1:00 a.m. and by the lower limit of sensitivity of the ionospheric measuring equipment (about 1 Mc/s) after this time.

*h′F2*—Only the minimum virtual height of the *F2* layer is drawn, regardless of the presence of spread echoes or other irregularities. It should be noted that *h′F2* on most nights cannot be considered as indicative of the true height of maximum ionization of the layer.

*h′Es*—The broad parts of the trace give the range of virtual height over all frequencies on which the *Es* echoes are observed and indicate that the virtual height increases gradually with increasing frequency. The shaded parts indicate the range of virtual height on which *E* region spread echoes are observed.

*Aurora*—A contour plot of the intensity of auroral light has been made on a grid of elevation of aurora above the northern horizon against time. The degree of shading represents the intensity of aurora on an arbitrary scale. The type of

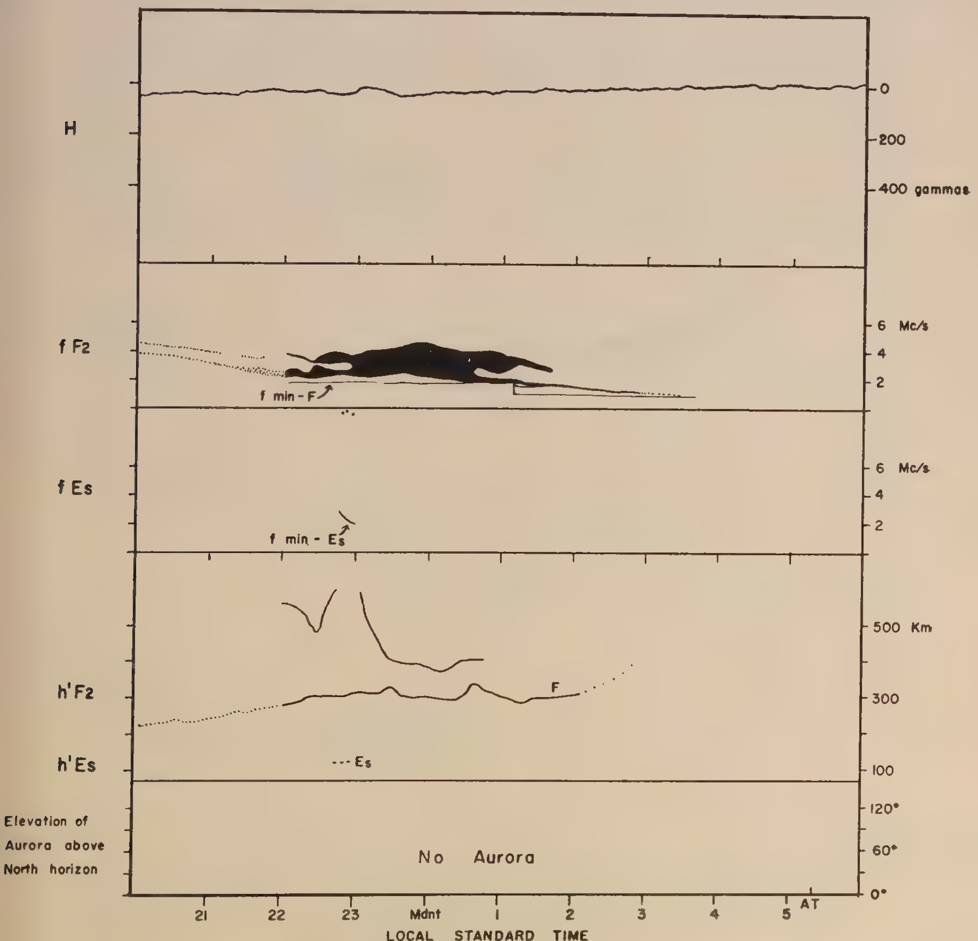


FIG. 3—FEBRUARY 22–23, 1952

measurements available does not show the structure of individual auroral arcs or displays.

*Figure 3, February 22-23, 1952*—This was a very quiet night, magnetically. Fluctuations of $H$ are less than 20 gammas in amplitude.

Radio echoes were received from the $F2$ layer throughout the night. Although ionospheric observations were available only from 10 a.m. to 3 a.m. on this night, estimated curves for earlier and later hours have been added on the basis of observations on other quiet nights.

The upper trace of $h'F2$ is quite separate from the regular $F2$ trace and is likely due to a type of scatter reflection from some oblique distance. It is not possible to say whether the appearance of the few $Es$ echoes has any relation to the increase in range of this $F$ region trace at the same time.

No aurora was observed during this night.

*Figure 4, March 25-26, 1952*—Fluctuations of $H$ were up to 40 gammas and were slightly greater than on February 22-23. In the early part of the night,

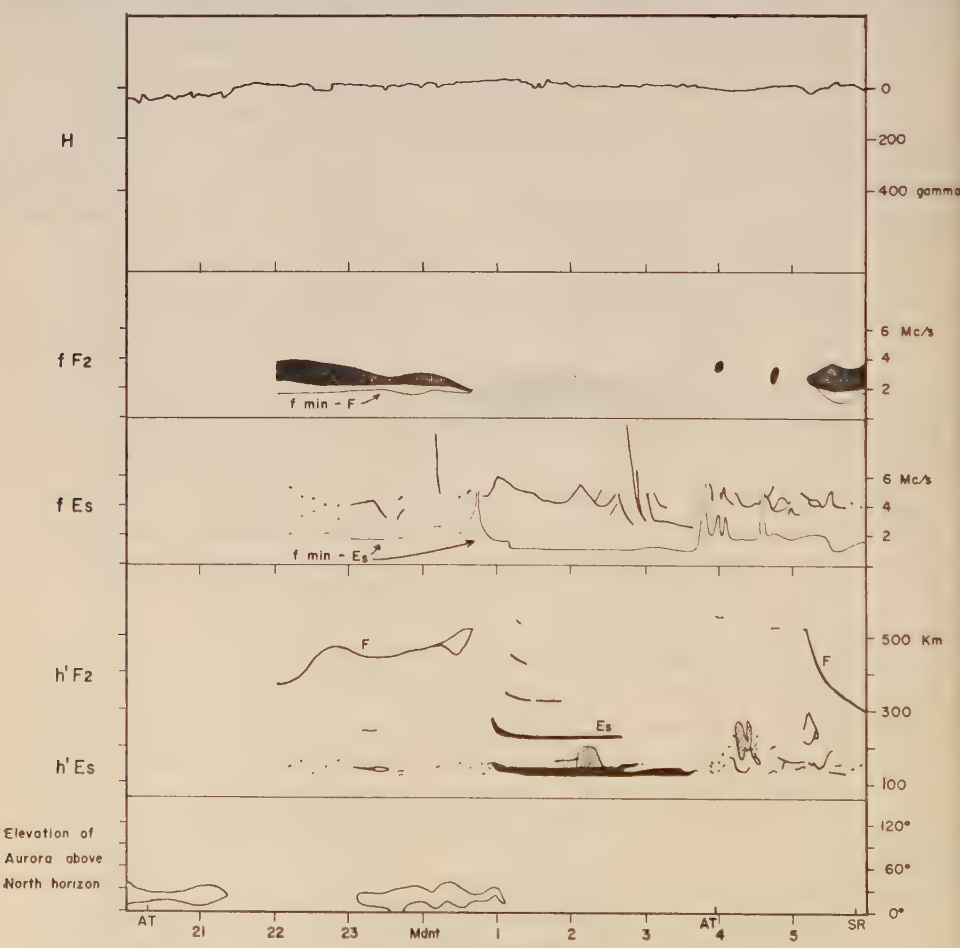


FIG. 4—MARCH 25-26, 1952

there were scattered *E* region echoes below the *F* region echoes. After a short period of high radio wave absorption at about 12:45, a blanketing type *Es* of high reflection coefficient and high *fEs* was observed. After 3 a.m., the *Es* became more scattered and the *F* region reappeared.

The *h'F*2 gradually increased until obscured by *Es*, and decreased again in the morning after the *Es* began to break up. This would indicate that the slight ionospheric disturbance has affected both the *E* and *F* regions.

Some faint aurora was observed low in the north sky (below 30° elevation), but there is no obvious relationship between the aurora and the changes observed in the ionospheric regions.

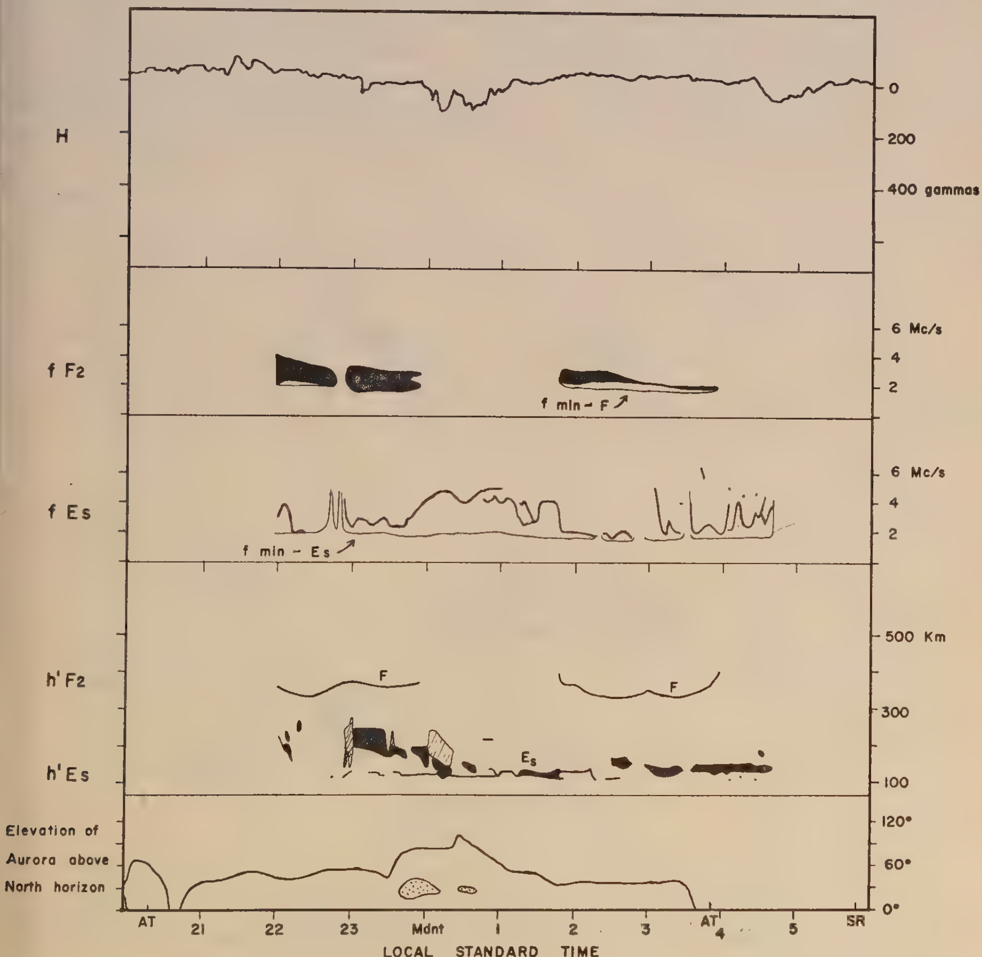


FIG. 5—MARCH 26-27, 1952

*Figure 5, March 26-27, 1952*—Several small magnetic bays were visible in *H*. The *F* region echoes were obscured during the hours 12:00 to 2:00 a.m., but not by the highly reflecting type of *E* layer. A thin layer at 100 km with *fEs* of about 5 Mc/s appears to be responsible. Other *Es* echoes occurring during the night

were rather erratic and showed considerable spread in the echoes. From about 4:45 a.m. on, no ionospheric reflections were observed, presumably due to strong radio wave absorption at a level below the $E$ region.

Although the magnetic disturbance was relatively small, aurora was visible low in the north all night. At the time of the midnight bay, its intensity increased and it was observed for a short time at elevations extending to near the zenith.

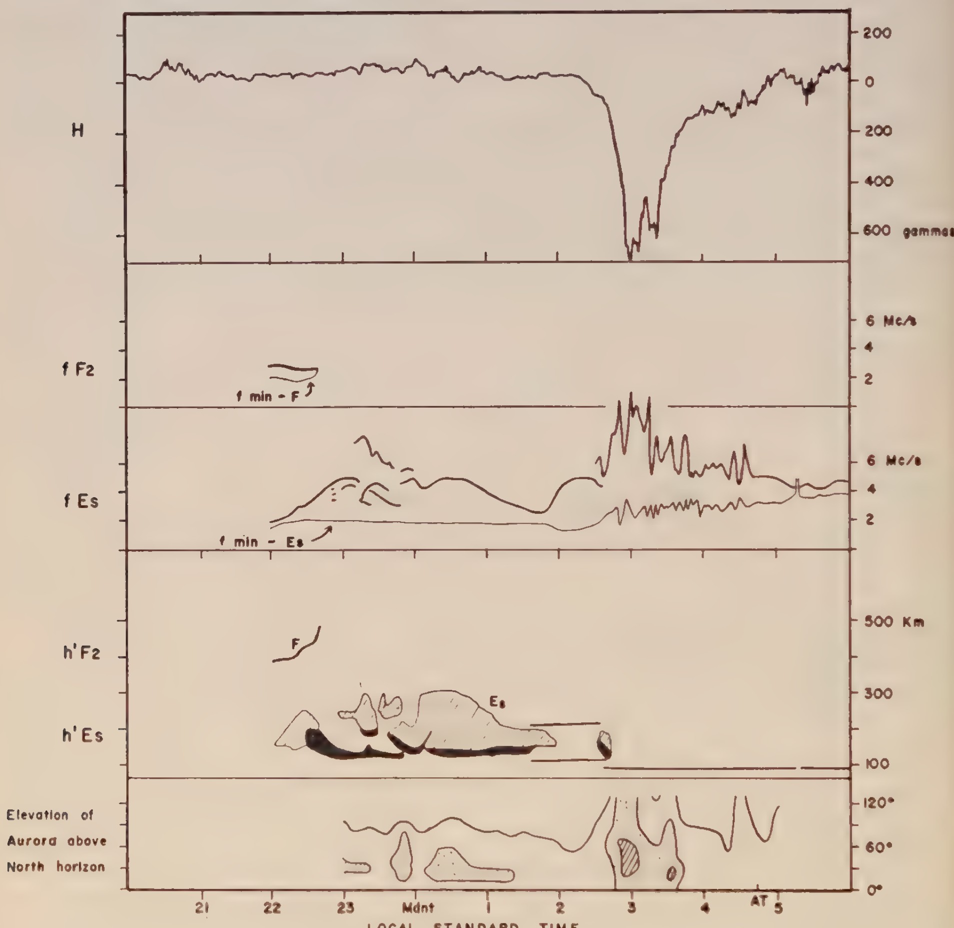


FIG. 6—MARCH 6-7, 1952

*Figure 6, March 6-7, 1952*—There were small fluctuations in $H$ several hours before the main magnetic bay. The recovery of $H$ after the main bay was rather slow and variable.

The $F$ region was obscured early in the night and did not reappear. Up to this time, the increase in $h'F2$ and in $fEs$ indicates the commencement of an ionospheric disturbance. The $Es$ was very variable.

A thin extremely variable echo at 90 km appeared at the time of the main drop in the $H$ component, and all other echoes disappeared. On this night, the

90-km echo lasted for several hours. For many bays, no echoes are observed during the maximum deviations of $H$.

Radio wave absorption was low up to the time of the main bay. With the appearance of the 90-km $Es$, the $f_{\min}Es$ rose and became very variable, indicating the increased absorption associated with the bay. At the time of the small sharp bay at 5:15 to 5:45, even the 90-km $Es$ echoes disappeared for a short period.

Faint aurora was present in the north all night and during most of the time it reached 70-80° elevation. At the time of the main drop in $H$, the auroral intensity increased, and it extended past the zenith and to the south. The enhancement of the aurora appears to be related to the rate of change of $H$ rather than the amplitude of the change. This is better illustrated in the next example.

*Figure 7, February 15-16, 1952*—A large positive bay was followed by what appears to be a number of negative bays, more or less overlapping.

As in the above example, the $F$ region was obscured by $Es$ early in the evening. The $fEs$ was well above normal all night.

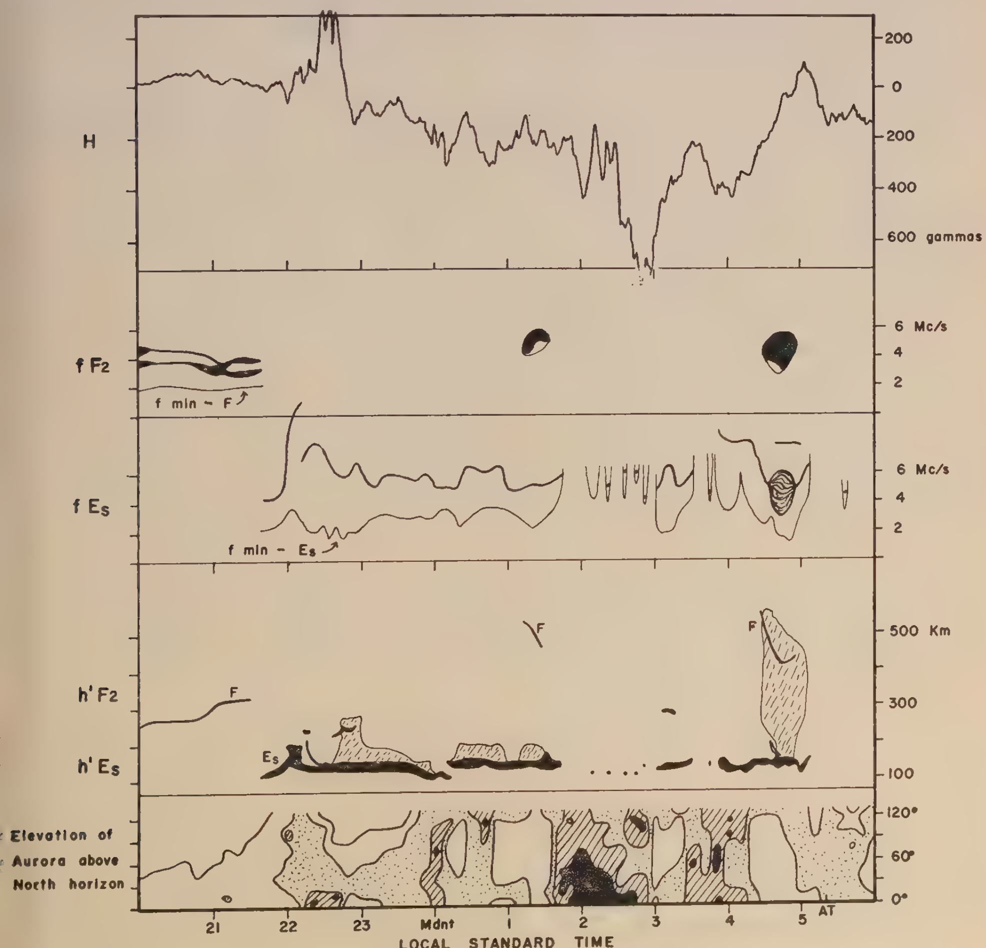


FIG. 7—FEBRUARY 15-16, 1952

The sharp negative bays from 2:00 a.m. on were accompanied by complete disappearance of all echoes wherever $H$ was decreasing rapidly. $Es$ reappeared when $H$ was increasing. The radio wave absorption was higher than normal most of the night. The absorption was at a minimum near 5 a.m., when the magnetic trace returned temporarily to near normal. Both $E$ and $F$ region echoes were then present at frequencies above normal.

The aurora was very pronounced all night and extended past the zenith at the start of the disturbance. The intensity increased during initial part of the positive bay. At other times, enhanced aurora was accompanied by sharp decreases in the $H$ component of the magnetic field. Maximum auroral intensities and the greatest magnetic and ionospheric changes corresponded.

## SUMMARY AND CONCLUSIONS

The maximum deviation of $H$ during a 24-hour period gives a simple criterion of general geophysical disturbance. The length of time during which the magnetic field is disturbed is quite variable, except for the isolated well-defined magnetic bays. We can say roughly that the larger the amplitude of the disturbance, the greater its duration.

The use of auroral and ionospheric observations as a criterion is not feasible because of the variety of possible measurements, each with different characteristics.

While the above criterion was found to be satisfactory for statistical work on a daily basis, when looking at the details of magnetic variations as related to auroral and ionospheric variations, it was found necessary to examine the data for each night individually and from minute to minute.

The occurrence of a large magnetic bay is related to simultaneous changes of auroral light and absorbing and reflecting properties of the ionospheric layers.

The maximum elevation of aurora above the northern horizon at Saskatoon is related closely to the amount of magnetic variation, although accurate quantitative measurements have not yet been made. If the elevation of the aurora above the northern horizon is less than 20°, the corresponding deviation in $H$ is less than 50 gammas. Aurora overhead corresponds to a deviation in $H$ of about 200 gammas. These results are comparable to those found by Rostad [2] at Potsdam.

An increase in intensity of the aurora is observed at the time of the rapid change in $H$ at the onset of a magnetic bay. The increase in intensity appears to be related to the rate of change of magnetic field (slope of the $H$ trace) rather than to the amount of change. The peak of auroral intensity is past by the time $H$ reaches its minimum value.

The critical frequencies of the $F$ region of the ionosphere decrease regularly throughout the night on undisturbed nights. However, when there is a disturbance, the $fF2$ when visible is higher than normal. This has been noted previously by Harang [3]. It is a reversal of the daytime disturbance effect where $fF2$ is well below normal [4]. It is generally assumed that the geophysical disturbance is caused by a stream of particles entering the ionosphere and increasing the amount of ionization. The decrease in daytime $fF2$ is assumed to be due to the heating effect of the impinging particles, which causes the layer to expand vertically,

thus lowering the maximum electron density. This is possible, since the daytime ionization is mostly due to the direct solar radiation. At night it appears that the main effect of the particles is to maintain the $F$ region ionization.

During the daytime there is very little disturbance observed in the $E$ region; however, at night it appears that the $E$ region is affected as much as, if not more than, the $F$ region. $Es$ is sometimes present on undisturbed nights, but it becomes quite prominent when there is even a slight disturbance, obscuring the $F$ region for the greater part of the night.

Several types of $Es$ are associated with geomagnetic disturbances. The observations of Lindquist [5], on the whole, are confirmed. His $N2$ type of $Es$ was observed only twice; while it occurred during disturbed periods, it did not correspond to specific changes in aurora or magnetic records. His $E1$ type (here called 90-km $Es$) was observed on a considerable number of occasions.

The type of $Es$ showing retardation and critical frequencies, and the type with high $fEs$ and high reflection coefficient, both appear more frequently on disturbed nights, but were not found to correlate with particular variations in aurora or magnetic field. This latter type of $Es$ is explained by Wells [6] as due to the same process which produces the intense absorbing region, but occurring at a slightly greater height where the collisional frequency is not so high and reflections of radio waves are possible. In this case, there is a considerable absorbing region still in existence below the reflecting level.

A regular sequence of events leads up to the commencement of a large magnetic bay. The $F$ region shows spread echoes and $h'F2$ begins to rise at about the time the $Es$ echoes become more prominent. Several hours before the main magnetic bay, $fEs$ begins to increase. If a positive bay precedes the main bay, spread echoes and a sharp increase in $fEs$ are observed, but little increase in absorption. After the positive bay, the occurrence of the spread echoes is less and multiple reflections are often seen. At the time of the main magnetic decrease, all ionospheric echoes disappear and, as noted above, the aurora is considerably enhanced. Sometimes weak $Es$ echoes are observed below 100 km during this period. The fact that a magnetic bay in high latitudes is accompanied by radio absorption was noted by Wells [6], while Harang [3] observed the increase in $fEs$ connected with a magnetic bay.

The material presented above supports the suggestion made by Wells [6] that the magnetic bay is due to horizontally moving electric currents at a level below 100 km (most estimates have been 125 to 150 km or higher), since auroral, magnetic, and ionospheric effects occur simultaneously, and at times when auroral and ionospheric measurements indicate heights below 100 km.

## ACKNOWLEDGMENTS

The author wishes to thank Prof. B. W. Currie, Head of the Physics Department, University of Saskatchewan, for making facilities available for this work, and also for the use of data from the auroral recorder. Considerable assistance in measuring and reducing the data was given by Mr. C. H. Costain.

## *References*


[1] J. H. Meek, J. Geophys. Res., **54**, 339 (1949).
[2] A. Röstad, Geofys. Pub., Oslo, **10**, No. 10 (1935).
[3] L. Harang, Terr. Mag., **41**, 143 (1936).
[4] J. H. Meek, J. Geophys. Res., **57**, 177 (1952).
[5] R. Lindquist, Arkiv Geofysik, **1**, No. 11 (1951).
[6] H. W. Wells, Terr. Mag., **52**, 315 (1947).

Journal of Geophysical Research Volume 58, No. 4 December, 1953

# ATOMIC AND MOLECULAR TRANSITIONS IN AURORAL SPECTRA

By Joseph W. Chamberlain and Norman J. Oliver

*Geophysics Research Directorate, Air Force Cambridge Research Center, 230 Albany Street, Cambridge 39, Mass.*

(Received March 21, 1953)

ABSTRACT

The identifications of lines and bands in auroral spectra, as reported by several observers over the past few years, are subjected to a critical analysis in order to determine which atomic transition arrays and molecular progressions are most important. The various transitions are analyzed from the standpoint of expected relative intensities of lines or bands originating from common upper levels, and the probable validity of the identifications is discussed.

Tables are presented listing the emissions that seem to be well established in at least some auroral displays. Variations in auroral spectra with latitude, type of display, etc., undoubtedly account for many of the discrepancies among the wavelength lists of different authors. Hence it is not always possible to differentiate between real and fortuitous identifications. A large number of fainter lines and bands still remain unidentified.

## I. INTRODUCTION

During the past several years, considerable research has been directed towards obtaining and analyzing auroral spectra. The complexity of the spectra obtained with modern high-speed equipment is such that it is very difficult to make proper identifications of many of the moderately strong and the weaker features. Even a casual comparison of the measured wavelengths shows a wide variance from one observer to the next. Instrumental effects arise from differences in dispersion, effective resolving power (including plate graininess), and wavelength sensitivity, which may cause errors in measuring the wavelengths or may blend or totally obscure various lines. There undoubtedly are also real differences in spectra made at different times of the night, year, or solar cycle. Spectra from different types of auroral forms or from different heights in the atmosphere must vary considerably. Some interesting spectral differences exist between high- and low-latitude aurorae. The correlation of spectral differences with these and other factors is extremely complicated because of the interdependence of some of the factors on one another.

Some of these problems are in only the initial stages of study and others have

Table 1—*Permitted atomic lines in aurorae*

| Mult. No. | Multiplet (Exc. Pot.) | *J* | λ | Ref. |
|---|---|---|---|---|
| | | *H* | | |
| 1 | $2^2P^0$–$3^2D$ *et al.* (12.04) | — | 6562.817 (Hα) | 3,4,6,8 |
| 1 | $2^2P^0$–$4^2D$ *et al.* (12.69) | — | 4861.332 (Hβ) | 1,2,3,6 |
| 1 | $2^2P^0$–$5^2D$ *et al.* (13.00) | — | 4340.468 (Hγ) | 1,3,6 |
| | | *N I* | | |
| 1 | $3s^4P$–$3p^4D^0$ (11.71) | 2½–3½ | 8680.24 | 8,9,10 |
| | | 1½–1½ | 8683.38 | 7,8,9 |
| | | 2½–2½ | 8718.82 | 10 |
| | | 1½–1½ | 8711.69 | 7,9,10 |
| | | ½–½ | 8703.24 | 8,10 |
| 2 | $3s^4P$–$3p^4P^0$ (11.79) | 2½–2½ | 8216.28 | 8,9,10 |
| | | 2½–1½ | 8242.34 | 8,10 |
| | | 1½–½ | 8223.07 | 10 |
| | | ½–1½ | 8187.95 | 8,10 |
| 5 | $3s^4P$–$4p^4P^0$ (13.21) | 2½–2½ | 4223.04* | 6 |
| 6 | $3s^4P$–$4p^4S^0$ (13.26) | 2½–1½ | 4151.46 | 1,9 |
| 9 | $3s^2P$–$4p^2S^0$ (13.14) | 1½–½ | 4935.03 | 6,10 |
| | | ½–½ | 4914.90 | 6,10 |
| 10 | $3s^2P$–$3p'^2D^0$ (13.64) | 1½–2½ | 4109.98* | 1,6 |
| 11 | $3s^2P$–$3p'^2P^0$ (13.86) | ½–½ | 3822.07* | 6 |
| | | *N II* | | |
| 1 | $2p^3\ ^1D^0$–$3p^1P$ (20.32) | 2–1 | 4895.20* | 10 |
| 3 | $3s^3P^0$–$3p^3D$ (20.57) | 2–3 | 5679.56 | 6,10 |
| | | 1–2 | 5666.64 | 10 |
| | | 0–1 | 5676.02 | 5,6,10 |
| | | 2–2 | 5710.76 | 10 |
| | | 1–1 | 5686.21 | 10 |
| | | 2–1 | 5730.67 | 10 |
| 4 | $3s^3P^0$–$3p^3S$ (20.85) | 2–1 | 5045.098 | 6,10 |
| | | 1–1 | 5010.620 | 10 |
| | | 0–1 | 5002.692 | 5 |
| 5 | $3s^3P^0$–$3p^3P$ (21.07) | 2–2 | 4630.537 | 6,10 |
| | | 1–0 | 4621.392 | 6,10 |
| | | 1–2 | 4601.478 | 10 |
| | | 0–1 | 4607.153 | 10 |
| | | *N II Cont.* | | |
| 6 | $3s^3P^0$–$3p^1D$ (21.51) | 1–2 | 3955.851* | 6 |
| 8 | $3s^1P^0$–$3p^1P$ (20.32) | 1–1 | 6482.07 | 4,10 |
| 9 | $3s^1P^0$–$3p^3D$ (20.56) | 1–2 | 5747.29* | 6 |
| | | 1–1 | 5767.43* | 6 |
| 12 | $3s^1P^0$–$3p^1D$ (21.51) | 1–2 | 3994.996 | 6,10 |
| 14 | $3p^1P$–$3d^3F^0$ (23.02) | 1–2 | 4564.78* | 6 |
| 19 | $3p^3D$–$3d^3F^0$ (23.04) | 3–4 | 5005.140* | 10 |
| | | 2–3, 1–2 | 5001.3* | 10 |
| | | 3–3 | 5025.665* | 10 |
| | | 2–2 | 5016.387* | 10 |
| 20 | $3p^3D$–$3d^3D^0$ (23.14) | 3–2 | 4810.286* | 6 |
| | | 2–1, 2–2 | 4791.* | 6 |
| | | 2–3, 1–1 | 4780.5* | 6 |
| 21 | $3p^3D$–$3d^3P^0$ (23.31) | 2–2 | 4488.15* | 6 |
| | | 3–2 | 4507.559* | 6 |
| 24 | $3p^3S$–$3d^3P^0$ (23.32) | 1–0 | 4987.377* | 6 |
| 28 | $3p^3P$–$3d^3D^0$ (23.14) | 2–1 | 5960.93* | 6 |
| 29 | $3p^3P$–$3d^3P^0$ (23.32) | 1–0 | 5454.26* | 6 |
| | | *O I* | | |
| 1 | $3^5S^0$–$3^5P$ (10.69) | 2– | 7774. | 7,8,9,10 |
| 3 | $3^5S^0$–$4^5P$ (12.23) | 2– | 3947.5* | 9 |
| 4 | $3^3S^0$–$3^3P$ (10.94) | 1– | 8446.5 | 7,8,9,10 |
| 5 | $3^3S^0$–$4^3P$ (12.31) | 1– | 4368.30 | 1,6,9,10 |
| 6 | $3^3S^0$–$5^3P$ (12.82) | 1– | 3692.44 | 1,9 |
| 9 | $3^5P$–$5^5S^0$ (12.61) | –2 | 6455.* | 6,9 |

TABLE 1—*Permitted atomic lines in aurorae—Continued*

| Mult. No. | Multiplet (Exc. Pot.) | *J* | λ | Ref. |
|---|---|---|---|---|
| | | *O I Cont.* | | |
| 10 | $3^5P-4^5D^o$ (12.70) | – | 6157. | 6, 9, 10 |
| 11 | $3^5P-6^5S^o$ (12.96) | –2 | 5436.* | 10 |
| 12 | $3^5P-5^5D^o$ (13.01) | – | 5330.* | 10 |
| 14 | $3^5P-6^5D^o$ (13.18) | – | 4968.* | 10 |
| 19 | $3^3P-3s'^3D^o$ (12.49) | 2–3<br>–2 | 7995.12*<br>7987.* | 8<br>8, 9 |
| 20 | $3^3P-5^3S^o$ (12.64) | –1 | 7254.4* | 6, 9 |
| 22 | $3^3P-6^3S^o$ (12.98) | –1 | 6046.* | 6 |
| | | *O II* | | |
| 1 | $3s^4P-3p^4D^o$ (25.54) | 1½–2½<br>½–1½<br>2½–2½<br>1½–1½<br>½–½ | 4641.811<br>4638.854<br>4676.234<br>4661.635<br>4650.841 | 10<br>10<br>10<br>10<br>6 |
| 2 | $3s^4P-3p^4P^o$ (25.74) | 2½–2½<br>1½–1½<br>1½–1½<br>1½–2½<br>½–1½ | 4349.426<br>4336.865<br>4345.562<br>4319.631<br>4317.139 | 6, 10<br>6<br>6<br>6, 10<br>10 |
| 3 | $3s^4P-3p^4S^o$ (26.19) | 2½–1½<br>1½–1½<br>½–1½ | 3749.49<br>3727.33*<br>3712.75 | 10<br>6<br>10 |
| 5 | $3s^2P-3p^2D^o$ (26.14) | 1½–2½ }<br>½–1½ }<br>1½–1½ | 4416.<br>4452.377 | 1, 6, 10<br>6 |
| 6 | $3s^2P-3p^2P^o$ (26.45) | 1½–1½<br>½–½<br>1½–½ | 3973.263<br>3954.372*<br>3982.719 | 1, 6<br>6<br>6 |

| Mult. No. | Multiplet (Exc. Pot.) | *J* | λ | Ref. |
|---|---|---|---|---|
| | | *O II Cont.* | | |
| 10 | $3p^4D^o-3d^4F$ (28.58) | 3½–4½<br>2½–3½<br>3½–3½ | 4075.868*<br>4072.164*<br>4092.940* | 6<br>10<br>6 |
| 11 | $3p^4D^o-3d^4P$ (28.71) | 1½–½<br>1½–1½ | 3872.45*<br>3882.45* | 6<br>6 |
| 12 | $3p^4D^o-3d^4D$ (28.73) | 3½–2½ | 3883.15* | 6 |
| 13 | $3p^4D^o-3d^2F$ (28.74) | 2½–2½<br>3½–2½ | 3857.18*<br>3875.82* | 6<br>6 |
| 15 | $3s'^2D-3p'^2F^o$ (28.24) | 2½–3½<br>1½–2½ | 4590.971*<br>4596.174* | 10<br>6, 10 |
| 16 | $3s'^2D-3p'^2D^o$ (28.39) | 1½–1½ | 4347.425* | 6 |
| 19 | $3p^4P^o-3d^4P$ (28.70) | 2½–2½<br>½–½ | 4169.230*<br>4121.48* | 6<br>6 |
| 20 | $3p^4P^o-3d^4D$ (28.73) | 2½– | 4120.* | 1, 6 |
| 21 | $3p^4P^o-3d^2F$ (28.74) | 2½–2½ | 4112.029* | 6 |
| 26 | $3p^2D^o-3d^2D$ (28.94) | 1½–1½ | 4369.28* | 6 |
| 28 | $3p^4S^o-3d^4P$ (28.71) | 1½–2½<br>1½–½ | 4924.60*<br>4890.93* | 6<br>6 |
| 29 | $3p^4S^o-3d^4D$ (28.73) | 1½–2½ | 4856.49* | 6 |
| 33 | $3p^2P^o-3d^2D$ (28.94) | ½–1½ | 4941.12* | 6 |
| | | *Na I* | | |
| 1 | $3^2S-3^2P^o$ (2.10) | ½–1½<br>½–½ | 5889.953* }<br>5895.923* } | 6, 10 |

not yet begun to be understood. Currently, many improvements are being made in the equipment used by several observers and the resultant higher dispersion and resolving power should lead to greatly improved wavelength measures in the not-too-distant future. Hence, it will be well for us at this time to critically examine the identifications made in recent years. An analysis of the data so far available should not only be of use to the important problem of auroral excitation

mechanisms, but should also provide a basis for the analysis of spectra yet to be obtained.

## II. THE TABLES OF IDENTIFICATION

In Tables 1, 2, and 3 we have listed those identifications that we consider well established in auroral spectra. In addition, a number of lines and bands have been included that may quite possibly be present, but which have not yet been definitely verified. The latter are indicated by an asterisk (*) in the wavelength column. In Table 3, an "*M*" after a wavelength indicates that multiple heads have been reported for this band in the aurora.

These Tables are based on the observational data of several observers [see 1 through 10 and 18 of "References" at end of paper]. Their observations represent several geomagnetic latitudes, auroral forms, etc., and give a fairly complete summary of the emissions that have been detected in aurorae. Although many

TABLE 2—*Forbidden atomic lines in aurorae*

| Transition (Mult. No.) | Multiplet (Exc. Pot.) | *J* | λ | Ref. |
|---|---|---|---|---|
| | *N I* | | | |
| Nebular (1F) | $2p^3\ ^4S^0$–$2p^3\ ^2D^0$ (2.37) | $1\frac{1}{2}$–$2\frac{1}{2}$ | 5200.7 | 9,10 |
| | | $1\frac{1}{2}$–$1\frac{1}{2}$ | 5198.5 | 5,9,10 |
| Trans-auroral (2F) | $2p^3\ ^4S^0$–$2p^3\ ^2P^0$ (3.56) | $1\frac{1}{2}$– | 3466.4 | 1,6,9,10 |
| | *N II* | | | |
| Auroral (3F) | $2p^2\ ^1D$–$2p^2\ ^1S$ (4.04) | 2–0 | 5754.8 | 6,18 |
| | *O I* | | | |
| Nebular (1F) | $2p^4\ ^3P$–$2p^4\ ^1D$ (1.96) | 2–2 | 6300.23 | 6,8,9,10 |
| | | 1–2 | 6363.88 | 6,8,9,10 |
| Auroral (3F) | $2p^4\ ^1D$–$2p^4\ ^1S$ (4.17) | 2–0 | 5577.350 | 6,9,10 |
| | *O II* | | | |
| Nebular (1F) | $2p^3\ ^4S^0$–$2p^3\ ^2D^0$ (3.31) | $1\frac{1}{2}$–$2\frac{1}{2}$, $1\frac{1}{2}$–$1\frac{1}{2}$ | 3727.5* | 1,6,10 |

TABLE 3—*Molecular bands in aurorae*

| $v' - v''$ | λ | Ref. |
|---|---|---|
| $N_2$ *First Positive* ($B^3\Pi \rightarrow A^3\Sigma$) | | |
| 1–0 | 8911.6 | 8,9,10 |
| 2–0 | 7753.2 *M* | 6,8,9,10 |
| 2–1 | 8722.3 | 8,9,10 |
| 3–0 | 6875.0 | 6,8,9,10 |
| 3–1 | 7626.2 *M* | 6,8,9,10 |
| 3–2 | 8541.8 | 8,9,10 |
| 4–0 | 6185.2* | 9,10 |
| 4–1 | 6788.6 *M* | 4,6,8,9,10 |
| 4–2 | 7503.9 *M* | 6,8,9,10 |
| 5–1 | 6127.4 | 6,9,10 |
| 5–2 | 6704.8 *M* | 4,6,8,9,10 |
| 5–3 | 7386.6 *M* | 6,8,9,10 |
| 5–4 | 8204.8* | 6 |
| 6–2 | 6069.7 | 6,9,10 |
| 6–3 | 6623.6 *M* | 4,6,8,9,10 |
| 6–4 | 7273.3 | 6,8,9,10 |
| 6–5 | 8047.4* | 6 |
| 7–3 | 6013.6 | 6,9,10 |
| 7–4 | 6544.8 *M* | 4,6,8,9,10 |
| 7–5 | 7164.8 | 8,9,10 |
| 7–6 | 7896.4* | 6 |
| 8–4 | 5959.0 | 6,9,10 |
| 8–5 | 6468.5 | 6,8,9,10 |
| 8–6 | 7059.0* | 6,10 |
| 8–7 | 7734.* | 6 |
| 9–4 | 5478.5* | 6 |
| 9–5 | 5906.0* | 10 |
| 9–6 | 6394.7 | 6,8,9,10 |
| 9–7 | 6967.8 | 8,10 |
| 9–8 | 7594.* | 6 |
| 10–6 | 5854.4 | 6,10 |
| 10–7 | 6322.9* | 10 |
| 10–8 | 6861.* | 6 |
| 10–9 | 7479.* | 6 |
| 11–7 | 5804.3* | 10 |
| 11–8 | 6252.8* | 10 |
| 11–9 | 6760.* | 6 |
| 11–10 | 7368.* | 6 |
| 12–8 | 5755.2* | 10 |
| 12–9 | 6185.2* | 6,10 |
| $N_2$ *Second Positive* ($C^3\Pi \rightarrow B^3\Pi$) | | |
| 0–0 | 3371.3 | 1,6,9,10 |
| 0–1 | 3576.9 | 1,6,9,10 |
| 0–2 | 3804.9 | 1,6,9,10 |
| $N_2$ *Second Positive* ($C^3\Pi \rightarrow B^3\Pi$) *Cont.* | | |
| 0–3 | 4059.4 | 1,6,9,10 |
| 0–4 | 4343.6* | 1,6 |
| 1–0 | 3159.3 | 1,6,9,10 |
| 1–1 | 3339. | 1,6,9,10 |
| 1–2 | 3536.7 | 1,6,9,10 |
| 1–3 | 3755.4 | 1,6,9,10 |
| 1–4 | 3998.4 | 1,6,9,10 |
| 1–6 | 4574.3 | 1,10 |
| 2–1 | 3136.0 | 1,6,9,10 |
| 2–2 | 3309. | 1,9,10 |
| 2–3 | 3500.5* | 6 |
| 2–4 | 3710.5 | 1,6,9,10 |
| 2–5 | 3943.0 | 1,6,9,10 |
| 3–2 | 3116.7 | 6,10 |
| 3–3 | 3285.3 | 1,6,10 |
| 3–4 | 3469.* | 6 |
| 3–5 | 3671.9 | 6,9,10 |
| 3–7 | 4141.8 | 1,6,10 |
| 4–4 | 3268.1* | 1 |
| 4–8 | 4094.8* | 1,6,10 |
| $N_2$ *Vegard-Kaplan* ($A^3\Sigma \rightarrow X^1\Sigma$) | | |
| 0–10 | 3603.0 | 1,6,9,10 |
| 0–12 | 4218.* | 6 |
| 1–9 | 3197.5 | 1,6,9,10 |
| 1–10 | 3424.6 | 1,6,9,10 |
| 1–11 | 3684. | 1,6,9,10 |
| 1–12 | 3979.1 | 1,9,10 |
| 1–13 | 4319.8* | 1,6,9 |
| 1–16 | 5751.* | 6 |
| 2–10 | 3269.* | 1,9 |
| 2–11 | 3502.7* | 1,9,10 |
| 2–12 | 3768. | 1,6,9,10 |
| 2–13 | 4072.5 | 1,6,9,10 |
| 2–14 | 4225. | 1,6,9 |
| 2–15 | 4837.1* | 10 |
| 3–13 | 3854.7 | 1,9 |
| 3–14 | 4171.2 | 1,6,9,10 |
| 3–15 | 4535.5 | 1,6,9,10 |
| 3–18 | 6068.* | 6 |
| 4–11 | 3192.* | 6 |
| 4–14 | 3948.* | 1,9 |
| 5–15 | 4044.* | 1,9 |
| 5–17 | 4771.* | 6,10 |

TABLE 3—*Molecular bands in aurorae*—*Concluded*

| $v' - v''$ | $\lambda$ | Ref. | $v' - v''$ | $\lambda$ | Ref. |
|---|---|---|---|---|---|
| $N_2^+$ *First Negative* ($B^2\Sigma \rightarrow X^2\Sigma$) | | | $N_2^+$ *Meinel* ($A^2\Pi \rightarrow X^2\Sigma$) | | |
| 0–0 | 3914.4 | 1,6,9,10 | 2–0 | 7828. *M* | 8,9,10 |
| 0–1 | 4278.1 | 1,6,9,10 | 3–0 | 6858. *M* | 4,8,9,10 |
| 0–2 | 4709.2 | 1,6,9,10 | 3–1 | 8057. *M* | 8,9,10 |
| 0–3 | 5228.3 | 5,10 | 4–1 | 7050. *M* | 8,9,10 |
| 1–0 | 3582.1 | 6,9,10 | 4–2 | 8298. *M* | 8,9,10 |
| 1–1 | 3884.3 | 1,6,9,10 | 5–2 | 7250. *M* | 8,9,10 |
| 1–2 | 4236.5 | 1,6,9,10 | | | |
| 1–3 | 4651.8 | 1,6,9,10 | | | |
| 1–4 | 5148.8 | 5,10 | $O_2$ *Atmospheric* ($A^1\Sigma_g^+ \rightarrow X^3\Sigma_g^-$) | | |
| 2–1 | 3563.9 | 6,9,10 | | | |
| 2–2 | 3857.9 | 1,9,10 | 0–1 | 8629. / 8665. | 8 |
| 2–3 | 4199.1 | 1,6,9,10 | | | |
| 2–4 | 4599.7 | 1,6,9,10 | | | |
| 2–5 | 5076.6 | 5,10 | | | |
| 3–2 | 3548.9 | 10 | | | |
| 3–3 | 3835.4* | 1,9 | $O_2^+$ *First Negative* ($b^4\Sigma_g^- \rightarrow a^4\Pi_u$) | | |
| 3–4 | 4166.8 | 1,9 | | | |
| 3–5 | 4554.1 | 1,6,9,10 | | | |
| 4–6 | 4515.9* | 1,10 | 0–0 | 6026.4 | 2,10 |
| 4–7 | 4957.9 | 10 | 0–1 | 6418.* | 2 |
| 5–6 | 4121.* | 1 | 1–0 | 5631.9 *M* | 2,5,10 |
| 5–7 | 4490.* | 1,6,10 | 1–1 | 5973.* | 2 |
| 6–7 | 4112.* | 1 | 2–0 | 5295.7 *M* | 2,5,10 |
| 6–8 | 4467.* | 1,10 | | | |

real differences certainly exist in the spectra reported by the various observers, we believe that there are also many improper identifications. Thus, the accompanying Tables list only those wavelengths that are consistent with our analysis discussed in the following sections of this paper.

A few words are in order regarding our choice of the observational data. Several papers have been included that considered in detail a few particular features of the spectrum [2,3,4,5,18]. Two papers by Meinel [7,8] dealt with the infrared regions exclusively. The remaining papers referred to in these Tables reported observations over a wide range of wavelengths. In a well-known paper, Barbier and Williams [1] discussed their observations near Fairbanks, Alaska, from 3100 to 5000 A. Their few identifications in the red have not been incorporated here. Petrie and Small [10] recently published their results obtained at Saskatoon from about 150 spectrograms and listed "only those features whose origin seems quite definite." From the numerous papers by Vegard and his coworkers, we have selected a wavelength list originally published in 1945 and which has been reprinted in Harang's book [6]. The Norwegian workers have published several tables since that time, which did not seem to be quite as complete as the earlier list [for example, 11, 12], or which contained so many spectral features [13] that

a comparison with the shorter lists of other observers would not have been profitable. Vegard and Kvifte have provided an interesting discussion of their identifications in the latter paper and we have considered some of their conclusions in this work. Finally, wavelengths listed in a review paper by Meinel [9] have been inserted.

The multiplet numbers used here are those of Miss Moore [14], and the excitation potentials for the upper levels are taken directly from her tables. She has obtained these potentials with the now outdated conversion-factor of $1.2345 \times 10^{-4}$ ev/cm$^{-1}$, and they should not be used for any excitation analysis requiring accurate potentials unless they are corrected. In the column labeled "$\lambda$" we have included whenever possible the laboratory wavelengths reported by Miss Moore for atomic lines and by Pearse and Gaydon [15] for the molecular bands. It should be pointed out that the auroral measures are usually made on the strongest part of the bands, rather than on the band heads, and small discrepancies should be expected between auroral and laboratory wavelengths.

Usually the observers have not specifically designated both the multiplets and the laboratory wavelengths that correspond to their measured atomic lines. Hence we have had to insert some information about these identifications that was only inferred from their papers. In the vast majority of cases, there was absolutely no doubt as to the observers' intent. In those cases where only the ion and a wavelength were listed, we have assigned the line to a low-level multiplet when there was some ambiguity. Whenever it seemed likely that two or more lines in the multiplet were blended, we included all of these lines.

## III. PERMITTED LINES OF NITROGEN AND OXYGEN

An accurate analysis of the permitted atomic lines to be expected in a given multiplet or supermultiplet is difficult, insofar as we have no accurate transition probabilities. Since the nitrogen and oxygen energy levels may deviate considerably from *LS* coupling, especially at the higher excitation potentials, the application of relative intensities obtained from the simple theory is severely limited. Laboratory estimates of relative intensities are of some help, but it must be emphasized that at best these estimates give only a rough indication of relative transition probabilities for lines in the same region of the spectrum and arising from common upper terms. The observed intensities, either in the aurora or laboratory sources, depend also on the population of the upper levels involved in the transitions and hence on the process of excitation. One of the ultimate objectives of auroral physics is to determine precisely the auroral excitation processes, but at this time we can do little more than make a few enlightened guesses.

An excitation analysis is further complicated by the fact that accurate line intensities have not been obtained from spectrophotometrically calibrated plates, although some observers list their "eye-estimates" of intensities.* Petrie and Small

**Note added in proof:* Petrie and Small [Can. J. Phys., **31**, 911, 1953] have recently published a list of relative multiplet intensities. It should be point out, however, that since the observed relative intensities might be approximately the same for several widely different excitation mechanisms (for example, inelastic collisions or ionization followed by recombinations), their conclusions regarding the excitation of atomic oxygen and nitrogen are open to some question.

[21], however, have attempted accurate intensity measures of the brighter ultraviolet bands. In any event, spectrophotometry is difficult, since the complexity of a well-exposed spectrum gives many overlapping features. Generally, it is not known just where to draw the continuum on the microphotometer tracings. Moreover, the ordinary difficulties inherent in accurate photometry are greatly magnified when we work with faint sources of light and the resulting long exposures. The use of higher resolution and dispersion and the extended application of photoelectric techniques may eventually simplify this difficult problem.

Some of Vegard's identifications of nitrogen and oxygen lines were criticized by Nicolet [16] in 1938 on the basis of relative intensities within multiplets or supermultiplets. A few of these identifications have been retained here because of later observations which have recorded the lines Nicolet suggested should be present. Most of his criticisms are still valid, however, although many of the identifications he questioned were again reported by the Norwegian workers in their later papers.

### (*a*) *N I*

Nearly all of the observed N I lines belong to the two transition arrays $2s^2\ 2p^2\ (^3P)\ 3s—2s^2\ 2p^2\ (^3P)\ 3p$ and $2s^2\ 2p^2\ (^3P)\ 3s—2s^2\ 2p^2\ (^3P)\ 4p$. This is to be expected, since most of the lines in the photographic region arising from other configurations have very high excitation potentials. These arrays are composed of multiplets 1 through 9, which we discuss now in some detail.

There is a line at 8686 A in multiplet 1 ($J = \frac{1}{2}$-$1\frac{1}{2}$), which should be present, and it is probably blended with the $J = 1\frac{1}{2}$-$2\frac{1}{2}$ line at 8683. Similarly, with multiplet 2, the line at 8185 may be blended with 8188. The three lines composing No. 3 are in the 7400 A region and have not been reported. One of these lines may be obscured by First Positive 4-2. Multiplet 7 is inaccessible and none of the lines from No. 8 have been found. However, the strongest line in the laboratory from No. 8 overlaps an $O_2$ atmospheric band and the entire multiplet is in the 8600 A region. Observers might well concentrate on searching for 8594.

Lines from the 4p configuration are somewhat less satisfactorily accounted for. Multiplets 4 and 5 should give lines at 4251, 4214, and 4230. Vegard and Kvifte's line at 4223 is probably a blend of two lines from No. 5. The strongest line of No. 6 seems to be present, and 4137 may be obscured by a Second Positive band. No. 9 apparently has been identified satisfactorily.

A few scattered lines from other configurations have been listed, but are by no means definite. There do not seem to be many laboratory lines arising from the $2s^2\ 2p^2\ (^1D)$ or $2s^2\ 2p^2\ (^1S)$ parent terms. Multiplets 10 and 11 have the $^1D$ parentage, and it would be well to search for other lines in these multiplets; it is quite possible that the auroral spectrum may have enhanced N I lines from the $^1D$ and $^1S$ parents.

### (*b*) *N II*

Most of the observed N II multiplets belong to the 3s-3p transition array (Nos. 2 through 13). Multiplets 2, 7, 10, 11, and 13 have not been detected at

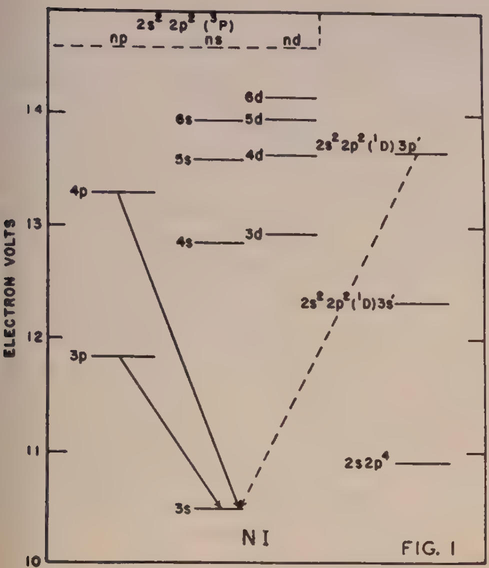


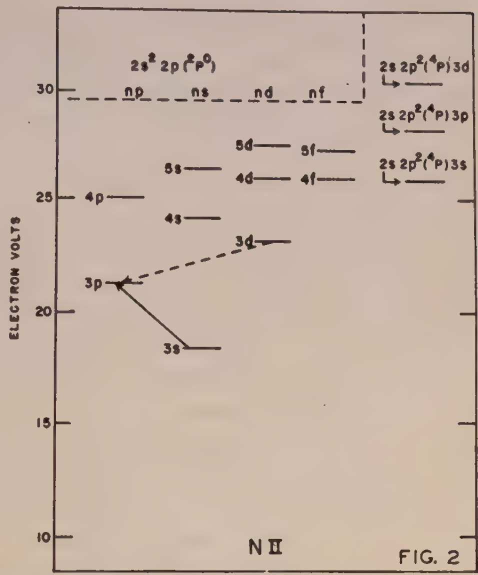


FIGS. 1 AND 2—CONFIGURATIONS AND AURORAL TRANSITION ARRAYS; THE TRANSITION INDICATED BY A BROKEN LINE IS NOT YET DEFINITELY ESTABLISHED

all. Some of these lines are probably obscured and No. 11 is weak in the laboratory, but lines 6380 and 3408 should be present. The multiplets that have been claimed are entirely satisfactory, except in the case of No. 5, where 4614 and 4643 should be listed. A line at 4642 was found by Petrie and Small, but was attributed solely to OII.

The 3p-3d transition is represented by several observed multiplets and several more may be accounted for by considering blended or obscured lines. It is interesting to note that the Saskatoon and Norway plates do not show the same multiplets for this transition array. There are many lines here that should be checked by other observers, but it seems quite probable that the low-level N II lines exist in at least some auroral spectra.

### (c) *N III*

Of the eight N III lines listed by Vegard and Kvifte [6], five may be successfully identified with various $N_2$ or $N_2^+$ bands or, in the case of 4633, with an N II line. Moreover, lines at 4103 and 4641 (multiplets 1 and 2) would almost certainly have been present and unobscured if N III were indeed recorded on the spectrograms. (Another strong line in multiplet 1 at 4097 might not be resolvable from the nearby Second Positive band.) Thus, the existence of N III cannot be accepted on the basis of the present data.

### (d) *O I*

In general, the lines composing an O I multiplet are so close together that they are blended into a single line in auroral spectra. Multiplets 1 through 6, which arise from transitions of the type 3s-np, are not completely consistent with laboratory intensities. Multiplet 2 at 6726 (3 $^5S^0$-3 $^3P$) has not been recorded, but

possibly it should not be very strong; its expected intensity is difficult to predict from the laboratory data, since there are no other low-level O I lines in its immediate neighborhood. Under *LS* coupling, 6726 would be forbidden. Multiplet 3, however, should probably be present, in view of the fact that No. 5 has been recorded by several observers. Meinel lists No. 3, but Petrie and Small [10] and Barbier and Williams [1] explicitly state that it is absent from their spectra. Multiplets 3 and 5 were obtained from different sources by Miss Moore [14], so their relative laboratory intensities are uncertain. Multiplet 6 (3s-5p) is also absent at Saskatoon and higher transitions are apparently not usually detected.

Emission from the *ns* configurations is also occasionally observed. The 3p-4s transition is in the inaccessible infrared, and the 3p-5s quintet multiplet (No. 9) may be partially blended with First Positive 8-5, although it has been listed by two observers. The corresponding triplet (No. 20) apparently exists. The quintet 3 $^5P$-6 $^5S^0$ (No. 11) was observed by Petrie and Small, and the triplet 3 $^3P$-6 $^3S^0$ (No. 22) was found by Vegard and Kvifte. (In 1951, Vegard, Tønsberg, and Kvifte [12] reported an observed wavelength for this line that agrees much better with the laboratory value than does the wavelength given in reference 6.) The 3p-7s lines at 5019 and 5555 probably have not been observed.

Although three quintets of the type 3p-nd have been reported (Nos. 10, 12, and 14), the corresponding triplets, which would normally be expected, have not yet been detected. However, 3 $^3P$-4 $^3D^0$ falls at 7002, which is in a spectral region that has not been very thoroughly observed, owing in part to low plate sensitivity and dispersion. The triplet 3 $^3P$-5 $^3D^0$ would be blended with First Positive 8-4 at 5959.

For the above transitions, all the atomic electrons, except the "jumping" electron, form the parent term $2s^2\,2p^3\,(^4S^0)$. If, however, the parentage is $2s^2\,2p^3\,(^2D^0)$ or $(^2P^0)$, we obtain configurations that are denoted by *nl′* and *nl″*, respectively. The corresponding transition arrays are observed to some extent in the laboratory and would be expected in aurorae. For example, if O I lines are formed by recombination of an electron with O II and subsequent cascading, then metastable O II would lead to *nl′* and *nl″* transition arrays. As we will point out in our discussion of forbidden lines, the presence of metastable O II has not been satisfactorily verified, but this does not necessarily mean that these O I transitions will not be present.

The 3p-3s′ (multiplet 19) transition is claimed by Meinel, but was not on the Saskatoon plates. The strongest line of 3p-3s″ (No. 30) at 3955 was reported by Vegard and Kvifte, but has not been repeated in some of their later papers [11,12]. Moreover, both O II and N II have probable lines at the same wavelength. We might expect lines at 8221 and 8230 (3s′-3p′); whereas the former has been found and interpreted as N I, no line has been reported at 8230. Another 3s′-3p′ multiplet should appear around 7950. All these multiplets have high excitation potentials and undoubtedly are weak, if indeed they are present at all. Some definite information on the existence of oxygen configurations with the $^2D^0$ and $^2P^0$ parentage would have important implications in the problem of excitation mechanisms.

(*e*) *O II*

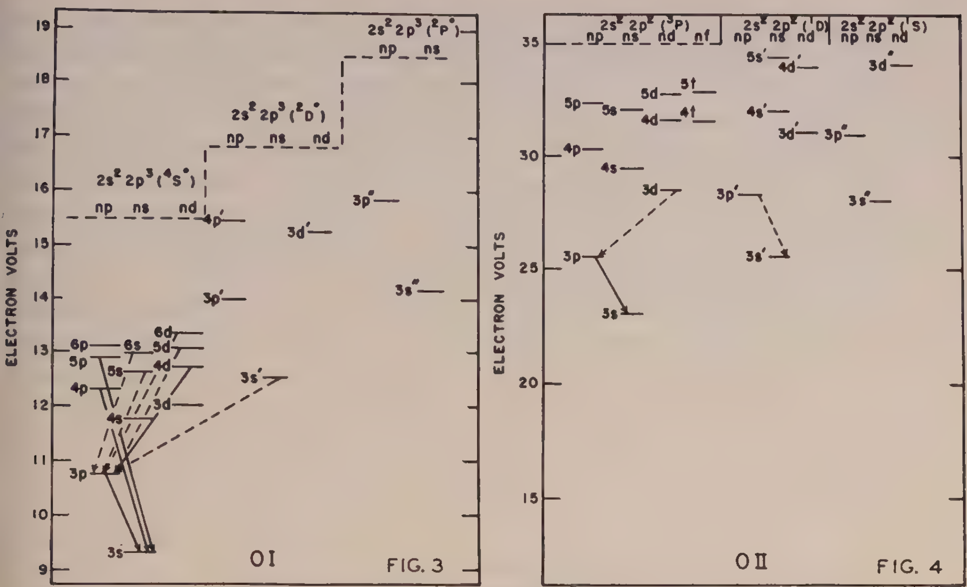


FIGS. 3 AND 4—CONFIGURATIONS AND AURORAL TRANSITION ARRAYS; THE TRANSITIONS INDICATED BY BROKEN LINES ARE NOT YET DEFINITELY ESTABLISHED

The lines arising from 3s-3p transitions have been fairly adequately identified. Observers disagree occasionally as to the particular lines that are in the spectra, but the totality of recorded lines shows few serious omissions that cannot be interpreted as obscured by other emissions or that probably have low transition probabilities.

Several 3p-3d lines have been listed, but unobscured lines at 3390 and 4105 are strong in laboratory spectra and should be looked for in aurorae. There are several other lines, for example 3134, 3377, 3846, and 3882, that are probably obscured by bands. The transition 3s′-3p′ (having $^1$D parentage) may well be present; one of the strongest lines in this transition would be covered by First Negative 0-0.

Several other transitions having high excitation potentials are suggested by Vegard and Kvifte, but it seems likely that many of their wavelength coincidences for O II are fortuitous. Since so few lines are reported from each of the higher transition arrays, it is difficult to know just which identifications should be accepted or discarded.

### (*f*) O *III*

Six out of the seven O III identifications made by Vegard and Kvifte [6], are blended with $N_2$ bands. Hence, there seems to be no justification for assuming that O III permitted lines are in auroral spectra. Moreover, these identifications have not been made by the Norwegian workers in their more recent papers.

## IV. FORBIDDEN ATOMIC LINES

The oxygen and nitrogen forbidden lines are of special significance to an understanding of ionospheric processes. Because they arise from low-energy metastable

levels, they are normally excited by processes quite different from those producing permitted lines. For N I, N II, O I, O II, and O III, the ground configurations each contain three terms. Transitions from the upper to the middle term, the so-called "auroral transitions," have the highest transition probabilities and hence are normally the strongest in aurorae. The "trans-auroral transitions" between the highest and lowest terms also have high $A$-values, but usually fall in the inaccessible ultraviolet. The "nebular transitions" connect the middle and ground terms, and have very low transition probabilities. But under conditions of extremely low density, de-exciting collisions are so rare that nearly every ion excited eventually radiates regardless of its Einstein $A$-value. In this case, because of its higher excitation potential, the auroral transition will no longer predominate, and even in the case of fairly high densities, selective excitation processes could conceivably enhance the nebular transition. (With *very* high densities, detailed balancing obtains between all levels, as in thermodynamic equilibrium, and no radiation is allowed to escape.)

Several observers have reported the [N I] nebular and trans-auroral transitions, but the auroral transition falls at 10,400 A. The presence of 3466 (trans-auroral) has been discussed in detail by Bernard [17] and there seems to be no doubt about its identity. The auroral and nebular [N II] transitions have been listed by Vegard and Kvifte, but their wavelength coincidences were rather poor. However, Petrie [18] has recently reported that 5755 (auroral) has definitely been identified on spectra made at Saskatoon. This discovery is most interesting, and it would be well to know if [N II] can be verified on spectra made at other latitudes.

The presence of [O I] is universally accepted, but [O II] poses an intriguing problem. The auroral transition has not been found at 7319 and 7330, in spite of the fact that many observers have explicitly sought it. Therefore, grave doubts must be raised as to the interpretation of 3727 as the [O II] doublet. If the infrared lines continue to evade detection and if high-resolution, high-dispersion spectra verify the wavelength coincidences and expected intensity ratio of 3726 and 3729, then a selective excitation process will have to be invoked, unless it can be shown that the transition takes place at extremely high altitudes. We must seriously question Vegard and Kvifte's identifications of the [O III] lines at 4363, 4959, and 5007, inasmuch as they have not been verified elsewhere.

## V. NITROGEN BANDS

The bands that may be expected in any $v''$ progression have been estimated from vibrational transition probabilities as calculated by R. W. Nicholls and his associates [19]. These transition probabilities or "$p$ values" are only approximate, in that the electronic transition moment, $R_e$, is assumed to be independent of the internuclear distance and the potential is characterized by a Morse function. The order of magnitude of the $p$ values, it is generally believed, is not affected by these approximations. However, should future improvements in the theory and computational procedure produce significant changes in the $p$ values, some of the following remarks would have to be modified.

### (a) $N_2$ *First Positive* ($B\,^3\Pi \rightarrow A\,^3\Sigma$)

These bands are degraded to the violet and occasionally several heads are observed in the stronger bands. Nearly all the bands in this system with $v' \leq 8$ that would be expected from the transition probabilities have been found. In addition, an occasional band, such as 4-0, that would not be expected, has been reported. It seems surprising that more observers have not found 7-6, 9-5, and 9-8, in view of the weaker bands that are listed. The identification of 8-6 is *very* doubtful. The 9-9, 10-10, and 11-11 bands should be detectable in the infrared, and 11-6 and 12-7 should appear near 5400, although some of these bands may be partially obscured. The available $p$ values do not go above $v' = 12$, and the observers (with the exception of Vegard and Kvifte) have not listed higher transitions. Thus, from the observations, it appears that the $B\ ^3\Pi$ state is excited up to quite high vibrational levels, and the few existing discrepancies will no doubt be clarified in the near future.

### (b) $N_2$ *Second Positive* ($C\ ^3\Pi \rightarrow B\ ^3\Pi$)

The Second Positive bands are also degraded to shorter wavelengths, and although laboratory spectra show close triple heads, auroral plates contain single-headed bands. The transitions 1-5, 2-6, 2-7, 3-6, and 4-7 would be anticipated from the $p$ values, but are probably blended with First Negative bands. Similarly, the 2-3 and 4-4 bands are blended with the Vegard-Kaplan system. The 0-4 band should be weak and may be confused with a broadened $H\gamma$, and 3-8 should probably be a weak band blended with 4417 of O II.

Thus, the progressions with $v' = 0$, 1, 2, and 3 are definitely established, but $v' = 4$ should be further investigated. Only two of the latter bands have been reported, but two of the stronger bands would be obscured by other emissions. Whereas 4-5 and 4-10 would not be expected, 4-6 and 4-9 should be faint but detectable at 3642 and 4355, respectively. Excitation to levels higher than the fourth is very doubtful and has probably not been observed.

### (c) $N_2$ *Vegard-Kaplan* ($A\ ^3\Sigma \rightarrow X\ ^1\Sigma$)

Although the presence of these forbidden transitions seems to be definitely established in auroral spectra, the contribution of the airglow transitions to the observed bands is still unknown. Unlike the other bands in the blue and ultraviolet, the Vegard-Kaplan system is degraded to the red. The relative intensities of these bands are quite different in aurorae and in airglow spectra, and a number of anomalies exist in the intensity ratios as reported by Barbier and Williams [1] and Bernard [20]. In general, it appears that the upper electronic state is excited to higher vibrational levels in the airglow than in the aurora, but nevertheless the relative intensities within a given $v''$ progression should be the same in all spectra, although the available eye-estimates do not bear this out.

Relative transition probabilities have recently been computed [19] for transitions with $v' = 0$, 1, 2, and 3, and with $v'' \leq 15$. It should be mentioned that for large values of $v''$, the assumption that $R_e$ remains constant may introduce some errors, although the present values should adequately suffice for our qualitative discussion. The auroral eye-estimates of Barbier and Williams show a nice correlation with these $p$ values, except that the observed intensities of 2-11 and 1-13 are

much stronger than would be expected. However, 2-11 is blended with Second Positive 2-3, which would be anticipated but has been listed only by the Norwegians. Similarly, the emission at 4319 may be primarily due to O II, multiplet 2, rather than the 1-13 band.

On the other hand, there is extremely poor correlation between the intensity estimates of the Vegard-Kaplan bands in the airglow and the computed intensities; therefore, we suggest that some of these identifications be reexamined. For example, it seems very unlikely that the airglow 1-12 and 1-13 bands have been correctly identified when the 1-9, 1-10, and 1-11 bands are not detected. There may be a number of discrepancies in the observed intensities because of various overlapping lines and bands, but the Vegard-Kaplan bands will require much more investigation before any definite statements can be made regarding the excitation of the A $^3\Sigma$ state in the airglow. During aurorae, we almost certainly can observe excitation to at least $v' = 3$. It seems rather strange, however, that the 0-10 band is the only one commonly observed arising from $v' = 0$.

### (*d*) $N_2^+$ *First Negative* ($B\,^2\Sigma \rightarrow X\,^2\Sigma$)

The bands from this system observed in aurorae are degraded to shorter wavelengths. The identifications up to $v' = 2$ are consistent with the theoretical predictions, except that 2-0 should be present, but possibly it is obscured by Second Positive 2-2. Also the 2-6 band at 5653 might be present, although weak. The 3-1 band has not been reported; however, Barbier and Williams found an emission at 3295 that they ascribed to a Herzberg airglow band. The 3-2 band should be the strongest in this progression, but was observed only by Petrie and Small. Again Barbier and Williams listed a Herzberg band at this wavelength. The identification of the emission at 3835 as the 3-3 band is entirely inconsistent with the present transition probabilities. The intensities fall off rapidly with increasing $v'$, but excitation up to $v' = 3$ has apparently been detected. The data are conflicting, however, for the higher progressions, and these identifications must be considered doubtful for the time being.

### (*e*) $N_2^+$ *Meinel* ($A\,^2\Pi \rightarrow X\,^2\Sigma$)

Several multiple-headed bands have been found in the infrared and identified by several lines of analysis. The evidence is greatly in favor of Meinel's [22] identifications.

## VI. MISCELLANEOUS EMISSIONS

The first three Balmer lines of hydrogen have been reported by numerous spectroscopists. It is well known that their intensity compared with other auroral lines varies greatly, but as yet no reliable estimates have been made of their relative intensities with respect to one another (the so-called Balmer decrement). It now seems that the Na "D" lines exist in aurorae independently of the airglow spectrum, but the relative importance of the two contributions is not known.

A few bands from the $O_2^+$ First Negative system ($b\,^4\Sigma_g^- \rightarrow a\,^4\Pi_u$) have been identified, primarily in type *B* aurorae. The 0-1 $O_2$ Atmospheric band was confirmed by Meinel [8], but the 0-0 band is apparently completely reabsorbed and is

not detected in emission. Vegard and Kvifte have identified a few $H_2$ bands, but further investigation is necessary before they can be accepted. Barbier and Williams listed several Herzberg bands from $O_2$ and an unidentified "*Y*" system that normally appear in the airglow. Their analysis of eye-estimates of intensity seems to verify their assignment of these bands to the airglow rather than the aurora. A number of He lines have been proposed by Bernard [23], but these identifications are extremely doubtful. The ratio of helium to hydrogen in the sun suggests that helium may be an important constituent bombarding the upper atmosphere, but Fan and Meinel [24] have not detected helium lines in their synthetic (laboratory) aurorae produced by high-energy $\alpha$ particles.

## VII. ACKNOWLEDGMENTS

We are deeply indebted to Mr. Stanley Wolnik and Miss Anne Carrigan for their assistance in consolidating the observational data and in preparing a number of extensive wavelength tables that were required for the above discussion. Also, it is a pleasure to thank Dr. Nicholls and Messrs. Fraser and Jarmain at the University of Western Ontario for the use of their vibrational transition probabilities prior to publication.

## *References*

[1] D. Barbier and D. R. Williams, Observations of the aurora borealis, J. Geophys. Res. **55**, 401 (1950).
[2] C. E. Dahlstrom and D. M. Hunten, $O_2^+$ and H in the auroral spectrum, Phys. Rev., **84**, 378 (1951).
[3] C. W. Gartlein, Hydrogen in aurora, Mém. Soc. roy. sci., Liege, **12**, 195 (1952). [Proceedings of the Liege Conference, 3 and 4 September 1951.]
[4] C. W. Gartlein and Sprague, First positive bands of nitrogen in aurora, Mém. Soc. roy. sci., Liege, **12**, 191 (1952). [Proceedings of the Liege Conference, 3 and 4 September 1951.]
[5] C. W. Gartlein and Sherman, Identification of $O_2$ bands and forbidden nitrogen in aurora, Mém. Soc. roy. sci., Liege, **12**, 187 (1952). [Proceedings of the Liege Conference, 3 and 4 September 1951.]
[6] L. Vegard and G. Kvifte, Geofys. Pub., **16**, No. 7 (1945); reprinted by L. Harang, The aurorae, New York, John Wiley and Sons, Inc., pp. 67-68 (1951).
[7] A. B. Meinel, Strong permitted OI and NI lines in the infrared auroral spectrum, Trans. Amer. Geophys. Union, **31**, 21 (1950).
[8] A. B. Meinel, The auroral spectrum from 6200 to 8900 A, Astroph. J., **113**, 583 (1951).
[9] A. B. Meinel, The spectrum of the airglow and the aurora, Rep. Prog. Phys., **14**, 121 (1951).
[10] W. Petrie and R. Small, The auroral spectrum in the wave-length range 3300-8900 A, Astroph. J., **116**, 433 (1952).
[11] L. Vegard, Paris, C.-R. Acad. sci., **230**, 1884 (1950).
[12] L. Vegard, E. Tönsberg, and G. Kvifte, Geofys. Pub., **18**, No. 4 (1949).
[13] L. Vegard and G. Kvifte, Geofys. Pub., **18**, No. 3 (1951).
[14] C. Moore, A multiplet table of astrophysical interest, Contrib. Princeton University Observatory, No. 20 (1945); also see R. W. B. Pearse, Proc. Conf. Auroral Physics, London, Ontario, July 1951, edited by N. C. Gerson (in press).
[15] R. W. B. Pearse and A. G. Gaydon, The identification of molecular spectra, New York, John Wiley and Sons, Inc. (1950).
[16] M. Nicolet, Ann. d'Astroph., **1**, 381 (1938).

[17] R. Bernard, Phys. Rev., 55, 511 (1939); International Conf. Gassiot Committee, London, The Physical Society, p. 91 (1948).

[18] W. Petrie, Phys. Rev., 87, 1002 (1952).

[19] Jarmain, Fraser, and Nicholls, University of Western Ontario, Contract AF 19(122)-470, Sci. Rep. No. 8 (1953), Astroph. J., **118**, 228 (1953), also see The Computational Laboratory, Harvard University, Prof. Rep. No. 27 (1951).

[20] R. Bernard, Proc. Conf. Auroral Physics, London, Ontario, July 1951, edited by N. C. Gerson (in press).

[21] W. Petrie and R. Small, J. Geophys. Res., 57, 51 (1952).

[22] A. B. Meinel, Astroph. J., **114**, 431 (1951).

[23] R. Bernard, International Conf. Gassiot Committee, London, The Physical Society, p. 93 (1948).

[24] C. Y. Fan and A. B. Meinel, Astroph. J., **118**, 205 (1953).

[25] Transitions in auroral spectra and many related problems were discussed by various physicists engaged in theoretical, experimental, and observational research at the Colloquium on Auroral Physics, London, Ontario, July 1951, edited by N. J. Oliver (in press).

Journal of Geophysical Research Volume 58, No. 4 December, 1953

# IRREGULARITIES IN THE IONOSPHERE

By R. Roy and J. K. D. Verma

*Institute of Nuclear Physics, Calcutta 9, India*
(Received May 15, 1953)

## ABSTRACT

Electron clouds, both in the $E$ and $F$ regions of the ionosphere, have been detected at vertical incidence by means of a high-precision ionosphere sounding equipment. The clouds give rise to scattered echoes, which are delineated on an expanded sweep as individual pips, resolved out from the normal echoes. An estimate of the received power by back-scattering, made on the basis of the theory of tropospheric radio scattering by Booker and Gordon, shows that it is far in excess of the receiver noise power. Some of the records indicate that sometimes at night the normal layer structure of the ionosphere ceases to hold; the ionospheric regions then contain only electron clouds at different heights. The scattered echoes generally appear for a very short duration. The short persistence (1 to 2 minutes) of these echoes has been explained by considering the drift of the clouds by the upper air winds.

## INTRODUCTION

It is now well known that, in addition to $E$, $F1$, and $F2$ layers, the origin of which has been explained to some extent by the Chapman mechanism, other types of reflection are obtained from thin layers and patches of ionization which are temporary and do not obey the above mechanism. All these irregularities contribute to the departure of ion density from the normal Chapman distribution and as a result give rise to several effects, such as the irregular group retardation of the ionosphere echoes, the random fading of the received signals, the persistence of the echo pattern over a large range of frequencies, the diffuse traces spread over the normal $h'-f$ curves, and the back-scattered radiation within the skip zone of a transmitter. The study of these phenomena has revealed that the irregularities may be classified into two broad categories, namely:

(*A*) *Thin-strata type*—Since the discovery of $E2$ layer by Appleton (1933), finer structures in the $E$ layer have been proposed and investigated by a large number of workers. Ratcliffe and White (1933) observed the doubling of night-time $E_s$ echoes and concluded that it was due to a double stratification in the $E$ region. Smith and Kirby (1937) arrived at a similar inference of stratification in the $E$ region while conducting the field-intensity measurements at oblique incidence at 1040 kc/sec. McKinley and Millman (1949) have proposed a theory of meteoric

ionization on the basis of the existence of stratifications in a narrow region within the $E$ layer. Helliwell and his coworkers (1951), at Stanford, found distinct evidence of multiple strata in the $E$ layer lying between 90 and 130 km. B. H. Briggs (1951), from his studies of the variation of amplitude with frequency by means of a rapid sweep-frequency recorder, has been able to compute the thickness of such types of thin layer in the $E$ region. The origin of such stratification, however, is not known.

($B$) *Electron-cloud type*.—This type of sporadic ionization characterizes itself by the absence of group retardation effects. They generally persist for short durations and give rise to short-length patches in the $h'$-$f$ traces. Eckersley (1932, 1937, 1939, 1944) ascribed the different scattering phenomena, which he denoted by $1 \times E$, $1 \times F$, $2 \times F$, and $G$, to ionized clouds in the $E$ layer. Echoes arising from some "bursts" of ionization at the 80- to 160-km level were first noted by Appleton and Piddington (1938) while working with a fairly high-resolving ionospheric recorder.

The existence of an extended region of electron clouds at or above the $F$ layer was assumed by Booker and Wells (1938) for explaining the diffuse traces above the penetration frequency in the night-time $h'$-$f$ records of Huancayo. Wells, Watts, and George (1946) detected rapidly moving ion-clouds in the $F$ layer during a magnetic storm. The presence of turbulent ion-clouds in the horizontal plane of the region $E$ was suggested by Ratcliffe (1948) for elucidating the phenomenon of random fading. Helliwell (1949), by means of a high-power ionospheric equipment at 100 kc/sec, found that most frequently at night the region between 86 to 106 km consists of clouds of ionization rather than any regular ion-density distribution. It may be pointed out that Dieminger (1951) has indicated that genuine irregularities occurring in the $F$ layer can also give rise to $1 \times F$ scattering.

The object of the present communication is to show some direct evidence of ionospheric irregularities, mainly the electron clouds both in the $E$ and $F$ regions, with the aid of the new ionospheric recorder evolved at the Institute of Nuclear Physics, Calcutta.

## EXPERIMENTAL ARRANGEMENT

The details of this high-precision ionospheric sounding equipment has been published elsewhere (Banerjee and Roy, 1952*b*). The apparatus utilizes a transmitter generating 50-kw sounding pulses of 6 to 30 microseconds duration, and a vertical delta antenna, terminated at the top with a non-inductive resistance of 800 ohms or alternatively 450 ohms. The echoes are received by a pair of horizontal dipole antennas situated on the top (140 feet above the ground-level) of the antenna-mast, which feed the signal into a wide-band amplifier, also kept at the same height. The amplified echo signal is carried through shielded twin cables to a superheterodyne receiver, the band-width of which is 90 kc/sec. The output of the receiver is fed to the vertical deflection plates of an oscilloscope containing a raster time-base (Banerjee and Roy, 1950) of 12 lines. Each line of the raster is executed from right to left and corresponds to only 50 km of equivalent height, and there are height-markers at intervals of 5 km on the raster.

In the conventional ionospheric recorders, pulses of duration of 200 microseconds are generally used, which limit the accuracy of height measurements to $\pm 15$ km and the resolving limit to 30 km. The best improvement over these limits was obtained by Helliwell, *et al.* (1951), who used a pulse time-constant of the order of 30 microseconds and a receiver of 50 kc/sec band-width, the resolving limit in the case being 5 km only. The need for further higher order of resolution was pointed out by Helliwell, *et al.* (1950) for an adequate observation of the phenomenon of splitting in the $E$ layer. The use of a wider-band receiver and the expanded sweep circuit in the high precision equipment described enables the height measurements to be made to an accuracy of 1 km, and the adjacent echoes discernible when their mutual separation is 2 km only.

## RESULTS

Various complex echo patterns have been recorded during a period of observation covering more than a year, a typical few of which have been reported earlier (1952*a*, 1952*b*).

Due to the high resolution, the echoes due to the $x$ and the $o$ waves from the $F$ layer remain resolved at frequencies much remote from the critical frequencies. The Plates (I to XII) illustrate a number of complex echo patterns on the raster, in which the ground pulse stands on the lowermost line taken as the first line (the faint lines in the background are due to the other beam of the CRO).

Photographs of the echo pattern were taken on a 35-mm film at intervals of half a minute, whenever such irregularities appeared. The duration of any echo was determined from a scrutiny of the consecutive records.

In some of the Plates (IV, V, VI, VII, VIII, XI), the sporadic $E$ echoes have been designated as the thin-layer type of $E_s$. The echoes due to scattering in the electron clouds rarely persist for more than two minutes, whereas those from the thin layer of ionization remained on the raster for 30 minutes to one hour. The scattered echoes are further characterised by their unsteady character, and they show periodic fluctuation of their amplitude (quasi-period of the order of one second). The amplitude of the echo from the thin layer, on the other hand, is fairly steady. Further, higher order of reflection can only be possible for a thin layer (Plates V, VII, XI).

## SCATTERED POWER FROM AN ELECTRON CLOUD

An estimate of the received scattered power from an electron cloud observed at vertical incidence can be obtained on the basis of the theory of radio scattering proposed by Booker and Gordon (1950). The original theory for the tropospheric scattering was later extended by Booker (1951) for the ionospheric case, namely, scattering from $E_s$ and also the $F$ region at the time of magnetic storms.

Following the analysis of Booker and Gordon, for the case of electron clouds in the ionosphere, it may be assumed that the cloud represents a region, the dielectric constant of which differs from the average dielectric constant of the region in which the cloud is embedded. If $(\Delta\epsilon)$ measures the departure of the capacitivity of the cloud from the average capacitivity $(\epsilon)$ of the ionospheric region, then the

PLATE I

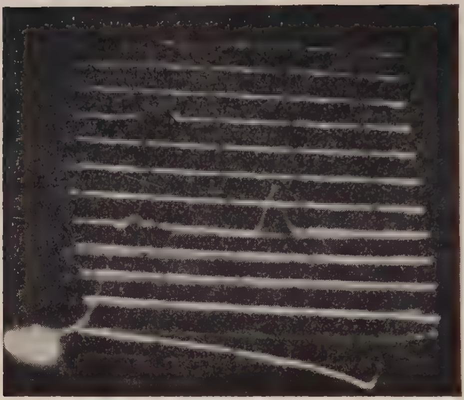

PLATE II

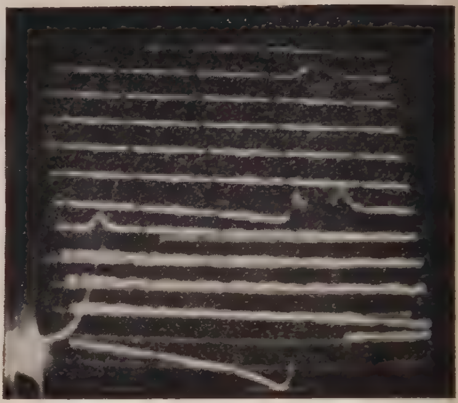

Plate I—*Freq., 3.4 Mc/sec; time, 15ʰ 53ᵐ IST; date, Dec. 27, 1952*

| Line | Height (km) | Type | Remarks* |
|---|---|---|---|
| 5 | 216 | $F_o$ | .......... |
| 5 | 234 | $F_x$ | .......... |
| 5 | 237 | Cloud $F_s$ | Duration 2 minutes |
| 9 | 430 | $F_o + F_s$ | Duration 1 minute |
| | | | The *o* wave meets a cloud in second hop |
| 9 | 432 | $2F_o$ | .......... |

*Duration stated only for transitory echoes.

Plate II—*Freq., 3.95 Mc/sec; time, 15ʰ 35ᵐ IST; date, Dec. 27, 1952*

| Line | Height (km) | Type | Remarks |
|---|---|---|---|
| 5 | 228 | $F_o$ | .......... |
| 6 | 245 | Cloud $F_s$ | Duration less than a minute |
| 6 | 248 | $F_x$ | .......... |
| 6 | 251 | Cloud $F_s$ | Duration less than a minute |
| 11 | 496 | $2F_x$ | .......... |

PLATE III

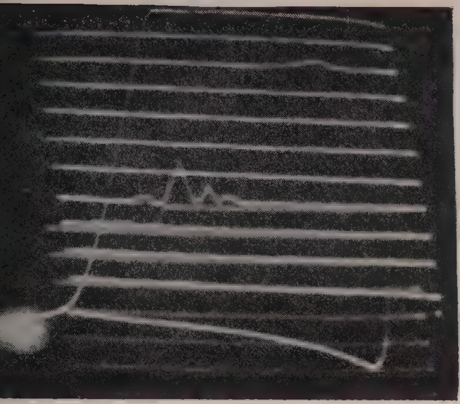

PLATE IV

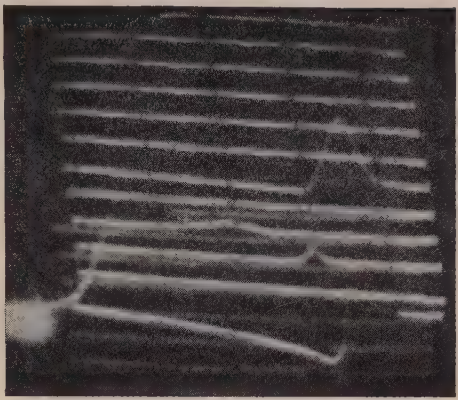

PLATE III—*Freq., 3.62 Mc/sec; time, 14^h 01^m IST; date, Jan. 1, 1953*

| Line | Height (km) | Type | Remarks |
|---|---|---|---|
| 4 | 189 | $F_o$ | Feeble |
| 5 | 222 | Cloud $F_s$ | Duration less than a minute |
| 5 | 225 | Cloud $F_s$ | Duration less than a minute |
| 5 | 229 | $F_x$ | .......... |
| 5 | 233 | Cloud $F_s$ | Duration less than a minute |
| 10 | 458 | $2F_x$ | .......... |

PLATE IV—*Freq., 4 Mc/sec; time, 12^h 52^m IST; date, Dec. 28, 1952*

| Line | Height (km) | Type | Remarks |
|---|---|---|---|
| 3 | 107 | Cloud $E_s$ | Duration 2 minutes |
| 4 | 167 | $E_s$ | Layer type of $E_s$ showing group retardation |
| 6 | 252 | $F_o$ | Broad echo of base-width 10 km |

PLATE V

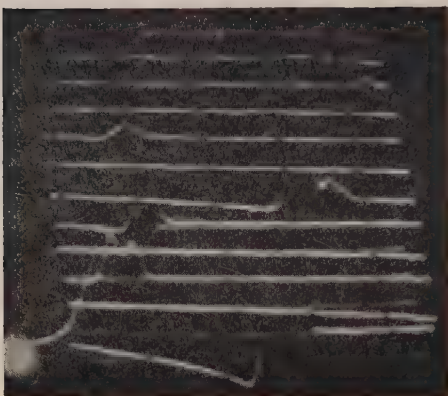

PLATE VI

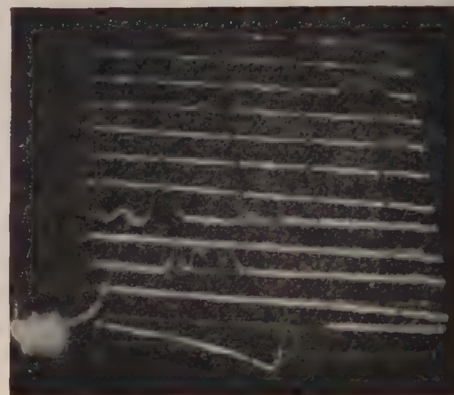

PLATE V—*Freq., 3.7 Mc/sec; time, 15^h 45^m IST; date, Jan. 1, 1953*

| Line | Height (km) | Type | Remarks |
|---|---|---|---|
| 3 | 118 | $E_s$ cloud | Duration less than a minute |
| 3 | 123 | $E_s$ | Thin-layer type |
| 5 | 217 | $F_o$ | .......... |
| 6 | 243 | $F_x$ | .......... |
| 6 | 246 | $2E_s$ | .......... |
| 8 | 368 | $3E_s$ | .......... |
| 10 | 434 | $2F_o$ | .......... |
| 11 | 493 | $4E_s$ | .......... |

PLATE VI—*Freq., 3.62 Mc/sec; time, 16^h 25^m IST; date, Jan. 1, 1953*

| Line | Height (km) | Type | Remarks |
|---|---|---|---|
| 3 | 110 | $E_s$ cloud | Duration 2 minutes |
| 3 | 113 | $E_s$ | Layer type |
| 3 | 115 | $E_s$ cloud | Duration 2 minutes |
| 3 | 118 | $E_s$ cloud | Duration 2 minutes |
| 5 | 204 | $F_o$ | .......... |
| 5 | 208 | Cloud $F_s$ | Duration 1 minute |
| 5 | 219 | $F_x$ | .......... |
| 5 | 225 | Cloud $F_s$ | Duration 1 minute |
| 8 | 336 | $F_x + E_s$ | The $x$ wave after ground reflection met the $E_s$ cloud at 118 km |
| 9 | 408 | $2F_o$ | .......... |
| 9 | 412 | $F_o$ + cloud $F_s$ | The $o$ wave after ground reflection met an electron cloud in $F$ region |
| 10 | 438 | $2F_x$ | .......... |
| 10 | 441 | $F_x$ + cloud $F_s$ | The $x$ wave after ground reflection met an electron cloud in $F$ region |

PLATE VII

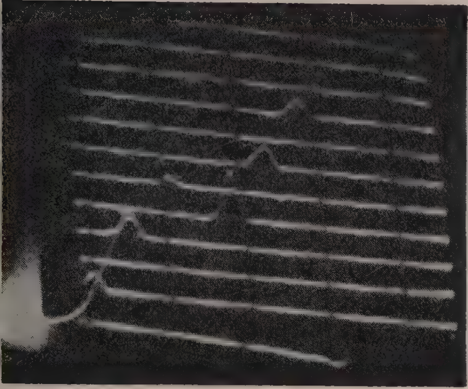

PLATE VIII

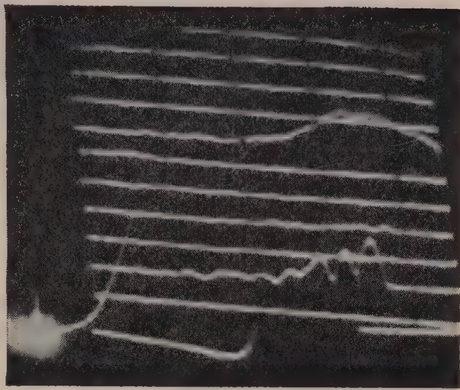

PLATE VII—*Freq., 2.05 Mc/sec; time, 06^h 12^m IST; date, Jan. 4, 1953*

| Line | Height (km) | Type | Remarks |
|---|---|---|---|
| 2 | 94 | $E_s$ | Thin layer |
| 4 | 188 | $2E_s$ | .......... |
| 5 | 226 | $F_o$ | .......... |
| 6 | 282 | $3E_s$ | .......... |
| 7 | 320 | $F_o + E_s$ | The *o* wave after ground reflection met the thin-layer type of $E_s$ |
| 9 | 414 | $F_o + 2E_s$ | The *o* wave meets the thin-layer $E_s$ twice |
| 10 | 452 | $2F_o$ | .......... |

PLATE VIII—*Freq., 1.77 Mc/sec; time, 05^h 47^m IST; date, Jan. 4, 1953*

| Line | Height (km) | Type | Remarks |
|---|---|---|---|
| 3 | 94 | $E_s$ | Thin layer |
| 3 | 99 | $E_s$ | All these pips persisted for a period of 25 minutes ($05^h$ $30^m$ to $05^h$ $55^m$); the intensity of these pips showed periodic fluctuations, suggesting the turbulent nature of the clouds to which they were due |
| 3 | 101 | $E_s$ | |
| 3 | 105 | $E_s$ | |
| 3 | 109 | $E_s$ | |
| 3 | 114 | $E_s$ | |
| 3 | 118 | $E_s$ | |
| 5 | 193 | Cloud $F_s$ | Very feeble echoes |
| 5 | 195 | Cloud $F_s$ | |
| 8 | 332-355 | $F_o$ | Broad echo extending over 23 km |

PLATE IX

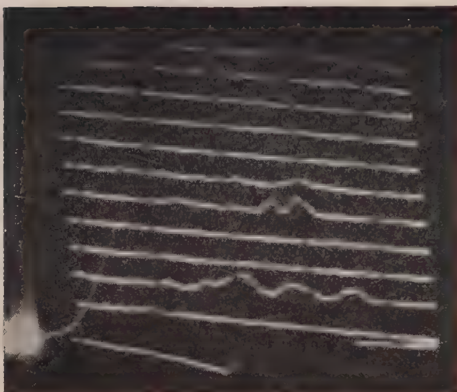

PLATE X

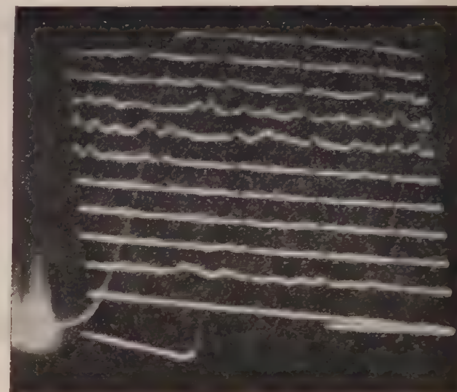

Plate IX—*Freq., 2.15 Mc/sec; time, 01^h 58^m IST; date, Jan. 4, 1953*

| Line | Height (km) | Type | Remarks |
|---|---|---|---|
| 3 | 97 | $E_s$ cloud | Nocturnal $E_s$ and $F_s$. The persistence of the $E_s$ clouds were of the order of 2 minutes and for $F_s$ only 1 minute. The structure of $E$ and $F$ layers has assumed a patchy nature. |
| 3 | 106 | $E_s$ cloud | |
| 3 | 112 | $E_s$ cloud | |
| 3 | 117 | $E_s$ cloud | |
| 3 | 122 | $E_s$ cloud | |
| 6 | 254 | Cloud $F_s$ | |
| 6 | 257 | Cloud $F_s$ | |
| 6 | 269 | Cloud $F_s$ | |
| 7 | 303 | Cloud $F_s$ | |
| 7 | 311 | Cloud $F_s$ | |
| 12 | 551 | Cloud above $F$ layer | |

Plate X—*Freq., 1.77 Mc/sec; time, 02^h 29^m IST; date, Jan. 4, 1953*

| Line | Height (km) | Type | Remarks |
|---|---|---|---|
| 3 | 92-132 | Seven $E_s$ clouds | Feeble scattered echoes from nocturnal $E_s$ |
| 7-10 | 318-468 | More than 30 $F_s$ clouds | The whole of $F$ region appears to be full of "bursts" of ionization |

PLATE XI

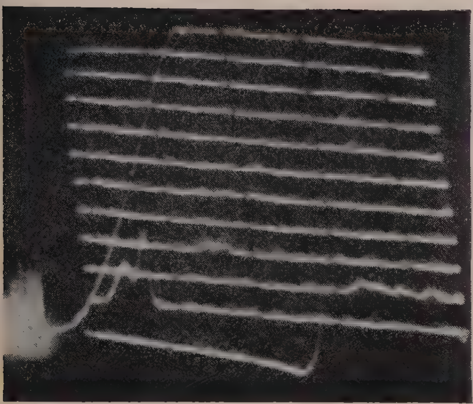

PLATE XII

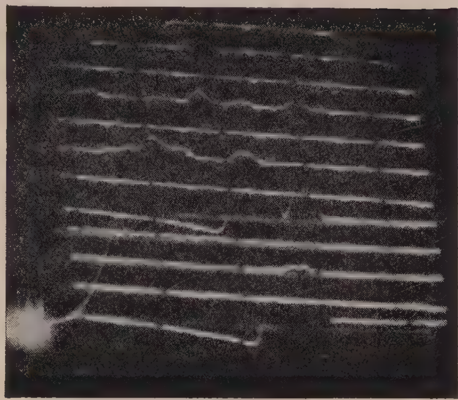

PLATE XI—*Freq., 1.8 Mc/sec; time, 03$^h$ 30$^m$ IST; date, Jan. 4, 1953*

| Line | Height (km) | Type | Remarks |
|---|---|---|---|
| 2 | 88 | Thin-layer $E_s$ | The strong twin owes its origin to thin double stratification in the $E$ layer |
| 2 | 90 | Thin-layer $E_s$ | |
| 3 | 101 | $E_s$ cloud | .......... |
| 3 | 104 | $E_s$ cloud | .......... |
| 3 | 109 | $E_s$ cloud | .......... |
| 4 | 176 | $2E_s$ | Second-order reflection from the double stratification in the $E$ layer |
| 4 | 179 | $2E_s$ | |

PLATE XII—*Freq., 3 Mc/sec; time, 18$^h$ 00$^m$ IST; date, Jan. 15, 1953*

| Line | Height (km) | Type | Remarks |
|---|---|---|---|
| 3 | 101 | $E_s$ cloud | Stayed for 5 minutes |
| 3 | 103 | $E_s$ cloud | Stayed for a minute |
| 5 | 199 | $F_o$ | .......... |
| 5 | 203 | $F_x$ | .......... |
| 7 | 306 | $F_x + E_s$ | The $x$ wave meets the $E_s$ cloud at 103 km in second hop |
| 7 | 314 | $F_s$ cloud | Stayed for 2 minutes |
| 7 | 318 | $F_s$ cloud | Stayed for 2 minutes |
| 7 | 321 | $F_s$ cloud | Stayed for 2 minutes |
| 9 | 398 | $2F_o$ | .......... |
| 9 | 406 | $2F_x$ | .......... |
| 9 | 410 | $F_x + F_s$ | The $x$ wave meets an extra cloud in the $F$ region in second hop |
| 9 | 425 | $F_x + F_s$ | The $x$ wave meets an extra cloud in the $F$ region in second hop |
| 11 | 510 | $2F_x + E_s$ | .......... |

scattered power $\sigma$ per unit solid angle, per unit incident power density, and per unit scattering volume in the backward direction can be written as

$$\sigma = \frac{1}{32\pi l}\cdot\overline{\left(\frac{\Delta\epsilon}{\epsilon}\right)^2}$$

where the scale of fine structure of the scattering irregularity

$$l \gg \frac{\lambda}{2\pi}$$

and $\lambda$ is the wavelength in the ionized medium.

Assuming further that the irregularity is isotropic in nature, the scattered power per unit solid angle from a volume d$v$ of the cloud in the direction of the receiver is

$$\frac{P_o}{4\pi h^2}\cdot G\cdot\sigma\cdot \mathrm{d}v$$

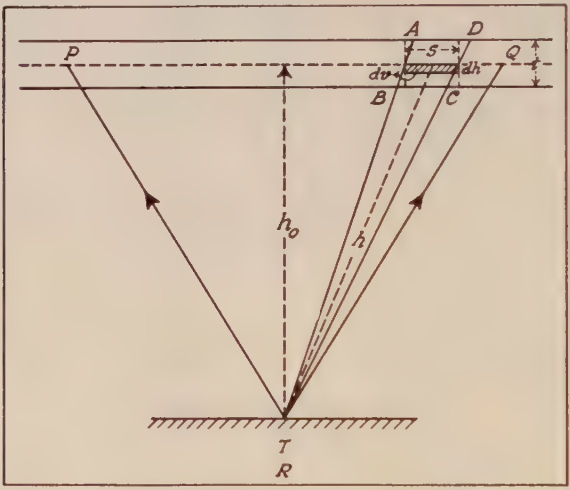


FIG. 1—THE TRANSMITTER AT T IS IRRADIATING THE ZONE PQ IN THE IONOSPHERE; ABCD REPRESENTS THE CLOUD GIVING RISE TO THE SCATTERED ECHO AT THE RECEIVER R

where $P_o$ is the transmitted power, $h$ the distance of the cloud from the receiving point, and $G$ the gain of the transmitting antenna. So the total scattered power at the receiver comes out as

$$P = \int_v \frac{P_o}{4\pi h^2}\cdot G\cdot\sigma\cdot\frac{A'}{h^2}\cdot \mathrm{d}v$$

where $A'$ is the equivalent antenna aperture of the receiving system. The total volume $V$ of the scattering irregularity may be taken as $S\cdot t$, where $S$ is the average cross-sectional area in the plane perpendicular to the direction of transmission and $t$ the thickness of the equivalent scattering cylinder (Fig. 1). Putting

the solid angle $\phi$ subtended by the cloud cross-section at the receiver as $\phi = S/h^2$, and $dv = S \cdot dh = \phi\, h^2\, dh$, the expression for the received power can be rewritten as

$$P = \frac{P_o}{4\pi} \cdot G \cdot \sigma \cdot \phi \cdot A' \int_{h-(t/2)}^{h+(t/2)} \frac{dh}{h^2}$$

$$= \frac{P_o}{4\pi h^2} \cdot G \cdot \sigma \cdot \phi \cdot A' \cdot t$$

since $t$ is small compared to $h$.

The above expression indicates that the scattered power would be appreciable only when the cross-section of the cloud is fairly large. Thus, a cloud in the zone, irradiated by the transmitted beam, but away from the zenith, may give rise to another echo at height $h$, over and above the normal echo obtained at vertical incidence at height $h_o$, provided this difference in height is amenable to resolution. In case the resolution of this height difference $h \sim h_o$ is not possible, the scattered power contributes to change the intensity of the normal echo. When the cloud is embedded in the same horizontal region as that responsible for normal reflection, the height $h$ is greater than $h_o$. When the seat of the cloud occurs in a lower region in the same layer, $h$ may also become less than $h_o$.

A tentative numerical calculation of the received scattered power can be obtained with some basic assumptions about the parameters involved. The value $\overline{(\Delta N/N)^2}$ may be taken as $10^{-4}$, as has been assumed by Bailey, *et al.* (1952) for explaining the long-distance radio propagation as a result of scattering from the $E$ region irregularities, while the scale of fine structure $l$ is taken as 100 metres, after Ratcliffe and Pawsey (1933). The expanse of the scattering cloud may be taken as 5 km, as suggested by Weekes (1951), who takes this dimension of the irregularities in the $F$ layer giving rise to ionospheric twinkling of the extra-terrestrial radio waves. Assuming $t = 1$ km, a plasma frequency $= 2.84$ Mc/sec for $E$ region, and the frequency of radio wave in propagation as 3 Mc/sec, the received power comes out to be

$$P = 1.1 \times 10^{-8} \text{ watt} = -\ 79.4 \text{ dbw}$$

when the main lobe of transmission is vertical and its semiangle is 20°, the radiated power is 25 kw, and the receiving aerial is a horizontal dipole (assumed to be resonant at the signal frequency). The receiver noise power for 90 kc/sec band-width and a noise figure of ten, comes out as $3.8 \times 10^{-15}$ watt. This clearly establishes the possibility of detecting a scattered echo above the noise level.

## DISCUSSION

Generally, the amplitude of the scattered echo is found to be smaller than those of the normally reflected echoes. But sometimes, these transitory echoes show an amplitude nearly equal to the normal echo amplitudes (Plate V). This means that the scattered power sometimes is of the same order as that obtained in normal reflection. A more precise knowledge of the parameters involved is essential for a correct evaluation of the scattered power.

In plates I, VI, and XII, it has been proposed that a scattered echo is appearing

at a higher height, due to the $x$ or $o$ wave meeting an electron cloud in the second hop of its propagation. Though the magnitude of the echo heights seems to suggest the above mechanism, an anomaly arises regarding the obtainable scattered power, unless the dimension of the cloud is appreciably large.

Plates IV and VIII show the broad type of echoes usually observed near the "tail" or the penetration limit of a layer. The lower side-bands in the spectrum of the short-duration pulse are reflected with smaller retardation than the higher side-bands; consequently the base-width of the echo envelope increases. In both the Plates, the $F_o$ echo has become broadened due to such differential group retardation suffered at the lower tail of the $F$ layer. The echo at 167 km in Plate IV is due to a retardation type of $E_s$ , evidently resembling a layer formation.

Plates IX and X show a very rare abnormal feature observed at midnight. The layer structure in both $E$ and $F$ regions has completely broken down, and the whole of the ionosphere seems to consist of only electron clouds distributed at different heights in the aforesaid regions. A solitary cloud above the $F$ region has been detected in Plate IX when the layer has assumed such patchy structure.

The occurrence of the resolved scattered echoes has been noted to be as low as 30 per cent in the $E$ region as compared to that in $F$. The radiation lobe of the transmitter intercepts a smaller surface area in the $E$ region; so the possibility of detecting $E$ region clouds is less, though it may be richer in such irregularities. The short persistence of these scattered echoes finds ready explanation when the existence of the upper air winds is taken into account. As a result of these winds, having a horizontal drift velocity of the order of 50 metres/sec (Mitra, 1949), the clouds cross the narrow cone of radiation within a few minutes. So the time-delay of the scattered echoes first decreases, then increases, finally disappearing when the cloud leaves the beam. Most of the scattered echoes described in the Plates showed such variation of time-delay.

## CONCLUSION

The presence of clouds in the ionosphere thus becomes detectable at vertical incidence when an ionospheric sounding equipment of high resolving power is utilized. A measurement of the persistence as well as the height variations of the scattered echo can give the average values of the wind velocities at the $E$ and $F$ regions. This necessitates a sufficiently rapid $h'$–$t$ recording, arrangements for which are now in progress in the laboratory.

## ACKNOWLEDGMENTS

The authors are indebted to Prof. M. N. Saha, D.Sc., F.R.S., for his kind interest and constant guidance during the progress of this work. Grateful thanks are also due to Messrs. B. M. Banerjee, B. K. Banerjee, and S. N. Mitra for their valuable discussions and criticisms.

## *References*

Appleton, E. V. (1933); Nature, **131**, 872-873.

Appleton, E. V., and J. A. Piddington (1938); Proc. R. Soc., A, **164**, 467-476.

Bailey, D. K., R. Bateman, L. V. Berkner, H. G. Booker, G. F. Montgomery, E. M. Purcell, W. W. Salesbury, and J. B. Weisner (1952); Phys. Rev., **86**, 141-145.
Banerjee, B. M., and R. Roy (1950); Indian J. Phys., **24**, 411-419.
Banerjee, B. M., and R. Roy (1952); (*a*) Science and Culture, **17**, 305-306.
Banerjee, B. M., and R. Roy (1952); (*b*) Indian J. Phys., **26**, 473-494.
Booker, H. G., and H. W. Wells (1938); Terr. Mag., **43**, 249.
Booker, H. G., and W. E. Gordon (1950); Proc. Inst. Radio Eng., **38**, 401-412.
Booker, H. G. (1951); The theory of electromagnetic waves (a symposium), S379.
Briggs, B. H. (1951); Proc. Phys. Soc., B, **64**, 255-274.
Dieminger, W. (1951); Proc. Phys. Soc., B, **64**, 142-158.
Eckersley, T. L. (1932); J. Inst. Elec. Eng., **71**, 405.
Eckersley, T. L. (1937); Nature, **140**, 846.
Eckersley, T. L. (1939); Nature, **143**, 33.
Eckersley, T. L., G. Millington, and J. W. Cox (1944); Nature, **153**, 341.
Helliwell, R. A. (1949); Proc. Inst. Radio Eng., **37**, 887.
Helliwell, R. A., A. J. Mallinckrodt, F. W. Kruse, and B. A. Wambsganss (1950); Pulse studies of the ionosphere at low frequencies, Electronics Research Laboratory, Stanford University, 36.
Helliwell, R. A., A. J. Mallinckrodt, and F. W. Kruse (1951); J. Geophys. Res., **56**, 53-62.
McKinley, D. W. R., and P. N. Millman (1949); Proc. Inst. Radio Eng., **37**, 364-374.
Mitra, S. N. (1949); J. Inst. Elec. Eng., Pt. 3, **96**, 441.
Ratcliffe, J. A. (1948); Nature, **162**, 9.
Ratcliffe, J. A., and E. L. C. White (1933); Phil. Mag., **16**, 125-144.
Ratcliffe, J. A., and J. L. Pawsey (1933); Proc. Cambridge Phil. Soc., **29**, 301-318.
Smith, N., and S. S. Kirby (1937); Phys. Rev., **51**, 890-891.
Weekes, K. (1951); Proceedings of the Conference on Ionospheric Physics at Pennsylvania State College, 3M.
Wells, H. W., J. M. Watts, and D. R. George (1946); Phys. Rev., **69**, 540.

Journal of Geophysical Research Volume 58, No. 4 December, 1953

# MAXIMUM USABLE FREQUENCIES AND LOWEST USABLE FREQUENCIES FOR THE PATH WASHINGTON TO RESOLUTE BAY*

By G. H. Hanson, H. V. Serson, and W. Campbell

*Defence Research Telecommunications Establishment, Radio Physics Laboratory, Defence Research Board, Ottawa, Canada*

(Received May 28, 1953)

## ABSTRACT

The standard frequency transmissions of WWV were monitored at Resolute Bay for one year. Using a method developed by Scott, maximum usable frequencies (MUF's) and lowest usable frequencies (LUF's) have been obtained for the path Washington to Resolute Bay for that period. Comparison with the predictions made by the Central Radio Propagation Laboratory in Washington indicates that the predicted MUF's are too low during the night and, for some months, too high during the day. The LUF's are lower than would be expected if the propagation were all by one reflection from the $F2$ layer.

## INTRODUCTION

From September 24, 1951, until September 30, 1952, each of the standard frequencies broadcast by WWV was monitored continuously at Resolute Bay (lat. 74°.7 north, long. 94°.9 west). A great deal of information about communication over the path from Washington to Resolute Bay is therefore available. In particular, it has been possible to compute the MUF's and LUF's for the whole period and to compare them with predictions. It is interesting to note that the control point for the circuit is close to the maximum of the auroral zone, and that the path is 4,009 km long and therefore corresponds to the maximum distance that a radio wave can be propagated by one reflection from the $F2$ layer.

## RECORDING APPARATUS AND PROCEDURE

Separate receiving equipments were constructed for each of the eight frequencies which were monitored. Doublet antennas were used for the five highest frequencies (15, 20, 25, 30, and 35 Mc), while vertical antennas, 20 feet high, were used for the lower frequencies (2.5, 5, and 10 Mc). The outputs of the fixed-frequency receivers were fed through DC amplifiers into Evershed-Vignoles triplex recorders. The limiting sensitivities of the receivers due to noise were between 1.0 and 10$\mu v$, differing somewhat from one to another. Thus, any signal strong enough to produce observable deflections of the traces on the recorders

*Research conducted under Defence Research Board Project D48-97-52-01.

could be considered strong enough so that a communication circuit using high-gain antennas could pass traffic.

At certain hours of the day, station WWVH in Hawaii produced a strong signal in Resolute Bay. During these periods, it was possible to avoid confusing the two stations by observing the deflection of the trace from the base-line during WWVH's four minutes of silence every half-hour.

## DETERMINATION OF MUF's AND LUF's FROM WWV SIGNAL STRENGTHS

Several years ago, Scott [see 1 of "References" at end of paper] developed a method of determining MUF's and LUF's from similar data. As the report was not widely distributed, the method will be described briefly here.

For each month, graphs are prepared on which, for each frequency, the number of days that WWV was not heard is plotted as a function of the time of day. Two types of diurnal curves are obtained, depending on whether reception of the frequency is predominately limited by the MUF or the LUF. Examples of these are shown in Figures 1 and 2. The times at which the curves cross a horizontal line, corresponding to one-half of the days in the month, are then transferred to another graph, on which the coordinates are frequency and time of day. At these times, the corresponding frequency is exactly either the monthly median MUF or LUF, by definition of these quantities. Additional points may be obtained on the second graph by interpolating between the curves on the first graph. Smooth curves of MUF and LUF may then be drawn.

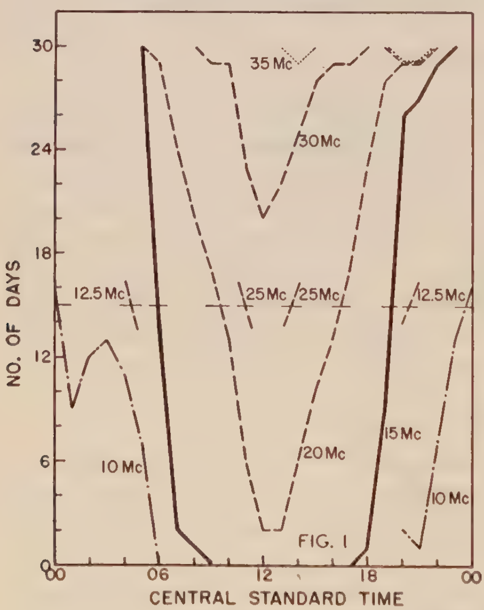


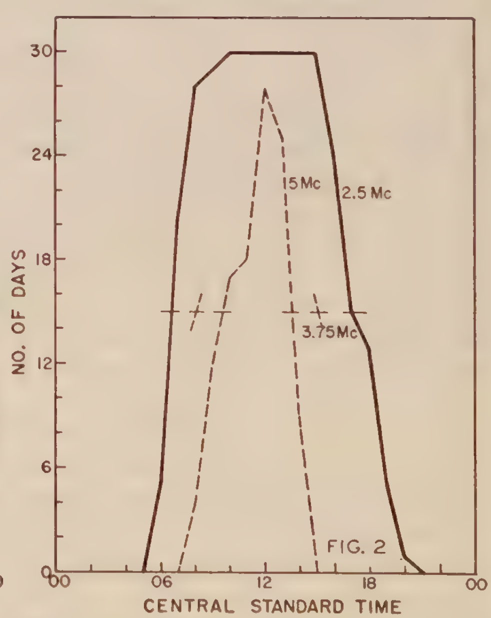


FIG. 1—NUMBER OF DAYS OF NIL RECEPTION OF WWV'S FIVE HIGHEST FREQUENCIES AS A FUNCTION OF TIME OF DAY FOR NOVEMBER 1951 (THERE IS NO CURVE FOR 25 MC BECAUSE THE RECEIVER WAS UNSERVICEABLE MOST OF THE MONTH)

FIG. 2—NUMBER OF DAYS OF NIL RECEPTION OF WWV'S THREE LOWEST FREQUENCIES AS A FUNCTION OF TIME OF DAY FOR NOVEMBER 1951

In this analysis, there was no attempt to distinguish between weak and strong signals. Any displacement of the trace above the base-line of the recorder was taken to mean that that frequency was below the MUF and above the LUF. The LUF, of course, is a function of the transmitter power, but the results give a very useful indication of what may be expected for any similar circuit.

## RESULTS

Graphs of the MUF and LUF are shown in Figures 3, 4, and 5, for November 1951, March 1952, and June 1952. Also shown on the same graphs, as dotted curves, are the predicted MUF's obtained from the prediction charts issued by the National Bureau of Standards [2], in Washington. These predicted MUF's refer to propagation via the $F2$ layer, since the MUF's for $E$ and $F1$ layer propagation are much lower, and it is not considered likely that sporadic $E$ would provide a reliable reflecting layer for a path 4,000 km long. It is clear from Figure 3 that the predicted MUF in November was much too low at night and too high in the day. The errors are as great as 33 per cent. These errors cannot be due to a wrong estimate of the sunspot-number, for it is the shape of the curve which is at fault, rather than the average value of the MUF. On the other hand, Figure 4 shows that the prediction for March 1952 was much better. The shapes of the two curves agree fairly well, and the largest error at any hour was 19 per cent.

A comparison of the measured and predicted MUF's for the whole year leads to the following general conclusions:

(1) In the winter, the predictions were much too low at night and too high in the day. Figure 3 is typical of the graphs for winter months.

(2) In the summer, the predictions were good during the night but too low in the day. Figure 5 is a typical graph for a summer month.

(3) In the spring and fall, the predictions were the most accurate. Figure 4 represents the closest agreement of any of the 12 months.

For long-path propagation by the $F2$ layer, the LUF is usually considered [3] to be very close to the higher of two 2,000-km $E$ layer MUF's, which are obtained by considering control points 1,000 km from either end of the circuit. This is based on the fact that the radio wave will not penetrate the $E$ layer unless its frequency is above the $E$ layer MUF corresponding to the angle of departure of the radiation. For a 4,000-km path, the angle of departure for one-hop $F2$ propagation is almost zero. The appropriate $E$ layer MUF then is that for 2,000 km, since that distance corresponds to zero angle of departure for $E$ layer propagation.

The observed LUF's are considerably lower than would be predicted from the above considerations. It is likely that frequencies just above the observed LUF reached Resolute Bay by a two-hop path, and thus penetrated the $E$ layer at a much higher angle of incidence.

Similar computations of LUF have been made for the path from Washington to Prince Rupert (5,400 km), using data obtained by monitoring WWV aurally. These data cannot be considered as accurate as those from Resolute Bay; nevertheless, they give very useful information. The same result is obtained; the LUF's

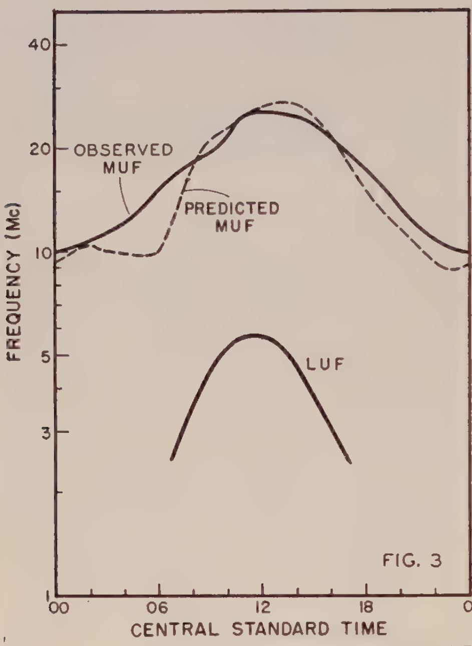


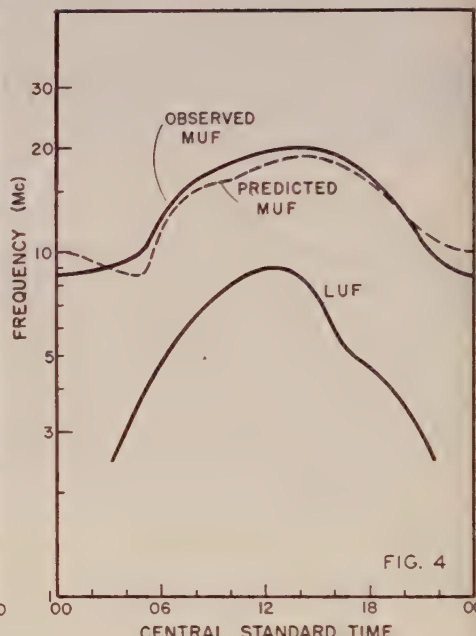


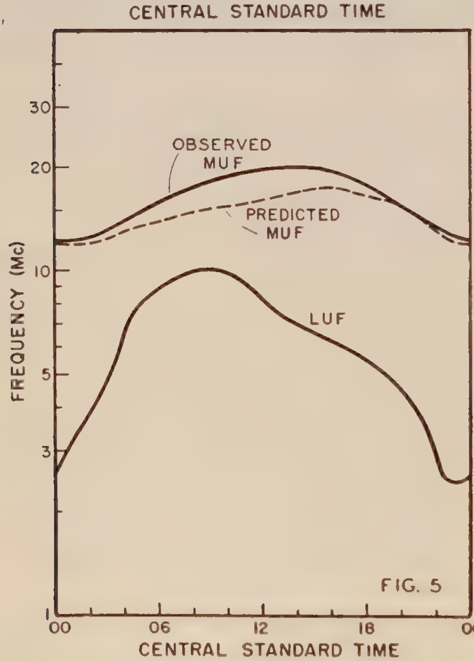


FIGS. 3-5—OBSERVED AND PREDICTED MEDIAN MUF AND OBSERVED MEDIAN LUF FOR THE PATH WASHINGTON TO RESOLUTE BAY

FIG. 3—NOVEMBER 1951

FIG. 4—MARCH 1952

FIG. 5—JUNE 1952

are much lower than would be the case if the transmission were exclusively by the 4,000-km $F2$ mode.

## DISCUSSION

The errors in the predicted MUF's are rather serious. No doubt they are due in part to inadequacies in the zonal method of prediction used by CRPL. However,

the consistently low values at night suggest that incorrect interpretation of the ionospheric records from northern stations may be the cause. Records taken at night at such stations almost invariably have badly spread echoes, large amounts of sporadic $E$, and reflections which appear to be from clouds of dense ionization in the $F2$ region. It may be that the higher MUF's result from scatter due to electron clouds or reflections from denser regions in the $F2$ layer. If this is the case, scaling techniques at northern stations will have to be reexamined.

The low values of the LUF's are of some importance, in that they indicate that multiple-hop propagation involving high angles of departure and arrival must be considered in operating circuits over similar paths.

## *References*

[1] J. C. W. Scott, Seasonal variation in WWV reception at St. Johns, Nfld., Canadian Radio Wave Propagation Committee Report No. 13 (July 1946).

[2] Basic Radio Propagation Predictions—Three months in advance, U. S. Department of Commerce, National Bureau of Standards, CRPL Series D, Nos. 84, 88, and 91.

[3] Ionospheric Radio Propagation, U. S. Department of Commerce, National Bureau of Standards, Circular 462 (June 25, 1948).

JOURNAL OF GEOPHYSICAL RESEARCH VOLUME 58, No. 4 DECEMBER, 1953

# MÉTHODE DE DÉTERMINATION DES HAUTEURS VRAIES DES COUCHES DE L'IONOSPHÈRE. II—UTILISATION DE LA VALEUR EXACTE DE L'INDICE DE RÉFRACTION (CAS DU RAYON ORDINAIRE)

PAR E. ARGENCE ET M. MAYOT

*Service de Prévision Ionosphérique Militaire, Fribourg, Germany, et Institut d'Astrophysique, Paris, France*

(Received June 22, 1953)

## ABSTRACT

Determination of the characteristic parameters of an ionized layer by the hypothesis where the variation of the electronic density ensues from a parabolic law, to the first approximation, is described. Also shown is the application of the exact value of the refractive index (Appleton-Hartree).

## NOTATIONS

Nous renvoyons pour les notations utilisées à la première partie de ce travail [1].

## 1—INTRODUCTION

Nous avons obtenu antérieurement pour expression de la hauteur virtuelle, comptée à partir de la base de la couche:

$$h_v(f) = \gamma \int_0^1 \mu'(\eta, \beta)\phi'(\eta\gamma)\, d\eta$$

où $\phi'(\eta\gamma)$ désigne la dérivée de $\phi(\eta\gamma)$, fonction caractérisant la variation de l'altitude à partir de $\eta\gamma$,

$$y = \phi(\eta\gamma)$$

Si l'on admet l'hypothèse d'une *variation parabolique* de la densité avec l'altitude nous avons:

$$\phi(\eta\gamma) = y_m(1 - \sqrt{1 - \eta\gamma})$$

D'où

$$h_v(f) = \frac{\gamma y_m}{2} \int_0^1 \mu'(\eta, \beta) \frac{d\eta}{\sqrt{1 - \eta\gamma}} \qquad (1)$$

$\mu'(\eta, \beta)$ a été calculé par Whale et Stanley [2]* à partir de la valeur rigoureuse de l'indice (Appleton-Hartree).

*Le résultat donné par ces auteurs est correct à un facteur 2 près.

## 2—RESOLUTION DE L'ÉQUATION INTÉGRALE

Nous avons intérêt à choisir l'origine au maximum de densité de la couche. Posons:

$$z = y_m - y \qquad (z > 0)$$

Nous pouvons écrire:

$$1 - \eta\gamma = a_2 z^2$$

avec:

$$z_m = \frac{1}{\sqrt{a_2}} \qquad \text{(demi-épaisseur)}$$

Plus généralement nous pouvons considérer le développement:

$$1 - \eta\gamma = a_2 z^2 + a_3 z^3 + a_4 z^4 + \cdots = g(z) \ldots\ldots\ldots\ldots\ldots (2)$$

développement qui sera convergent en général étant donnée la bonne approximation fournie par le modèle parabolique.

Si nous posons:

$$u = 1 - \eta\gamma$$

nous avons les deux fonctions inverses:

$$\left.\begin{matrix} z_1 \\ \\ z_2 \end{matrix}\right\} = C_1 u^{1/2} + C_2 u + C_3 u^{3/2} + \cdots$$

Les coefficients $C_i$ étant déterminés à partir des coefficients $a_i$ à l'aide des relations:

$$\left.\begin{aligned} 1 &= C_1^2 a_2 \\ 0 &= 2a_2 C_1 C_2 + C_1^3 a_3 \\ 0 &= (2C_1C_3 + C_2^2)a_2 + 3C_1^2 C_2 a_3 + C_1^4 a_4 \end{aligned}\right\} \ldots\ldots\ldots\ldots\ldots (3)$$

et nous obtenons pour expression de la hauteur virtuelle:

$$h_v(f) = \frac{\gamma}{2} \int_0^1 \frac{\mu'(\eta, \beta)}{\sqrt{1 - \eta\gamma}} \left[C_1 + 2C_2(1 - \eta\gamma)^{1/2} + 3C_3(1 - \eta\gamma) + \cdots\right] d\eta$$

La fonction $\mu'(\eta, \beta)$ devenant infinie pour $\eta = 1$ nous pouvons écrire:

$$\mu'(\eta, \beta) = \frac{\Delta(\eta, \beta)}{\sqrt{1 - \eta}}$$

$\Delta(\eta, \beta)$ étant bornée dans l'intervalle $0 < \eta < 1$.

Posons à nouveau:

$$1 - \eta = v^2$$

il vient:

$$h_v(f) = \gamma \int_0^1 \Delta(v, \beta) \frac{dv}{\sqrt{1 - \gamma + \gamma v^2}}$$

$$\cdot [C_1 + 2C_2(1 - \gamma + \gamma v^2)^{1/2} + 3C_3(1 - \gamma + \gamma v^2) + \cdots] \quad \ldots .(4)$$

c'est à dire:

$$h_v(f) = C_1\psi_1(f) + 2C_2\psi_2(f) + 3C_3\psi_3(f) + \cdots .$$

$\psi_1$, $\psi_2$, $\psi_3$ désignant les intégrales:

$$\left.\begin{aligned} \psi_1(f) &= \gamma \int_0^1 \frac{\Delta(v, \beta)\, dv}{\sqrt{1 - \gamma + \gamma v^2}} \\ \psi_2(f) &= \gamma \int_0^1 \Delta(v, \beta)\, dv \\ \psi_3(f) &= \gamma \int_0^1 \Delta(v, \beta) \sqrt{1 - \gamma + \gamma v^2}\, dv \\ &\cdots\cdots\cdots\cdots \end{aligned}\right\} \quad \ldots\ldots\ldots\ldots(5)$$

Nous devons déterminer les paramétres $C_1$, $C_2$, $C_3 \cdots$. Si nous pouvons écrire la hauteur virtuelle mesurée:

$$h_{obs}(f) = \lambda_0 + \lambda_1\psi_1 + \lambda_2\psi_2 + \lambda_3\psi_3 + \cdots \quad \ldots\ldots\ldots\ldots(6)$$

les différents paramètres seront définis à l'aide des relations:

$$\begin{aligned} \lambda_0 &= h_0 \qquad \text{(base de la couche)} \\ \lambda_1 &= C_1 \\ \lambda_2 &= 2C_2 \\ \lambda_3 &= 3C_3 \\ &\cdots\cdots \end{aligned}$$

On déterminera ensuite $a_2$, $a_3$, $a_4 \cdots$ à l'aide de (3). Le développement:

$$1 - \eta\gamma = a_2 z^2 + a_3 z^3 + a_4 z^4 + \cdots$$

étant défini, nous en déduirons l'épaisseur de la couche après avoir posé $\eta = 0$, c'est à dire:

$$a_2 z_m^2 + a_3 z_m^3 + a_4 z_m^4 + \cdots = 1$$

## 3—APPLICATION

La détermination des coefficients $\lambda_2$, $\lambda_3$, $\cdots$ exigeant un grand nombre de valeurs, nous avons limité le développement au premier terme:

$$h_{obs}(f) = h_0 + \lambda_1\psi_1$$

Dans le cas de l'enregistrement examiné [1] nous obtenons

$$\begin{cases} h_0 = 270 \text{ [km]} \pm 2 \\ y_m = 87 \text{ [km]} \pm 6 \end{cases}$$

TABLE 1—*Hauteurs virtuelles (avec champ magnétique, valeur exacte de l'indice)*

| $f$ | $H_{obs}$ | $H_{cal}$ | $\Delta H$ | $f$ | $H_{obs}$ | $H_{cal}$ | $\Delta H$ |
|---|---|---|---|---|---|---|---|
| 1.45 | 287 | 284 | 3 | 2.40 | 312 | 313 | −1 |
| 1.50 | 288 | 285 | 3 | 2.50 | 316 | 317 | −1 |
| 1.55 | 289 | 287 | 2 | 2.60 | 320 | 322 | −2 |
| 1.60 | 289 | 288 | 1 | 2.70 | 327 | 327 | 0 |
| 1.65 | 290 | 289 | 1 | 2.80 | 332 | 333 | −1 |
| 1.70 | 290 | 290 | 0 | 2.90 | 336 | 339 | −3 |
| 1.75 | 291 | 291 | 0 | 3.00 | 341 | 346 | −5 |
| 1.80 | 292 | 293 | −1 | 3.10 | 349 | 354 | −5 |
| 1.85 | 293 | 294 | −1 | 3.20 | 356 | 362 | −6 |
| 1.90 | 294 | 295 | −1 | 3.30 | 365 | 372 | −7 |
| 1.95 | 295 | 297 | −2 | 3.40 | 383 | 384 | −1 |
| 2.00 | 301 | 299 | 2 | 3.50 | 401 | 398 | −3 |
| 2.10 | 304 | 302 | 2 | 3.60 | 414 | 415 | −1 |
| 2.20 | 307 | 305 | 2 | 3.70 | 440 | 442 | −2 |
| 2.30 | 310 | 309 | 1 | 3.80 | 486 | 476 | 10 |

## 4—CONCLUSION

La formule complète de l'indice nous donne une valeur un peu plus grande que celle donnée par l'emploi des formules d'approximation [1].

Dans l'hypothèse envisagée nous avons supposé que le modèle de variation de $\eta$ était rigoureusement quadratique. La détermination des intégrales $\psi_2$, $\psi_3$, $\cdots$, permet d'étendre la méthode à des couches du type de Chapman (variation de la densité électronique supposée parabolique en première approximation), mais ceci suppose que de nombreuses mesures ont pu être effectuées sur un même enregistrement, en raison semble-t-il de la grande sensibilité des paramètres $\lambda_2$, $\lambda_3$, $\cdots$.

### *Références*

[1] E. Argence et M. Mayot, J. Geophys. Res., 58, 147-165 (1953).
[2] H. A. Whale and J. P. Stanley, J. Atmos. Terr. Phys., 1, 82-94 (1950).

# ON A SELF-EXCITING PROCESS IN MAGNETO-HYDRODYNAMICS

By HITOSHI TAKEUCHI AND YASUO SHIMAZU

*Geophysical Institute, Tokyo University, Tokyo, Japan*

(Received June 27, 1953)

ABSTRACT

In connection with the convection-current model proposed by E. C. Bullard, the problem here considered is whether the magneto-hydrodynamical equations have a solution representing the self-exciting process which is appropriate to the model. In §2, the general expressions for the magneto-hydrodynamical couplings are obtained. In §3, using the results in §2, the problem is reduced to solve (3.6) under the boundary conditions (3.3). This is the eigen-value problem for $4\pi\kappa aV$ ($\kappa$ is the electric conductivity, $a$ the radius of the earth's core, and $V$ the fluid velocity). This eigen-value problem is solved in an approximate way. In §4 and §5, this approximate solution is shown to be good enough for studying the present problem. The results obtained in this paper show that such a self-exciting dynamo is possible by which the earth's main magnetic field is produced and maintained.

§1. The main part of the earth's magnetic field and its secular variations are known to have nothing to do with things outside the earth. Here lies the most difficult point of the problem concerning the earth's magnetic field. What is going on within the earth in order that its magnetic field can undergo sensible changes in a hundred years or so and in order that the field itself can, nevertheless, be maintained? Recently, a simple and plausible explanation of the non-dipole geomagnetic field and its secular variations was proposed by W. M. Elsasser (1946, 1947) and E. C. Bullard (1948, 1949). The variations are attributed to hydrodynamical eddies occurring in the earth's core and to changes in electric current systems in the outer part of the core caused by the eddies. After examining all possibilities, it is now believed that these eddies are caused by the thermal convection of the fluid within the earth's core (Bullard, 1949). The success above referred to leads us to the idea that the whole magnetic field of the earth is ultimately produced and maintained by a mechanism of induction. Elsasser discusses the relation between the field and motion in a very general way and concludes that there may exist chains of relation in which a field $H_1$ interacts with a motion $V_1$ to produce a field $H_2$, which, in turn, interacts with another motion $V_2$ to

reproduce $H_1$. If it is possible to show the existence of such a "self-exciting dynamo" in the earth's core, the main magnetic field might also be explained. Thus, the problem is reduced to examine whether Maxwell's equation of electrodynamics possesses solutions representing such a self-exciting dynamo. In this connection, Bullard (1949) proposed a process by which the earth's main magnetic field may be produced and maintained. The self-exciting dynamo proposed by Bullard is considered to be driven by the convection current in the earth's core. It is this convection-current model that we are going to study in the present paper.

§2. In order to study the maintenance of magnetic fields by electro-magnetic induction, the following equations must be solved under certain boundary conditions (Alfvén, 1950):

$$\operatorname{curl} H = 4\pi I = 4\pi\kappa(E + V \times H) \qquad (2.1)$$

$$\operatorname{curl} E = -\frac{\partial H}{\partial t} = 0 \qquad (2.2)$$

$$\operatorname{div} H = 0 \qquad (2.3)$$

$$\operatorname{div} E = 4\pi\rho c^2\epsilon^{-1} \qquad (2.4)$$

Customary notations are adopted. From (2.1), (2.2), and (2.3), we get

$$\nabla^2 H + 4\pi\kappa \operatorname{curl}(V \times H) = 0 \qquad (2.5)$$

In spherical coordinates, it is shown that the equation (2.3) is satisfied by the following two expressions for the magnetic fields:

*S*-type (poloidal type) magnetic field

$$H_S = \left\{ \begin{array}{l} -n(n+1) S_n^m(r) r^{n-1} Y_n^m, \\[2ex] -\left[ r \dfrac{dS_n^m}{dr} + (n+1) S_n^m \right] r^{n-1} \dfrac{\partial Y_n^m}{\partial \theta}, \\[2ex] -\left[ r \dfrac{dS_n^m}{dr} + (n+1) S_n^m \right] r^{n-1} \dfrac{\partial Y_n^m}{\sin\theta\, \partial \phi} \end{array} \right\} \qquad (2.6)$$

*T*-type (toroidal type) magnetic field

$$H_T = \left\{ \begin{array}{l} 0, \\[2ex] -T_n^m(r) r^n \dfrac{\partial Y_n^m}{\sin\theta\, \partial\phi}, \\[2ex] T_n^m(r) r^n \dfrac{\partial Y_n^m}{\partial \theta} \end{array} \right\} \qquad (2.7)$$

In (2.6) and (2.7), $Y_n^m$ is a surface spherical harmonic with degree $n$ and order $m$.

$$Y_n^m = P_n^m(\cos\theta) \begin{array}{c}\cos\\ \sin\end{array} m\phi \qquad (2.8)$$

Curl $H$ and $\nabla^2 H$ for the magnetic fields in (2.6) and (2.7) are calculated as follows:

*S*-type magnetic field

$$\left.\begin{aligned}
\operatorname{curl} H_S &= \begin{cases} 0, \\[2ex] \left[r\dfrac{d^2S_n^m}{dr^2} + 2(n+1)\dfrac{dS_n^m}{dr}\right]r^{n-1}\dfrac{\partial Y_n^m}{\sin\theta\,\partial\phi}, \\[2ex] -\left[r\dfrac{d^2S_n^m}{dr^2} + 2(n+1)\dfrac{dS_n^m}{dr}\right]r^{n-1}\dfrac{\partial Y_n^m}{\partial\theta} \end{cases} \\[2ex]
\nabla^2 H_S &= \begin{cases} -n(n+1)\left[\dfrac{d^2S_n^m}{dr^2} + \dfrac{2(n+1)}{r}\dfrac{dS_n^m}{dr}\right]r^{n-1}Y_n^m, \\[2ex] -\left[r\dfrac{d^3S_n^m}{dr^3} + 3(n+1)\dfrac{d^2S_n^m}{dr^2} + \dfrac{2n(n+1)}{r}\dfrac{dS_n^m}{dr}\right]r^{n-1}\dfrac{\partial Y_n^m}{\partial\theta}, \\[2ex] -\left[r\dfrac{d^3S_n^m}{dr^3} + 3(n+1)\dfrac{d^2S_n^m}{dr^2} + \dfrac{2n(n+1)}{r}\dfrac{dS_n^m}{dr}\right]r^{n-1}\dfrac{\partial Y_n^m}{\sin\theta\,\partial\phi} \end{cases}
\end{aligned}\right\}\ldots(2.9)$$

*T*-type magnetic field

$$\left.\begin{aligned}
\operatorname{curl} H_T &= \begin{cases} -n(n+1)T_n^m r^{n-1}Y_n^m, \\[2ex] -\left[r\dfrac{dT_n^m}{dr} + (n+1)T_n^m\right]r^{n-1}\dfrac{\partial Y_n^m}{\partial\theta}, \\[2ex] -\left[r\dfrac{dT_n^m}{dr} + (n+1)T_n^m\right]r^{n-1}\dfrac{\partial Y_n^m}{\sin\theta\,\partial\phi} \end{cases} \\[2ex]
\nabla^2 H_T &= \begin{cases} 0, \\[2ex] -\left[\dfrac{d^2T_n^m}{dr^2} + \dfrac{2(n+1)}{r}\dfrac{dT_n^m}{dr}\right]r^n\dfrac{\partial Y_n^m}{\sin\theta\,\partial\phi}, \\[2ex] \left[\dfrac{d^2T_n^m}{dr^2} + \dfrac{2(n+1)}{r}\dfrac{dT_n^m}{dr}\right]r^n\dfrac{\partial Y_n^m}{\partial\theta} \end{cases}
\end{aligned}\right\}\ldots\ldots\ldots(2.10)$$

In the Bullard's convection-current model, the velocity field in the earth's core is assumed to be expressed as an arbitrary linear combination of the following two fields:

*S*-type velocity field

$$V_S = \begin{cases} -n(n+1)V_{S,n}^m(r)r^{n-1}Y_n^m, \\[2ex] -\left[r\dfrac{dV_{S,n}^m}{dr} + (n+1)V_{S,n}^m\right]r^{n-1}\dfrac{\partial Y_n^m}{\partial\theta}, \\[2ex] -\left[r\dfrac{dV_{S,n}^m}{dr} + (n+1)V_{S,n}^m\right]r^{n-1}\dfrac{\partial Y_n^m}{\sin\theta\,\partial\phi} \end{cases}\Bigg\}\ldots\ldots\ldots(2.11)$$

with $n = 2$ and $m = 2c$ [$2c$ means $\cos 2\phi$ in the expression (2.8)].

$T$-type velocity field

$$V = \begin{Bmatrix} 0, \\ -V_{T,n}^m(r) r^n \dfrac{\partial Y_n^m}{\sin\theta\,\partial\phi}, \\ V_{T,n}^m(r) r^n \dfrac{\partial Y_n^m}{\partial\theta} \end{Bmatrix} \qquad (2.12)$$

with $n = 1$ and $m = 0$.

The expressions for the magneto-hydrodynamical couplings of general (poloidal and toroidal) magnetic fields by general (poloidal and toroidal) velocity fields are given as follows. With the suffixes

$\alpha$: primary (inducing) magnetic field

$\beta$: velocity field

$\gamma$: secondary (induced) magnetic field

the orthogonal condition for Maxwell's equation (2.5) is expressed by

$$\int_0^a \int_0^\pi \int_0^{2\pi} \sum_\alpha [\nabla^2 H_\alpha + 4\pi\kappa \operatorname{curl}(V_\beta \times H_\alpha)] \cdot H_\gamma r^2 \sin\theta \, dr \, d\theta \, d\phi = 0 \qquad (2.13)$$

Executing integrations with respect to $\theta$ and $\phi$, we get

$$\left.\begin{aligned} \int_0^a [\sum_\alpha \widehat{S_\alpha S_\gamma} + \sum_\alpha \widehat{T_\alpha S_\gamma}] r^2 \, dr = 0 \\ \int_0^a [\sum_\alpha \widehat{S_\alpha T_\gamma} + \sum_\alpha \widehat{T_\alpha T_\gamma}] r^2 \, dr = 0 \end{aligned}\right\} \qquad (2.14)$$

where

$$\left.\begin{aligned} \widehat{S_\alpha S_\gamma} &= \int_0^\pi \int_0^{2\pi} [\nabla^2 H_{S\alpha} + 4\pi\kappa \operatorname{curl}(\sum_\beta V_\beta \times H_{S\alpha})] \cdot H_{S\gamma} \sin\theta \, d\theta \, d\phi \\ \widehat{T_\alpha S_\gamma} &= \int_0^\pi \int_0^{2\pi} [\nabla^2 H_{T\alpha} + 4\pi\kappa \operatorname{curl}(\sum_\beta V_\beta \times H_{T\alpha})] \cdot H_{S\gamma} \sin\theta \, d\theta \, d\phi \\ &\text{etc.} \end{aligned}\right\} \qquad (2.15)$$

We shall call $\widehat{S_\alpha S_\gamma}$, $\widehat{T_\alpha S_\gamma}$, $\widehat{S_\alpha T_\gamma}$, and $\widehat{T_\alpha T_\gamma}$ the coupling coefficients. Changing the independent and dependent variables by the following equations,

$$r = a\xi \quad (a\text{: radius of the earth's core})$$

$$\begin{pmatrix} S_n^m(r) \\ V_{S,n}^m(r) \end{pmatrix} = \frac{1}{a^{n-1}} \begin{pmatrix} S_n^m(\xi) \\ V_{S,n,m} V_{S,n}^m(\xi) \end{pmatrix}, \quad \begin{pmatrix} T_n^m(r) \\ V_{T,n}^m(r) \end{pmatrix} = \frac{1}{a^n} \begin{pmatrix} T_n^m(\xi) \\ V_{T,n,m} V_{T,n}^m(\xi) \end{pmatrix} \qquad (2.16)$$

we get the following expressions for the coupling coefficients.

Coupling by $S$-type velocity field:

$$\left.\begin{aligned}\widehat{S_\alpha S_\gamma} = {} & [I(\alpha,\gamma)n_\alpha(n_\alpha+1)f_S + yK(\alpha\gamma,\beta)n_\beta(n_\beta+1)g_1 \\ & - yK(\gamma\beta,\alpha)n_\alpha(n_\alpha+1)g_2]\underline{n_\gamma(n_\gamma+1)S_\gamma\xi^{n_\gamma-1}} \\ & + \left[I(\alpha,\gamma)n_\alpha(n_\alpha+1)\frac{\mathrm{d}(f_S\xi^2)}{\mathrm{d}\xi} + yK(\alpha\gamma,\beta)n_\beta(n_\beta+1)\frac{\mathrm{d}(g_1\xi^2)}{\mathrm{d}\xi}\right. \\ & \left. - yK(\gamma\beta,\alpha)n_\alpha(n_\alpha+1)\frac{\mathrm{d}(g_2\xi^2)}{\mathrm{d}\xi}\right]\underline{\overline{S}_\gamma\xi^{n_\gamma-2}}\end{aligned}\right\}\ldots(2.17)$$

$$\left.\begin{aligned}\widehat{T_\alpha S_\gamma} = {} & yL(\gamma\alpha,\beta)n_\beta(n_\beta+1)g_3\underline{n_\gamma(n_\gamma+1)S_\gamma\xi^{n_\gamma-1}} \\ & + yL(\gamma\alpha,\beta)n_\beta(n_\beta+1)\frac{\mathrm{d}(g_3\xi^2)}{\mathrm{d}\xi}\,\underline{\overline{S}_\gamma\xi^{n_\gamma-2}}\end{aligned}\right\}\ldots(2.18)$$

$$\left.\begin{aligned}\widehat{S_\alpha T_\gamma} = {} & \left[yL(\alpha\beta,\gamma)n_\gamma(n_\gamma+1)\overline{S}_\alpha\overline{V}_{S\beta}\,\xi^{n_\alpha+n_\beta-2}\right. \\ & + yL(\alpha\gamma,\beta)n_\beta(n_\beta+1)\frac{\mathrm{d}(g_1\xi^2)}{\mathrm{d}\xi} \\ & \left. + yL(\gamma\beta,\alpha)n_\alpha(n_\alpha+1)\frac{\mathrm{d}(g_2\xi^2)}{\mathrm{d}\xi}\right]\underline{T_\gamma\xi^{n_\gamma-1}}\end{aligned}\right\}\ldots(2.19)$$

$$\left.\begin{aligned}\widehat{T_\alpha T_\gamma} = {} & \left[I(\alpha,\gamma)n_\alpha(n_\alpha+1)f_T + yK(\alpha\beta,\gamma)n_\gamma(n_\gamma+1)T_\alpha\overline{V}_{S\beta}\,\xi^{n_\alpha+n_\beta-1}\right. \\ & \left. + yK(\alpha\gamma,\beta)n_\beta(n_\beta+1)\frac{\mathrm{d}(g_3\xi^2)}{\mathrm{d}\xi}\right]\underline{T_\gamma\xi^{n_\gamma-1}}\end{aligned}\right\}\ldots(2.20)$$

Coupling by $T$-type velocity field

$$\left.\begin{aligned}\widehat{S_\alpha S_\gamma} = {} & [I(\alpha,\gamma)n_\alpha(n_\alpha+1)f_S + xL(\beta\gamma,\alpha)n_\alpha(n_\alpha+1)g_4]\underline{n_\gamma(n_\gamma+1)S_\gamma\xi^{n_\gamma-1}} \\ & + \left[I(\alpha,\gamma)n_\alpha(n_\alpha+1)\frac{\mathrm{d}(f_S\xi^2)}{\mathrm{d}\xi} + xL(\beta\gamma,\alpha)n_\alpha(n_\alpha+1)\frac{\mathrm{d}(g_4\xi^2)}{\mathrm{d}\xi}\right]\underline{\overline{S}_\gamma\xi^{n_\gamma-2}}\end{aligned}\right\}(2.21)$$

$$\widehat{T_\alpha S_\gamma} = 0 \ldots\ldots(2.22)$$

$$\left.\begin{aligned}\widehat{S_\alpha T_\gamma} = {} & -\left[xK(\alpha\beta,\gamma)n_\gamma(n_\gamma+1)\overline{S}_\alpha V_{T\beta}\,\xi^{n_\alpha+n_\beta-1}\right. \\ & \left. + xK(\gamma\beta,\alpha)n_\alpha(n_\alpha+1)\frac{\mathrm{d}(g_4\xi^2)}{\mathrm{d}\xi}\right]\underline{T_\gamma\xi^{n_\gamma-1}}\end{aligned}\right\}\ldots(2.23)$$

$$\left.\begin{aligned}\widehat{T_\alpha T_\gamma} = \Big[ & I(\alpha, \gamma) n_\alpha (n_\alpha + 1) f_T \\ & + xL(\alpha\beta, \gamma) n_\gamma (n_\gamma + 1) T_\alpha V_{T\beta}\, \xi^{n_\alpha + n_\beta} \Big] \underline{T_\gamma \xi^{n_\gamma - 1}}\end{aligned}\right\} \quad \ldots (2.24)$$

where

$$\left.\begin{aligned} & y = 4\pi\kappa a V_{S,2,2c}\,, \qquad x = 4\pi\kappa a V_{T,1,0} \\ & \overline{S} = \left[\xi \frac{d}{d\xi} + (n+1)\right] S, \qquad \overline{V}_S = \left[\xi \frac{d}{d\xi} + (n+1)\right] V_S \\ & f_{\substack{S\\T}} = \left[\frac{d^2}{d\xi^2} + \frac{2(n+1)}{\xi}\frac{d}{d\xi}\right]\begin{bmatrix} S \\ T \end{bmatrix} \xi^{\left[\substack{n-1\\n+1}\right]} \\ & g_1 = \overline{S}_\alpha V_{S\beta} \xi^{n_\alpha + n_\beta - 3}, \qquad g_2 = S_\alpha \overline{V}_{S\beta} \xi^{n_\alpha + n_\beta - 3} \\ & g_3 = T_\alpha V_{S\beta} \xi^{n_\alpha + n_\beta - 2}, \qquad g_4 = S_\alpha V_{T\beta} \xi^{n_\alpha + n_\beta - 2} \end{aligned}\right\} \quad \ldots (2.25)$$

and

$$I(\alpha, \gamma) = \int_0^\pi \int_0^{2\pi} Y_\alpha Y_\gamma \sin\theta \, d\theta \, d\phi \quad \ldots (2.26)$$

$$K(\alpha\beta, \gamma) = \int_0^\pi \int_0^{2\pi} \left(\frac{\partial Y_\alpha}{\partial\theta}\frac{\partial Y_\beta}{\partial\theta} + \frac{\partial Y_\alpha}{\sin\theta\,\partial\phi}\frac{\partial Y_\beta}{\sin\theta\,\partial\phi}\right) Y_\gamma \sin\theta \, d\theta \, d\phi \quad \ldots (2.27)$$

$$L(\alpha\beta, \gamma) = \int_0^\pi \int_0^{2\pi} \left(\frac{\partial Y_\alpha}{\partial\theta}\frac{\partial Y_\beta}{\sin\theta\,\partial\phi} - \frac{\partial Y_\alpha}{\sin\theta\,\partial\phi}\frac{\partial Y_\beta}{\partial\theta}\right) Y_\gamma \sin\theta \, d\theta \, d\phi \quad \ldots (2.28)$$

In (2.26) to (2.28), $Y_\alpha$, for example, denotes $Y_{n_\alpha}^{m_\alpha}$.

The selection rules for the coupling coefficient integrals in (2.26) to (2.28) are as follows.

As to the integral $I\ (\alpha, \gamma)$, we must have

$$n_\alpha = n_\gamma\,, \qquad m_\alpha = m_\gamma \quad \ldots (2.29)$$

Otherwise the integral vanishes. $K\ (\alpha, \beta, \gamma)$ vanishes unless

$$n_\alpha + n_\beta + n_\gamma = \text{even}, \qquad m_\alpha \pm m_\beta = m_\gamma \quad \ldots (2.30)$$

$L\ (\alpha, \beta, \gamma)$ vanishes unless

$$n_\alpha + n_\beta + n_\gamma = \text{odd}, \qquad m_\alpha \pm m_\beta = m_\gamma \quad \ldots (2.31)$$

These are the selection rules for the magneto-hydrodynamical couplings.

In the Bullard convection-current model, the self-exciting dynamo is considered to be driven by $T_1^0$ and $S_2^{2c}$ types of velocity. Furthermore, it is a well-known fact that the magnetic field in the earth's mantle is of the dipole ($S_1^0$) type. So we shall now study the magneto-hydrodynamical couplings, which are main-

tained by $T_1^0$ and $S_2^{2c}$ types of velocity and in which the $S_1^0$ type of magnetic field is found as an element. In Figure 1 is shown the chain of couplings of magnetic fields up to the fourth harmonics. The arrows along (between) rows denote the couplings by the $T_1^0$ ($S_2^{2c}$) type of velocity. It is needless to say that the chain is continued infinitely with infinite number of magnetic fields. As is seen in Figure 1, magnetic fields of $S_1^0$, $T_2^0$, $T_2^{2c}$, and $T_2^{2S}$ types make a closed circuit of couplings with harmonics up to the second degree. We shall call this chain the $A$ approximation for the self-exciting process. Magnetic fields of $S_3^0$, $S_3^{2c}$, and $S_3^{2S}$ types become the elements of the coupling chain if harmonics up to the third are taken into consideration. This step may be called the $B$ approximation. Including harmonics up to the fourth, the chain expands and includes 12 types of magnetic fields. This step will be called the $C$ approximation. From the physical point of view, the self-exciting dynamo may be considered to be driven by magnetic fields of comparatively lower harmonics. Therefore, we shall, in the next section, study the problem in its $A$ step of approximation.

§3. The system in which we are going to solve the problem is shown in Figure 2. Since the equations (2.1) to (2.5) do not change if we go from a system at rest

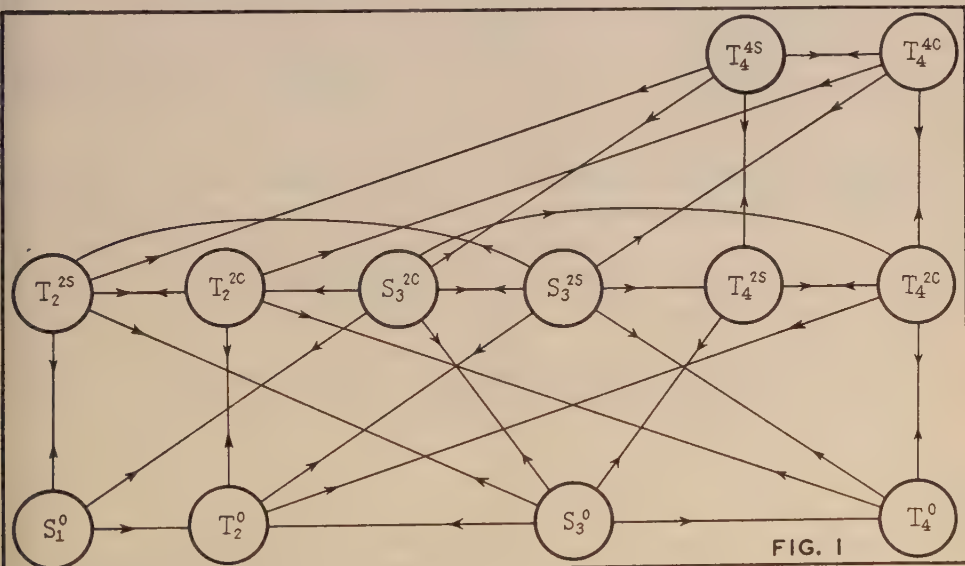


FIG. 1

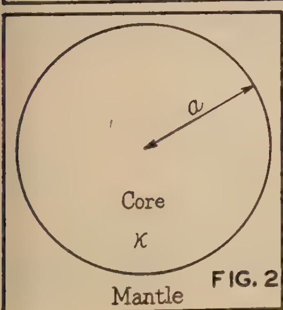


FIG. 2

FIG. 1—CHAIN OF COUPLINGS OF MAGNETIC FIELDS BY $T_1^0$ AND $S_2^{2C}$ TYPES OF FLUID MOTION

FIG. 2—SYSTEM OF THE CORE AND MANTLE

to a uniformly-rotating system of reference, we shall use the coordinates that are fixed to the rotating mantle. Therefore, $V_1^0(\xi)$ and $V_2^{2c}(\xi)$ in (2.11) to (2.25) denote the velocities relative to the rotating mantle. In (2.16), we put

$$V_1^0(r) = \frac{1}{a} V_{1,0} V_1^0(\xi), \qquad V_2^{2c}(r) = \frac{1}{a} V_{2,2c} V_2^{2c}(\xi) \quad \ldots\ldots\ldots\ldots (3.1)$$

where $V_{1,0}$ and $V_{2,2c}$ are constants of dimensions of velocities. In our present problem, $V_1^0(\xi)$ and $V_2^{2c}(\xi)$ are thought to be given *a priori*. Taking (2.11) and (2.12) into consideration and assuming "viscous" liquid in the earth's core, we shall put tentatively

$$V_1^0(\xi) = \begin{cases} 1-\xi \\ 0 \end{cases}, \qquad V_2^{2c}(\xi) = \begin{cases} (1-\xi)^2 \\ 0 \end{cases}, \qquad \text{for} \quad \begin{cases} 0 \le \xi \le 1 \\ \xi \ge 1 \end{cases} \quad \ldots\ldots (3.2)$$

Furthermore, we shall assume that the only magnetic field in the mantle is of the $S_1^0$ type (dipole type). The boundary conditions are that $H_r$, $H_\theta$, and $H_\phi$ are continuous and $I_r = 0$ at $\xi = 1$ $(r = a)$. These boundary conditions will be satisfied by putting

$$\left.\begin{aligned} S_1^0 + \frac{\xi}{3}\frac{dS_1^0}{d\xi} = 0, \qquad S_n^m = \frac{dS_n^m}{d\xi} = 0 \qquad (n \ne 1,\ m \ne 0) \\ T_n^m = 0, \qquad \text{at} \qquad \xi = 1 \end{aligned}\right\} \ldots\ldots (3.3)$$

We shall now study the problem in its $A$ step of approximation. Taking the results in §2 into consideration, we get

$$\left.\begin{aligned} &\int_0^1 [\widehat{S_1^0 S_1^0} + \widehat{T_2^0 S_1^0} + \widehat{T_2^{2c} S_1^0} + \widehat{T_2^{2S} S_1^0}]\xi^2 \, d\xi = 0, \\ &\int_0^1 [\widehat{S_1^0 T_2^0} + \widehat{T_2^0 T_2^0} + \widehat{T_2^{2c} T_2^0} + \widehat{T_2^{2S} T_2^0}]\xi^2 \, d\xi = 0, \\ &\text{etc.} \end{aligned}\right\} \ldots\ldots\ldots\ldots (3.4)$$

where

$$\widehat{S_1^0 S_1^0} = \frac{16}{3}\left(\frac{d^2 S_1^0}{d\xi^2} + \frac{4}{\xi}\frac{dS_1^0}{d\xi}\right)S_1^0 + \frac{8}{3}\frac{1}{\xi}\frac{d}{d\xi}\left[\xi^2\left(\frac{d^2 S_1^0}{d\xi^2} + \frac{4}{\xi}\frac{dS_1^0}{d\xi}\right)\right]\left(\xi\frac{dS_1^0}{d\xi} + 2S_1^0\right)$$

$$\widehat{T_2^0 S_1^0} = 0$$

$$\widehat{T_2^{2c,S} S_1^0} = -\frac{48 \times 24}{5}\binom{0}{1} y\xi^2 V_2^{2c} T_2^{2c,S} S_1^0$$

$$- \frac{48 \times 12}{5}\binom{0}{1} y \frac{1}{\xi}\frac{d}{d\xi}(\xi^4 V_2^{2c} T_2^{2c,S})\left(\xi\frac{dS_1^0}{d\xi} + 2S_1^0\right)$$

$$\widehat{S_1^0 T_2^0} = -\frac{16}{5} x S_1^0 \frac{\mathrm{d}V_1^0}{\mathrm{d}\xi} \xi^3 T_2^0$$

$$\widehat{T_2^0 T_2^0} = \frac{24}{5}\left(\xi \frac{\mathrm{d}^2 T_2^0}{\mathrm{d}\xi^2} + 6 \frac{\mathrm{d}T_2^0}{\mathrm{d}\xi}\right)\xi^3 T_2^0$$

$$\widehat{T_2^{2c,S} T_2^0} = -\frac{288 \times 6}{35}\begin{pmatrix}1\\0\end{pmatrix} y\left\{\frac{\mathrm{d}}{\mathrm{d}\xi}(\xi^4 V_2^{2c} T_2^{2c,S}) + \frac{\mathrm{d}}{\mathrm{d}\xi}(\xi^3 V_2^{2c})\xi T_2^{2c,S}\right\}\xi T_2^0$$

$$\widehat{S_1^0 T_2^{2c,S}} = -\frac{96 \times 2}{5}\begin{pmatrix}0\\1\end{pmatrix} y\left\{3\xi^3 V_2^{2c} \frac{\mathrm{d}}{\mathrm{d}\xi}\left[\frac{1}{\xi}\left(\xi \frac{\mathrm{d}S_1^0}{\mathrm{d}\xi} + 2S_1^0\right)\right]\right.$$

$$\left. + \frac{\mathrm{d}}{\mathrm{d}\xi}\left[\frac{\mathrm{d}}{\mathrm{d}\xi}(\xi^3 V_2^{2c}) S_1^0\right]\right\}\xi T_2^{2c,S}$$

$$\widehat{T_2^0 T_2^{2c,S}} = -\frac{288 \times 6}{35}\begin{pmatrix}1\\0\end{pmatrix} y\left\{\frac{\mathrm{d}}{\mathrm{d}\xi}(\xi^4 V_2^{2c} T_2^0) + \frac{\mathrm{d}}{\mathrm{d}\xi}(\xi^3 V_2^{2c})\xi T_2^0\right\}\xi T_2^{2c,S}$$

$$\widehat{T_2^{2c,S} T_2^{2c}} = \frac{48 \times 6}{5}\begin{pmatrix}1\\0\end{pmatrix}\left(\xi \frac{\mathrm{d}^2 T_2^{2c,S}}{\mathrm{d}\xi^2} + 6 \frac{\mathrm{d}T_2^{2c,S}}{\mathrm{d}\xi}\right)\xi^3 T_2^{2c} + \frac{96 \times 6}{5}\begin{pmatrix}0\\1\end{pmatrix} x\xi T_2^{2c,S} V_1^0 \xi^3 T_2^{2c}$$

$$\widehat{T_2^{2c,S} T_2^{2S}} = \frac{48 \times 6}{5}\begin{pmatrix}0\\1\end{pmatrix}\left(\xi \frac{\mathrm{d}^2 T_2^{2c,S}}{\mathrm{d}\xi^2} + 6 \frac{\mathrm{d}T_2^{2c,S}}{\mathrm{d}\xi}\right)\xi^3 T_2^{2S} - \frac{96 \times 6}{5}\begin{pmatrix}1\\0\end{pmatrix} x\xi T_2^{2c,S} V_1^0 \xi^3 T_2^{2S} \qquad \ldots.(3.5)$$

In (3.5), $\langle{}^0_1\rangle$ in the expression for $\widehat{T_2^{2cS} S_1^0}$, for example, means 0 and 1 for $T_2^{2c}$ and $T_2^{2S}$, respectively. From (3.4) and (3.5), we get

$$\xi \frac{\mathrm{d}^2 S_1^0}{\mathrm{d}\xi^2} + 4 \frac{\mathrm{d}S_1^0}{\mathrm{d}\xi} = \frac{9 \times 24}{5} y\xi^3 V_2^{2c} T_2^{2S}$$

$$\xi \frac{\mathrm{d}^2 T_2^0}{\mathrm{d}\xi^2} + 6 \frac{\mathrm{d}T_2^0}{\mathrm{d}\xi} = \frac{2}{3} x \frac{\mathrm{d}V_1^0}{\mathrm{d}\xi} S_1^0 + \frac{72}{7}\frac{y}{\xi^2}\left[\frac{\mathrm{d}}{\mathrm{d}\xi}(\xi^4 V_2^{2c} T_2^{2c}) + \frac{\mathrm{d}}{\mathrm{d}\xi}(\xi^3 V_2^{2c})\xi T_2^{2c}\right]$$

$$\xi \frac{\mathrm{d}^2 T_2^{2c}}{\mathrm{d}\xi^2} + 6 \frac{\mathrm{d}T_2^{2c}}{\mathrm{d}\xi} = \frac{6}{7}\frac{y}{\xi^2}\left[\frac{\mathrm{d}}{\mathrm{d}\xi}(\xi^4 V_2^{2c} T_2^0) + \frac{\mathrm{d}}{\mathrm{d}\xi}(\xi^3 V_2^{2c})\xi T_2^0\right] - 2x V_1^0 \xi T_2^{2S}$$

$$\xi \frac{\mathrm{d}^2 T_2^{2S}}{\mathrm{d}\xi^2} + 6 \frac{\mathrm{d}T_2^{2S}}{\mathrm{d}\xi} = 2x V_1^0 \xi T_2^{2c} + \frac{2}{3}\frac{y}{\xi^2}\left[3\xi^3 V_2^{2c} \frac{\mathrm{d}}{\mathrm{d}\xi}\left\{\frac{\mathrm{d}S_1^0}{\mathrm{d}\xi} + \frac{2}{\xi} S_1^0\right\} + \frac{\mathrm{d}}{\mathrm{d}\xi}\left\{\frac{\mathrm{d}}{\mathrm{d}\xi}(\xi^3 V_2^{2c}) S_1^0\right\}\right] \qquad \ldots.(3.6)$$

These are the differential equations for the radial functions $S_1^0$, $T_2^0$, $T_2^{2c}$, and $T_2^{2S}$.

Thus our problem is reduced to solve (3.6) under the boundary conditions in (3.3). It is easily seen that this is an eigen-value problem for $x = 4\pi\kappa a V_{1,0}$ and $y = 4\pi\kappa a V_{2,2c}$. If we get real eigen-values for $x$ and $y$ by solving the problem, we

can thus prove that the process proposed by Bullard is self-exciting. It is, however, almost hopeless to find the eigen-values by the trial-and-error method. We shall try to find them in an approximate method. Taking (3.3) into consideration, we shall put

$$S_1^0(\xi) = A_0\left(1 - \frac{3}{4}\xi\right) + A_1\xi\left(1 - \frac{4}{5}\xi\right) + \cdots + A_n\xi^n\left(1 - \frac{n+3}{n+4}\xi\right) + \cdots \quad (3.7)$$

$$\begin{Bmatrix} T_2^0(\xi) \\ T_2^{2c}(\xi) \\ T_2^{2S}(\xi) \end{Bmatrix} = (1-\xi)\left[\begin{Bmatrix} B_0 \\ C_0 \\ D_0 \end{Bmatrix} + \begin{Bmatrix} B_1 \\ C_1 \\ D_1 \end{Bmatrix}\xi + \cdots + \begin{Bmatrix} B_n \\ C_n \\ D_n \end{Bmatrix}\xi^n + \cdots\right] \ldots (3.8)$$

where $A_0$, $A_1$, $\cdots$ are constants to be determined. Inserting (3.7) and (3.8) into (3.4), we get the following types of equations:

$$-6A_0 - \frac{8}{3}A_1 - \frac{2}{3}A_2 - \frac{24}{35}yD_0 - \frac{72}{175}yD_1 - \frac{72}{25 \times 11}yD_2 + \cdots = 0 \ldots (3.9)$$

In order that these equations are compatible, the determinant formed by the coefficients must be equal to zero. Putting

$$\alpha = \frac{x}{y} \ldots\ldots\ldots\ldots (3.10)$$

in the determinant equation, we get the value of $y = 4\pi\kappa a V_{2,2c}$ as the function of $\alpha$. The results obtained by putting the coefficients of $(A_j, B_j, C_j, D_j)$ with $j \geq n$ equal to zero will be called the $n$th approximations. It is to be noted that all the $n$th approximations thus obtained are the $A$ approximation in the sense of §2. In view of these circumstances, it may be preferred to call the above $n$th approximations as the $A_n$ approximations. In Table 1 is shown the determinant for the $A_3$ approximation. The results of computations for the $A_1$, $A_2$, and $A_3$ approximations are shown in Table 2. In order to express "magnetic Reynold's

TABLE 2—*Eigen-values obtained by the approximate method*

| $\alpha$ | $Y = 8/3\,y$ | | | $X = 1/4\,x$ |
|---|---|---|---|---|
| | $A_1$ | $A_2$ | $A_3$ | $A_3$ |
| 0 | 169.36 | 269.7 | 323.2 | 0 |
| 1 | 163.54 | 265.6 | 267 | 25.0 |
| 10 | 82.322 | 94.80 | 111 | 105 |
| 100 | 68.664 | 72.05 | 92.8 | 870 |
| $\infty$ | 68.507 | 71.71 | 92.3 | $\infty$ |

number" in terms of the maximum velocities of $T_1^0$ and $S_2^{2c}$ types, $Y = 8/3\,y$ and $X = 1/4\,x$ are shown in Table 2. From Table 2, we see that our method of

TABLE 1—*Equations for the $A_3$ approximation*

| $A_0$ | $A_1$ | $A_2$ | $B_0$ | $B_1$ | $B_2$ | $C_0$ | $C_1$ | $C_2$ | $D_0$ | $D_1$ | $D_2$ |
|---|---|---|---|---|---|---|---|---|---|---|---|
| $-6$ | $-\frac{8}{3}$ | $-\frac{2}{3}$ | 0 | 0 | 0 | 0 | 0 | 0 | $-\frac{24}{35}y$ | $-\frac{72}{175}y$ | $-\frac{72}{25\times 11}y$ |
| $-\frac{56}{15}$ | $-\frac{32}{9}$ | $-\frac{8}{3}$ | 0 | 0 | 0 | 0 | 0 | 0 | $-\frac{32}{175}y$ | $-\frac{288}{175\times 11}y$ | $-\frac{32}{25\times 11}y$ |
| $-\frac{8}{3}$ | $-\frac{32}{9}$ | $-\frac{220}{63}$ | 0 | 0 | 0 | 0 | 0 | 0 | $\frac{24}{35\times 11}y$ | 0 | $-\frac{16}{65\times 11}y$ |
| $\frac{1}{30}x$ | $\frac{34}{35\times 45}x$ | $\frac{2}{15\times 9}x$ | $-\frac{24}{35}$ | $-\frac{18}{35}$ | $-\frac{2}{5}$ | $\frac{72}{35\times 55}y$ | $\frac{48}{35\times 55}y$ | $\frac{432}{35\times 55\times 13}y$ | 0 | 0 | 0 |
| $\frac{1}{42}x$ | $\frac{2}{125}x$ | $\frac{28}{(15)^2\times 11}x$ | $-\frac{18}{35}$ | $-\frac{44}{35\times 3}$ | $-\frac{26}{25\times 3}$ | $\frac{72}{35\times 55}y$ | $\frac{48}{35\times 55}y$ | $\frac{432}{35\times 55\times 13}y$ | 0 | 0 | 0 |
| $\frac{4}{25\times 9}x$ | $\frac{8\times 19}{25\times 45\times 11}x$ | $\frac{2}{(15)^2}x$ | $-\frac{2}{5}$ | $-\frac{26}{25\times 3}$ | $-\frac{248}{25\times 33}$ | $\frac{8\times 102}{35\times 55\times 13}y$ | $\frac{9\times 432}{(35)^2\times 11\times 13}y$ | $\frac{72\times 38}{(35)^2\times 11\times 13}y$ | 0 | 0 | 0 |
| 0 | 0 | 0 | $\frac{72}{35\times 55}y$ | $\frac{48}{35\times 55}y$ | $\frac{432}{35\times 55\times 13}y$ | $-\frac{288}{35}$ | $-\frac{216}{35}$ | $-\frac{24}{5}$ | $\frac{24}{35\times 5}x$ | $\frac{24}{25\times 11}x$ | $\frac{16}{25\times 11}x$ |
| 0 | 0 | 0 | $\frac{72}{35\times 55}y$ | $\frac{48}{35\times 55}y$ | $\frac{432}{35\times 55\times 13}y$ | $-\frac{216}{35}$ | $-\frac{176}{35}$ | $-\frac{104}{25}$ | $\frac{24}{25\times 11}x$ | $\frac{16}{25\times 11}x$ | $\frac{144}{25\times 11\times 13}x$ |
| 0 | 0 | 0 | $\frac{8\times 102}{35\times 55\times 13}y$ | $\frac{9\times 432}{(35)^2\times 11\times 13}y$ | $\frac{72\times 38}{(35)^2\times 11\times 13}y$ | $-\frac{24}{5}$ | $-\frac{104}{25}$ | $-\frac{16\times 62}{25\times 11}$ | $\frac{16}{25\times 11}x$ | $\frac{144}{25\times 11\times 13}x$ | $\frac{144}{35\times 11\times 13}x$ |
| $\frac{38}{35}y$ | $\frac{72}{125}y$ | $\frac{1532}{35\times 15\times 11}y$ | 0 | 0 | 0 | $-\frac{24}{35\times 5}x$ | $-\frac{24}{25\times 11}x$ | $-\frac{16}{25\times 11}x$ | $-\frac{288}{35}$ | $-\frac{216}{35}$ | $-\frac{24}{5}$ |
| $\frac{62}{35\times 3}y$ | $\frac{4\times 2546}{35\times 25\times 33}y$ | $\frac{8\times 19}{25\times 33}y$ | 0 | 0 | 0 | $-\frac{24}{25\times 11}x$ | $-\frac{16}{25\times 11}x$ | $-\frac{144}{25\times 11\times 13}x$ | $-\frac{216}{35}$ | $-\frac{176}{35}$ | $-\frac{104}{25}$ |
| $\frac{274}{25\times 33}y$ | $\frac{8\times 113}{125\times 33}y$ | $\frac{8\times 13}{25\times 33}y$ | 0 | 0 | 0 | $-\frac{16}{25\times 11}x$ | $-\frac{144}{25\times 11\times 13}x$ | $-\frac{144}{35\times 11\times 13}x$ | $-\frac{24}{5}$ | $-\frac{104}{25}$ | $-\frac{16\times 62}{25\times 11}$ |

approximation gives slowly increasing and converging real eigen-values, and it seems plausible that the process proposed by Bullard is self-exciting and is capable of maintaining the magnetic fields. As this is an important conclusion, we shall, in the next section, make some numerical checks for it.

§4. As is shown in Table 2, we have got the approximate value $Y = 92.3$ in the case when $\alpha = x/y \to \infty$. We shall show that this value of $Y$ is a good approximation for the eigen-value for this case. Assuming that the $S_1^0$ type of magnetic field is of finite order, we get, from the first equation in (3.6), the $T_2^{2s}$ field of finite order. Making $x \to \infty$ in the fourth equation, we see that the $T_2^{2c}$ field becomes zero. The $T_2^0$ field becomes the order of $x$ by the second and also by the third equations. Thus putting

$$T_2^0(\xi) = x\overline{T}_2^0(\xi) \qquad (4.1)$$

and making $x \to \infty$, we get, taking (3.2) and (3.6) into consideration,

$$\left.\begin{aligned} S_1^0(\xi) &= -\frac{3}{2}\left(\xi\frac{d^2\overline{T}_2^0}{d\xi^2} + 6\frac{d\overline{T}_2^0}{d\xi}\right) \\ T_2^{2c}(\xi) &= 0 \\ T_2^{2S}(\xi) &= \frac{3}{7}y\left[\xi(1-\xi)\frac{d\overline{T}_2^0}{d\xi} + (7-11\xi)\overline{T}_2^0\right] \end{aligned}\right\} \qquad (4.2)$$

$$\left.\begin{aligned} &\frac{d^4\overline{T}_2^0}{d\xi^4} + \frac{12}{\xi}\frac{d^3\overline{T}_2^0}{d\xi^3} + \frac{28}{\xi^2}\frac{d^2\overline{T}_2^0}{d\xi^2} \\ &\qquad + \frac{36 \times 12}{35}y^2(1-\xi)^2\xi\left[\xi(1-\xi)\frac{d\overline{T}_2^0}{d\xi} + (7-11\xi)\overline{T}_2^0\right] = 0 \end{aligned}\right\} \qquad (4.3)$$

The boundary conditions in (3.3) will be satisfied by putting

$$\overline{T}_2^0(\xi) = 0 \qquad (4.4)$$

and

$$Q(\xi) = \frac{d^3\overline{T}_2^0}{d\xi^3} + 10\frac{d^2\overline{T}_2^0}{d\xi^2} + 18\frac{d\overline{T}_2^0}{d\xi} = 0 \qquad (4.5)$$

at $\xi = 1$. $\overline{T}_2^0$ must also be finite at $\xi = 0$. Thus, the problem in this special case is reduced to solve (4.3) under the boundary conditions (4.4) and (4.5). The exact eigen-value $Y$ for this case is obtained by the trial-and-error method as follows. Expanding $\overline{T}_2^0(\xi)$ in (4.3) in power-series of $\xi$, we get the following two independent solutions

$$\left.\begin{aligned} &\text{Solution I for which} && \overline{T}_2^0 = 1, && \frac{d\overline{T}_2^0}{d\xi} = \frac{d^2\overline{T}_2^0}{d\xi^2} = \frac{d^3\overline{T}_2^0}{d\xi^3} = 0 \\ &\text{Solution II for which} && \frac{d\overline{T}_2^0}{d\xi} = 1, && \overline{T}_2^0 = \frac{d^2\overline{T}_2^0}{d\xi^2} = \frac{d^3\overline{T}_2^0}{d\xi^3} = 0 \end{aligned}\right\} \qquad (4.6)$$

at $\xi = 0$. The most general solution of (4.3) is given by

$$\overline{T}_2^0(\xi) = A \times \text{Solution I} + B \times \text{Solution II} \qquad (4.7)$$

where $A$ and $B$ are undetermined constants. Integrating (4.3) with (4.6) numerically, we can determine the solutions I and II, and using the numerical values thus obtained, we get two equations to determine $A$ and $B$. The determinant $\Delta$ formed by the coefficients of $A$ and $B$ in these two equations

$$\Delta = \begin{vmatrix} \overline{T}_2^0(\xi = 1) \text{ for Sol. I} & \overline{T}_2^0(\xi = 1) \text{ for Sol. II} \\ Q(\xi = 1) \text{ for Sol. I} & Q(\xi = 1) \text{ for Sol. II} \end{vmatrix} \qquad (4.8)$$

will become zero for the exact eigen-value $Y$. In order to obtain the exact eigen-value $Y$, the value of the determinant $\Delta$ is evaluated for several $Y$'s. The results obtained are shown in Table 3.

TABLE 3—*Values of $\Delta$ for $Y$'s*

| $y^2$ | $Y$ | $\Delta$ |
|---|---|---|
| 0 | 0 | +18 |
| 1200 | 92.37 | +12 |
| 1658 | 108.5 | + 8.2 |
| 2400 | 130.6 | − 0.3 |
| 3600 | 160.0 | −23 |
| 4800 | 184.8 | −63 |

The exact eigen-value is thus shown to be at $Y = 130.6$ ($y^2 = 2400$). The value $Y = 92.3$ in Table 2 is a fairly good approximation to this exact value.

An effective method of approximation in treating the above problem is devised as follows. Putting

$$T_2^0(\xi) = x\overline{T}_2^0(\xi) \qquad (4.9)$$

in (3.6) and making $x \to \infty$, we get as in (4.2) and (4.3),

$$T_2^{2S}(\xi) = \frac{3y}{7\xi^3 V_1^0(\xi)} \left[\frac{d}{d\xi}(\xi^4 V_2^{2c}\overline{T}_2^0) + \frac{d}{d\xi}(\xi^3 V_2^{2c})\xi\overline{T}_2^0\right] \qquad (4.10)$$

$$\frac{d^2 S_1^0}{d\xi^2} + \frac{4}{\xi}\frac{dS_1^0}{d\xi} = \frac{9 \times 24}{5} y\xi^2 V_2^{2c}(\xi) T_2^{2S} \qquad (4.11)$$

$$\frac{d^2\overline{T}_2^0}{d\xi^2} + \frac{6}{\xi}\frac{d\overline{T}_2^0}{d\xi} = \frac{2}{3\xi}\frac{dV_1^0}{d\xi} S_1^0 \qquad (4.12)$$

The boundary conditions are

$$\overline{T}_2^0(\xi) = 0 \qquad (4.13)$$

$$\frac{dS_1^0}{d\xi} + \frac{3}{\xi} S_1^0 = 0 \qquad (4.14)$$

at $\xi = 1$. Generalizing (3.2), we shall assume

$$V_1^0(\xi) = \xi^r(1 - \xi), \qquad V_2^{2*}(\xi) = \xi^r(1 - \xi)^2 \ldots\ldots\ldots\ldots (4.15)$$

Taking (4.13) into consideration, we shall put

$$\overline{T}_2^0(\xi) = \sum_n^\infty A_n \overline{T}_2^0(\xi, n), \qquad \overline{T}_2^0(\xi, n) = \xi^n(1 - \xi) \ldots\ldots\ldots (4.16)$$

for $\overline{T}_2^0(\xi)$. $A_n$'s ($n = 0, 1, \cdots$) in (4.16) are constants to be determined. Inserting (4.16) into (4.10) and (4.11), and taking (4.14) into consideration, we get

$$S_1^0(\xi) = \frac{24 \times 27}{35} y^2 \sum A_n S_1^0(\xi, n) \ldots\ldots\ldots\ldots\ldots (4.17)$$

in which $S_1^0(\xi, n)$ is

$$\left.\begin{aligned} S_1^0(\xi, n) = &-\frac{1}{3}\left(\frac{n'+7}{N+4} - \frac{4n'+33}{N+5} + \frac{6n'+57}{N+6} - \frac{4n'+43}{N+7} + \frac{n'+12}{N+8}\right) \\ &+ \frac{n'+7}{(N+4)(N+7)}\xi^{N+4} - \frac{4n'+33}{(N+5)(N+8)}\xi^{N+5} + \frac{6n'+57}{(N+6)(N+9)}\xi^{N+6} \\ &- \frac{4n'+43}{(N+7)(N+10)}\xi^{N+7} + \frac{n'+12}{(N+8)(N+11)}\xi^{N+8} \end{aligned}\right\} (4.18)$$

In (4.18), $n'$ and $N$ are

$$n' = n + 2\sigma, \qquad N = n' - \tau = n + 2\sigma - \tau \ldots\ldots\ldots\ldots (4.19)$$

respectively. In this way, we can satisfy the two equations (4.10) and (4.11) among the required three. The third equation (4.12) is replaced by

$$\int_0^1 \xi^6 \overline{T}_2^0(\xi, n)\left[\frac{d^2\overline{T}_2^0}{d\xi^2} + \frac{6}{\xi}\frac{d\overline{T}_2^0}{d\xi} - \frac{2}{3\xi}\frac{dV_1^0}{d\xi} S_1^0\right] d\xi = 0 \qquad (n = 0, 1, 2, \cdots) \ldots (4.20)$$

in which $\overline{T}_2^0$ and $S_1^0$ are to be taken as those in (4.16) and (4.17). If we take (4.16) into consideration, we see at once that (4.20) is nothing but the second equation in (3.4) from which (4.12) itself is obtained. Executing the integral in (4.20), we get the equations of the same types as those in Table 1. Equating the determinant formed by the coefficients of $A_n$'s to zero, we have the equation by which the eigen-value $y = 4\pi\kappa a V_{2,2c}$ is determined. By the present method, better approxi-

Table 4—*Eigen-values for the case $\sigma = \tau = 0$ obtained by the new approximate method*

| Approximation | $Y$ |
|---|---|
| 1 | 111.7 |
| 2 | 129.3 |
| 3 | 130.2 |
| exact | 130.6 |

mation for $y$ is obtained with less numerical computations than by that in §3. In fact, putting $\sigma = \tau = 0$ in (4.15) and using (4.20), we get the value of $Y = 8/3y$ as is shown in Table 4. In Table 4, the second approximation, for example, means the value of $Y$ which is obtained by using $\overline{T}_2^0(\xi) = A_0\overline{T}_2^0(\xi, 0) + A_1\overline{T}_2^0(\xi, 1)$ and solving the determinant equation of rank 2. From this Table, we see that our approximate values for $Y$ agree with the exact value satisfactorily well. Looking at the result from a different angle, we may say that the results in §3 and the present section are checked in an independent way.

In (3.2), we put

$$V_1^0(\xi) = 1 - \xi, \qquad V_2^{2c}(\xi) = (1 - \xi)^2 \quad \text{(4.21)}$$

tentatively, for the radial parts of the velocity fields. There is, however, no reason why the radial functions should be of these types. In order to make the matter clearer, we put

$$V_1^0(\xi) = \xi^\tau(1 - \xi), \qquad V_2^{2c}(\xi) = \xi^\sigma(1 - \xi)^2 \quad \text{(4.22)}$$

in (4.15). We shall now study whether or not the self-exciting dynamo is possible by the fluid motions of the types as in (4.22). For the larger values of $\sigma$ or $\tau$, the depth of the maximum fluid motions becomes the shallower. Thus, the value of $\xi$ for which the radial component of the velocity field of $S_2^{2c}$ type becomes maximum is given by

$$\xi = \xi_m \text{ (say)} = \frac{\sigma + 1}{\sigma + 3} \quad \text{(4.23)}$$

The maximum value of the radial velocity of $S_2^{2c}$ type is given by

$$\text{Max. vel.} = 18\xi_m^{\sigma+1}(1 - \xi_m)^2 V_{2,2c} \quad \text{(4.24)}$$

where $V_{2,2c}$ is the constant in (4.22). Defining $Y$ by the following equation

$$Y = 4\pi\kappa a \text{ (Max. vel.)} \quad \text{(4.25)}$$

the values of $Y$ are calculated for several $\sigma = \tau$ up to the second approximation. The first approximations for $Y$ differ but little from the second approximations which are shown in Table 5.

TABLES 5 AND 6—*Eigen-values for the cases with various $\sigma$ and $\tau$*

TABLE 5

| $\sigma = \tau$ | $Y$ |
|---|---|
| 0 | 129.3 |
| 2 | 98.2 |
| 4 | 44.5 |
| 8 | 28.9 |
| 16 | 25.6 |

TABLE 6

| $\sigma$ | $\tau$ | $Y$ |
|---|---|---|
| 2 | 0 | 56.2 |
| 4 | 0 | 42.2 |
| 8 | 0 | 32.2 |
| 0 | 2 | 154.0 |
| 0 | 8 | 90.8 |

From Table 5, we see that the self-exciting dynamo is possible for all $\sigma = \tau$ studied and the values of $Y$ do not differ much from that for $\sigma = \tau = 0$. In addition

to the results in Table 5, the values of $Y$ are calculated for several $\sigma$ and $\tau$ ($\neq \sigma$). Only the first approximation for $Y$ is calculated, and the results of calculations are shown in Table 6.

In view of the results obtained in §3 and the present section, we may say that the self-exciting dynamo is possible by a considerable variety of fluid motions. The only condition required for the existence of the self-exciting dynamo is that the radial velocity is of the order of magnitude for which $Y$ in (4.25) becomes

$$Y \approx 10^2 \qquad (4.26)$$

Putting $a = 3.5 \times 10^8$ cm and $\kappa = 3 \times 10^{-6}$ *emu*, the corresponding maximum velocity in the earth's core is calculated to be

$$\text{Max. vel.} \approx 0.01 \text{ cm/sec} \qquad (4.27)$$

§5. So far, we have studied the problem in its $A$ step of approximation. In our discussions in §3 and §4, only the magnetic fields of $n$, $m \leq 2$ are taken into account. It is, however, not self-evident from the beginning that the magnetic fields of higher harmonics play no important roles in our self-exciting dynamo. We shall now estimate the relative importance of the magnetic fields of higher harmonics in driving the dynamo. We shall study the problem in its $B$ and $C$ steps of approximations. As is stated in §2, in the $C$ step of approximation, the following 12 types of magnetic fields are included in our induction chain: $S_1^0$, $T_2^0$, $T_2^{2c}$, $T_2^{2S}$, $S_3^0$, $S_3^{2c}$, $S_3^{2S}$, $T_4^0$, $T_4^{2c}$, $T_4^{2S}$, $T_4^{4c}$, $T_4^{4S}$. In the same way as in §3, the following 12 equations are obtained from (2.14) to (2.28):

$$\frac{8}{3}\left(\frac{d^2 S_1^0}{d\xi^2} + \frac{4}{\xi}\frac{dS_1^0}{d\xi}\right) - \frac{96 \times 6}{5} y T_2^{2S} V_2^{2c} \xi^2$$
$$+ \frac{96 \times 12}{7} y\left[\left(\xi \frac{dS_3^{2c}}{d\xi} + 4S_3^{2c}\right)V_2^{2c} + S_3^{2c}\left(\xi \frac{dV_2^{2c}}{d\xi} + 3V_2^{2c}\right)\right]\xi^2 = 0$$

$$\frac{16}{5} x\left[\left(\xi \frac{dS_1^0}{d\xi} + 2S_1^0\right)V_1^0 \xi - \frac{d}{d\xi}(S_1^0 V_1^0 \xi^2)\right] + \frac{24}{5}\left(\frac{d^2 T_2^0}{d\xi^2} + \frac{6}{\xi}\frac{dT_2^0}{d\xi}\right)\xi^3$$
$$- \frac{288 \times 6}{35} y\left[T_2^{2c}\left(\xi \frac{dV_2^{2c}}{d\xi} + 3V_2^{2c}\right)\xi^3 + \frac{d}{d\xi}(T_2^{2c} V_2^{2c} \xi^4)\right]$$
$$- \frac{48 \times 6}{35} x\left[\left(\xi \frac{dS_3^0}{d\xi} + 4S_3^0\right)V_1^0 \xi^3 - \frac{d}{d\xi}(S_3^0 V_1^0 \xi^4)\right]$$
$$+ \frac{288 \times 6}{7} y\left[-\left(\xi \frac{dS_3^{2S}}{d\xi} + 4S_3^{2S}\right)\left(\xi \frac{dV_2^{2c}}{d\xi} + 3V_2^{2c}\right)\xi^3 + \frac{d}{d\xi}\left\{\left(\xi \frac{dS_3^{2S}}{d\xi} + 4S_3^{2S}\right)V_2^{2c}\xi^4\right\}\right.$$
$$\left. + 2\frac{d}{d\xi}\left\{S_3^{2S}\left(\xi \frac{dV_2^{2c}}{d\xi} + 3V_2^{2c}\right)\xi^4\right\}\right]$$
$$+ \frac{480 \times 6}{7} y\left[T_4^{2c}\left(\xi \frac{dV_2^{2c}}{d\xi} + 3V_2^{2c}\right)\xi^5 + \frac{d}{d\xi}(T_4^{2c} V_2^{2c} \xi^6)\right] = 0$$

$$-\frac{288 \times 6}{35} y\left[T_2^0\left(\xi \frac{dV_2^{2c}}{d\xi} + 3V_2^{2c}\right)\xi^3 + \frac{d}{d\xi}(T_2^0 V_2^{2c} \xi^4)\right]$$

$$
\begin{aligned}
&+ \frac{48 \times 6}{5}\left(\frac{\mathrm{d}^2 T_2^{2c}}{\mathrm{d}\xi^2} + \frac{6}{\xi}\frac{\mathrm{d}T_2^{2c}}{\mathrm{d}\xi}\right)\xi^3 + \frac{96 \times 6}{5}\, xT_2^{2S} V_1^0 \xi^3 \\
&- \frac{192 \times 6}{7}\, x\left[\left(\xi \frac{\mathrm{d}S_3^{2c}}{\mathrm{d}\xi} + 4S_3^{2c}\right)V_1^0\xi^3 - \frac{\mathrm{d}}{\mathrm{d}\xi}\,(S_3^{2c} V_1^0 \xi^4)\right] \\
&+ \frac{32 \times 6}{7}\, y\left[T_4^0\left(\xi \frac{\mathrm{d}V_2^{2c}}{\mathrm{d}\xi} + 3V_2^{2c}\right)\xi^5 + \frac{\mathrm{d}}{\mathrm{d}\xi}\,(T_4^0 V_2^{2c} \xi^6)\right] \\
&+ 96 \times 40 \times 6y\left[T_4^{4c}\left(\xi \frac{\mathrm{d}V_2^{2c}}{\mathrm{d}\xi} + 3V_2^{2c}\right)\xi^5 + \frac{\mathrm{d}}{\mathrm{d}\xi}\,(T_4^{4c} V_2^{2c} \xi^6)\right] = 0
\end{aligned}
$$

$$
\begin{aligned}
&\frac{96 \times 6}{5}\, y\left[\left(\xi \frac{\mathrm{d}S_1^0}{\mathrm{d}\xi} + 2S_1^0\right)\left(\xi \frac{\mathrm{d}V_2^{2c}}{\mathrm{d}\xi} + 3V_2^{2c}\right)\xi - \frac{\mathrm{d}}{\mathrm{d}\xi}\left\{\left(\xi \frac{\mathrm{d}S_1^0}{\mathrm{d}\xi} + 2S_1^0\right)V_2^{2c}\xi^2\right\}\right. \\
&\quad \left. - 2\frac{\mathrm{d}}{\mathrm{d}\xi}\left\{S_1^0\left(\xi \frac{\mathrm{d}V_2^{2c}}{\mathrm{d}\xi} + 3V_2^{2c}\right)\xi^2\right\}\right] \\
&\quad - \frac{96 \times 6}{5}\, xT_2^{2c} V_1^0 \xi^3 + \frac{48 \times 6}{5}\left(\frac{\mathrm{d}^2 T_2^{2S}}{\mathrm{d}\xi^2} + \frac{6}{\xi}\frac{\mathrm{d}T_2^{2S}}{\mathrm{d}\xi}\right)\xi^3 \\
&\quad + \frac{288 \times 6}{35}\, y\left[-\left(\xi \frac{\mathrm{d}S_3^0}{\mathrm{d}\xi} + 4S_3^0\right)\left(\xi \frac{\mathrm{d}V_2^{2c}}{\mathrm{d}\xi} + 3V_2^{2c}\right)\xi^3 + \frac{\mathrm{d}}{\mathrm{d}\xi}\left\{\left(\xi \frac{\mathrm{d}S_3^0}{\mathrm{d}\xi} + 4S_3^0\right)V_2^{2c}\xi^4\right\}\right. \\
&\quad \left. + 2\frac{\mathrm{d}}{\mathrm{d}\xi}\left\{S_3^0\left(\xi \frac{\mathrm{d}V_2^{2c}}{\mathrm{d}\xi} + 3V_2^{2c}\right)\xi^4\right\}\right] \\
&\quad - \frac{192 \times 6}{7}\, x\left[\left(\xi \frac{\mathrm{d}S_3^{2S}}{\mathrm{d}\xi} + 4S_3^{2S}\right)V_1^0\xi^3 - \frac{\mathrm{d}}{\mathrm{d}\xi}\,(S_3^{2S} V_1^0 \xi^4)\right] \\
&\quad + 96 \times 40 \times 6y\left[T_4^{4S}\left(\xi \frac{\mathrm{d}V_2^{2c}}{\mathrm{d}\xi} + 3V_2^{2c}\right)\xi^5 + \frac{\mathrm{d}}{\mathrm{d}\xi}\,(T_4^{4S} V_2^{2c} \xi^6)\right] = 0
\end{aligned}
$$

$$
\begin{aligned}
&\frac{288 \times 6}{35}\, yT_2^{2S} V_2^{2c}\xi^2 + \frac{48}{7}\left(\frac{\mathrm{d}^2 S_3^0}{\mathrm{d}\xi^2} + \frac{8}{\xi}\frac{\mathrm{d}S_3^0}{\mathrm{d}\xi}\right)\xi^2 \\
&\qquad + \frac{288 \times 2}{7}\, y\left[-3\left(\xi \frac{\mathrm{d}S_2^{2c}}{\mathrm{d}\xi} + 4S_3^{2c}\right)V_2^{2c}\xi^2 + 2S_3^{2c}\left(\xi \frac{\mathrm{d}V_2^{2c}}{\mathrm{d}\xi} + 3V_2^{2c}\right)\xi^2\right] \\
&\qquad - \frac{480 \times 6}{7}\, yT_4^{2S} V_2^{2c}\xi^4 = 0
\end{aligned}
$$

$$
\begin{aligned}
&\frac{384}{7}\, y\left[3\left(\xi \frac{\mathrm{d}S_1^0}{\mathrm{d}\xi} + 2S_1^0\right)V_2^{2c} - 2S_1^0\left(\xi \frac{\mathrm{d}V_2^{2c}}{\mathrm{d}\xi} + 3V_2^{2c}\right)\right] \\
&\qquad + \frac{576}{7}\, y\left[-3\left(\xi \frac{\mathrm{d}S_3^0}{\mathrm{d}\xi} + 4S_3^0\right)V_2^{2c}\xi^2 + 2S_3^0\left(\xi \frac{\mathrm{d}V_2^{2c}}{\mathrm{d}\xi} + 3V_2^{2c}\right)\xi^2\right] \\
&\qquad + \frac{240 \times 12}{7}\left(\frac{\mathrm{d}^2 S_3^{2c}}{\mathrm{d}\xi^2} + \frac{8}{\xi}\frac{\mathrm{d}S_3^{2c}}{\mathrm{d}\xi}\right)\xi^2 + \frac{480 \times 12}{7}\, xS_3^{2S} V_1^0\xi^2 \\
&\qquad - 96 \times 40 \times 6yT_4^{4S} V_2^{2c}\xi^4 = 0
\end{aligned}
$$

$$\frac{288 \times 6}{7} yT_2^0 V_2^{2c}\xi^2 - \frac{480 \times 12}{7} xS_3^{2c} V_1^0 \xi^2 + \frac{240 \times 12}{7}\left(\frac{d^2 S_3^{2S}}{d\xi^2} + \frac{8}{\xi}\frac{dS_3^{2S}}{d\xi}\right)\xi^2$$

$$- \frac{160 \times 6}{7} yT_4^0 V_2^{2c}\xi^4 + 96 \times 40 \times 6yT_4^{4c} V_2^{2c}\xi^4 = 0$$

$$\frac{64}{7} y\left[-4T_2^{2c}\left(\xi\frac{dV_2^{2c}}{d\xi} + 3V_2^{2c}\right)\xi^3 + 3\frac{d}{d\xi}(T_2^{2c}V_2^{2c}\xi^4)\right]$$

$$- \frac{16 \times 20}{21} x\left[-\left(\xi\frac{dS_3^0}{d\xi} + 4S_3^0\right)V_1^0\xi^3 + \frac{d}{d\xi}(S_3^0 V_1^0 \xi^4)\right]$$

$$+ \frac{160}{7} y\left[20\left(\xi\frac{dS_3^{2S}}{d\xi} + 4S_3^{2S}\right)\left(\xi\frac{dV_2^{2c}}{d\xi} + 3V_2^{2c}\right)\xi^3\right.$$

$$\left.- 6\frac{d}{d\xi}\left\{\left(\xi\frac{dS_3^{2S}}{d\xi} + 4S_3^{2S}\right)V_2^{2c}\xi^4\right\} - 12\frac{d}{d\xi}\left\{S_3^{2S}\left(\xi\frac{dV_2^{2c}}{d\xi} + 3V_2^{2c}\right)\xi^4\right\}\right]$$

$$+ \frac{80}{9}\left(\frac{d^2T_4^0}{d\xi^2} + \frac{10}{\xi}\frac{dT_4^0}{d\xi}\right)\xi^5$$

$$- \frac{480 \times 6}{77} y\left[10T_4^{2c}\left(\xi\frac{dV_2^{2c}}{d\xi} + 3V_2^{2c}\right)\xi^5 + 17\frac{d}{d\xi}(T_4^{2c}V_2^{2c}\xi^6)\right] = 0$$

$$\frac{960}{7} y\left[-4T_2^0\left(\xi\frac{dV_2^{2c}}{d\xi} + 3V_2^{2c}\right)\xi^3 + 3\frac{d}{d\xi}(T_2^0 V_2^{2c}\xi^4)\right]$$

$$- \frac{480 \times 20}{7} x\left[-\left(\xi\frac{dS_3^{2c}}{d\xi} + 4S_3^{2c}\right)V_1^0\xi^3 + \frac{d}{d\xi}(S_3^{2c}V_1^0\xi^4)\right]$$

$$- \frac{480 \times 6}{77} y\left[10T_4^0\left(\xi\frac{dV_2^{2c}}{d\xi} + 3V_2^{2c}\right)\xi^5 + 17\frac{d}{d\xi}(T_4^0 V_2^{2c}\xi^6)\right]$$

$$+ 80 \times 20\left(\frac{d^2T_4^{2c}}{d\xi^2} + \frac{10}{\xi}\frac{dT_4^{2c}}{d\xi}\right)\xi^5 + 160 \times 20xT_4^{2S}V_1^0\xi^5$$

$$- \frac{480 \times 48}{11} y\left[10T_4^{4c}\left(\xi\frac{dV_2^{2c}}{d\xi} + 3V_2^{2c}\right)\xi^5 + 17\frac{d}{d\xi}(T_4^{4c}V_2^{2c}\xi^6)\right] = 0$$

$$\frac{480}{7} y\left[20\left(\xi\frac{dS_3^0}{d\xi} + 4S_3^0\right)\left(\xi\frac{dV_2^{2c}}{d\xi} + 3V_2^{2c}\right)\xi^3\right.$$

$$\left.- 6\frac{d}{d\xi}\left\{\left(\xi\frac{dS_3^0}{d\xi} + 4S_3^0\right)V_2^{2c}\xi^4\right\} - 12\frac{d}{d\xi}\left\{S_3^0\left(\xi\frac{dV_2^{2c}}{d\xi} + 3V_2^{2c}\right)\xi^4\right\}\right]$$

$$- \frac{480 \times 20}{7} x\left[-\left(\xi\frac{dS_3^{2S}}{d\xi} + 4S_3^{2S}\right)V_1^0\xi^3 + \frac{d}{d\xi}(S_3^{2S}V_1^0\xi^4)\right]$$

$$- 160 \times 20xT_4^{2c}V_1^0\xi^5 + 80 \times 20\left(\frac{d^2T_4^{2S}}{d\xi^2} + \frac{10}{\xi}\frac{dT_4^{2S}}{d\xi}\right)\xi^5$$

$$- \frac{480 \times 48}{11} y\left[10T_4^{4S}\left(\xi\frac{dV_2^{2c}}{d\xi} + 3V_2^{2c}\right)\xi^5 + 17\frac{d}{d\xi}(T_4^{4S}V_2^{2c}\xi^6)\right] = 0$$

$$96 \times 80y\Big[-4T_2^{2c}\Big(\xi\frac{dV_2^{2c}}{d\xi} + 3V_2^{2c}\Big)\xi^3 + 3\frac{d}{d\xi}(T_2^{2c}V_2^{2c}\xi^4)\Big]$$
$$+ 96 \times 40y\Big[-20\Big(\xi\frac{dS_3^{2S}}{d\xi} + 4S_3^{2S}\Big)\Big(\xi\frac{dV_2^{2c}}{d\xi} + 3V_2^{2c}\Big)\xi^3$$
$$+ 6\frac{d}{d\xi}\Big\{\Big(\xi\frac{dS_3^{2S}}{d\xi} + 4S_3^{2S}\Big)V_2^{2c}\xi^4\Big\} + 12\frac{d}{d\xi}\Big\{S_3^{2S}\Big(\xi\frac{dV_2^{2c}}{d\xi} + 3V_2^{2c}\Big)\xi^4\Big\}\Big]$$
$$- \frac{480 \times 48}{11}y\Big[10T_4^{2c}\Big(\xi\frac{dV_2^{2c}}{d\xi} + 3V_2^{2c}\Big)\xi^5 + 17\frac{d}{d\xi}(T_4^{2c}V_2^{2c}\xi^6)\Big]$$
$$+ 256 \times 35 \times 20\Big(\frac{d^2T_4^{4c}}{d\xi^2} + \frac{10}{\xi}\frac{dT_4^{4c}}{d\xi}\Big)\xi^5 + 256 \times 140 \times 20xT_4^{4S}V_1^0\xi^5 = 0$$

$$96 \times 80y\Big[-4T_2^{2S}\Big(\xi\frac{dV_2^{2c}}{d\xi} + 3V_2^{2c}\Big)\xi^3 + 3\frac{d}{d\xi}(T_2^{2S}V_2^{2c}\xi^4)\Big]$$
$$+ 96 \times 40y\Big[20\Big(\xi\frac{dS_3^{2c}}{d\xi} + 4S_3^{2c}\Big)\Big(\xi\frac{dV_2^{2c}}{d\xi} + 3V_2^{2c}\Big)\xi^3$$
$$- 6\frac{d}{d\xi}\Big\{\Big(\xi\frac{dS_3^{2c}}{d\xi} + 4S_3^{2c}\Big)V_2^{2c}\xi^4\Big\} - 12\frac{d}{d\xi}\Big\{S_3^{2c}\Big(\xi\frac{dV_2^{2c}}{d\xi} + 3V_2^{2c}\Big)\xi^4\Big\}\Big]$$
$$- \frac{480 \times 48}{11}y\Big[10T_4^{2S}\Big(\xi\frac{dV_2^{2c}}{d\xi} + 3V_2^{2c}\Big)\xi^5 + 17\frac{d}{d\xi}(T_4^{2S}V_2^{2c}\xi^6)\Big]$$
$$- 256 \times 140 \times 20xT_4^{4c}V_1^0\xi^5 + 256 \times 35 \times 20\Big(\frac{d^2T_4^{4S}}{d\xi^2} + \frac{10}{\xi}\frac{dT_4^{4S}}{d\xi}\Big)\xi^5 = 0$$
$$\ldots.(5.1)$$

These are the differential equations for the radial functions $S_1^0$ , $T_2^0$ , $\cdots$ . The boundary conditions to be satisfied are shown in (3.3). Thus, in the $C$ step of approximation for our problem, we must solve (5.1) under the conditions in (3.3).

Making $x = 4\pi\kappa a V_{1,0} \to \infty$ in (5.1), and taking the similar way as in the last section, we have $T_2^0$ , $T_4^0 \to x$ and $T_2^{2c}$, $S_3^{2S}$, $T_4^{2c}$, $T_4^{4c}$, and $T_4^{4S} = 0$. Thus, the 12 simultaneous equations in (5.1) are reduced to seven in this special case. We shall now make a study on this special case. Putting

$$T_2^0(\xi) = x\overline{T}_2^0(\xi), \qquad T_4^0(\xi) = x\overline{T}_4^0(\xi)$$

in which $\overline{T}_2^0$ and $\overline{T}_4^0$ are of finite order, and making $x \to \infty$, we have

$$\frac{8}{3}\Big(\frac{d^2S_1^0}{d\xi^2} + \frac{4}{\xi}\frac{dS_1^0}{d\xi}\Big) - \frac{96 \times 6}{5}yT_2^{2S}V_2^{2c}\xi^2$$
$$+ \frac{96 \times 12}{7}y\Big[\Big(\xi\frac{dS_3^{2c}}{d\xi} + 4S_3^{2c}\Big)V_2^{2c} + S_3^{2c}\Big(\xi\frac{dV_2^{2c}}{d\xi} + 3V_2^{2c}\Big)\Big]\xi^2 = 0$$

$$-\frac{16}{5}S_1^0\frac{dV_1^0}{d\xi}\frac{1}{\xi} + \frac{24}{5}\Big(\frac{d^2\overline{T}_2^0}{d\xi^2} + \frac{6}{\xi}\frac{d\overline{T}_2^0}{d\xi}\Big) + \frac{48 \times 6}{35}S_3^0\frac{dV_1^0}{d\xi}\xi = 0$$

$$-\frac{288\times 6}{35}\,y\left[\overline{T}{}_2^0\left(\xi\frac{dV_2^{2c}}{d\xi}+3V_2^{2c}\right)+\frac{d}{d\xi}\left(\overline{T}{}_2^0V_2^{2c}\xi^4\right)\frac{1}{\xi^3}\right]+\frac{96\times 6}{5}T_2^{2S}V_1^0$$
$$+\frac{192\times 6}{7}S_3^{2c}\frac{dV_1^0}{d\xi}\xi+\frac{32\times 6}{7}\,y\left[\overline{T}{}_4^0\left(\xi\frac{dV_2^{2c}}{d\xi}+3V_2^{2c}\right)\xi^2+\frac{d}{d\xi}\left(\overline{T}{}_4^0V_2^{2c}\xi^6\right)\frac{1}{\xi^3}\right]=0$$

$$\frac{288\times 6}{35}\,yT_2^{2S}V_2^{2c}+\frac{48}{7}\left(\frac{d^2S_3^0}{d\xi^2}+\frac{8}{\xi}\frac{dS_3^0}{d\xi}\right)+\frac{288\times 2}{7}\,y\left[-3\left(\xi\frac{dS_3^{2c}}{d\xi}+4S_3^{2c}\right)V_2^{2c}\right.$$
$$\left.+2S_3^{2c}\left(\xi\frac{dV_2^{2c}}{d\xi}+3V_2^{2c}\right)\right]-\frac{480\times 6}{7}\,yT_4^{2S}V_2^{2c}\xi^2=0$$

$$\frac{288\times 6}{7}\,y\overline{T}{}_2^0V_2^{2c}-\frac{480\times 12}{7}S_3^{2c}V_1^0-\frac{160\times 6}{7}\,y\overline{T}{}_4^0V_2^{2c}\xi^2=0$$

$$-\frac{16\times 20}{21}S_3^0\frac{dV_1^0}{d\xi}\frac{1}{\xi}+\frac{80}{9}\left(\frac{d^2\overline{T}{}_4^0}{d\xi^2}+\frac{10}{\xi}\frac{d\overline{T}{}_4^0}{d\xi}\right)=0$$

$$\frac{960}{7}\left[-4\overline{T}{}_2^0\left(\xi\frac{dV_2^{2c}}{d\xi}+3V_2^{2c}\right)+3\frac{d}{d\xi}\left(\overline{T}{}_2^0V_2^{2c}\xi^4\right)\frac{1}{\xi^3}\right]-\frac{480\times 20}{7}S_3^{2c}\frac{dV_1^0}{d\xi}\xi$$
$$-\frac{480\times 6}{77}\,y\left[10\overline{T}{}_4^0\left(\xi\frac{dV_2^{2c}}{d\xi}+3V_2^{2c}\right)\xi^2+17\frac{d}{d\xi}\left(\overline{T}{}_4^0V_2^{2c}\xi^6\right)\frac{1}{\xi^3}\right]$$
$$+160\times 20T_4^{2S}V_1^0\xi^2=0\qquad\ldots(5.2)$$

As in §3, we shall put tentatively

$$V_1^0(\xi)=1-\xi,\qquad V_2^{2c}(\xi)=(1-\xi)^2\ldots\ldots\ldots(5.3)$$

in (5.1). The boundary conditions to be satisfied are shown in (3.3). It is, even in this reduced case, almost hopeless to solve the eigen-value problem for $y=4\pi\kappa aV_{2,2c}$ by the trial-and-error method. In order to solve the problem in an approximate way, taking (3.3) into consideration, we shall put

$$\left.\begin{aligned}&S_1^0(\xi)=A_1^0(1-\tfrac{3}{4}\xi),\\&\begin{pmatrix}S_3^0(\xi)\\S_3^{2c}(\xi)\end{pmatrix}=\begin{pmatrix}A_3^0\\A_3^{2c}\end{pmatrix}(1-\xi)^2,\end{aligned}\qquad\begin{pmatrix}\overline{T}{}_2^0(\xi)\\T_2^{2S}(\xi)\\\overline{T}{}_4^0(\xi)\\T_4^{2S}(\xi)\end{pmatrix}=\begin{pmatrix}\overline{B}{}_2^0\\\overline{B}{}_2^{2s}\\\overline{B}{}_4^0\\B_4^{2S}\end{pmatrix}(1-\xi),\right\}\ldots\ldots(5.4)$$

where $A_1^0$, $A_3^0$, $\cdots$ are undetermined constants. Since only one adjustable parameter $A_n^m$(or $B_n^m$) is given for each $S_n^m$(or $T_n^m$), the present approximations using (5.4) may be called the $B_1$ and $C_1$ approximations in contrast with the $A_1$, $A_2$, and $A_3$ approximations in §3. Inserting (5.4) into (2.14) and thereby taking the results in (5.2) into consideration, we get the equations of the following types:

$$-6A_1^0-\frac{24}{35}yB_2^{2S}+\frac{96}{35\times 7}yA_3^{2c}=0,\qquad\text{etc.,}\ldots\ldots\ldots(5.5)$$

All of these equations for the $C_1$ approximation are shown in Table 7. By putting the coefficients of $\overline{B}_4^0$ and $B_4^{2S}$ in Table 7 equal to zero, we have the equations for the $B_1$ approximation. Similarly, if we put the coefficients of $\overline{B}_4^0$, $B_4^{2S}$, $A_3^0$, and $A_3^{2c}$ in Table 7 equal to zero, we get the equations for the $A_1$ approximation. Thus, Table 7 is considered to be a generalization of Table 1. In any case, in order that

TABLE 7—*Equations for the $C_1$ approximation*

| $A_1^0$ | $\overline{B}_2^0$ | $B_2^{2S}$ | $A_3^0$ | $A_3^{2c}$ | $\overline{B}_4^0$ | $B_4^{2S}$ |
|---|---|---|---|---|---|---|
| $-6$ | $0$ | $-\frac{24}{35}y$ | $0$ | $\frac{96}{35\times 7}y$ | $0$ | $0$ |
| $\frac{1}{30}$ | $-\frac{24}{35}$ | $0$ | $-\frac{12}{35\times 55}$ | $0$ | $0$ | $0$ |
| $0$ | $\frac{72}{35\times 55}y$ | $\frac{24}{35\times 5}$ | $0$ | $-\frac{48}{35\times 11}$ | $-\frac{48}{35\times 11\times 13}y$ | $0$ |
| $0$ | $0$ | $\frac{24\times 12}{35\times 55}y$ | $-\frac{24\times 8}{49}$ | $-\frac{320}{77\times 13}y$ | $0$ | $-\frac{24\times 12}{49\times 13}y$ |
| $0$ | $\frac{24\times 12}{35\times 11}y$ | $0$ | $0$ | $-\frac{24\times 8}{77}$ | $-\frac{96}{49\times 13}y$ | $0$ |
| $0$ | $0$ | $0$ | $\frac{16}{21\times 11\times 13}$ | $0$ | $-\frac{80}{99}$ | $0$ |
| $0$ | $-\frac{48}{77\times 13}y$ | $0$ | $0$ | $\frac{480}{77\times 13}$ | $\frac{48\times 23}{77\times 91}y$ | $\frac{800}{77\times 13}$ |

the equations are compatible with each other, the determinant formed by the coefficients must be equal to zero. By putting the determinants in the $A_1$, $B_1$, and $C_1$ approximations equal to zero, we can determine the eigen-values

$$Y = \frac{8}{3}y, \qquad y = 4\pi\kappa a V_{2,2c} \qquad \text{(5.6)}$$

for the respective cases. The values of $Y$ thus calculated are shown in Table 8.

TABLE 8—*Eigen-values $Y$ for the $A_1$, $B_1$, and $C_1$ approximations*

| Approximation | $Y$ |
|---|---|
| $A_1$ | 68.51 |
| $B_1$ | 77.79 |
| $C_1$ | 80.91 |

The value $Y = 68.51$ is nothing but the one obtained in §3. Other values of $Y$ in Table 8 do not differ much from this. We may infer from this result that our self-exciting dynamo is driven by the fields of comparatively lower harmonics. Thus, the results in §3 and §4 are shown to remain true even if we include magnetic fields of higher harmonics in our dynamo model.

§6. As is shown at the end of §4, the only condition required for the existence of the self-exciting dynamo in the earth's core is that the maximum radial velocity of the fluid there is of the order of magnitude $10^{-2}$ cm/sec. The corresponding lateral velocity is obtained from Table 2. It is of the order of $10^{-2} \sim 10^{-1}$ cm/sec for $\alpha = 10 \sim 100$. This is of the order of magnitude for the lateral velocity which is obtained by Elsasser and Bullard in their discussions on the secular variations of the earth's magnetic field. Thus, using the results in the present paper, we may construct a self-exciting dynamo by which the earth's magnetic field is produced and maintained. The self-exciting dynamo is considered to have a similar character as that supposed by Elsasser and Bullard in their studies on the secular variation of the earth's magnetic field. In order to make the study on the self-exciting dynamo complete, however, there remains another problem to be solved. That is the problem on the fluid motion itself. Is it possible that the required fluid motion takes place in the earth's core? Is the fluid motion appropriate to maintain the self-exciting dynamo? These questions will be considered in another paper.

*Acknowledgments.* The authors express their sincere thanks to Prof. Ch. Tsuboi (Tokyo University), Prof. T. Nagata (Tokyo University), Prof. E. C. Bullard (National Physical Laboratory), and Mr. H. Gellman (Toronto University) for their helpful discussions. A part of the present paper has been published in the "Journal of Physics of The Earth" (H. Takeuchi and Y. Shimazu, 1952). The authors thank the Editor of J.P.E. (Prof. Ch. Tsuboi) for his generous permission to reproduce in part from the Journal.

## *References*

Alfvén, H. (1950): Cosmical electrodynamics, Oxford, Clarendon Press, 76-97.

Bullard, E. C. (1948): The secular change in the earth's magnetic field, Mon. Not. R. Astr. Soc., Geophys. Sup., 5, 248.

——— (1949): The magnetic field within the earth, Proc. R. Soc., **197**, 433.

——— (1949): Electromagnetic induction in a rotating sphere, Proc. R. Soc., **199**, 413.

Elsasser, W. M. (1946): Induction effects in terrestrial magnetism (Part 1), Phys. Rev., **69**, 106.

——— (1946): Induction effects in terrestrial magnetism (Part 2), Phys. Rev., **70**, 202.

——— (1947): Induction effects in terrestrial magnetism (Part 3), Phys. Rev., **72**, 821.

Takeuchi, H., and Y. Shimazu (1952): On a self-exciting process in magneto-hydrodynamics, J. Phys. Earth, **1**, 1.

——— (1952): On a self-exciting process in magneto-hydrodynamics (II), J. Phys. Earth, **1**, 57.

# A SERIES OF STRATOSPHERIC TEMPERATURE PROFILES OBTAINED WITH THE SEARCHLIGHT TECHNIQUE

By L. ELTERMAN

*Geophysics Research Directorate, Air Force Cambridge Research Center, Air Research and Development Command, Cambridge 39, Massachusetts*

(Original manuscript received June 26, 1953; revised manuscript, October 19, 1953)

ABSTRACT

Measurements of atmospheric densities have been made with the searchlight technique, using improved instrumentation. The density distributions are sufficiently accurate so that corresponding temperature profiles are readily obtained. The density-temperature equation requires the evaluation of an integration constant, which is accomplished by using radiosonde information and, in addition, considering physically acceptable temperature lapse rates. Five temperature profiles are obtained which represent stratospheric conditions over New Mexico during October 1952. The average height of the temperature maximum is 53 km and the mean value of the temperature maximum is 313°K. The average temperatures are calculated to 67.6 km.

## 1. INTRODUCTION

Recent publications [see 1 and 2 of "References" at end of paper] have described the searchlight technique as a method for deriving densities to about 67.6 km. In brief, the intensity from a 60-inch searchlight is modulated by a shutter mechanism fronting the searchlight, which allows differentiation of the scattered light from the light of the night sky. The sensing instrumentation comprises a 60-inch parabolic mirror, with a photomultiplier tube mounted at its focus which feeds into a narrow-band amplifier tuned to the modulating frequency, as well as suitable monitoring and recording components. The response from portions of the beam scanned at various altitudes permits derivation of the densities. It has been shown [1, 2] that the densities are closely approximated by the relationship,

$$N = \frac{E_o}{C(1 + \cos^2 \beta)} \qquad (1)$$

where $N$ is the number density (cm$^{-3}$), $E_o$ is the instrumentation response (microvolts), $\beta$ is the angle of scatter determined from the searchlight scene geometry, and $C$ is a constant evaluated from local radiosonde data taken during the same night that the light-scattering measurements were carried out.

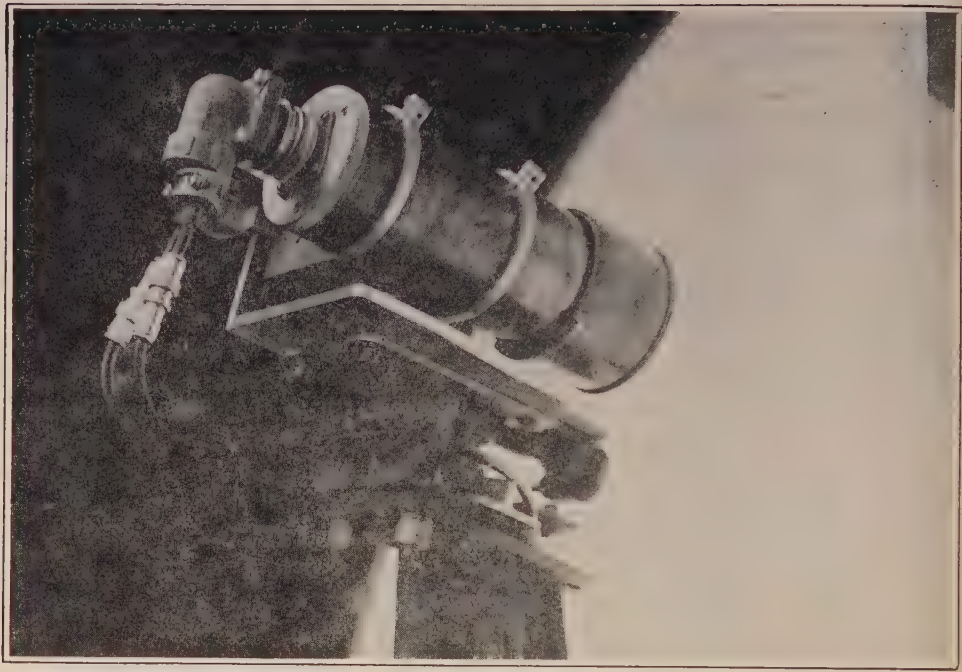

FIG. 1—PHOTOMULTIPLIER ASSEMBLY MOUNTED IN MIRROR

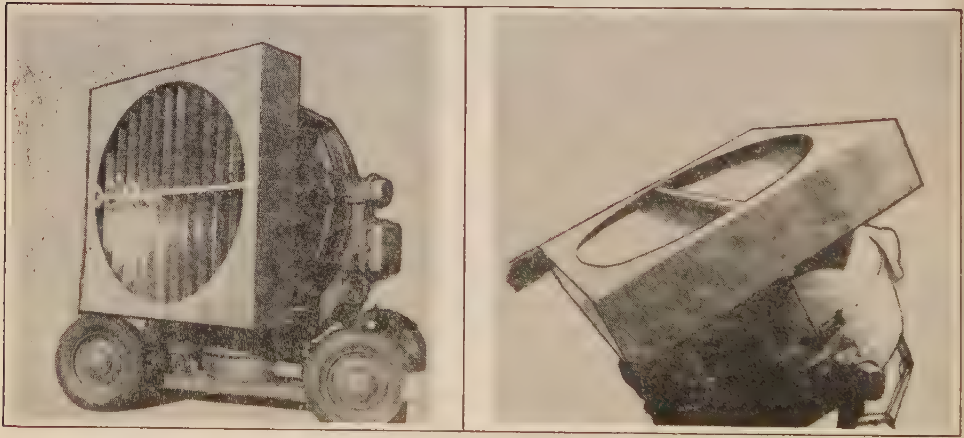

ZERO ELEVATION 60° ELEVATION

FIG. 2—MODULATING SHUTTER

## 2. THE CALCULATED DENSITIES

Since 1950, when the last searchlight measurements were conducted, some refinements were made in the instrumentation and techniques of measurement. These resulted in improved accuracy and acquisition of data to 67.6 km. The shutter and photomultiplier assemblies are shown in Figures 1 and 2. The outer brass case and an inner mu-metal cylinder fitted around the type 5819 photomultiplier tube serve as electrostatic and magnetic shields. A No. 39 glass-type Wratten filter effectively screened the photomultiplier from the high oxygen and sodium

night-glow occurring between 5500 and 6500 A. The background level of light intensity (necessary for correcting the instrumentation response) was measured by setting the field of view of the receiving mirror at 120° elevation so that it is parallel to the searchlight beam. This background level represents both the night skylight and multiple scattering from the beam. An Esterline-Angus was used to record all measurements.

Table 1 presents the instrumentation response for six sets of data taken during a typical night's operation. The background value ($E_{120} = 1.491$) subtracted from the average values ($E_{avg}$) provides the corrected response ($E_o$) from which the densities ($N_c$) were calculated. These density values were plotted on expanded scales, from which the smoothed values ($N$) were obtained. Figure 3 presents the densities listed in Table 1. Five density distributions determined for October 1952 are tabulated in Table 2. Up to 40 km, the distributions are markedly similar

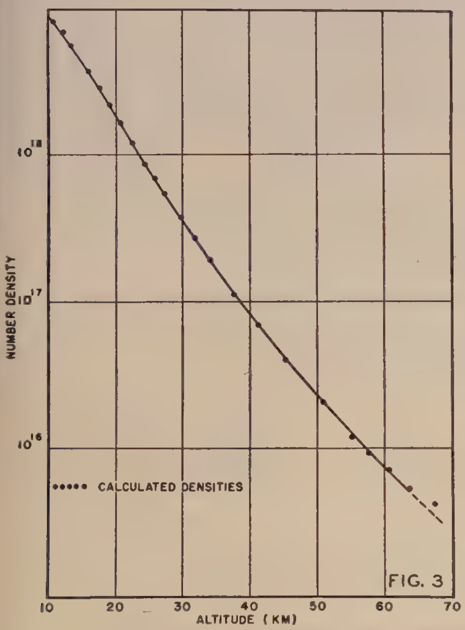


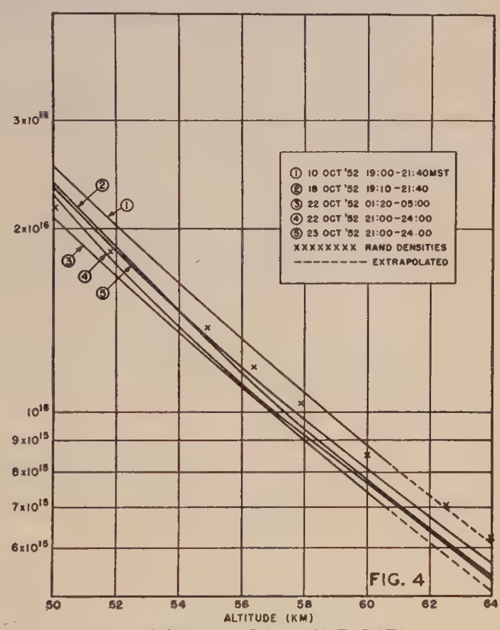


FIG. 3—DENSITY DISTRIBUTION OVER NEW MEXICO FROM SEARCHLIGHT DATA, 22 OCTOBER 1952, 21:00-24:00 MST

FIG. 4—DENSITY DISTRIBUTIONS WITH THE SEARCHLIGHT TECHNIQUE IN THE REGION 50-64 KM

and are hardly distinguishable from each other when plotted on normal-size graph paper. Above 40 km, the density curves diverge slightly and distinction among them can be made when plotted with expanded scales (Fig. 4).

Let us consider the errors involved in the measurements. The distance between the transmitter and receiver sites is 20.5 km ±0.3 km. The error in setting of the elevation scales for the mirrors is ±3 minutes of arc. Nonlinearity of the amplifier would result in less than one per cent error. The constant for calculating temperatures is determined by radiosonde data between 20 to 25 km, the error in pressure being ±4 mb; the radiosonde temperature error in the absence of solar

Table 1—*Data and densities for a typical night, 22 October 1952, 21:00 to 24:00 MST, New Mexico*

| $h$ | $E_1$ | $E_2$ | $E_3$ | $E_4$ | $E_5$ | $E_6$ | $E_{avg}$ | $E_o$ | $N_c$ | $N$ |
|---|---|---|---|---|---|---|---|---|---|---|
| 9.50 | 555 | 550 | 550 | 540 | 540 | 530 | 544.3 | 542.7 | $9.81 \times 10^{18}$ | 9.81 |
| 10.82 | 460 | 457 | 448 | 457 | 453 | 440 | 452.5 | 451.0 | 8.33 " | 8.33 |
| 12.12 | 390 | 380 | 372 | 375 | 380 | 378 | 379.1 | 377.6 | 7.03 " | 7.03 |
| 13.42 | 320 | 317 | 304 | 312 | 312 | 300 | 310.8 | 309.3 | 5.71 " | 5.71 |
| 14.74 | 266 | 260 | 250 | 267 | 262 | 250 | 259.1 | 257.6 | 4.66 " | 4.66 |
| 16.10 | 220 | 215 | 210 | 220 | 218 | 212 | 215.8 | 214.3 | 3.74 " | 3.74 |
| 17.53 | 180 | 180 | 173 | 179 | 180 | 172 | 177.3 | 175.8 | 2.93 " | 2.93 |
| 19.06 | 150 | 142 | 140 | 144 | 147 | 140 | 143.8 | 142.3 | 2.25 " | 2.25 |
| 20.70 | 127 | 120 | 120 | 122 | 125 | 120 | 122.3 | 120.8 | 1.80 " | 1.69 |
| 22.53 | 92.0 | 89.5 | 88.5 | 89.2 | 89.0 | 89.4 | 89.6 | 88.1 | 1.23 " | 1.23 |
| 24.60 | 68.0 | 68.8 | 67.8 | 67.7 | 66.5 | 69.3 | 68.01 | 66.50 | $8.75 \times 10^{17}$ | 8.75 |
| 25.98 | 56.5 | 56.7 | 56.0 | 57.0 | 55.5 | 59.0 | 56.78 | 55.28 | 7.03 " | 7.03 |
| 27.51 | 47.0 | 46.0 | 46.0 | 45.8 | 44.0 | 47.5 | 46.05 | 44.56 | 5.45 " | 5.45 |
| 29.83 | 33.9 | 33.0 | 33.2 | 34.0 | 31.3 | 34.0 | 33.23 | 31.74 | 3.73 " | 3.73 |
| 31.85 | 26.0 | 25.7 | 25.9 | 26.0 | 25.0 | 26.0 | 25.77 | 24.27 | 2.75 " | 2.75 |
| 34.16 | 19.6 | 18.8 | 19.0 | 20.0 | 18.0 | 18.7 | 19.01 | 17.51 | 1.93 " | 1.93 |
| 37.87 | 12.0 | 12.0 | 12.0 | 12.0 | 12.0 | 12.0 | 12.00 | 10.50 | 1.12 " | 1.12 |
| 41.29 | 8.70 | 8.20 | 8.00 | 8.20 | 8.00 | 8.01 | 8.185 | 6.685 | $6.95 \times 10^{16}$ | 6.95 |
| 45.51 | 5.51 | 5.39 | 5.35 | 5.29 | 5.01 | 5.30 | 5.308 | 3.818 | 3.88 " | 3.97 |
| 50.84 | 3.45 | 3.49 | 3.76 | 3.75 | 3.56 | 3.50 | 3.585 | 2.094 | 2.09 " | 2.04 |
| 55.28 | 2.61 | 2.47 | 2.92 | 2.75 | 2.67 | 2.74 | 2.693 | 1.202 | 1.18 " | 1.21 |
| 57.87 | 2.25 | 2.44 | 2.40 | 2.61 | 2.43 | 2.49 | 2.436 | .945 | $9.26 \times 10^{15}$ | 9.26 |
| 60.74 | 2.04 | 2.27 | 2.22 | 2.45 | 2.17 | 2.23 | 2.230 | .739 | 7.20 " | 7.20 |
| 63.97 | 1.86 | 2.11 | 2.16 | 2.15 | 1.96 | 2.01 | 2.041 | .550 | 5.33 " | 5.33 |
| *67.60 | 1.78 | 1.92 | 2.06 | 2.03 | 1.94 | 1.86 | 1.931 | .440 | 4.24 " | |
| $E_{120}$ | 1.49 | 1.69 | 1.48 | 1.41 | 1.48 | 1.40 | 1.491 | | | |

Time of measurements (Mountain Standard Time)

$E_1$ = 21:00–21:30
$E_2$ = 21:30–22:00
$E_3$ = 22:00–22:30
$E_4$ = 22:30–23:00
$E_5$ = 23:00–23:30
$E_6$ = 23:30–24:00

$h$ = altitude (km)
$E_1$ to $E_6$ = sets of measurements (microvolts)
$E_{avg}$ = average of measurements (microvolts)
$E_{120}$ = background (microvolts)
$E_o$ = $E_{avg} - E_{120}$
$N_c$ = calculated densities ($cm^{-3}$)
$N$ = smoothed densities ($cm^{-3}$)

TABLE 2—*Densities and temperatures over New Mexico for October 1952*

| $h$ | 10 Oct. 1952 19:00–21:40 | | 18 Oct. 1952 19:10–21:40 | | 22 Oct. 1952 01:20–05:00 | | 22 Oct. 1952 21:00–24:00 | | 23 Oct. 1952 21:00–24:00 | |
|---|---|---|---|---|---|---|---|---|---|---|
| | $N$ | $T$ | $N$ | $T$ | $N$ | $T$ | $N$ | $T$ | $N$ | $T$ |
| 9.50 | $9.41 \times 10^{18}$ | 237 | $9.88 \times 10^{18}$ | 230 | $9.86 \times 10^{18}$ | 223 | $9.81 \times 10^{18}$ | 227 | $9.92 \times 10^{18}$ | 229 |
| 10.82 | 7.98 " | 231 | 8.54 " | 217 | 8.36 " | 214 | 8.33 " | 218 | 8.44 " | 220 |
| 12.12 | 6.84 " | 221 | 7.22 " | 209 | 6.97 " | 208 | 7.03 " | 210 | 7.07 " | 214 |
| 13.42 | 5.78 " | 214 | 5.94 " | 205 | 5.67 " | 207 | 5.71 " | 209 | 5.86 " | 209 |
| 14.74 | 4.74 " | 211 | 4.74 " | 206 | 4.60 " | 205 | 4.66 " | 206 | 4.73 " | 209 |
| 16.10 | 3.87 " | 206 | 3.79 " | 205 | 3.68 " | 204 | 3.74 " | 204 | 3.82 " | 206 |
| 17.53 | 3.08 " | 204 | 3.00 " | 204 | 2.89 " | 204 | 2.93 " | 205 | 3.03 " | 205 |
| 19.06 | 2.38 " | 205 | 2.31 " | 206 | 2.21 " | 207 | 2.25 " | 208 | 2.31 " | 209 |
| 20.70 | 1.78 " | 209 | 1.74 " | 209 | 1.67 " | 209 | 1.69 " | 212 | 1.76 " | 211 |
| 22.53 | 1.29 " | 215 | 1.27 " | 213 | 1.21 " | 215 | 1.23 " | 217 | 1.28 " | 217 |
| 24.60 | $9.05 \times 10^{17}$ | 222 | $8.82 \times 10^{17}$ | 221 | $8.61 \times 10^{17}$ | 218 | $8.75 \times 10^{17}$ | 221 | $9.10 \times 10^{17}$ | 220 |
| 25.98 | 7.20 " | 226 | 7.03 " | 225 | 6.83 " | 222 | 7.03 " | 223 | 7.20 " | 225 |
| 27.51 | 5.54 " | 234 | 5.50 " | 229 | 5.32 " | 227 | 5.45 " | 228 | 5.62 " | 229 |
| 29.83 | 3.80 " | 246 | 3.80 " | 235 | 3.66 " | 234 | 3.73 " | 238 | 3.89 " | 236 |
| 31.85 | 2.82 " | 251 | 2.74 " | 245 | 2.68 " | 239 | 2.75 " | 242 | 2.86 " | 240 |
| 34.16 | 2.03 " | 256 | 1.93 " | 254 | 1.88 " | 246 | 1.93 " | 251 | 1.98 " | 252 |
| 37.87 | 1.19 " | 270 | 1.12 " | 271 | 1.08 " | 260 | 1.12 " | 265 | 1.15 " | 267 |
| 41.29 | $7.42 \times 10^{16}$ | 285 | $7.06 \times 10^{16}$ | 282 | $6.63 \times 10^{16}$ | 274 | $6.95 \times 10^{16}$ | 279 | $7.15 \times 10^{16}$ | 281 |
| 45.51 | 4.23 " | 309 | 4.16 " | 291 | 3.70 " | 298 | 3.97 " | 298 | 4.08 " | 301 |
| 50.84 | 2.30 " | 311 | 2.16 " | 297 | 1.91 " | 312 | 2.04 " | 314 | 2.11 " | 317 |
| 55.28 | 1.42 " | 311 | 1.27 " | 307 | 1.21 " | 303 | 1.21 " | 332 | 1.29 " | 326 |
| 57.87 | 1.09 " | 305 | $9.53 \times 10^{15}$ | 308 | $9.26 \times 10^{15}$ | 296 | $9.26 \times 10^{15}$ | 334 | $9.87 \times 10^{15}$ | 325 |
| 60.74 | $8.27 \times 10^{15}$ | 291 | 7.25 " | 294 | 6.97 " | 282 | 7.20 " | 320 | 7.62 " | 311 |
| 63.97 | | | 5.40 " | 278 | | | 5.33 " | 305 | 5.66 " | 292 |

$h$ = altitude (km); $N$ = number density ($cm^{-3}$); $T$ = temperature (°K).

radiation is $\pm 1°$. The density values derived with the searchlight method were based on averaging five or six sets of measurements spread over a period of about four hours.

## 3. THE TEMPERATURE EQUATION

The "hydrostatic equation" is

$$dp = -mgN\,dh \quad \ldots\ldots(2)$$

and from the "equation of state," we have

$$dp = k\,d(NT) \quad \ldots\ldots(3)$$

or,

$$d(NT) = -\frac{mg}{k} N\,dh \quad \ldots\ldots(4)$$

where $p$ = pressure (gm cm$^{-1}$ sec$^{-2}$), $T$ = temperature (°K), $k$ = Boltzmann's constant ($1.372 \times 10^{-16}$ ergs deg$^{-1}$), $g$ = apparent gravity (cm sec$^{-2}$), $m$ = mean molecular mass ($4.8 \times 10^{-23}$ gm), and $h$ = altitude (cm). Integrating Eq. (4),

$$N_2T_2 - N_1T_1 = \frac{mg}{k} \int_{h_1}^{h_2} N\,dh \quad \ldots\ldots(5)$$

and

$$T_2 = \frac{1}{N_2}\left(N_1T_1 - \frac{mg}{k}\overline{N}\,\Delta h\right) \quad \ldots\ldots(6)$$

so that for a given atmospheric layer, $N_1T_1$ and $N_2T_2$ represent the number densities and temperatures at the bottom and top of the layer and $\overline{N}$ is the average density of the layer.

It is desirable to have a convenient expression for evaluating $\overline{N}$. This can be done by considering that the density-height relationship is well approximated by

$$N = N_1 e^{-bh} \quad \ldots\ldots(7)$$

or for a specific layer,

$$N_2 = N_1 e^{-b\,\Delta h} \quad \ldots\ldots(8)$$

where $b$ is a constant. For such a layer, the average density is

$$\overline{N} = \int_0^{\Delta h} \frac{N\,dh}{\Delta h} = N_1 \int_0^{\Delta h} \frac{e^{-bh}\,dh}{\Delta h}$$

Integrating yields

$$\overline{N} = \frac{N_1(1 - e^{-b\,\Delta h})}{b\,\Delta h} = \frac{N_1 - N_2}{b\,\Delta h}$$

but from Eq. (8)

$$ln\,\frac{N_2}{N_1} = -b\,\Delta h$$

Therefore,

$$\overline{N} = \frac{N_1 - N_2}{ln \frac{N_1}{N_2}} \qquad (9)$$

Substituting in Eq. (6),

$$T_2 = \frac{N_1 T_1}{N_2} - \frac{mg}{k} \quad \Delta h \frac{\left(\frac{N_1}{N_2} - 1\right)}{ln \frac{N_1}{N_2}} \qquad (10)$$

## 4. THE TEMPERATURE PROFILE APPROACH

Equation (10) is the basic equation from which the temperature profiles are derived. If the density distribution is established by the searchlight method and a temperature at a known height is taken from radiosonde data, then the temperature at the top of a layer $\Delta h$ can be determined. In this way, the temperatures can be calculated successively to the heights probed by the searchlight beam. This approach is quite simple, except that the value $N_1 T_1$ is critical and must be of high accuracy in order to develop the temperature profile to high altitude, that is, above 50 km. This is due to the successive nature of the calculation. Any error in $N_1 T_1$ builds up exponentially, so that the temperatures at great altitudes become unacceptably large or small, depending on whether this error is negative or positive.

It is evident from Eqs. (4) and (5) that this critical factor is in reality a constant of integration, which we shall designate as $B$, so that

$$B = N_1 T_1 \qquad (11)$$

Since this constant will be determined from radiosonde data,

$$B = 7.29 \times 10^{18} P \qquad (12)$$

where $P$ is the radiosonde pressure in millibars. The value of $B$ (although applicable only to the first of the successive series of calculations) will materially determine the shape and position of the temperature profile. This is demonstrated by Figure 5, where a family of curves results from different values of $B$, even though these values are well within the limit of error of the radiosonde pressure. In this Figure, the following should be noted as representing conditions above 50 km:

$B_1$ —lapse rate attains a value greater than 10°C/km
$B_{min}$—lapse rate attains a value equal to 10°C/km
$B_{med}$—lapse rate attains a value of 5°C/km
$B_{max}$—temperatures are approximately constant; lapse rate is zero
$B_2$ —temperatures continue to increase indefinitely.

A lapse rate greater than 9°.8 C per km would result in a thermodynamically unstable atmosphere and this condition is unlikely. Further, a persisting zero lapse rate above 50 km also is unacceptable from our present knowledge of the upper atmosphere. This suggests that the temperature spread caused by the

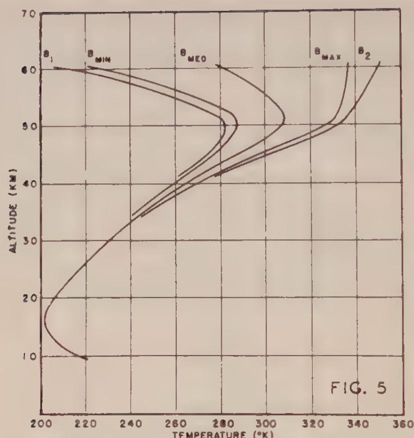


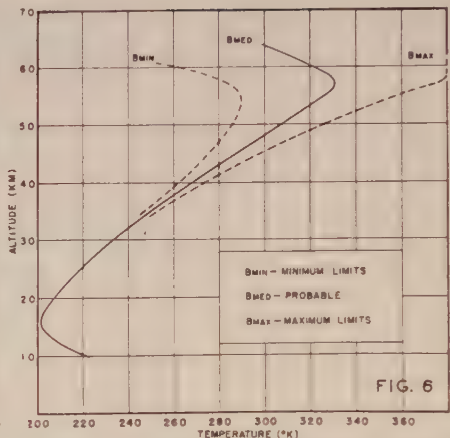


FIG. 5—TEMPERATURE PROFILE FAMILY FROM A DENSITY DISTRIBUTION USING DIFFERENT INTEGRATION CONSTANTS B, 22 OCTOBER 1952, 01:20-05:00 MST

FIG. 6—TEMPERATURE PROFILE, NEW MEXICO, 22 OCTOBER 1952, 21:00-24:00 MST

family of curves can be limited by discarding all values of $B < B_{\min}$ and all values of $B > B_{\max}$. Thus, for any temperature distribution derived with the searchlight technique, three useful profiles can be presented, that is, possible minimum limits ($B_{\min}$), possible maximum limits ($B_{\max}$), and finally a temperature profile based on averaging the constants $B_{\min}$ and $B_{\max}$. This average value ($B_{\mathrm{med}}$) will generate a most probable temperature distribution which is equidistant between the limiting profiles. Accordingly, Eq. (10) can take the form,

$$T_2 = \frac{B}{N_2} - \frac{mg\,\Delta h}{k}\,\frac{\left(\frac{N_1}{N_2} - 1\right)}{ln\,\frac{N_1}{N_2}} \qquad (13)$$

## 5. THE TEMPERATURE PROFILE CALCULATION

Since any error may be perpetuated significantly in a successive calculation, it is advisable to start the calculation in the vicinity of one of the higher altitudes available from the radiosonde. Then the calculations are carried upward to the height attained by searchlight probing. Subsequently, the calculations are carried downward from the initial altitude to 9.5 km, where the searchlight measurements begin.

As an example, for the night represented by Figure 1, calculations were started at 20.70 km. The radiosonde pressure at this altitude is 50.0 mb ± 4 mb. From Eq. (12),

$$B_{-4} = 335.34 \times 10^{18}$$

$$B_{+4} = 393.66 \times 10^{18}$$

Whatever values of $B$ are used, they must necessarily fall in the range $B_{-4}$ to $B_{+4}$. An arbitrarily chosen value in this range can be applied in Eq. (13) to produce

the temperature at 22.53 km (the next higher searchlight altitude). With $T_2$ established at 22.53 km, Eq. (10) is used to determine the successive higher altitude temperatures. This phase of the calculation can be simplified by

$$\alpha = \frac{N_1}{N_2}$$

so that Eq. (10) takes the form

$$T_2 = \alpha T_1 - \frac{mg}{k} \quad \Delta h \frac{(\alpha - 1)}{ln\ \alpha} \quad \text{.....................} (14)$$

By this means, various values of $B$ in the range $B_{-4}$ to $B_{+4}$ were tried, until it was determined that for 22 October 1952, 21:00-24:00 Mountain Standard Time,

$$B_{min} = 357.07 \times 10^{18}$$

$$B_{max} = 357.99 \times 10^{18}$$

$$B_{med} = 357.54 \times 10^{18}$$

Figure 6 shows the profiles generated by these constants. In these calculations, the temperatures, like the constant $B$, are worked to two decimal places in order to avoid systematic error in the calculation. The values for the apparent gravity, $g$, were taken from the Rand report [3].

In following this procedure, it can be shown that if the values of the integration constants $B_{min}$ and $B_{max}$ are chosen so that the temperature profiles attain the limiting lapse rates at the highest level of measurement, then the temperature profile will be affected somewhat by the level to which data are available. It is desirable, therefore, to compute all lapse rates to the same altitude, so that a better comparison can be made between profiles representing different nights. Accordingly, the values of $B_{min}$ and $B_{max}$ were chosen so that the limiting lapse rates occur in the layer 57.87 to 60.74 km. On 10 October 1952 (19:00-22:00 MST) and 22 October 1952 (01:20-05:00 MST), dependable data were acquired to 57.87 km, so that it was necessary, in this instance, to extrapolate the density curve to 60.74 km. On other nights, however, dependable data were acquired to 63.97 km. A temperature representing this additional level is then added to the median profile (by Eq. 14) after the median profile has been determined to 60.74 km, as indicated above.

## 6. DISCUSSION OF RESULTS

The density information obtained for October 1952 shows the distributions to be almost identical in the region from 10 to 45 km (Tables 1 and 2, and Fig. 3). Above 45 km, the rigid nature of the distribution yields to a flexible region, where the densities vary as much as 17 per cent (Fig. 4).* The mean of the densities for October 1952 are in good agreement with the Rand densities [3] to 55 km. Beyond this altitude, the searchlight densities drop below the Rand values (about 11 per cent lower at 64 km).

The radiosonde temperatures entered on the profiles in Figure 7 show them

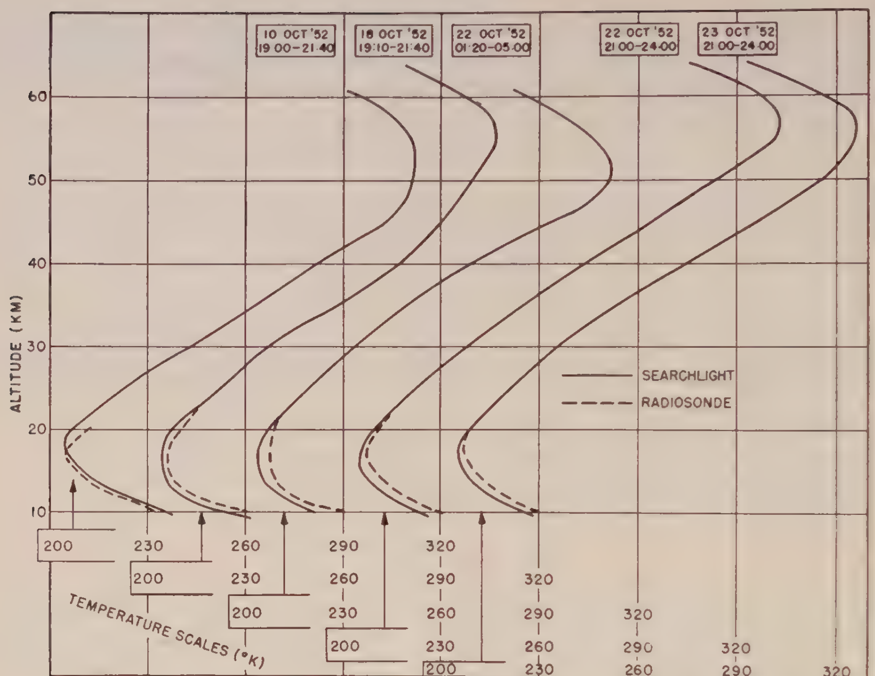


FIG. 7—STAGGERED SCALE PRESENTATION OF TEMPERATURE PROFILES, NEW MEXICO, OCTOBER 1952

to be higher by a few degrees than the searchlight temperatures. This is attributed to the presence of water vapor and dust, which increases the scattered light in the region where the discrepancy is evident. Although, in the region 9.5 to 18 km, the density error due to accumulation of dust in the tropopause region is small, the nature of the temperature calculation results in a discrepancy of several degrees which is in the right direction.

It is seen in Figures 5 and 6 that, up to 45 km, the limiting temperature profiles ($B_{max}$ , $B_{min}$) cover a relatively narrow temperature spread. This applies to all the five nights treated in this discussion. The deviation from the probable temperature profile ($B_{med}$) becomes increasingly smaller at reduced heights, as shown by the following tabulation (Table 3).

TABLE 3—*Deviation of limiting profiles from probable temperature profile*

| Altitude | Deviation from probable temperature profile | | | | |
|---|---|---|---|---|---|
| | 10 Oct. 1952 19:00–21:40 | 18 Oct. 1952 19:10–21:40 | 22 Oct. 1952 01:20–05:00 | 22 Oct. 1952 21:00–24:00 | 23 Oct. 1952 21:00–24:00 |
| *km* | °*C* | °*C* | °*C* | °*C* | °*C* |
| 30 | ± 1 | ± 1 | ± 1 | ± 1 | ± 1 |
| 40 | ± 5 | ± 6 | ± 5 | ± 5 | ± 6 |
| 45 | ±11 | ±12 | ±10 | ±11 | ±12 |

Thus, up to 45 km, the temperatures derived with the searchlight technique are well defined and considered reliable because of their small dependency on the integrating constant $B$.

Above 50 km, the temperatures encompassed by the limiting profiles are less constricted. However, the unlikely lapse rates (above 50 km) of the limiting profiles suggest that the true temperatures approach reasonably close to the median (most probable) profile. Figure 8 compares the median profiles for the five nights (Table 2). The temperatures up to 50 km do not vary significantly from night to night.

In order to obtain a representative profile for the month, the densities for the five nights were averaged for each layer. The resulting distribution produces the profile shown in Figure 9. The average height of the temperature maximum is 53 km and the maximum temperature is 313°K. Calculations are in progress covering a season's measurements, from which it will be possible to evaluate the significance of the differently positioned profiles.

As explained previously, the constants for the minimum limiting profile and maximum limiting profile are chosen so that ultimately they terminate in 10° C/km and zero lapse rate, respectively. The median temperature profile, necessarily, will attain a lapse rate of 5° C/km. The following tabulation (Table 4) gives the

TABLE 4

| Mountain Standard Time | Derived temperature at 60.74 km | Extrapolated stratopause conditions | |
|---|---|---|---|
| | | Height | Temperature |
| | °K | km | °K |
| 10 Oct. 1952 19:00–21:40 | 291 | 79 | 201 |
| 18 Oct. 1952 19:10–21:40 | 290 | 79 | 200 |
| 22 Oct. 1952 01:20–05:00 | 282 | 77 | 202 |
| 22 Oct. 1952 21:00–24:00 | 320 | 85 | 200 |
| 23 Oct. 1952 21:00–24:00 | 311 | 83 | 201 |
| | | Avg. = 80.6 | Avg. = 200.8 |

height of the stratopause (height of minimum temperature) if the derived temperature profiles are extrapolated from 60.74 km upward with the 5° C/km lapse rate. The 5° C/km lapse rate, therefore, is reasonable, since it leads to temperatures of

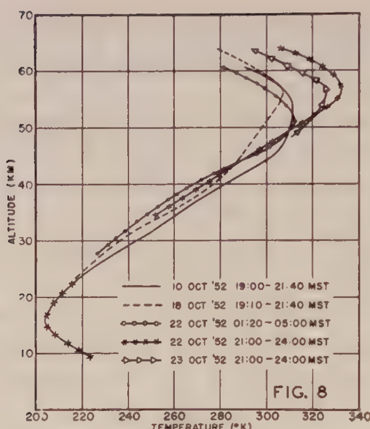


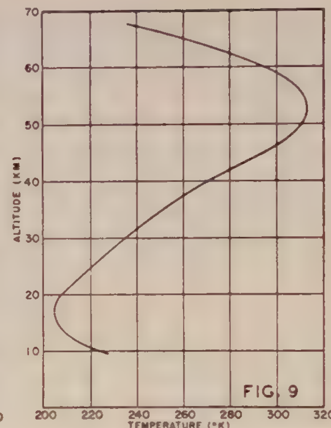


FIG. 8—COMPARISON OF TEMPERATURE PROFILES, NEW MEXICO, OCTOBER 1952

FIG. 9—AVERAGE TEMPERATURE PROFILE FOR OCTOBER 1952, NEW MEXICO

about 200°K in the vicinity of 80 km—conditions which are in agreement with results of previous investigators.

## 7. ACKNOWLEDGMENT

Acknowledgment is due Sgt. James C. Cunningham, of the Air Force Cambridge Research Center, for his skilled operation of the searchlight equipment and for his assistance with the calculations; to Walter Wysoczanski, formerly of this laboratory, for his expert assistance with the electronic equipment, and to my other laboratory colleagues for their generous interest and suggestions.

## *References*

[1] L. Elterman, The measurement of stratospheric density distribution with the searchlight technique, Geophysics Research Directorate, Air Force Cambridge Research Center, Cambridge, Mass., Geophysical Research Paper No. 10 (Dec. 1951).

[2] L. Elterman, The measurement of stratospheric density distribution with the searchlight technique, J. Geophys. Res., 56, 509-520 (1951).

[3] G. Grimminger, Analysis of temperature, pressure and density of the atmosphere extending to extreme altitudes, Rand Corporation, Santa Monica, Calif., Rep. No. 105 (Nov. 1948).

JOURNAL OF GEOPHYSICAL RESEARCH VOLUME 58, No. 4 DECEMBER, 1953

# ON THE PRODUCTION OF GLOW DISCHARGES IN THE IONOSPHERE BY WINDS

By OLIVER R. WULF

*United States Weather Bureau, California Institute of Technology, Pasadena, California*

(Received September 2, 1953)

ABSTRACT

It is suggested that a source of excitation of the airglow and aurora is to be found in potential differences generated by zonal ionospheric winds cutting the earth's magnetic field. A return path of current flow (glow discharge) in the higher ionosphere appears plausible. The principal effect in this process arises from the cutting of the vertical component of the field by broad horizontal winds. An auroral zone results as the region where the product of wind velocity and vertical field intensity has a maximum. From this point of view, the aurora and the airglow (at least a portion of it) are manifestations of the same thing. The aurora occurs under high excitation when the winds are strong in high latitudes, while this portion of the airglow is always present in some measure in most latitudes, arising from lower velocity winds. Patterns in the large-scale air circulation should lead to patterns in the intensity of the emission, and the regular diurnal disturbance of these upper atmosphere zonal winds should lead to diurnal features in the aurora and airglow.

Movements of air in the ionosphere across the lines of force of the earth's permanent magnetic field give rise to electromotive forces, which in turn cause the separation of ions of opposite sign. This may lead to a closed circuit of electric current if there is an outer path over which opposing electromotive forces do not prevent such. The widely accepted dynamo theory of the daily variation of the earth's magnetic field ascribes this phenomenon to the magnetic field of such an electric current.

Information concerning winds in the ionosphere can be gained, for example, from the movement of irregularities of ion density there. In an article in which a method of this kind is described, Maxwell and Little [see 1 of "References" at end of paper] have reported observations of winds in the $F$ region from which some idea of velocities and directions, as well as variability in time, may be had.

It seems from the data existing at present that the winds in the ionosphere can be roughly described as similar to the winds in the lower atmosphere, except that, in the average, higher velocities are observed in the ionosphere and that

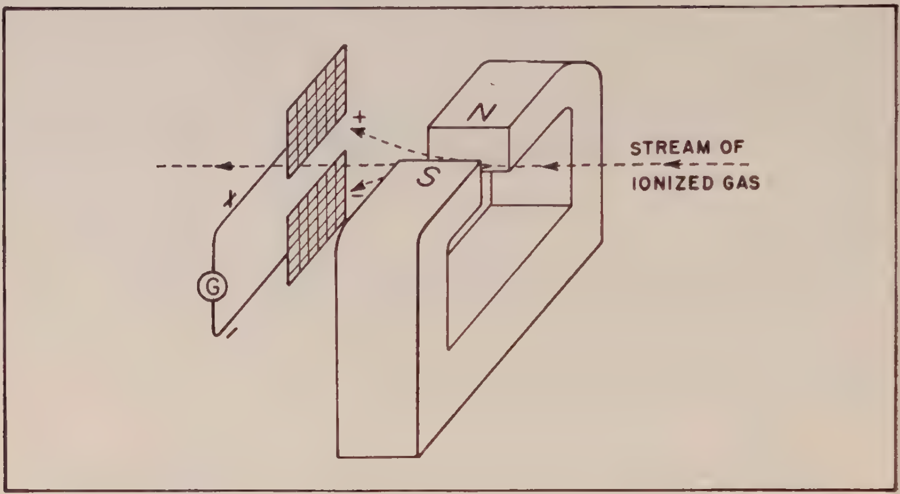


FIG. 1—AN ILLUSTRATIVE EXPERIMENT (SCHEMATIC). A STREAM OF IONIZED GAS AT LOW PRESSURE BLOWS THROUGH (AT RIGHT-ANGLES TO) A MAGNETIC FIELD LEADING TO CHARGES OF OPPOSITE SIGNS ON THE TWO COLLECTING SCREENS AND A CURRENT FLOW THROUGH THE GALVANOMETER IN THE EXTERNAL CIRCUIT. ON THE REMOVAL OF THE COLLECTING SCREENS AND OUTER CIRCUIT, AND WITH LARGE FIELD AND HIGH GAS VELOCITY, A GLOW DISCHARGE MIGHT BE PRODUCED IN THE SPACE BETWEEN THE PLACES WHERE THE SCREENS WERE, CAUSED BY IMPACTS OF ELECTRONS ACCELERATED IN THE POTENTIAL DROP ACROSS THE GAS STREAM AFTER LEAVING THE MAGNETIC FIELD.

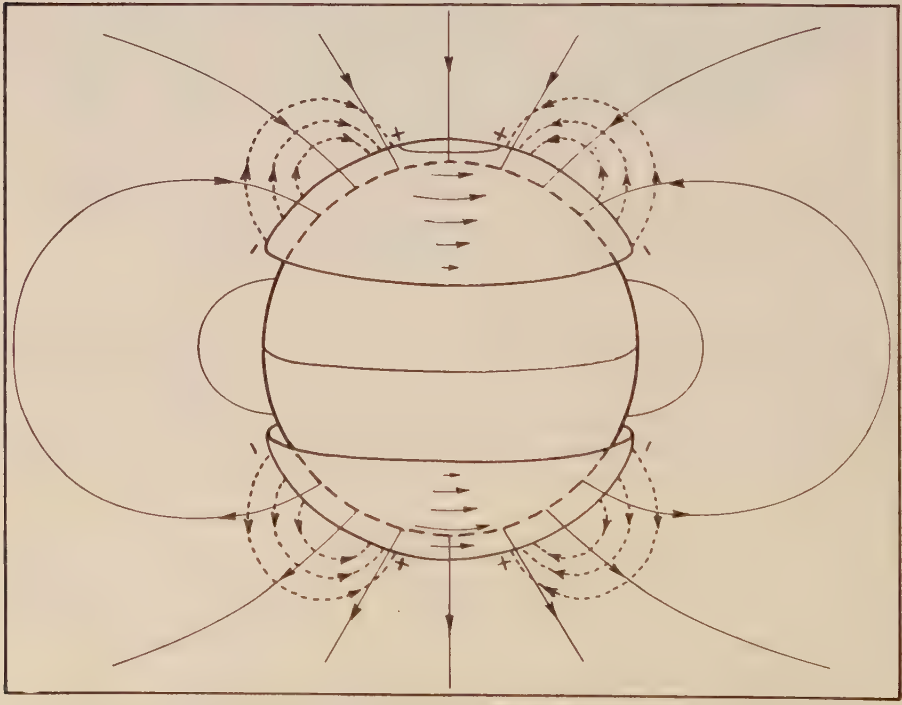

FIG. 2—SCHEMATIC REPRESENTATION OF A POSSIBLE SOURCE OF EXCITATION OF THE AURORA AND AIRGLOW

diurnal variations are more pronounced there. Turbulent motions are indicated by some of the observations, which is not surprising in view of the high wind-speeds that are found. Kellogg and Schilling [2] have proposed a model of the circulation in the upper stratosphere, and in their paper an extensive bibliography is given.

There is a thermodynamic source of large-scale air circulation in the high atmosphere arising from temperature gradients produced there by the absorption of solar radiation and of radiation from below by oxygen, nitrogen, ozone, water vapor, and carbon dioxide, and the emission of long wavelength radiation (the condenser element of the engine) by ozone, water vapor, and carbon dioxide, as well as by OH and possibly other photochemical constituents that also have radiative properties in the infrared. Thus there may be motions in the high atmosphere that originate there, as well as motions that the lower atmosphere may cause in it.

Such absorption and emission of radiation should result in temperature gradients (and accompanying density and pressure gradients) that are roughly symmetrical around the earth's axis of rotation. They should therefore be in a sense to produce meridional flow of air, which, with the deflecting force of the earth's rotation, should lead predominantly to zonal flow, just as in the lower atmosphere. One would therefore expect in the high atmosphere broad zonal flow of air, in breadth a considerable part of the distance from the equator to the pole, say several thousand kilometers, with diurnal motions superposed. This entire flow occurs on a river-bed whose contours vary with time, namely, on the lower atmosphere, which has its own thermodynamic source of circulation, and is subject to continual change arising from the instability of fluid flow that occurs within it.

The relative dimensions of the system appear to be important. From the *F* region of the ionosphere to the ground is a small distance compared with the distance from the equator to the pole. The latter distance is of the order of the width of the river-bed. The zonal circulation is, in other words, a very broad but shallow flow.

Across such zonal winds, considerable potential differences may exist, arising from the separation of charge and illustrated hypothetically in Figure 1. Horizontal winds cutting the vertical component of the earth's magnetic field will experience lateral (north $\leftrightarrow$ south) electric polarization,* which should result in current flow if an external path exists over which a closed circuit can form or over which a discharge can occur. This is shown schematically in Figure 2, where zonal westerly winds are pictured in the lower ionosphere. The author earlier suggested that such potential differences may play a role in the excitation of the aurora. They may also be a source of excitation of the airglow [3].

A rough estimate can be made of the possible potential differences that may arise. Let us, for example, consider the higher latitudes where horizontal wind will cut principally the vertical component of the earth's permanent field. Taking

*Vertical polarization arising from horizontal winds cutting the horizontal component of the field will be small because of the relative thinness of all large-scale horizontal winds. The author has earlier discussed [3*a*] the possible geomagnetic importance of large-scale vertical air-motions in low latitudes cutting the horizontal component of the field.

the latter to be around 0.5 gauss, a horizontal wind of 50 meters per second will be associated with an electric field of $0.5 \times 5 \times 10^3$ emu, or roughly a potential difference of $10^{-5}$ volt/cm, which is 1 volt/km. If this wind be zonal, the potential differences will be in a north-south direction, and if the wind stream be a few thousand kilometers in width the potential difference across the stream may be of the order of a thousand volts.*

The radiations coming from the airglow and from the aurora require excitation energies of only a few volts, or, at most, of the order of ten volts. Since it seems that ionospheric winds may lead to much greater potential differences than this, it appears plausible that such winds may actually produce glow discharges in the ionosphere, that is, cause the excitation by ordinary electron impact of molecular and atomic species existing there, the emission from which appears as a part at least of the aurora and of the airglow. The principal questions seem to be whether there exists a region in which adequate charge separation by zonal winds may occur, and whether there then remains a path over which a closed circuit in the form of a glow discharge may be set up.

In order that such winds can effect separation of charge most favorably, they presumably must be in an altitude range where molecular collisions are sufficiently frequent to minimize the restricting influence of the earth's magnetic field on the motion of the ions in the wind-created electric field. This suggests that the winds which may lead to potential differences sufficient to produce such glow discharges blow in the $D$ and $E$ regions, and that the discharge (return path) occurs at much greater altitudes.† Such winds may reasonably extend to depths where the ion density is small. Under these circumstances, the only likely return path for the current closure would be upward and over in a meridional direction, well above the wind stream, at altitudes where the latter does not exist or even where zonal winds of opposite direction may prevail.

Current flow under a potential difference in a gas in which ionization already exists (for example, the ionosphere), and at a pressure where the mean free path is sufficiently large that electrons attain critical excitation velocities, is essentially a glow discharge. Such a discharge in the high atmosphere differs from that commonly produced at low pressure in the laboratory in that the ionization already exists in the ionosphere and does not depend on the discharge for its production, though it may of course be enhanced by the passage of the discharge.

The paths of electrons in the ionosphere moving under the potential difference established near its base are suggested in Figure 2 by the dotted lines with arrowheads. The first portions of the paths, upward and poleward over the accumulation of charge in the lower latitude band of the wind stream, will be across the lines of force of the earth's field. But in this region there are relatively large numbers of collisions which should be favorable to the steady drift of electrons along this

*Early and Dow [4] have described a laboratory experiment in which a very high velocity wind is produced by an electric discharge (arc) at low pressure in a magnetic field. This seems to be a sort of inverse process to the one being discussed here.

†Dr. Fred Hoyle has suggested to the author that the dissipation of energy in such glow discharges in the high atmosphere might contribute importantly to the temperature there. In such a process, kinetic energy of the atmospheric circulation lower down would be utilized in heating the air in the upper ionosphere.

path. This will probably be the high resistance portion of the path, along which the greater part of the potential drop may occur (see, however, a further suggestion below). Electron velocities over this portion of the path will remain low, seldom if ever reaching critical excitation velocities.

The collisions which the electrons make will be elastic, with only small energy loss per collision (because of the much greater mass of the molecules with which they collide) so long as the electron energies remain below the excitation energies of the existing atomic and molecular species. The terminal velocities in the direction of the potential drop will remain low over the first portion of the path, however, because of the large number of collisions. As higher altitudes are attained with greater mean free paths, higher terminal velocities should be reached.

Recent evidence indicates that the atomic oxygen and sodium radiations in the airglow come from average heights of about 200 km or more [5]. At such altitudes it is probably not possible to call on the energy of any chemical reaction as a source of excitation because of the very low rates of reaction at such low molecular densities [6]. These altitudes of emission seem plausible, however, if ionospheric winds lead to such excitation. We may ask at what mean free path, that is, at what altitude, the electrons may acquire the necessary terminal speeds for excitation under a potential drop that seems likely to be present there. The outstanding low excitation potential in the upper ionosphere is the $^3\text{P} \rightarrow {}^1\text{D}$ transition in the oxygen atom of about 2 volts. If an appreciable number of oxygen atoms are present in the $^1\text{D}$ state, there is the excitation $^1\text{D} \rightarrow {}^1\text{S}$, the energy of which is about 2.2 volts. And if an appreciable number of free sodium atoms are present, there is the excitation of the Na D lines requiring about 2.1 volts.

The terminal energy of an electron moving in a gas under an electric field $E$ is given in sufficient approximation for the present purpose [7] by

$$U_T = \frac{\lambda \cdot E}{2.31}\left(\frac{M}{m}\right)^{1/2}$$

where $U_T$ is expressed in terms of equivalent potential drop, $E$ is the electric field, $\lambda$ is the mean free path, and $M$ and $m$ are the masses of the gas molecules and electrons, respectively. We saw above that ionospheric winds of reasonable velocity may lead to electric fields of the order of $10^{-5}$ volt/cm or more. If we assume that the exciting electrons in this portion of the airglow move in the upper region where excitation may occur under a remaining field of one-tenth this value, we find for the mean free path at which terminal energies of 2 electron volts may be attained, the approximate value

$$\lambda = \frac{2.31 \times 2}{10^{-6}}\left(\frac{1}{1850 \times 20}\right)^{1/2} \approx 2 \times 10^4 \text{ cm}$$

where the average molecular weight has been taken as 20. This value of the free path for an electron probably occurs where the molecular free path is several times smaller, probably somewhat above 150-km altitude [8]. While the electric field actually available may be different than that assumed, this calculation may perhaps be taken as showing that a not unreasonable value of the field would be

in accord with excitation of these airglow radiations in the altitude range indicated by recent observations.

In the higher latitudes, the discharge would occur where the electron path is closely parallel to the field, the field acting as a guide but interposing little obstacle. In middle latitudes, the excitation path is not so clear, but there seems to be a process by which the discharge may still occur largely along the lines of force. The diffusion upward of electrons over the first portion of the path, partially obstructed by the need of crossing the magnetic field, may build up the negative charge to considerable altitudes, from which poleward fall along the lines of force is possible. A similar effect can hardly occur in the positive-ion excess in high latitudes because of the low mobility of the heavy ions. Electrons originating in any manner above this excess can fall into it, with the possibility of attaining excitation velocities in the trajectory. The lower altitude limit of the aurora, from this point of view, represents the greatest depth at which the electrons can acquire excitation velocities under the highest electric fields that occur.

The path over which a gas discharge at low pressure occurs is sensitive to gas density. Over a field of uniform horizontal density at the various heights, a general auroral glow might be expected from such large-scale wind-generated potential differences. But if pressure waves form in the high atmosphere or large-scale turbulence occurs, patterns in the glow discharge may occur, caused by the discharge taking paths of favored gas density, as well as by spatial variations in the exciting electromotive force. This would seem to be a plausible source of patterns in the aurora. From this point of view, the aurora may give indication of meteorological conditions in the high atmosphere, and there may be a partial similarity between conditions that lead to auroral forms and those that lead to some forms of clouds.

Aurorae would be expected at times of high-velocity ionospheric winds and where the vertical component of the earth's magnetic field is large, while during low-velocity ionospheric winds and particularly in middle latitudes a weaker glow discharge representing a portion of the airglow may occur. On a large scale, the convergence of air toward the poles in the meridional component of flow, with ultimate descent or ascent, probably makes the range of latitudes prior to the descent or ascent of the air, regions of high and variable winds. Times of especially high winds resulting from the precipitation of cumulated instability in the atmospheric circulation should be fairly distinct from times of lower winds when this is absent.

Of interest in connection with these general considerations are the observations of Little and Maxwell [9] on the scintillation of radio stars during aurorae and magnetic storms, which indicate an increase in the velocity of ionospheric winds during magnetically disturbed periods and during aurorae. While high winds in the ionosphere at the time of magnetic disturbance and aurorae might have other significance than that given them in the present picture of auroral excitation by winds, they seem at least in accord with this. They seem also in accord with an atmospheric theory of magnetic disturbance outlined by Nicholson and Wulf [10], where a discussion is given of important aspects of magnetic disturbance not mentioned in the present paper, such as its relation to solar features, and the

maxima near the equinoxes in its seasonal variation. In this theory, magnetic disturbance arises from electric currents in the ionosphere produced through dynamo action by winds of the large-scale atmospheric circulation, and the present paper simply suggests that a glow discharge in the upper ionosphere may be a part of this.*

Inelastic impacts at excitation potentials tend to limit the attainable electron velocities. At low densities, however, there should be a considerable distribution of velocities about the average, and the electrons of higher velocities may produce ionoization. (It is possible that it is the higher end of the distribution that is utilized in the production of the airglow and aurora themselves.) Thus it seems possible that ionospheric winds may lead to the production of some of the ionization in the ionosphere, such as irregular ionization and the residual $E$-layer ionization that persists through the night. When electromotive forces build up rapidly, the enhancement of ionization over a particular path of current flow may lead to a relatively large current in a short time, though not as abruptly of course as the breakdown that occurs in the lower atmosphere as lightning. However, in the present picture, the element of atmospheric instability is also involved in the production of the former process.

The magnetic field of the current flowing in such a circuit should be a part of magnetic disturbance [12]. Such electromotive forces generated by the large-scale atmospheric circulation in the concentric conducting spherical shell of the ionosphere should have world-wide effects, occurring at the same time, but with different intensities depending on the character of the electromotive force. From this point of view, magnetic disturbance may have an appreciable part of the energy of the entire atmospheric circulation to draw on for its production [3*a*], and this latter appears to be large compared with the energy of a magnetic storm [13]. Pressure waves in the atmosphere may lead to oscillations between different current paths and to pulsations in the disturbance. Zonal winds of opposite directions at different levels above and below one another (a circumstance not unlikely where the winds have their origin in meridional flow) may lead directly to vertical electric fields.†

The excitation in this manner of the airglow by large-scale winds would have a further feature that appears to be in accord with observation. Thus it has been found [5*a*] that there are patterns of intensity in the OI 5577 A radiation in the night sky (rather than uniform luminosity) and that these exhibit a diurnal variation,** with a fairly definite average behavior, but with significant differences from night to night. This is suggestive of wind excitation, particularly that of a diurnal wind pattern [14] superposed on the large-scale circulation of the air in the lower ionosphere. With change from day to day in the pattern of the circulation in the lower

*The author wishes to call attention to the work of Hulbert and Maris [11] in this general field, and also to the work of Alfvén [15].

†It seems possible that the long enduring meteor train, a phenomenon that has been difficult to explain, may be caused by the flow of current over the path of ionization left by a meteor that, in its descent, has cut through two layers of excess charge of opposite sign.

**This has also been found [5*a*] for the oxygen atom radiation at 6300 A and for the sodium radiation at 5893 A, but the behaviors differ. Here emphasis is only on the finding of patterns and their diurnal variation. The oxygen atom radiation 5577 A has received most study.

ionosphere, the pattern of the diurnal winds produced in this circulation would likewise show departures from the average from day to day, and with this also the pattern of excitation. It would seem that in the high atmosphere the sun is constantly sending a "bow wave" of air [3a] toward both poles, which may tend to force the large-scale zonal circulation into an eccentric motion that rotates with the sun around the poles, leading to a flow of air across the polar regions, with important fluctuations depending on changes in the ultraviolet solar radiation and on instability in the large-scale atmospheric circulation.

### *Acknowledgment*

Discussions with Dr. F. E. Roach and his collaborators concerning their work on the airglow led the author to extend the suggestion he had earlier made regarding the production of aurora by winds to the airglow, and to develop the suggestion somewhat further. He gratefully acknowledges the stimulation received from these conversations. He is also grateful for very helpful discussions with Professors Verner Schomaker and Leverett Davis, Jr., of the California Institute of Technology.

### *References*

[1] A. Maxwell and C. G. Little, Nature, **169**, 746 (1952). See also references at the end of their article.
[2] W. W. Kellogg and G. F. Schilling, J. Met., **8**, 222 (1951).
[3] (*a*) O. R. Wulf, Terr. Mag., **50**, 185 (1945). (*b*) See also F. E. Roach and N. B. Pettit, L'étude optique de l'atmosphère terrestre, Mem. Soc. roy sci. Liége, **12**, 13 (1952).
[4] H. C. Early and W. G. Dow, Phys. Rev., **79**, 186 (1950).
[5] (*a*) F. E. Roach and H. B. Pettit, J. Geophys. Res., **56**, 325 (1951); L'étude optique de l'atmosphère terrestre, Mém. Soc. roy. sci. Liége, **12**, 13 (1952); F. E. Roach, D. R. Williams, and H. B. Pettit, J. Geophys. Res., **58**, 73 (1953); (*b*) D. Barbier, Mém. Soc. roy. sci. Liége, **12**, 43 (1952).
[6] In this connection, see D. R. Bates and M. Nicolet, J. Geophys. Res., **55**, 235 (1950).
[7] See, for example, K. T. Compton and I. Langmuir, Rev. Modern Phys., **2**, 123 (1930).
[8] The Rocket Panel, Phys. Rev., **88**, 1027 (1952).
[9] C. G. Little and A. Maxwell, J. Atmos. Terr. Phys., **2**, 356 (1952).
[10] O. R. Wulf and S. B. Nicholson, Pub. A. S. P., **60**, 37, 259 (1948); **61**, 166 (1949); **62**, 202 (1950); Phys. Rev., **73**, 1204 (1948); S. B. Nicholson and O. R. Wulf, Pub. A. S. P., **64**, 265 (1952).
[11] E. O. Hulbert, Rev. Modern Phys., **9**, 44 (1937).
[12] In this connection, see J. M. Stagg and J. Paton, Nature, **143**, 941 (1939).
[13] O. R. Wulf and L. Davis, Jr., J. Met., **9**, 82 (1952).
[14] Concerning diurnal effects in the aurora and in the airglow, see also A. B. Meinel and D. H. Schulte, Astroph. J., **117**, 454 (1953), and F. E. Roach, D. R. Williams, and H. Pettit, Astroph. J. **117**, 456 (1953).
[15] H. Alfvén, Cosmical electrodynamics, Oxford, Clarendon Press (1950); see p. 204.

Journal of Geophysical Research Volume 58, No. 4 December, 1953

# NOTE ON GEOMAGNETIC DISTURBANCE AS AN ATMOSPHERIC PHENOMENON

By E. H. Vestine

*Department of Terrestrial Magnetism, Carnegie Institution of Washington, Washington 15, D. C.*

(Received September 28, 1953)

ABSTRACT

Recent studies indicate that magnetic storm currents, even including SC's and the initial phase, are in the atmosphere immediately overhead. The possible relationships of these currents to wind motions are briefly discussed.

This note (prepared at the request of the Editor) concerns some speculative studies recently undertaken at the Department of Terrestrial Magnetism, Carnegie Institution of Washington, on the general subject of the dynamo theory of geomagnetic disturbance. There is, of course, nothing radically new about such a theory. In fact, it seems to have been first proposed by Balfour Stewart [see 1 of "References" at end of paper] as long ago as 1882. It is also probably true that every student of the subject of magnetic storms has had some thoughts on the general subject of winds as the direct cause of magnetic storms. As is well known, the idea is simple. A mass of moving electrically conducting air in cutting the lines of force of the earth's main magnetic field generates electromotive forces. These in turn create variable electric current systems in the atmosphere, and the magnetic field when observed at the earth's surface undergoes time fluctuations. Hence, given a suitable air circulation in the ionosphere, as well as adequate electric conductivity, it should be possible to devise a speculative theory which would purport to explain the most complicated magnetic storm ever observed.

Strange to say, up to the present time, a developed dynamo theory for even a "simple" magnetic storm has not appeared, in spite of obvious opportunities to draw upon analogies with tropospheric storms (though they might prove to be false analogies), which would not require a great strain on the imagination. This defect is the more noteworthy in view of the classical success achieved by Schuster and Chapman in developing the dynamo theory of the ordinary quiet-day solar and lunar diurnal magnetic variations [1]. Can it be that students of magnetic storms have been so fascinated by the great Birkeland's early experiments and studies of corpuscular radiation, and the later elegant studies of solar corpuscular streams by Chapman and Ferraro [1], that they have shrunk from the task of providing a less spectacular alternate, a dynamo theory of disturbance? As far as the writer is aware, there is only one man, Oliver Wulf, who with evidently fervent

enthusiasm believes in the dynamo theory of magnetic disturbance, although he has not yet developed his approach to it from the solar and meteorological side [2]. And in Japan, a young student, Fukushima [3], has recently successfully considered the dynamo theory of disturbance pulses common in polar areas.

A subject such as magnetic storms is apt to prove somewhat dull if the only well-developed theory (for the early phases of a storm only) is one based on electric currents flowing in solar streams far out in space, and hence rather inaccessible to either proof or disproof. There is then a certain tendency to accept such a theory, which of course makes for progress in the subject if the theory is correct. But if the theory is incorrect, or only partially correct, effort proceeding mainly along very specialized lines may be unrewarding, and the subject becomes known as "difficult." It is in this spirit that the (slightly prejudiced) writer has sought to extend the development of Balfour Stewart's dynamo theory of disturbance. As the work proceeded, it became increasingly clear that the dynamo theory of disturbance is likely to be at least partially correct. Hence the foregoing comments are not in any sense written apologetically. These recent calculations will now be summarized at the request of the Editor.

As a first approach, a wind system was sought which could reproduce the monthly means of disturbance over the earth, using for this purpose the monthly means for the 12 years, 1922–33. The advantage of this approach was that the observed field changes are confined almost entirely within the geomagnetic meridian planes, so that only the effective transverse conductivity (averaged around parallels of geomagnetic latitude) needed consideration in the dynamo equations. Using Chapman's law of conductivity, and westward current densities estimated from the data, a compatible though not a unique wind system was found. In this system, the air near the equator flows poleward and returns in the less conducting region below. The only incompatibility found was that at the auroral zone the theoretical conductivity had to be multiplied by a factor of three to preserve continuity. The wind system was found to closely resemble that from meteorology due to Kellogg and Schilling [4], even to the seasonal component derived from the so-called sinusoidal part of the geomagnetic annual variation. Of course, comparisons with derived winds in this case are limited to monthly mean meridional winds, averaged along parallels of latitude.

The dynamo theory of the accompanying eastward zonal winds, strongest near the auroral zone at the upper level of circulation, was next considered. It was found that where a vertical gradient in eastward zonal wind speed exists, closed toroidal fields with a maximum axial field strength of as much as a gauss might not be unexpected in auroral regions. Such fields, of course, are likely to exist in the upper atmosphere, as will be clear from the Elsasser-Bullard dynamo theory of the earth's core [5]. In so far as circuits are available, the zonal winds thus generate toroidal currents, and when circuits are not available give rise to polarization, increasing the effective transverse conductivity of the atmosphere. Of course, the toroidal fields themselves assist in augmenting the transverse conductivity.

Qualitative wind systems were next derived for the storm-time and disturbance "daily" variations, for the maximum of the main phase of the magnetic storm of

May 1, 1933. The wind systems found were highly conjectural. Nevertheless, the wind system for the diurnally varying part appears to agree with that indicated by motion of noctilucent clouds at the lower level, and with the results of Meinel from auroral motions, and Little and Maxwell from radio star scintillations, at the upper level, with reversals in wind directions at noon and midnight [6].

An interesting speculation which arises naturally in a dynamo theory of the auroral electrojets is that, due to differential motions in growing zonal winds, there may appear a growing toroidal or solenoidal field nearly parallel to the auroral zone. It may be possible that this action serves to generate auroral particles, in a manner analogous to the familiar case of the betatron. However, an electric conductivity of the order $10^{-12}$ cgs is probably needed to start the mechanism, so that an additional source of ionization present on disturbed days must be available if this is to happen. The mechanism would seem also to predict the generation of magnetohydrodynamic waves, possibly visibly in evidence in the regular patterns of flaming aurora. It may hence be worthy of further consideration.

Important elements of the dynamo theory of disturbance have not yet been forthcoming to explain the sudden commencement and initial phase of a magnetic storm, although currents producing each of these effects appear in the atmosphere immediately overhead (see Letters to Editor by Sugiura and by the writer in this same issue). There is also need for an improved understanding of the electric conductivity of ionized media, in the presence of a magnetic field. The wind system for the storm-time variation also shows features which may tax the ingenuity of the meteorologist concerned with its driving forces.

It is believed that this approach is not without considerable promise, and that the study should be extended. It will provide interesting opportunities to the experimentalist who may be in a position to determine the extent to which the general circulation of the atmosphere contributes to the generation of magnetic storms.

A fuller presentation of this study is scheduled for the next issue (March 1954) of this JOURNAL.

## *References*

[1] S. Chapman and J. Bartels, Geomagnetism, Vols. 1 and 2, Oxford, Clarendon Press (1940).
[2] O. R. Wulf, Terr. Mag., **50**, 185-197 and 259-278 (1945).
[3] N. Fukushima, Polar magnetic storms and geomagnetic bays, J. Fac. Sci., Univ. Tokyo, 8, 293–412 (1953).
[4] W. W. Kellogg and G. F. Schilling, J. Met., **8**, 222 (1951).
[5] W. M. Elsasser, Rev. Modern Phys., **22**, 1-35 (1950).
[6] A. B. Meinel, Astroph. J., **113**, 50-59 (1951); C. G. Little and A. Maxwell, J. Atmos. Terr. Phys., **2**, 356 (1952); Nature, **159**, 746 (1952); M. Ryle and A. Hewish, Mon. Not. R. Astr. Soc., **110**, 381–394 (1950).

## *GEOMAGNETIC AND SOLAR DATA*

### INTERNATIONAL DATA ON MAGNETIC DISTURBANCES, SECOND QUARTER, 1953

#### Preliminary Report on Sudden Commencements

S.c.'s given by five or more stations are in italics. Times given are mean values, with special weight on data from quick-run records.

*Sudden commencements followed by a magnetic storm or a period of storminess (s.s.c.)*

1953 April *24d 17h 50m:* seven.
1953 May *05d 21h 15m:* sixteen.—14d 16h 40: SM Ap.—15d 04h 11: Ci Te.
1953 June *29d 07h 36m:* five.

*Sudden commencements of polar or pulsational disturbances (p.s.c.)*

1953 April 01d 00h 25m: Ci CF.—*02d 00h 24:* thirteen.—02d 19h 05: Fu Qu.—02d 20h 28: Ma Eb Qu Ta.—03d 01h 10: SM Ta.—*03d 18h 44:* fourteen.—*04d 18h 48:* five.—04d 22h 21: Ma SM Ta.—05d 19h 27: So Qu.—06d 22h 18: Le Es Ma El.—08d 20h 48: Fu Eb.—08d 21h 20: CF SM Ta.—09d 00h 03: Fu Eb SF Ta.—09d 03h 10: SM Hu.—*10d 21h 17:* thirteen.—13d 00h 44: SM SF Ta.—15d 02h 08: CF Eb SM Hr.—16d 01h 04: CF Eb.—16d 16h 18: Fu SM Ta.—16d 20h 12: Wn Ma Fu Tn.—*16d 20h 50:* eleven.—18d 01h 58: CF Ta.—19d 03h 30: CF IK Ci Ta.—19d 11h 50: Ka AM.—*20d 21h 10:* nine.—*21d 00h 04:* five.—*21d 17h 37:* eleven.—21d 22h 34: Fu Ta.—*23d 18h 40:* seven.—23d 22h 57: CF Ta.—*25d 22h 22:* five.—*25d 23h 05:* sixteen.—*26d 22h 09:* sixteen.—27d 01h 06: SM Ta.—*27d 23h 15:* five.—29d 11h 12: Ka Am.—30d 01h 15: Eb Va.—*30d 16h 24:* five.

1953 May *03d 20h 00m:* five.—*04d 20h 50:* eleven.—05d 03h 30: SM Hr.—*05d 18h 47:* ten.—06d 01h 34: Tn Hr.—06d 20h 50: Tr Do Ta Hr.—08d 01h 08: Ci Ta Hr.—08d 18h 09: Ta Te.—11d 01h 27: Eb Hr.—15d 20h 10: Ci Tn.—15d 21h 59: IK Tn.—16d 21h 18: Ci Tn.—18d 22h 06: SM Ta.—*19d 00h 10:* ten.—19d 20h 27: Wi Qu Ta.—21d 20h 15: Es El.—*22d 19h 29:* six.—23d 20h 10: SM Ta.—*24d 18h 58:* five.—*25d 22h 42:* seven.—27d 07h 01: Te Am.—*29d 23h 45:* six.—30d 21h 46: Wn IK El.—*31d 19h 52:* seven.

1953 June *02d 03h 00m:* thirteen.—02d 06h 32: Ma Pr.—*05d 19h 14:* eleven.—*11d 21h 44:* eleven.—12d 18h 07: Qu Tn.—12d 20h 35: Eb El Tn.—13d 18h 09: Fu Qu.—13d 18h 55: SM El.—14d 17h 59: Fu Qu.—15d 13h 09: Ka To Am.—20d 13h 44: Ka To Am.—20d 20h 18: Fu Tn.—21d 18h 05: IK Eb Qu.—*21d 21h 55:* six.—*25d 20h 11:* six.—26d 17h 55: Eb Bi El.—*27d 22h 04:* six.—29d 07h 40: Pr Qu Tn.—29d 09h 18: Tn Am.

*Geomagnetic planetary three-hour-range indices Kp, preliminary magnetic character-figure C, and final selected days, April to June, 1953*

| | April 1953 | | | | | | | | | May 1953 | | | | | | | | |
|---|---|---|---|---|---|---|---|---|---|---|---|---|---|---|---|---|---|---|
| E | 1 | 2 | 3 | 4 | 5 | 6 | 7 | 8 | Sum | 1 | 2 | 3 | 4 | 5 | 6 | 7 | 8 | Sum |
| 1 | 4 + | 3o | 2 + | 4o | 3 − | 2o | 1 + | 2 − | 21 + | 1o | 1 − | 1 + | 2 − | 2 − | 2 + | 0 + | 1o | 10o |
| 2 | 4o | 3 + | 3 + | 3o | 1 + | 2o | 3 + | 2 + | 23 − | 2o | 1 + | 0 + | 2 − | 1 + | 0 + | 1 − | 1 − | 8 − |
| 3 | 4 − | 3 + | 2 − | 1o | 1o | 2o | 3 + | 3 + | 19 + | 0 + | 0 + | 1o | 1 − | 1o | 2 − | 2 − | 1 + | 8o |
| 4 | 6o | 6 − | 3o | 3o | 4o | 3 + | 4 + | 3 + | 33 − | 1 + | 2 + | 1 + | 2 + | 0 + | 1o | 1 − | 2 − | 11o |
| 5 | 2 + | 0 + | 2o | 2o | 2 − | 2o | 2o | 2 − | 14o | 2 − | 3 + | 3 − | 3o | 2o | 2 − | 2 + | 3 − | 19 − |
| 6 | 2o | 3o | 2 + | 2 + | 1 + | 1 − | 1 + | 2 − | 15 − | 5 − | 3 + | 4 + | 6 − | 5 − | 3 + | 4o | 5o | 35o |
| 7 | 0 + | 0 + | 1 − | 0 + | 1o | 1o | 1o | 2 − | 6 + | 4 + | 5 − | 5 − | 5 − | 3 + | 2 + | 2 − | 3o | 29 − |
| 8 | 2 + | 2 + | 2o | 2o | 2 − | 1o | 1 + | 3o | 16 − | 4 + | 4 + | 5o | 3 + | 4 − | 3o | 5 − | 4 − | 32o |
| 9 | 3o | 3 + | 0 + | 2 − | 1 + | 2 − | 2 − | 1o | 14o | 4 + | 4o | 4o | 4o | 3 − | 3o | 3o | 4 − | 29 − |
| 10 | 2 − | 3 + | 3 − | 4 − | 4 − | 3o | 2 + | 3 + | 24 − | 2o | 1 + | 2 + | 3 − | 3 + | 2 + | 3o | 2o | 19o |
| 11 | 2 − | 5 − | 4 + | 4 + | 3 + | 5 − | 3o | 3 − | 29 − | 3 − | 2o | 2 + | 3o | 2o | 1 + | 1o | 1o | 15 + |
| 12 | 3 + | 3 − | 3 + | 4o | 3 + | 1 + | 2 + | 2o | 22 + | 1 + | 2o | 2 − | 0 + | 1o | 1 − | 1 + | 1 + | 10 − |
| 13 | 4o | 2o | 4 − | 4o | 4 + | 4 − | 3o | 1o | 26 − | 1o | 1o | 0 + | 1 + | 1o | 0 + | 1o | 0 + | 6 + |
| 14 | 2o | 2 + | 2 − | 1 + | 2 + | 1 + | 2 − | 1 + | 14o | 1o | 1 − | 1 − | 0 + | 1o | 1o | 1o | 2o | 8 − |
| 15 | 3 + | 3o | 2 + | 3 + | 2 + | 1 + | 2o | 2 − | 19 + | 1o | 3o | 3 − | 2 + | 5 + | 5 + | 8 − | 7 − | 34o |
| 16 | 4o | 5 + | 4 + | 4 − | 4 − | 5 + | 5 − | 5 + | 36 + | 6 − | 6o | 5 − | 5 + | 6 + | 6o | 7 − | 7 + | 48o |
| 17 | 4o | 2 − | 3 + | 3 + | 4 − | 2o | 1 + | 1 + | 21 − | 7 − | 5 − | 3o | 1 + | 2o | 3o | 3 − | 4 − | 27o |
| 18 | 3 − | 3 − | 4 − | 3o | 2o | 2 + | 2 + | 2 + | 21o | 3 + | 4 − | 4 − | 3 + | 3 − | 2 − | 2 + | 3 + | 24o |
| 19 | 3 − | 5o | 3o | 3o | 5 − | 4 − | 2o | 4 − | 28 − | 4o | 5o | 4 − | 4 + | 4 − | 1 + | 4 − | 4 + | 30o |
| 20 | 5 − | 5 + | 5o | 4 − | 4o | 4 − | 4 − | 5o | 35o | 4 − | 2 + | 4 − | 3o | 2 + | 2 + | 3o | 3 + | 24 − |
| 21 | 4 − | 4 − | 5 − | 4 − | 3o | 4 + | 5o | 4o | 32o | 2 + | 3 − | 3o | 2 − | 1 + | 2 + | 3o | 2 + | 19 − |
| 22 | 3 + | 3 + | 3o | 3 + | 4o | 4 + | 4o | 4 − | 29o | 2o | 4 − | 2o | 2o | 3 − | 2 + | 5 − | 3 + | 23 − |
| 23 | 4 − | 5o | 4o | 3 − | 4 − | 3o | 4 − | 3 + | 29o | 2 + | 1 + | 2o | 2 + | 2 − | 1 + | 2 + | 2 − | 15o |
| 24 | 2 + | 1o | 1 + | 1 + | 2 + | 3o | 3o | 2 + | 17 − | 1o | 1 − | 2o | 1o | 2 + | 2o | 2 + | 2 − | 13o |
| 25 | 3 − | 2 − | 2 − | 3 − | 3 − | 3 − | 3o | 4 − | 21 − | 1 − | 1 − | 1 + | 1 + | 1 + | 2o | 1 − | 2 + | 10 − |
| 26 | 3o | 3 − | 4 − | 2o | 4 − | 3 − | 2 − | 3 + | 23 − | 1 + | 1o | 1 + | 1 + | 1 + | 1 − | 3o | 3 − | 13 − |
| 27 | 3 + | 2o | 2 + | 2o | 2 + | 2o | 2 − | 2 + | 18o | 3 + | 5 − | 5 + | 4 + | 3 − | 3 + | 2 − | 2 − | 28 − |
| 28 | 2 + | 2 + | 3 − | 3 − | 2o | 1 + | 0 + | 0o | 14 − | 2o | 3 − | 2 − | 2 − | 2o | 2 + | 2o | 1o | 15 + |
| 29 | 1 + | 1 + | 2 + | 3 − | 4 − | 2 + | 1 + | 1 − | 16 − | 1 − | 1o | 2 − | 2o | 2 + | 1 + | 1 − | 1 − | 11o |
| 30 | 3 − | 2 + | 3o | 3 − | 2 + | 4 − | 3 + | 2 − | 22 − | 2 + | 1 + | 1 − | 1 − | 1o | 1o | 1o | 2 − | 10 − |
| 31 | | | | | | | | | | 2 − | 0 + | 1 − | 2o | 2 + | 2 + | 4 − | 1 − | 14 − |

| | June 1953 | | | | | | | | | Preliminary C, 1953 | | |
|---|---|---|---|---|---|---|---|---|---|---|---|---|
| E | 1 | 2 | 3 | 4 | 5 | 6 | 7 | 8 | Sum | Apr. | May | June |
| 1 | 2 − | 2 − | 2 − | 1 − | 1 − | 1o | 2 − | 1 + | 10 + | 0.7 | 0.2 | 0.1 |
| 2 | 3 − | 4 + | 6o | 6 − | 5o | 5o | 6 − | 5 − | 39o | 0.8 | 0.1 | 1.5 |
| 3 | 5 − | 4 + | 6o | 3o | 4 + | 4 − | 4o | 3o | 33o | 0.8 | 0.1 | 1.4 |
| 4 | 4 + | 5 − | 5 − | 4o | 3 + | 3o | 2 + | 2o | 28 + | 1.2 | 0.1 | 1.0 |
| 5 | 2 − | 3 + | 4o | 3o | 1 + | 2 + | 6 − | 2 + | 24 − | 0.2 | 1.0 | 1.0 |
| 6 | 3o | 4 − | 3o | 3 − | 2 + | 3o | 2 + | 1 + | 21 + | 0.3 | 1.5 | 0.7 |
| 7 | 2 + | 2 − | 3 + | 2o | 2 − | 2 − | 1 + | 2 − | 16 − | 0.1 | 1.1 | 0.4 |
| 8 | 2 − | 2 − | 2 − | 1o | 1 + | 2 − | 1o | 1o | 11o | 0.6 | 1.1 | 0.1 |
| 9 | 1 − | 1 + | 2o | 2 − | 1 + | 1o | 1 + | 1o | 10 + | 0.4 | 1.0 | 0.1 |
| 10 | 1 + | 3o | 4 − | 2 + | 2o | 2o | 3 + | 2 + | 20o | 0.9 | 0.6 | 0.6 |
| 11 | 2o | 2o | 2 + | 2o | 2o | 1 + | 1 + | 3 + | 16 + | 1.1 | 0.3 | 0.5 |
| 12 | 1 − | 1 + | 1 + | 2 + | 2 + | 3 + | 4 + | 4o | 20 − | 0.8 | 0.0 | 0.9 |
| 13 | 4 − | 3 + | 2 + | 2o | 2 + | 2o | 3 + | 3 − | 22 − | 0.9 | 0.0 | 0.8 |
| 14 | 2 + | 2o | 2o | 1o | 2o | 2o | 3 − | 2o | 16o | 0.1 | 0.1 | 0.5 |
| 15 | 1 − | 1 + | 1 + | 0 + | 2 − | 1 − | 2 + | 2o | 10 + | 0.6 | 1.5 | 0.2 |
| 16 | 0 + | 0 + | 1o | 2 − | 2 − | 1 − | 1o | 1 + | 8o | 1.4 | 1.8 | 0.2 |
| 17 | 2o | 1 + | 2 + | 1 + | 3 + | 3o | 1 + | 2 + | 17o | 0.7 | 1.2 | 0.5 |
| 18 | 2o | 2o | 2o | 1 − | 1 − | 0 + | 2 − | 2o | 11 + | 0.7 | 0.9 | 0.2 |
| 19 | 1o | 1o | 2 − | 0 + | 1 + | 1 + | 1 − | 1 + | 9 − | 1.1 | 1.1 | 0.2 |
| 20 | 1o | 2 − | 2 − | 3o | 4 − | 3o | 5 − | 4 − | 22 + | 1.3 | 0.9 | 0.8 |
| 21 | 2o | 3o | 4 − | 3o | 2 − | 2o | 3o | 3o | 21 + | 1.3 | 0.6 | 0.7 |
| 22 | 1 + | 2 − | 2 + | 3 − | 3o | 2o | 2o | 2 + | 17 + | 1.1 | 0.8 | 0.8 |
| 23 | 1 + | 1 − | 1 − | 0 + | 1 − | 0 + | 0 + | 2o | 6 + | 1.0 | 0.3 | 0.0 |
| 24 | 2o | 2o | 1 + | 1 − | 1 − | 1 + | 3o | 2 + | 13 + | 0.5 | 0.3 | 0.4 |
| 25 | 2 + | 1 + | 1o | 1o | 1o | 1o | 1 + | 1 + | 10 + | 0.7 | 0.2 | 0.1 |
| 26 | 0o | 0o | 0 + | 0 + | 0 + | 1o | 1 + | 1o | 4 + | 1.0 | 0.4 | 0.0 |
| 27 | 0 + | 1 − | 1 − | 1 + | 1 − | 1 + | 1 + | 2 − | 8o | 0.5 | 1.1 | 0.2 |
| 28 | 1 − | 2 − | 0 + | 1 − | 1 − | 0 + | 1 + | 2 + | 8o | 0.2 | 0.4 | 0.2 |
| 29 | 2 − | 1o | 3 + | 6 − | 6 + | 6 − | 5 − | 5 − | 33o | 0.5 | 0.2 | 1.5 |
| 30 | 6 − | 4 + | 5o | 5 + | 4 − | 4 − | 4 − | 3 + | 35 − | 0.6 | 0.2 | 1.4 |
| 31 | | | | | | | | | | | 0.4 | |

| Final selected days | | |
|---|---|---|
| Apr. | May | June |
| *Five quiet* | | |
| 5 | 2 | 16 |
| 6 | 3 | 19 |
| 7 | 12 | 23 |
| 14 | 13 | 26 |
| 28 | 14 | 27 |
| *Five disturbed* | | |
| 4 | 6 | 2 |
| 10 | 8 | 3 |
| 20 | 15 | 4 |
| 21 | 16 | 29 |
| 23 | 19 | 30 |
| *Ten quiet* | | |
| 5 | 1 | 1 |
| 6 | 2 | 8 |
| 7 | 3 | 9 |
| 8 | 4 | 16 |
| 9 | 12 | 19 |
| 14 | 13 | 23 |
| 24 | 14 | 25 |
| 27 | 25 | 26 |
| 28 | 29 | 27 |
| 29 | 30 | 28 |

*Sudden impulses found in the magnetograms (s.i.)*

1953 April 10d 18h 00m: SM Qu.—12d 12h 40: Le Es.—14d 06h 30: Ta Hr.—*15d 05h 00:* five.—21d 11h 59: Le Es Ab Ma.—24d 19h 45: Ma Pr.—27d 18h 23: Wn IK Qu.

1953 May *06d 07h 40m:* nine.—15d 20h 01: Wn Pr.—*15d 20h 41:* five.—*26d 07h 21:* eight.—27d 09h 00: Ka Tn Hr.

1953 June 18d 19h 06m: Ma Tn.

Preliminary Report on Solar-flare Effects

Effects confirmed by ionospheric or solar observations are in italics.

1953 April 05d 08h 12m: Ma.—23d 23h 10–24d 01h 00: Tu.—24d 19h 36: Ma.—25d 10h 24: El.—25d 10h 36–10h 41: Ma SM.—25d 14h 53: Ma Pr.—26d 14h 14: Pr.—27d 13h 22: Hu.—28d 10h 17: Pr.—29d 14h 00–14h 50: Tu.—30d 10h 31–10h 36: SM.

1953 May 02d 11h 08m: Tl.—06d 13h 30–13h 40: Te.—08d 20h 09–20h 19: Te.—10d 20h 16–20h 23: Te.—13d 18h 51–19h 45: Tu.—13d 22h 10–22h 18: Tu.—14d 16h 37–24h 00: Tu.—15d 06h 30: El.—18d 06h 44: Pr Ci.—23d 20h 08–20h 36: Te.—24d 21h 27–21h 46: Te.—25d 17h 42–17h 56: Tu.—25d 21h 03–21h 15: Te.

1953 June 06d 16h 15,: Pr.—*06d 20h 39–20h 50:* Te.—*07d 21h 21–21h 30:* Te.—08d 15h 02–18h 00: Tu.—*09d 21h 05–21h 16:* Te.—*10d 19h 21–19h 34:* Te.—*10d 22h 52–23h 11:* Te.—13d 01h 21–02h 10: Te.—19d 15h 33–17h 50: Tu.—*20d 20h 07–20h 21:* Te.—24d 19h 00–24h 00: Tu.—*24d 22h 33–22h 46:* Te.—25d 00h 00–00h 55: Tu.

*Ionospheric or solar disturbances without clear geomagnetic effect*

None.

Minor disturbances reported by one station only are listed in the De Bilt quarterly circular, but omitted here.

Committee on Characterization of Magnetic Disturbances

J. Bartels, *Chairman*
University
Göttingen, Germany

J. Veldkamp
Kon. Nederlandsch Meteorologisch Instituut
De Bilt, Holland

## PROVISIONAL SUNSPOT-NUMBERS FOR JULY TO SEPTEMBER, 1953

(Dependent on observations at Zurich Observatory and its stations at Locarno and Arosa)

| Day | July | Aug. | Sep. |
|---|---|---|---|
| 1 | 0 | 0 | 0 |
| 2 | 7 | 7 | 0 |
| 3 | 0 | 12 | 7 |
| 4 | 0 | 12 | 0 |
| 5 | 0 | 11 | 7 |
| 6 | 7 | 10 | 7 |
| 7 | 7 | 16 | 9 |
| 8 | 0 | 10 | 24 |
| 9 | 9 | 29 | 23 |
| 10 | 20 | 48 | 27 |
| 11 | 22 | 73 | 32 |
| 12 | 16 | 77 | 29 |
| 13 | 23 | 73 | 18 |
| 14 | 24 | 65 | 30 |
| 15 | 40 | 62 | 43 |
| 16 | 19 | 54 | 42 |
| 17 | 16 | 47 | 38 |
| 18 | 21 | 31 | 38 |
| 19 | 11 | 26 | 34 |
| 20 | 8 | 24 | 17 |
| 21 | 14 | 17 | 25 |
| 22 | 0 | 10 | 16 |
| 23 | 0 | 8 | 9 |
| 24 | 0 | 0 | 15 |
| 25 | 0 | 0 | 14 |
| 26 | 0 | 0 | 14 |
| 27 | 0 | 0 | 0 |
| 28 | 0 | 0 | 9 |
| 29 | 0 | 0 | 7 |
| 30 | 0 | 0 | 9 |
| 31 | 0 | 0 | |
| Means........ | 8.5 | 23.3 | 18.1 |
| No. days...... | 31 | 31 | 30 |

*Mean for quarter: 16.6 (92 days)*

M. Waldmeier

Swiss Federal Observatory
*Zurich, Switzerland*

## CHELTENHAM THREE-HOUR-RANGE INDICES $K$ FOR JULY TO SEPTEMBER, 1953

[$K9 = 500\gamma$; scale-values of variometers in $\gamma$/mm: $D = 5.4$; $H = 2.5$; $Z = 4.3$]

| Gr. day | July 1953 | | August 1953 | | Sep. 1953 | |
|---|---|---|---|---|---|---|
| | Values $K$ | Sum | Values $K$ | Sum | Values $K$ | Sum |
| 1 | 4455 4344 | 33 | 4322 2344 | 24 | 3343 4223 | 24 |
| 2 | 4553 3344 | 31 | 2424 2232 | 21 | 5453 3222 | 26 |
| 3 | 4333 3233 | 24 | 2231 2222 | 16 | 3132 2336 | 23 |
| 4 | 3343 3323 | 24 | 3332 2332 | 21 | 6655 3344 | 36 |
| 5 | 3352 2223 | 22 | 2233 1132 | 17 | 5443 2233 | 26 |
| 6 | 4233 1113 | 18 | 1112 2223 | 14 | 1252 2133 | 19 |
| 7 | 4441 3334 | 26 | 4214 1123 | 18 | 2334 2323 | 22 |
| 8 | 4332 2333 | 23 | 3332 2213 | 19 | 3334 1110 | 16 |
| 9 | 3221 1244 | 19 | 4432 3243 | 25 | 4322 1011 | 14 |
| 10 | 3241 0212 | 15 | 3353 2234 | 25 | 2122 2213 | 15 |
| 11 | 2301 1012 | 10 | 5433 2233 | 25 | 5332 3121 | 20 |
| 12 | 1210 1144 | 14 | 4455 3433 | 31 | 2223 2234 | 20 |
| 13 | 2354 2233 | 24 | 4332 3354 | 27 | 4333 1122 | 19 |
| 14 | 1222 2453 | 21 | 4423 2233 | 23 | 1111 0111 | 7 |
| 15 | 3444 3232 | 25 | 3221 1132 | 15 | 0333 3344 | 23 |
| 16 | 2211 0011 | 8 | 3323 2233 | 21 | 3333 2233 | 22 |
| 17 | 1233 1112 | 14 | 2101 2111 | 9 | 5332 2132 | 21 |
| 18 | 3311 1112 | 13 | 3310 2122 | 14 | 3322 1245 | 22 |
| 19 | 3220 1133 | 15 | 2211 2011 | 10 | 7666 5533 | 41 |
| 20 | 3322 2112 | 16 | 1111 1112 | 9 | 6653 3345 | 35 |
| 21 | 2232 0112 | 13 | 1201 1111 | 8 | 5453 3333 | 29 |
| 22 | 1011 1223 | 11 | 1322 2111 | 13 | 5463 2144 | 29 |
| 23 | 4445 4354 | 33 | 3344 3446 | 31 | 4464 4444 | 34 |
| 24 | 5223 2334 | 24 | 5653 4456 | 38 | 4455 4133 | 29 |
| 25 | 1221 2343 | 18 | 4555 4233 | 31 | 4233 3222 | 21 |
| 26 | 4343 2244 | 26 | 5442 3344 | 29 | 2132 1233 | 17 |
| 27 | 5654 3343 | 33 | 5644 3444 | 34 | 5453 2110 | 21 |
| 28 | 5454 3334 | 31 | 5544 3434 | 32 | 3332 1121 | 16 |
| 29 | 4444 3445 | 32 | 4555 4353 | 34 | 0211 1211 | 9 |
| 30 | 5343 4334 | 29 | 5555 4434 | 35 | 1132 1033 | 14 |
| 31 | 4344 3223 | 25 | 4443 4334 | 29 | | |

Ralph R. Bodle
*Observer-in-Charge*

Cheltenham Magnetic Observatory
*Cheltenham, Maryland, U.S.A.*

## PRINCIPAL MAGNETIC STORMS

(Advance knowledge of the character of the records at some observatories as regards disturbances)

| bservatory (Observer-n-Charge) | Green-wich date | Storm-time: GMT of begin. | Storm-time: GMT of ending[1] | Sudden commencement: Type[2] | Amplitudes[3]: D | Amplitudes[3]: H | Amplitudes[3]: Z | C-figure, degree of activity[4] | Maximal activity on K-scale 0 to 9: Gr. day | Gr. 3-hr. period | K-index | Ranges: D | Ranges: H | Ranges: Z |
|---|---|---|---|---|---|---|---|---|---|---|---|---|---|---|
| (1) | (2) | (3) | (4) | (5) | (6) | (7) | (8) | (9) | (10) | (11) | (12) | (13) | (14) | (15) |
| | *1953* | h m | d h | | ′ | γ | γ | | | | | ′ | γ | γ |
| lege | July 23 | 00 .. | 24 02 | ..... | .... | .... | .... | ms | 23 | 4,6 | 6 | 225 | 1270 | 950 |
| J. Beers) | July 26 | 01 .. | 31 16 | ..... | .... | .... | .... | ms | 28 | 4 | 7 | 150 | 1520 | 830 |
| | | | | | | | | | 29 | 4 | 7 | | | |
| | | | | | | | | | 30 | 4,5 | 7 | | | |
| | Aug. 12 | 01 .. | 13 06 | ..... | .... | .... | .... | ms | 12 | 3,4 | 7 | 250 | 1590 | 970 |
| | Aug. 23 | 00 24 | 25 20 | s.c.* | 9 | 7 | 10 | ms | 24 | 5 | 7 | 240 | 1440 | 610 |
| | Aug. 27 | 02 .. | 31 22 | ..... | .... | .... | .... | ms | 27 | 3,4 | 7 | 250 | 1730 | 1060 |
| | | | | | | | | | 28 | 4 | 7 | | | |
| | | | | | | | | | 30 | 3,5,6 | 7 | | | |
| | | | | | | | | | 31 | 5 | 7 | | | |
| | Sep. 3 | 08 30 | 5 13 | ..... | .... | .... | .... | ms | 4 | 3,4 | 7 | 180 | 1300 | 1090 |
| | Sep. 18 | 18 02 | 22 15 | ..... | .... | .... | .... | s | 19 | 4 | 8 | 370 | 2600 | 1460 |
| | Sep. 23 | 04 .. | 24 20 | ..... | .... | .... | .... | s | 24 | 4 | 8 | 320 | 1900 | 790 |
| a | July 23 | 03 .. | 24 02 | ..... | .... | .... | .... | ms | 23 | 4 | 7 | 70 | 645 | 664 |
| L.Skillman) | July 25 | 02 30 | 31 18 | ..... | .... | .... | .... | ms | 27 | 3 | 7 | 80 | 695 | 703 |
| | Aug. 12 | 00 45 | 14 20 | ..... | .... | .... | .... | ms | 12 | 3,4 | 7 | 137 | 717 | 670 |
| | Aug. 23 | 00 23 | 31 22 | s.c.* | +5 | −5 | −4 | ms | 23 | 4 | 7 | 103 | 746 | 686 |
| | | | | | | | | | 27 | 4 | 7 | | | |
| | | | | | | | | | 29 | 3 | 7 | | | |
| | | | | | | | | | 30 | 3,6 | 7 | | | |
| | | | | | | | | | 31 | 5 | 7 | | | |
| | Sep. 3 | 08 21 | 5 11 | ..... | .... | .... | .... | ms | 4 | 2,3,4 | 7 | 96 | 824 | 598 |
| | Sep. 18 | 18 00 | 24 16 | ..... | .... | .... | .... | s | 19 | 4 | 8 | 169 | 1155 | 1117 |
| teveen | Apr. 13 | 18 00 | 4 24 | ..... | .... | .... | .... | m | 3 | 7 | 5 | 30 | 155 | 60 |
| van Sabben) | | | | | | | | | 4 | 1,2,7 | 5 | | | |
| | Apr. 16 | 00 00 | 16 24 | ..... | .... | .... | .... | ms | 16 | 6,8 | 6 | 30 | 285 | 95 |
| | Apr. 19 | 08 00 | 23 24 | ..... | .... | .... | .... | m | 19 | 8 | 5 | 25 | 155 | 65 |
| | | | | | | | | | 20 | 8 | 5 | | | |
| | | | | | | | | | 21 | 6,7 | 5 | | | |
| | | | | | | | | | 23 | 7 | 5 | | | |
| | May 5 | 21 16 | 9 24 | s.c. | 0 | +25 | 0 | m | 6 | 1,4,7,8 | 5 | 25 | 200 | 60 |
| | | | | | | | | | 8 | 3,7 | | | | |
| | | | | | | | | | 9 | 1 | | | | |
| | May 15 | 09 00 | 17 07 | ..... | .... | .... | .... | ms | 15 | 7 | 7 | 55 | 250 | 180 |
| | | | | | | | | | 16 | 8 | 7 | | | |
| | June 2 | 02 00 | 4 24 | ..... | .... | .... | .... | m | 2 | 2nd-7th | 5 | 25 | 190 | 75 |
| | | | | | | | | | 3 | 1,3,5 | 5 | | | |
| | June 5 | 16 00 | 6 21 | ..... | .... | .... | .... | ms | 5 | 7 | 6 | 25 | 185 | 40 |
| | June 12 | 10 00 | 12 24 | ..... | .... | .... | .... | m | 12 | 8 | 5 | 15 | 100 | 60 |
| | June 29 | 07 00 | 4 24 | ..... | .... | .... | .... | ms | 29 | 5,6 | 6 | 30 | 225 | 100 |
| | July 7 | 14 25 | 8 24 | s.c. | +2 | +20 | 0 | m | 7 | 8 | 5 | 20 | 100 | 45 |
| | July 23 | 08 08 | 24 24 | s.c.* | +4 | −10 | +2 | ms | 23 | 6,8 | 6 | 35 | 200 | 100 |
| | July 26 | 00 00 | 31 24 | ..... | .... | .... | .... | ms | 27 | 6 | 6 | 30 | 205 | 65 |
| | Aug. 9 | 10 00 | 14 07 | ..... | .... | .... | .... | ms | 12 | 6 | 6 | 35 | 235 | 120 |
| | Aug. 23 | 00 24 | 31 24 | s.c.* | −1 | +28 | 0 | ms | 23 | 8 | 6 | 45 | 260 | 125 |
| | | | | | | | | | 24 | 6,7,8 | 6 | | | |
| | | | | | | | | | 27 | 6,7 | 6 | | | |
| | | | | | | | | | 29 | 7 | 6 | | | |
| | | | | | | | | | 30 | 6 | 6 | | | |

[1]Approximate time of ending of storm construed as the time of cessation of reasonably marked disturbance movements in the es; more specifically, when the *K*-index measure diminished to 2 or less for a reasonable period.

[2]s.c. = sudden commencement; s.c.* = small initial impulse followed by main impulse (the amplitude in this case is that of the *n impulse only*, neglecting the initial brief pulse; . . . = gradual commencement.

[3]Signs of amplitudes of *D* and *Z* taken algebraically; *D* reckoned positive if towards the east and *Z* reckoned positive if ver-y downwards.

[4]Storm described by three degrees of activity: *m* for moderate (when *K*-index as great as 5); *ms* for moderately severe (when = 6 or 7); *s* for severe (when *K* = 8 or 9).

PRINCIPAL MAGNETIC STORMS—*Continued*

| Observatory (Observer-in-Charge) (1) | Greenwich date (2) | Storm-time: GMT of begin. (3) | Storm-time: GMT of ending[1] (4) | Sudden commencement: Type[2] (5) | Amplitudes[3] D (6) | Amplitudes[3] H (7) | Amplitudes[3] Z (8) | C-figure, degree of activity[4] (9) | Maximal activity on K-scale 0 to 9: Gr. day (10) | Gr. 3-hr. period (11) | K-index (12) | Ranges D (13) | Ranges H (14) | Ranges Z (15) |
|---|---|---|---|---|---|---|---|---|---|---|---|---|---|---|
| | *1953* | *h m* | *d h* | | ′ | γ | γ | | | | | ′ | γ | γ |
| Witteveen—*Continued* (D. van Sabben) | Sep. 3 | 09 00 | 5 24 | ..... | .... | .... | .... | ms | 3 | 6 | 7 | 50 | 295 | [illegible] |
| | | | | | | | | | 4 | 1 | 7 | | | |
| | Sep. 15 | 02 59 | 16 24 | s.c.* | −2 | +10 | 0 | m | 15 | 7 | 5 | 30 | 105 | [illegible] |
| | | | | | | | | | 16 | 7 | 5 | | | |
| | Sep. 18 | 16 09 | 24 24 | s.c.* | −1 | +19 | 0 | ms | 19 | 6 | 7 | 65 | 300 | [illegible] |
| Cheltenham (R.R.Bodle) | July 14 | 17 .. | 15 24 | ..... | .... | .... | .... | m | 14 | 7 | 5 | 14 | 99 | [illegible] |
| | July 23 | 03 .. | 24 02 | ..... | .... | .... | .... | m | 23 | 4 | 5 | 23 | 97 | [illegible] |
| | July 26 | 20 .. | 31 17 | ..... | .... | .... | .... | ms | 27 | 2 | 6 | 31 | 151 | [illegible] |
| | Aug. 9 | 01 .. | 13 06 | ..... | .... | .... | .... | m | 12 | 3,4 | 5 | 28 | 152 | [illegible] |
| | Aug. 23 | 00 24 | 2 04 | s.c. | −1 | −52 | 0 | ms | 24 | 8 | 6 | 48 | 161 | [illegible] |
| | Sep. 3 | 21 .. | 5 07 | ..... | .... | .... | .... | ms | 3 | 8 | 6 | 36 | 154 | [illegible] |
| | | | | | | | | | 4 | 1 | 6 | | | |
| | Sep. 18 | 18 .. | 24 02 | ..... | .... | .... | .... | ms | 19 | 1 | 7 | 50 | 165 | [illegible] |
| Tucson (M.L.Cleven) | June 29 | 07 00 | 3 15 | ..... | .... | .... | .... | m | 1 | 3,4 | 5 | 17 | 154 | [illegible] |
| | | | | | | | | | 2 | 1,2,3 | 5 | | | |
| | July 23 | 03 00 | 24 01 | ..... | .... | .... | .... | m | 23 | 4 | 5 | 10 | 104 | [illegible] |
| | | | | | | | | | 24 | 1 | 5 | | | |
| | July 26 | 00 00 | 31 16 | ..... | .... | .... | .... | ms | 27 | 2,3 | 6 | 21 | 114 | [illegible] |
| | Aug. 23 | 00 24 | 31 21 | s.c. | −1 | 13 | 2 | ms | 24 | 8 | 6 | 20 | 136 | [illegible] |
| | | | | | | | | | 27 | 2 | 6 | | | |
| | | | | | | | | | 30 | 1 | 6 | | | |
| | Sep. 3 | 18 00 | 5 10 | ..... | .... | .... | .... | ms | 3 | 8 | 7 | 19 | 185 | [illegible] |
| | Sep. 18 | 18 00 | 24 15 | ..... | .... | .... | .... | ms | 19 | 1,2,4 | 6 | 27 | 162 | [illegible] |
| | | | | | | | | | 20 | 2 | 6 | | | |
| | | | | | | | | | 22 | 3 | 6 | | | |
| Honolulu (R.F.White) | July 25 | 18 00 | 28 15 | ..... | .... | .... | .... | m | 27 | 2,3 | 5 | 9 | 105 | [illegible] |
| | Aug. 23 | 03 50 | 31 24 | ..... | .... | .... | .... | m | 29 | 2,3,4 | 5 | 10 | 102 | [illegible] |
| | Sep. 3 | 15 00 | 5 21 | ..... | .... | .... | .... | ms | 3 | 8 | 7 | 14 | 162 | [illegible] |
| | Sep. 18 | 17 55 | 24 15 | ..... | .... | .... | .... | ms | 22 | 3 | 6 | 9 | 102 | [illegible] |
| Instituto Geofísico de Huancayo (A.A.Giesecke M.Casaverde) | Apr. 9 | 03 11 | 11 20 | s.c. | 0 | +26 | 0 | m | 10 | 6 | 5 | 9 | 200 | [illegible] |
| | Apr. 19 | 02 53 | 23 04 | ..... | .... | .... | .... | m | 21 | 6 | 5 | 6 | 177 | [illegible] |
| | May 5 | 21 16 | 7 08 | s.c. | 0 | +17 | −3 | m | 6 | ... | 4 | 4 | 191 | [illegible] |
| | May 15 | 06 47 | 17 06 | ..... | .... | .... | .... | m | 15 | 5,6 | 5 | 7 | 280 | [illegible] |
| | June 2 | 01 17 | 4 04 | ..... | .... | .... | .... | m | 2 | 3,6 | 5 | 6 | 178 | [illegible] |
| | June 29 | 07 24 | 1 14 | ..... | .... | .... | .... | ms | 29 | 6 | 6 | 7 | 226 | [illegible] |
| | July 23 | 02 42 | 3 01 | ..... | (*Note:* Rough day; *K*-index not greater than 4) | | | | | | | | | |
| | July 27 | .. .. | .. .. | ..... | (*Note:* Rough day; *K*-index not greater than 4) | | | | | | | | | |
| | Aug. 10 | 21 52 | 14 05 | ..... | .... | .... | .... | m | 13 | 5,6 | 5 | 6 | 227 | [illegible] |
| | Aug. 23 | 00 23 | 25 17 | s.c. | 0 | +22 | −3 | m | 23 | 6,7 | 5 | 5 | 189 | [illegible] |
| | Sep. 3 | 19 12 | 5 09 | ..... | .... | .... | .... | ms | 4 | 1 | 6 | 6 | 253 | [illegible] |
| | Sep. 15 | 02 59 | 16 20 | s.c. | 0 | +26 | −3 | m | 15 | 5,7 | 5 | 3 | 284 | [illegible] |
| | Sep. 18 | 15 31 | 20 21 | ..... | .... | .... | .... | m | 19 | 1,5,6 | 5 | 6 | 276 | [illegible] |
| Binza (J. Leroy) | Jan. 5 | 05 44 | 5 24 | s.c. | −1 | +27 | −2 | ms | 5 | 4,5,6 | ... | 10 | 216 | [illegible] |
| | Feb. 22 | 15 40 | 23 04 | s.c.* | +2 | −35 | +2 | m | 22 | 6,7,8 | ... | 2 | 121 | [illegible] |
| | May 6 | 7 43 | 6 24 | s.c.* | +1 | −50 | +3 | m | 6 | 4,5 | ... | 3 | 108 | |
| Vassouras (Lelio I. Gama) | May 5 | 21 16 | 7 12 | s.c. | 0 | 10 | +4 | m | 6 | 3 | 5 | 7 | 105 | [illegible] |
| | May 15 | 12 00 | 17 07 | s.c.? | .... | .... | .... | ms | 15 | 7 | 6 | 14 | 208 | [illegible] |
| | | (*Note:* S.c. probably occurred during changing of trace) | | | | | | | | | | | | |
| | June 2 | 02 .. | 3 05 | ..... | .... | .... | .... | ms | 2 | 3 | 6 | 7 | 126 | [illegible] |
| Apia (P.J.Gill) | June 28 | 21 .. | 1 14 | ..... | .... | .... | .... | m | 29 | 3,4 | 5 | 4 | 116 | [illegible] |
| | July 12 | 12 .. | 13 17 | ..... | .... | .... | .... | m | 13 | 3 | 5 | 3 | 91 | [illegible] |
| | July 23 | 08 09 | 24 06 | s.c. | 0 | +13 | −4 | m | 23 | 3,4 | 4 | | | |
| | | | | | | | | | 24 | 2 | 4 | | | |
| | July 25 | 14 .. | 1 13 | ..... | .... | .... | .... | m | 27 | 2,3 | 5 | 3 | 104 | [illegible] |
| | Aug. 23 | 00 23 | 2 11 | s.c. | 0 | +22 | −4 | m | 23 | 4,8 | 5 | 6 | 121 | [illegible] |
| | | | | | | | | | 24 | 2,8 | 5 | | | |
| | | | | | | | | | 25 | 4 | 5 | | | |
| | | | | | | | | | 29 | 2,3,4 | 5 | | | |
| | | | | | | | | | 30 | 3 | 5 | | | |

## PRINCIPAL MAGNETIC STORMS—*Continued*

| Observatory (Observer-in-Charge) (1) | Greenwich date (2) | Storm-time: GMT of begin. (3) | Storm-time: GMT of ending[1] (4) | Sudden commencement: Type[2] (5) | Amplitudes[3]: D (6) | Amplitudes[3]: H (7) | Amplitudes[3]: Z (8) | C-figure, degree of activity[4] (9) | Maximal activity on K-scale 0 to 9: Gr. day (10) | Gr. 3-hr. period (11) | K-index (12) | Ranges: D (13) | Ranges: H (14) | Ranges: Z (15) |
|---|---|---|---|---|---|---|---|---|---|---|---|---|---|---|
| | *1953* | h m | d h | | ′ | γ | γ | | | | | ′ | γ | γ |
| …ia—*Continued* | Sep. 3 | 18 .. | 7 18 | ..... | .... | .... | .... | ms | 3 | 8 | 6 | 5 | 172 | 36 |
| …(P.J.Gill) | Sep. 18 | 15 .. | 25 00 | ..... | .... | .... | .... | m | 18 | 8 | 5 | 5 | 120 | 29 |
| | | | | | | | | | 19 | 4,5 | 5 | | | |
| | | | | | | | | | 20 | 3 | 5 | | | |
| | | | | | | | | | 22 | 3 | 5 | | | |
| | | | | | | | | | 23 | 2 | 5 | | | |
| | | | | | | | | | 24 | 4 | 5 | | | |
| …ermanus | June 29 | 07 .. | 1 14 | ..... | .... | .... | .... | m | 29 | 4,5,6 | 5 | 18 | 99 | 85 |
| …M. | July 6 | 00 37 | 6 02 | s.c. | (Large bay) | | | m | 6 | 1 | 5 | .... | .... | .... |
| …van Wijk) | July 23 | 08 08 | 24 02 | s.c. | +1 | +1 | +3 | m | 23 | 5,8 | 5 | 13 | 108 | 83 |
| | Aug. 12 | 00 45 | 13 09 | s.c. | 0 | +13 | +10 | m | 12 | 2 | 5 | 18 | 96 | 80 |
| | Aug. 23 | 00 24 | 26 08 | s.c. | +1 | +13 | +11 | ms | 23 | 8 | 6 | 17 | 124 | 90 |
| | Aug. 26 | 17 .. | 1 00 | ..... | .... | .... | .... | m | 29 | 7 | 5 | 19 | 89 | 83 |
| | | | | | | | | | 30 | 6 | 5 | | | |
| | Sep. 3 | 16 .. | 5 10 | ..... | .... | .... | .... | ms | 3 | 8 | 6 | 24 | 106 | 130 |
| | | | | | | | | | 5 | 1 | 6 | | | |
| | Sep. 11 | 00 55 | 11 03 | s.c. | (Large bay) | | | m | 11 | 1 | 5 | .... | .... | .... |
| | Sep. 15 | 02 59 | 17 04 | s.c. | −1 | +14 | +11 | m | 15 | 7 | 5 | 15 | 114 | 126 |
| | Sep. 18 | 16 10 | 24 00 | s.c. | +1 | +4 | +4 | ms | 19 | 6 | 6 | 24 | 160 | 133 |
| …atheroo | June 29 | 07 24 | 1 14 | ..... | .... | .... | .... | m | 29 | 4,5,6 | 5 | 18 | 127 | 126 |
| …E.Webb) | | | | | | | | | 30 | 1,4 | 5 | | | |
| | | | | | | | | | 1 | 3,4 | 5 | | | |
| | July 23 | 08 09 | 24 23 | s.c.* | −1 | 19 | .... | ms | 23 | 5 | 6 | 20 | 122 | .... |
| | (*Note:* No Z record from July 23, 00^h^ 31^m^ to July 24, 02^h^ 20^m^) | | | | | | | | | | | | | |
| | July 25 | 16 40 | 31 15 | ..... | .... | .... | .... | m | 26 | 5 | 5 | 13 | 154 | 98 |
| | | | | | | | | | 27 | 3,5,6 | 5 | | | |
| | | | | | | | | | 28 | 3 | 5 | | | |
| | | | | | | | | | 29 | 4 | 5 | | | |
| | | | | | | | | | 30 | 4,5 | 5 | | | |
| | Aug. 23 | 00 24 | 25 20 | s.c. | 1 | 3 | 5 | m | 23 | 4,5,7,8 | 5 | 15 | 104 | 94 |
| | | | | | | | | | 24 | 6,8 | 5 | | | |
| | | | | | | | | | 25 | 4,5 | 5 | | | |
| | Aug. 27 | 08 40 | 31 18 | ..... | .... | .... | .... | m | 27 | 4,5,6 | 5 | 17 | 130 | 98 |
| | | | | | | | | | 28 | 1,4 | 5 | | | |
| | | | | | | | | | 29 | 4,7 | 5 | | | |
| | | | | | | | | | 30 | 3,5,6 | 5 | | | |
| | | | | | | | | | 31 | 5 | 5 | | | |
| | (*Note:* No trace for 00^h^ to 12^h^ GMT on August 31) | | | | | | | | | | | | | |
| | Sep. 3 | 11 50 | 5 10 | ..... | .... | .... | .... | ms | 3 | 8 | 7 | 29 | 119 | 130 |
| | Sep. 15 | 02 59 | 16 23 | s.c.* | −1 | 15 | 2 | m | 15 | 7 | 5 | 10 | 86 | 64 |
| | Sep. 18 | 15 30 | 22 16 | ..... | .... | .... | .... | ms | 19 | 4,6 | 6 | 19 | 150 | 111 |
| | Sep. 23 | 00 00 | 24 24 | ..... | .... | .... | .... | m | 23 | 2,3,5 | 5 | 14 | 110 | 96 |
| | | | | | | | | | 24 | 4,5 | 5 | | | |
| …oolangi | July 22 | 23 .. | 24 02 | ..... | .... | .... | .... | ms | 23 | 4 | 6 | 27 | 101 | 46 |
| …P. McGregor) | July 25 | 16 .. | 31 15 | ..... | .... | .... | .... | m | 27 | 2,3,5 | 5 | 23 | 161 | 48 |
| | | | | | | | | | 28 | 3,4 | 5 | | | |
| | | | | | | | | | 29 | 4 | 5 | | | |
| | | | | | | | | | 30 | 4,5 | 5 | | | |
| | Aug. 10 | 07 .. | 14 06 | ..... | .... | .... | .... | m | 12 | 3,4 | 5 | 22 | 152 | 62 |
| | Aug. 23 | 00 23 | 5 12 | s.c.* | +1 | −6 | .... | ms | 30 | 3 | 6 | 38 | 231 | 60 |
| | (*Note:* Record for August 27 incomplete from 12^h^) | | | | | | | | | | | | | |
| | Sep. 15 | 02 58 | 17 21 | s.c.* | .... | +28 | −4 | m | 15 | 6,7 | 5 | 20 | 135 | 35 |
| | Sep. 18 | 16 10 | 24 20 | s.c. | +1 | +10 | −1 | ms | 19 | 4 | 6 | 27 | 162 | 74 |
| Amberley | June 29 | 07 26 | 2 15 | ..... | .... | .... | .... | ms | 1 | 4 | 6 | 23 | 165 | 45 |
| (H.F.Baird) | July 23 | 08 10 | 24 05 | ..... | .... | .... | .... | ms | 23 | 4 | 6 | 22 | 124 | 60 |
| | July 26 | 06 .. | 31 15 | ..... | .... | .... | .... | m | 27 | 2,3 | 5 | 18 | 132 | 51 |
| | | | | | | | | | 28 | 3 | 5 | | | |
| | | | | | | | | | 29 | 4 | 5 | | | |

PRINCIPAL MAGNETIC STORMS—*Concluded*

| Observatory (Observer-in-Charge) | Green-wich date | Storm-time: GMT of begin. | Storm-time: GMT of ending[1] | Sudden commencement: Type[2] | Amplitudes[3]: D | Amplitudes[3]: H | Amplitudes[3]: Z | C-figure, degree of activity[4] | Maximal activity on K-scale 0 to 9: Gr. day | Gr. 3-hr. period | K-index | Ranges: D | Ranges: H | Ranges: Z |
|---|---|---|---|---|---|---|---|---|---|---|---|---|---|---|
| (1) | (2) | (3) | (4) | (5) | (6) | (7) | (8) | (9) | (10) | (11) | (12) | (13) | (14) | (1[illegible]) |
| | *1953* | h m | d h | | ′ | γ | γ | | | | | ′ | γ | γ |
| Amberley—*Continued* (H.F.Baird) | Aug. 12 | 01 .. | 12 18 | ..... | .... | .... | .... | m | 12 | 3,4 | 5 | 27 | 102 | [illegible] |
| | Aug. 23 | 00 24 | 25 15 | s.c.* | −1 | −20 | +4 | m | 23 | 4 | 5 | 17 | 170 | [illegible] |
| | | | | | | | | | 24 | 2,8 | 5 | | | |
| | | | | | | | | | 25 | 3,4 | 5 | | | |
| | Aug. 26 | 21 .. | 31 18 | ..... | .... | .... | .... | m | 27 | 3,4 | 5 | 22 | 139 | [illegible] |
| | | | | | | | | | 29 | 3,4 | 5 | | | |
| | | | | | | | | | 30 | 3 | 5 | | | |
| | Sep. 3 | 17 .. | 5 11 | ..... | .... | .... | .... | ms | 3 | 8 | 6 | 27 | 188 | [illegible] |
| | Sep. 15 | 02 59 | 16 13 | s.c.* | +1 | +35 | −7 | m | 15 | 7 | 5 | 17 | 77 | [illegible] |
| | Sep. 18 | 16 10 | 22 12 | s.c. | +1 | +5 | −3 | m | 19 | 3,4,5 | 5 | 22 | 143 | [illegible] |
| | | | | | | | | | 20 | 2 | 5 | | | |
| | | | | | | | | | 21 | 3 | 5 | | | |
| | | | | | | | | | 22 | 3 | 5 | | | |
| | Sep. 22 | 21 .. | 24 15 | ..... | .... | .... | .... | m | 23 | 4 | 5 | 17 | 124 | [illegible] |
| | | | | | | | | | 24 | 4 | 5 | | | |

# FURTHER DISCUSSION OF KELSO'S PAPER ON A METHOD FOR DETERMINATION OF THE DISTRIBUTION OF ELECTRON DENSITY IN THE IONOSPHERE

In his recent paper, Dr. Kelso[1] described a procedure for numerical evaluation of the integral which gives the actual distribution of ionization of an ionospheric layer from experimental data on the virtual height as a function of frequency. Manning[2] makes a number of criticisms of this procedure, the major ones being these:

(1) The result is "simple" and "elementary," since it can be interpreted as evaluating a certain derived integral by the crude method of averaging equally-spaced ordinates. The application of the "esoteric" Gauss-Christoffel (G.C.) formula in this case is "not well-founded."

(2) The procedure is "basically futile," since it depends on a polynomial approximation to observed data.

These remarks are apparently based on a misunderstanding of the *significance* of the procedure employed and seem to be directed at standard numerical methods in general.

As indicated by Kelso, the G.C. formula was applied by B. Friedman[3] to the calculation of theoretical virtual-height curves for various assumed distributions, taking into account the earth's magnetic field. The general procedure was then used for the inverse problem by the present writer, and a number of formulas were developed, one of which is exhibited in Kelso's paper. The formula finally suggested by Kelso is probably the most useful in practice, since it can be applied with a minimum of computation.

The integral in question for the true height of reflection $h_t$ as a function of critical frequency $f_v$ can be expressed in terms of the experimental virtual-height curve. This curve is given as a function of the operating frequency $h'(f)$ by the formula

$$h_t(f_v) = \frac{2}{\pi}\int_0^{f_v} \frac{h'(f)\,\mathrm{d}f}{\sqrt{f_v^2 - f^2}} = \frac{2}{\pi} f_v \int_0^1 \frac{h'(f_v x)}{\sqrt{1 - x^2}}\,\mathrm{d}x$$

A simple trigonometric transformation reduces the integral to $2/\pi \int_0^{\frac{\pi}{2}} h'(f_v \sin\theta)\,\mathrm{d}\theta$. The integrand $h'(f_v \sin\theta)$ as a function of $\theta$ is the so-called derived curve.

The G.C. quadrature formula as applied to this case states that if $h'(f_v x)$ is a polynomial of degree $2n - 1$, the *exact* value of the integral (1) is half the average

[1]J. M. Kelso, A procedure for the determination of the vertical distribution of the electron density in the ionosphere, J. Geophys. Res., 57, 357-367 (1952).

[2]L. A. Manning, Discussion of the Kelso paper . . . , J. Geophys. Res., 58, 117-118 (1953).

[3]B. Friedman, Numerical methods for evaluation of the integrals for virtual height, New York University, Math. Res. Group, Research Report EM-17 (Feb. 1950).

of the values of $h'(f_v x)$ evaluated at the zeros of the polynomial of order $n$, which belongs to the set of polynomials orthogonal over double the given interval with weight function $(1 - x^2)^{-1/2}$. If the experimental curve is approximated by a polynomial, then the G.C. formula gives an approximation to the integral. From the derivation of the formula, it is readily seen that this approximation may be interpreted as follows:

If we approximate the experimental curve by polynomials of degree $n$, then the mean-square error of the value of the integral is least if the G.C. formula is used. From another viewpoint, if we approximate the given curve by a polynomial of degree $n$ so as to minimize the mean-square error, the G.C. formula gives the exact value of the integral for the approximating curve.

The suggested formula, then, far from being "crude," gives the *best* possible result—best in the sense of the method of the least squares as defined above.

It is true that the result in this case may also be interpreted as evaluating the "derived curve" by the method of averaging equally-spaced ordinates. It is true that the latter method is, in general, crude. However, in this case, that is, when the weight function is $(1 - x^2)^{-1/2}$ and the interval is $(-1, 1)$, and only in this case, does the method of averaging equally-spaced ordinates coincide with the G.C. formula.

The use of a polynomial approximation to an experimental curve is always possible. Indeed, in a closed interval, every continuous curve can be approximated by a polynomial to any degree of accuracy.[4] The use of orthogonal polynomials insures an approximation such that for a polynomial of any degree the mean-square error is a minimum. For the case in question, the experimental curve $h'(f)$ is approximated by a polynomial of degree $n$ taken from the set of Tchebysheff polynomials. It will be noted that the polynomial approximation need not be calculated in practice, but it is implicit in the derivation of the final formula.

Manning states that the method of equally-spaced ordinates is inaccurate when applied even to second-degree polynomial integrands. In general, this is true. However, if in the integral (1), $h'(f)$ is a polynomial of the second degree, two ordinates chosen according to the G.C. formula give the exact result. Indeed, if $h'(f)$ were a polynomial of degree $2n - 1$, the result would be exact by averaging the ordinates of $n$ properly selected points.

Manning remarks that it is "equally logical" to apply numerical methods to the derived curve. For example, in an earlier paper by Manning,[5] the derived curve is integrated by a planimeter. However, no single derived curve exists. A plurality of derived curves must be computed from the experimental data, one for each value of the parameter, $f_v$. To obtain these derived curves, it is necessary to replot the experimental curve for each value of this parameter. In the neighborhood of the zero and the critical frequencies, the data are usually poor and all the errors in any part of the data, plus all the replotting errors, are incorporated in each derived curve, and the exactitude obtained by using a planimeter at this

[4]R. Courant, Differential and integral calculus, New York, Oxford University Press, Vol. I, p. 423, Ex. 4 (1937).

[5]L. A. Manning, Determination of ionospheric electron distribution, Proc. Inst. Radio Eng., 35, 1203-1207 (1947).

stage of the calculation is illusory. A reference to Manning's paper will indicate the essential impracticability of the procedure he used. This, in fact, led the present writer to try numerical integration procedures, which do not require replotting the data for each desired point of the true height curve. The G.C. procedure gives this point as the average of predetermined ordinates of the given curve. The number of these ordinates used determines the accuracy of the result.

To illustrate the accuracy of the approximation procedure, let us consider the case of the parabolic layer for which all calculations can be carried out explicitly. The virtual height is given by the well-known formula

$$h'(R) = \frac{R}{2} \log \frac{1+R}{1-R}, \qquad R = \frac{f}{f_v}$$

Note that $h'(R)$ is not a polynomial; in fact, it becomes infinite at the critical frequency $R = 1$. (Experimentally, at this point the value of the function becomes very large.) Assuming that this formula represents the experimental curve, we shall calculate the distribution by the G.C. scheme and compare the result with the known distribution. The following table shows the results:

| $R$ . . . . . . . | 0.30 | 0.60 | 0.75 | 0.85 | 0.90 | 0.94 | 0.98 | 1.0 |
|---|---|---|---|---|---|---|---|---|
| $h_t$ actual . . . . | 0.0461 | 0.2000 | 0.33856 | 0.47322 | 0.56411 | 0.65883 | 0.80100 | 1.0 |
| $h_t$ approximation: | | | | | | | | |
| Using 3 pts . . | 0.0461 | 0.2000 | 0.3385 | 0.4730 | 0.5634 | 0.6563 | 0.7865 | 0.8828 |
| Using 4 pts . . | 0.0461 | 0.2000 | 0.3386 | 0.4733 | 0.5641 | 0.6586 | 0.7962 | 0.9125 |
| Using 5 pts . . | 0.0461 | 0.2000 | 0.3386 | 0.7433 | 0.5640 | 0.6586 | 0.7995 | 0.9290 |

It will be noted that a high degree of accuracy is obtained by averaging only three ordinates, except at the critical frequency. In the neighborhood of the critical frequency, or cusps, if such exist, 4, 5, or 10 ordinates may be averaged to increase the accuracy at these points. Similar accuracy has been obtained by applying this method to other theoretical distributions.

Finally, Manning suggested that the method might be useful for automatic machine computation. Actually, the calculations above took only a few minutes and any $h'(f)$ curve to which the integral (1) may be applied can be done in that time without any mechanical aids whatsoever.

Lester Kraus

Mathematics Research Group,*
Washington Square College of Arts and Science,
New York University,
*New York 3, N.Y., June 2, 1953*
(Received July 7, 1953)

*This work was performed at Washington Square College of Arts and Science, New York University, and was supported in part by Contract No. AF-19(122)-42 with the U. S. Air Force through sponsorship of the Geophysics Research Directorate of the Air Force Cambridge Research Center, Air Research and Development Command.

# THE LUNAR DIURNAL-VARIATION OF THE EARTH'S MAGNETIC FIELD FOR ALL ELEMENTS AT AMBERLEY, NEW ZEALAND

Five years of hourly values were analyzed for lunar variations by the earlier Chapman method.[1] The period chosen was the sunspot-minimum of 1931-35. Each lunation was divided into eight phases, which were reduced to new moon by the use of Chapman's phase-law.[2] An estimate of the probable error was obtained by this means. It should be noted that Chapman's phase-law was not verified due to the smallness of the sample taken. A large sample could not be analyzed because of the lack of computing facilities.

It will be noticed, on comparing Tables 2 and 3, that only the second harmonic may be regarded as reliable. Table 4 gives the mean harmonics of the solar diurnal-variation over the corresponding period. For the second harmonic in the vertical intensity, the ratio $S_2 : L_2$ is extremely low in comparison with evaluations obtained by other observatories.

TABLE 1

| | |
|---|---|
| *Coordinates of Amberley:* | |
| Geographic | 43°.2 south, 172°.8 west |
| Geomagnetic | 47°.7 south, 252° east |
| *Mean values of elements over corresponding period:* | |
| Horizontal intensity | 22319.4 gammas |
| Declination | 18° 0′.2 east |
| Vertical intensity | 55229.7 gammas |
| *Sample size:* | |
| 1,561 lunar days | declination |
| 1,857 lunar days | horizontal intensity |
| 1,660 lunar days | vertical intensity |

(Taken during sunspot-minimum conditions.)

[1]S. Chapman, Phil. Trans. London, A, 218, 1-118 (1919).
[2]S. Chapman, Phil. Trans. London, A, 225, 49-91 (1925).

TABLE 2—*Lunar diurnal-variation of magnetic elements at Amberley*

[Expressed as the series $\Sigma_{n=1}^{4} C_n \sin (nt + \phi_n)$ at new moon]

| | $C_1$ | $\phi_1$ | $C_2$ | $\phi_2$ | $C_3$ | $\phi_3$ | $C_4$ | $\phi_4$ |
|---|---|---|---|---|---|---|---|---|
| | | ° | | ° | | ° | | ° |
| | *Horizontal intensity* (unit 1 gamma) | | | | | | | |
| Summer | 1.33 | 337 | 1.63 | 346 | 0.95 | 330 | 0.14 | 355 |
| Equinox | 0.58 | 334 | 1.10 | 332 | 0.63 | 291 | 0.14 | 340 |
| Winter | 0.20 | 258 | 0.59 | 330 | 0.15 | 198 | 0.12 | 106 |
| Total | 0.64 | 331 | 1.09 | 339 | 0.47 | 310 | 0.06 | 351 |
| | *Declination* (unit 1′ east) | | | | | | | |
| Summer | 0.20 | 63 | 0.42 | 29 | 0.11 | 50 | 0.02 | 76 |
| Equinox | 0.02 | 75 | 0.20 | 39 | 0.06 | 6 | 0.02 | 117 |
| Winter | 0.03 | 288 | 0.11 | 15 | 0.01 | 110 | 0.00 | 163 |
| Total | 0.09 | 34 | 0.24 | 29 | 0.05 | 31 | 0.01 | 103 |
| | *Northern intensity* (unit 1 gamma) | | | | | | | |
| Summer | 1.30 | 327 | 1.10 | 329 | 0.89 | 338 | 0.14 | 8 |
| Equinox | 0.56 | 337 | 0.95 | 325 | 0.58 | 301 | 0.17 | 359 |
| Winter | 0.14 | 251 | 0.43 | 324 | 0.14 | 212 | 0.11 | 133 |
| Total | 0.55 | 322 | 0.82 | 327 | 0.44 | 319 | 0.07 | 0 |
| | *Eastern intensity* (unit 1 gamma) | | | | | | | |
| Summer | 1.31 | 52 | 2.97 | 37 | 0.80 | 52 | 0.14 | 88 |
| Equinox | 0.20 | 22 | 1.38 | 41 | 0.46 | 5 | 0.11 | 133 |
| Winter | 0.27 | 289 | 0.82 | 21 | 0.08 | 277 | 0.05 | 156 |
| Total | 0.66 | 26 | 1.71 | 35 | 0.38 | 31 | 0.08 | 121 |
| | *Vertical intensity* (unit 1 gamma, increasing to zenith) | | | | | | | |
| Summer | 0.47 | 130 | 2.39 | 204 | 0.25 | 194 | 0.04 | 200 |
| Equinox | 0.13 | 132 | 2.07 | 201 | 0.09 | 113 | 0.07 | 165 |
| Winter | 0.05 | 33 | 1.96 | 207 | 0.00 | 219 | 0.02 | 230 |
| Total | 0.20 | 126 | 2.14 | 204 | 0.10 | 177 | 0.04 | 182 |

TABLE 3—*Probable error of amplitude*

| Season | $\Delta C_1$ | $\Delta C_2$ | $\Delta C_3$ | $\Delta C_4$ |
|---|---|---|---|---|
| | *Horizontal intensity* | | | |
| Summer | 0.98 | 0.50 | 0.30 | 0.24 |
| Equinox | 0.68 | 0.42 | 0.27 | 0.22 |
| Winter | 0.86 | 0.47 | 0.29 | 0.26 |
| Total | 0.53 | 0.33 | 0.19 | 0.16 |
| | *Declination* | | | |
| Summer | 0.16 | 0.09 | 0.05 | 0.03 |
| Equinox | 0.16 | 0.09 | 0.05 | 0.02 |
| Winter | 0.14 | 0.06 | 0.04 | 0.03 |
| Total | 0.12 | 0.07 | 0.03 | 0.01 |
| | *Vertical intensity* | | | |
| Summer | 0.54 | 0.23 | 0.11 | 0.11 |
| Equinox | 0.49 | 0.23 | 0.08 | 0.06 |
| Winter | 0.29 | 0.16 | 0.09 | 0.06 |
| Total | 0.37 | 0.10 | 0.06 | 0.05 |

Table 4—*Solar diurnal-variation of magnetic elements at Amberley*

[Expressed as the series $\Sigma_{n=1}^{4} C_n \sin (nt + \phi_n)$]

| Season | $C_1$ | $\phi_1$ | $C_2$ | $\phi_2$ | $C_3$ | $\phi_3$ | $C_4$ | $\phi_4$ |
|---|---|---|---|---|---|---|---|---|
| | | ° | | ° | | ° | | ° |
| | *Horizontal intensity* (unit 1 gamma) | | | | | | | |
| Summer | 13.94 | 302 | 8.99 | 304 | 4.61 | 310 | 0.88 | 347 |
| Equinox | 9.51 | 272 | 6.30 | 286 | 3.80 | 296 | 0.90 | 318 |
| Winter | 4.42 | 199 | 3.95 | 226 | 2.47 | 220 | 0.88 | 210 |
| Total | 7.68 | 277 | 5.59 | 285 | 2.98 | 288 | 0.40 | 310 |
| | *Declination* (unit 1′ east) | | | | | | | |
| Summer | 2.68 | 13 | 2.02 | 356 | 0.83 | 22 | 0.20 | 40 |
| Equinox | 1.63 | 29 | 1.79 | 345 | 0.80 | 358 | 0.32 | 353 |
| Winter | 0.84 | 54 | 0.99 | 322 | 0.49 | 327 | 0.32 | 297 |
| Total | 1.66 | 25 | 1.58 | 345 | 0.66 | 01 | 0.22 | 346 |
| | *Vertical intensity* (unit 1 gamma, increasing to zenith) | | | | | | | |
| Summer | 1.67 | 317 | 2.58 | 195 | 1.13 | 194 | 0.11 | 167 |
| Equinox | 2.69 | 343 | 1.66 | 195 | 0.74 | 207 | 0.29 | 189 |
| Winter | 3.03 | 329 | 0.19 | 305 | 0.39 | 310 | 0.09 | 105 |
| Total | 2.43 | 332 | 1.40 | 198 | 0.59 | 209 | 0.14 | 182 |

Table 5—*Comparison with northern hemisphere stations*

| Observatory | Latitude | | Western | | Northern | | Horizontal | | Declination | | | Vertical | | Reference |
|---|---|---|---|---|---|---|---|---|---|---|---|---|---|---|
| | Geogr. | Geomg. | $C_2$ | $\phi_2$ | $C_2$ | $\phi_2$ | $C_2$ | $\phi_2$ | $C_2$ | $C_2'$ | $\phi_2$ | $C_2$ | $\phi_2$ | |
| | ° | ° | | ° | | ° | | ° | | | ° | | ° | |
| Greenwich | 51.5 N | 54.2 N | ..... | .... | .... | ... | .... | ... | ..... | 1.14 | 59 | .... | ... | Chapman |
| Val Joyeux | 48.8 N | 51.3 N | ..... | .... | .... | ... | .... | ... | 0.13 | ..... | 9 | 0.38 | 357 | Rougerie |
| Pola | 44.9 N | 45.1 N | 0.68 | 62 | 0.70 | 35 | 0.79 | 39 | 0.09 | ..... | 68 | 0.39 | 132 | Chapman |
| Amberley | 43.2 S | 47.7 S | 1.71* | 35 | 0.82 | 327 | 1.09 | 339 | 0.24* | 1.56* | 29 | 2.14 | 204 | Bullen and Cummack |

*Opposite convention of sign is taken in these cases.

J. M. Bullen and C. H. Cummack

Geophysical Observatory,
*Christchurch, New Zealand, July 21, 1953*
(Received July 28, 1953)

# INTERNATIONAL UNION OF GEODESY AND GEOPHYSICS, ASSOCIATION OF TERRESTRIAL MAGNETISM AND ELECTRICITY CIRCULAR LETTER NO. 312/53/8 TO MAGNETIC OBSERVATORIES AND GEOPHYSICAL INSTITUTIONS

*Subject*: Proposed program of recording rapid magnetic pulsations during the coming International Geophysical Year 1957-58

Dear Colleagues:

At the recent meeting in Brussels of the Special Committee for the International Geophysical Year 1957-58, the AGI, a working group on geomagnetism, considered the possibility of obtaining, during the AGI, observational material for a more comprehensive understanding of rapid magnetic pulsations, that is, pulsations having periods between, say, one second and one minute. Recent investigations by means of special recording equipment have revealed that such pulsations are far more frequent than should be inferred from an examination of magnetic records of the normal type, and it is felt that the AGI would represent a unique opportunity for a more detailed study of these phenomena. Simultaneous records from an appropriate net of stations would provide not only material for a closer investigation of the morphology of the pulsations, but also material from which conclusions could be drawn as to whether the different types of pulsations are of a purely local or more regional character. This again would mean a possibility of locating the origin of these pulsations and of studying such relations as they may have to ionospheric phenomena.

It was agreed that a special instrumental equipment would be required to obtain adequate records of the pulsations here mentioned, and, in order to take advantage of any experience that may already have been obtained in this domain, the International Association of Terrestrial Magnetism and Electricity was requested to implement an inquiry on the subject among all magnetic observatories and geophysical institutions. It is in pursuance of this request that the Association now urges that you lend your assistance to the project outlined above by preparing at your earliest convenience a brief statement, summarizing any experience you may have in recording magnetic pulsations of periods shorter than one minute. Your statement should give full details of the instrumental equipment used, and points of special interest would be as follows: (1) Paper speed; (2) special devices aiming at a reduction of the consumption of photographic paper; (3) timing of the magnetograms; (4) elements recorded; (5) scale values of variometers; (6) special procedures adopted in order to obtain very high sensitivity of the variometers; (7) character of damping used; (8) any other details as you may deem essential for a proper functioning of the equipment and an adequate registration of the pulsations; and (9) such additional suggestions as you may wish to make as to the design of a recording equipment for the purpose here outlined.

It would be highly appreciated if a specimen copy of the records obtained could be included with your statement, which should be sent *not later than October the 1st, 1953*, to the Chairman of the IATME Committee on Observational Tech-

nique, as follows: Prof. E. Thellier, Observatoire du Parc Saint-Maur, Saint-Maur-des-Fossés (Seine), France.

On the basis of the material received, the Committee is to make definite recommendations as to the instrumental equipment which should be used during the International Geophysical Year for this special investigation.

V. Laursen
Secretary, IATME

Meteorological Institute,
*Charlottenlund, Denmark, July 28, 1953*
(Received August 7, 1953)

## THE SOLAR DIURNAL VARIATION IN THE AMPLITUDE OF SUDDEN COMMENCEMENTS OF MAGNETIC STORMS AT THE GEOMAGNETIC EQUATOR

The question of whether or not the sudden commencement of magnetic storms is abnormally large at the geomagnetic equator was studied by comparing SC's at Huancayo to those at Cheltenham. It was found that the sudden commencement is enhanced during sunlit hours at Huancayo, which is located near the geomagnetic equator.

The present statistics are based on 183 SC's in the period 1922 to 1946. SC's were chosen only when they took the typical form at all of three stations, Huancayo, Watheroo, and Cheltenham, so that "crochets" were excluded from the statistics. It is not likely from studies on *Sq* that changes in magnetic field of crochets manifest themselves as rises in the horizontal component at all of the three stations at any hour of local time. In Figure 1 are plotted the mean of the ratios of amplitudes of the horizontal component of SC's for Huancayo to those

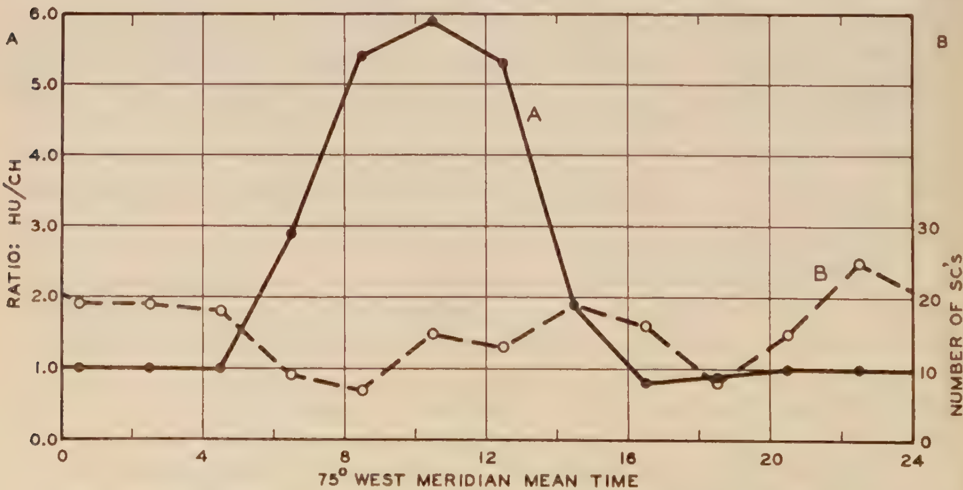


FIG. 1—THE DIURNAL VARIATION OF THE RATIO OF AMPLITUDES OF SC's ($\Delta H$) AT HUANCAYO TO THOSE AT CHELTENHAM, 183 SC's, 1922-46

for Cheltenham (the curve $A$) and the number of SC's (the curve $B$) against 75th Meridian Mean Time. Cheltenham was chosen because the station is located nearly on the same meridian as Huancayo, thus eliminating the factor coming from the relative positions to the sun of the two stations for which the ratio is taken.

The curve $A$ clearly shows that there exists a solar diurnal variation in the sudden commencement at Huancayo. The ratio starts increasing in the morning, reaches as high as 5 or 6 between $08^h$ and $13^h$, with a maximum around $11^h$, and decreases towards the evening; it remains constant throughout the night, the ratio being approximately 1. Thus, as in the case of the solar daily variation, the sudden commencement field is augmented during sunlit hours. This suggests that the immediate source of the main portion of SC which occurs during sunlit hours at the geomagnetic equator is within the upper atmosphere of the earth.

The frequency of occurrence of SC's as shown by the curve $B$ well agrees with Newton's result on Greenwich data. That is, there is a minimum centered around $08^h$, and there are afternoon and night maxima with a break by a secondary minimum at about $18^h$. It might be that the frequency of SC's depends upon the local time, not upon the universal time; or, rather it should be stated, in view of the world-wide nature of SC's, that this frequency curve represents the probability that SC's are of the "typical" form.

One might question* whether the diurnal variation of the above ratio is due to abnormally small SC's at Cheltenham during the daytime instead of SC's at Huancayo being so large. Although quantitative investigation of this point has not yet been made, it was clear to the writer by inspection of curves that this effect is due mainly to an enhancement of the sudden commencement at Huancayo. This is further confirmed by the fact that the same ratio of SC's at Huancayo to those at Watheroo is also large during sunlit hours. The details of the results of the present study will be published later.

The writer is indebted to Dr. E. H. Vestine for suggestions and discussions which led to this finding of the sudden commencement being abnormal at the geomagnetic equator. He also wishes to express his thanks to Dr. M. A. Tuve, the Director of the Department of Terrestrial Magnetism, Carnegie Institution of Washington, for his kind arrangements by which this work was made possible while the writer was a visiting investigator at the Department, and for his constant encouragement, and to the Director of the U. S. Coast and Geodetic Survey for making records available.

MASAHISA SUGIURA

GEOPHYSICAL INSTITUTE,
UNIVERSITY OF ALASKA,
*College, Alaska, September 21, 1953*
(Received September 22, 1953)

*This question was raised by Prof. S. Chapman, with whom the author had discussions at Ann Arbor, Michigan.

# THE IMMEDIATE SOURCE OF THE FIELD OF MAGNETIC STORMS

The purpose of this letter is to call attention to the fact that major sources of magnetic field changes during storms in all phases are either within or cannot be located much beyond the atmosphere.

Magnetic storms often begin with a sharp increase or pulse in horizontal magnetic intensity enduring for a few minutes. Some years ago, the writer sought to derive the world-wide field distribution for the maximum amplitude of this pulse, for the storm of May 1, 1933. The attempt failed for polar regions, even though the pulse appeared on a magnetically quiet day. There were considerable differences in the time of maximum amplitude, and in the amplitude itself at stations only some hundreds of kilometers away. At the time, the failure was attributed to electromagnetic induction by sources outside, within an atmosphere of patchy conductivity, or to other chance disturbances unrelated to the magnetic storm. Similar difficulties were found in the case of three other sudden commencements; accordingly, the possibility that sudden commencements mainly arise from atmospheric electric currents was suspected. The writer has been informed by Mr. Sugiura that this interpretation was probably correct, because he has noted that a large local difference also appears in sudden commencements between the station Huancayo, Peru, very near the magnetic equator and more northerly stations, in the daytime. In fact, he found that sudden commencements are augmented abnormally at Huancayo by day, as in the case of the solar daily magnetic variation.[1] Since from potential theory the linear cross-section of local field pattern at the ground cannot be ascribed to overhead sources much farther away than this length, the major component is due to atmospheric sources or electric currents.

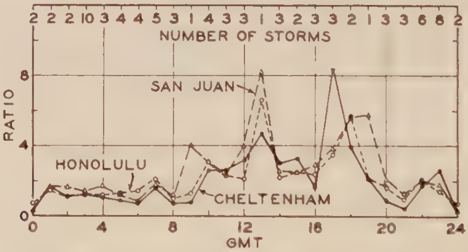


FIG. 1—RATIO OF MEAN HOURLY VALUE OF INITIAL PHASE OF MAGNETIC STORM AT HUANCAYO, PERU, TO THAT AT STATIONS INDICATED, FIRST HOUR OF STORM, $0^h-(-1)^h$, FOR STORMS BEGINNING AT VARIOUS HOURS GMT, 1922–1944; CORRECTED FOR Sq

Figure 1 shows similar results for the initial phase of magnetic storms. Strange to say, it would appear that the augmentation of the initial phase at Huancayo was also unnoticed in the cursory examinations which must have been made in the past. The initial phases of the storms of October 14, 1932, and April 30, 1933,

[1] S. Chapman and J. Bartels, Geomagnetism, Vols. 1 and 2, Oxford, Clarendon Press (1940).

which were studied in some detail by the writer did not show this augmentation at Huancayo, although both storms began within some hours of local noon.[2] But the augmentation is found on an average basis to occur during local daytime. These findings are further verified in Figure 2 (*A*) to (*E*), where the average local

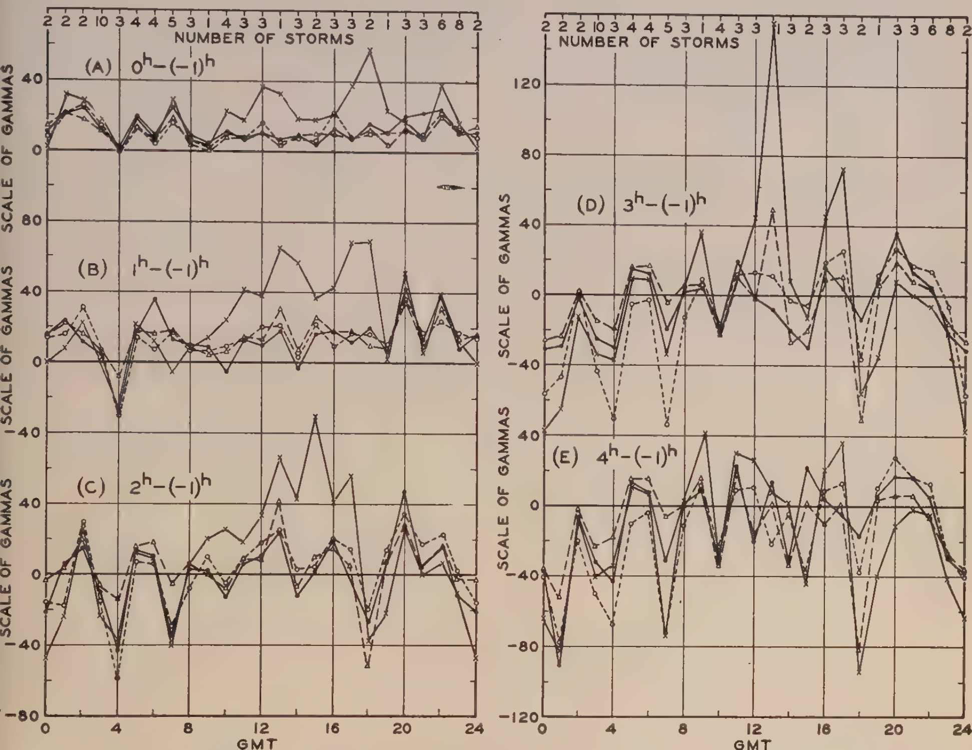


FIG. 2—MEAN HOURLY VALUES OF INITIAL PHASE AT SUCCESSIVE HOURS OF STORM, $0^h-(-1)^h$ TO $4^h-(-1)^h$, VARIOUS STATIONS, FOR STORMS BEGINNING AT VARIOUS HOURS GMT, 1922–1944; VALUES (E) MOSTLY FOR MAIN PHASE; CORRECTED FOR $S_q$

LEGEND: × = HUANCAYO • = CHELTENHAM ○ = HONOLULU ▵ = SAN JUAN

daytime values at Huancayo show augmentation not apparent at Cheltenham, Md., and San Juan, Porto Rico. During the main phase, there is no abnormal augmentation shown at Huancayo.

During the main phase of a magnetic storm, the electric current system responsible for the so-called diurnally varying part is accepted as atmospheric, because the dominant electric currents flowing along the auroral zone must flow within the atmosphere.[1,3] It may also be noted that Nagata and Ono[3] have found this current system to be present to some degree in the initial phase also.

On inspection, the oscillatory pulses of considerable strength recorded from time to time during the main phase of a magnetic storm show considerable variability from one station to the next, in low latitudes. This indicates the presence of a

[2]E. H. Vestine, L. Laporte, I. Lange, and W. E. Scott, The geomagnetic field, its description and analysis, Washington, D.C., Carnegie Inst. Pub. 580 (1947).

[3]T. Nagata and H. Ōno, J. Geomag. Geoelectr., 4, 108-113 (1952).

substantial "noise level" of atmospheric origin. These pulses should be examined to get the net pulse, if any, averaged around parallels of latitude (storm-time variation) for adjacent stations differing in latitude. It may then be possible to determine whether these averaged pulses are compatible in latitude distribution with sources such as a ring current encircling the earth at a distance of several earth radii. Unfortunately, it is not quite clear that the existing network of observatories in low latitudes is adequate for this purpose. In the meantime, it may be noted that a polar part simulating the storm-time variation is clearly of atmospheric origin.

Accordingly, there are now good grounds for concluding that the major immediate source of field is atmospheric in all phases of a magnetic storm, except possibly in the case of the storm-time changes in low latitudes. Of course, all magnetic storms are with good reason regarded as of solar origin, but it would appear that some magnetic changes previously ascribed in theory to electric currents flowing in solar streams may be smaller than was originally supposed.

The writer is indebted to Mr. M. Sugiura, Geophysical Institute, College, Alaska, for various interesting discussions of these matters.

E. H. Vestine

Department of Terrestrial Magnetism,
Carnegie Institution of Washington,
*Washington 15, D.C., September 21, 1953*
(Received September 22, 1953)

# *NOTES*

(26) *Geomagnetic three-hour-range indices K for the years 1937-1939 and planetary indices, Kp*—These are ready for publication in the forthcoming IATME Bulletin No. 12g, together with the indices for 1952. Tables of *Kp* have already appeared in the August 1953 issue of "Ionospheric Data" (*F*-series of the Central Radio Propagation Laboratory, Washington, D. C.). This completes a project of the Committee on Characterization of Magnetic Disturbances of the IATME, namely, to extend the current tables of *K*-indices of magnetic activity to cover the whole period of intensive ionospheric research beginning about 1937.

(27) *International Geophysical Year, 1957-58*—The year 1957-58, when sunspot activity is expected to be at its next maximum, has been designated an International Geophysical Year, and world-wide observations are planned in astronomy, geophysics, meteorology, geography, and radio science. Similar international geophysical years, called Polar Years, were conducted in 1882-83 and 1932-33; then observations were confined mostly to polar regions, whereas the current plans are global in scope. The program has been instigated by the International Council of Scientific Unions. A committee to plan the United States' part in the observations has been selected by the National Academy of Sciences and the National Research Council, with Dr. Joseph Kaplan, of the University of California at Los Angeles, as its chairman.

(28) *"Rockoons" reach height of 64 miles*—Physicists of the State University of Iowa, for the second successive summer, have sent up "rockoons," combinations of balloons and rockets, to establish new records for altitude and to collect information about cosmic rays. To reach the new height, rockets were launched from balloons at an altitude of 12.7 miles. Main interest was on cosmic radiation above 25 miles, that is, before the rays speeding to the earth from outer space change from their original nature through collisions with atmospheric atoms. The flights began about 100 miles east of Boston, Massachusetts, and continued up the coasts of Nova Scotia and Laborador as far north as 800 miles above the Arctic Circle in the waters west of Greenland.

(29) *Release of total-intensity aeromagnetic maps*—The United States Geological Survey has announced the release in open files for consultation of the following: (1) Two preliminary total-intensity aeromagnetic maps of the Mother Lode district, California; and (2) preliminary total-intensity aeromagnetic map of Morristown quadrangle, New Jersey. The latter map is the latest in a series of aeromagnetic maps of the New Jersey-New York magnetite district.

(30) *Geophysical Observatory, Quetta, Pakistan*—Quetta Magnetic Observatory has recently issued its first publications in the form of quarterly bulletins of magnetic character figures and special phenomena for the period January to June, 1953. Quetta, with its central position and dry climate, was found to be an ideal site for a magnetic observatory. Construction work commenced in 1951. In September 1952, A Ruska magnetograph was temporarily installed in a house in

Quetta. The base values of the variometers are controlled by means of three QHM's and two BMZ's. Two Askania balances also compose part of the equipment. The permanent magnetic observatory was to have been completed and occupied during the past summer.

(31) *New offices of the Society of Exploration Geophysicists*—Headquarters offices of the Society of Exploration Geophysicists have been moved to the Elm Oil Building, at 624 South Cheyenne, Tulsa, Oklahoma. The Society, an international organization of scientists engaged in exploration for minerals, primarily petroleum, established headquarters in Tulsa in 1946. In the seven years since that time, the Society has grown from 1500 to 3500 members. The Society publishes "Geophysics," a quarterly journal of general and applied geophysics.

(32) *Magnetic disturbance*—The United States *Hydrographic Bulletin* (No. 31 of August 1, 1953) contained the following account of a magnetic disturbance in the North Pacific Ocean:

"The Second Officer of the American S. S. *President Madison*, Captain Valdemar Nielsen, reported that while on passage from Iloilo to Hong Kong, on June 23, 1953, he noticed erratic westerly increases in the magnetic compass error to the southwest of Panay Island. They began in a position approximately 8 miles east of Juraojurao Island and the greatest disturbance was observed on a line connecting latitude 10° 41′ north, longitude 121° 41′ east, and latitude 11° 13′ north, longitude 121° 25′ east. North-northwest of the latter position, the variation became normal. The vessel's course was checked by radar fixes, which verified the accuracy of the gyrocompass.

(33) *Geomagnetic activities of the United States Coast and Geodetic Survey*—"Magnetic Observatory Manual," by H. E. McComb, Special Publication No. 283 of the United States Coast and Geodetic Survey, was issued. This publication is sold by the Superintendent of Documents, Government Printing Office, Washington 25, D. C., at the price of $1.50 per copy.

Mr. *Joel Campbell* was transferred from the Tucson Magnetic Observatory to the Cheltenham Magnetic Observatory on October 1, 1953.

Mr. *Ralph R. Bodle* was transferred from the Cheltenham Magnetic Observatory to the Washington office on October 1, 1953.

Mr. *Bernardo Grunebaum*, of the Empresa Nacional del Petróleo of Chile, was a guest of the United States Coast and Geodetic Survey, studying the magnetic work of the Division of Geophysics.

(34) *Personalia*—Dr. *Edwin P. Hubble*, noted astronomer and one of the scientists who developed the expanding universe theory, died on September 28, 1953, at the age of 63, in San Marino, California. Dr. Hubble joined the Mount Wilson Observatory, of the Carnegie Institution of Washington, in 1919. With Dr. Milton Humason, he used the Mount Wilson 100-inch and the Mount Palomar 200-inch telescopes to gather evidence concerning the expanding universe idea.

*Th. Laessöe Müller*, the Danish instrument-maker, who proposed the optical temperature compensation of magnetic variometers and with the support of D. la Cour constructed the monad *Z*-balance, died on July 10, 1953, in his 77th year.

The seventh Charles Chree Medal and prize of the Physical Society was presented to Prof. *J. Bartels*, of the University of Göttingen, in recognition of his

valuable work in the field of geomagnetism, at a meeting of the Society held in the Science Museum, London, on October 23, 1953. Prof. Bartels delivered a lecture on "Chree's influence on present-day geophysics."

Dr. *Tsuneji Rikitake*, of the Earthquake Research Institute, Tokyo University, Japan, will visit in England for the next year or two. His address will be "C/o Prof. A. T. Price, University College of the South West, Exeter, Devon, England."

On March 19 and 20, 1953, Messrs. *H. E. Garlick* and *V. B. Gerard*, of the Magnetic Survey, Christchurch, Geophysics Division, Department of Scientific and Industrial Research, New Zealand, obtained diurnal-variation curves of $D$ and $H$ on Campbell Island at station Vannevar Bush. Reoccupation values in $D$, $H$, and $Z$ were also obtained. Later, by courtesy of the Civil Aviation Branch, Air Department, Messrs. *H. E. Garlick* and *A. L. Burrows* obtained diurnal-variation curves of $D$, $H$, and $Z$ on Nandi airport (August 18, 1953) and Rarotonga airport (August 26, 1953).

# *LIST OF RECENT PUBLICATIONS*

By W. E. Scott

*Department of Terrestrial Magnetism,*
*Carnegie Institution of Washington,*
*Washington 15, D. C.*

(Received September 18, 1953)

## A—*Terrestrial Magnetism*

Apia Observatory. Magnetic and meteorological results for 1950. Issued under the authority of the Hon. R. M. Algie, Minister of Scientific and Industrial Research. Wellington, R. E. Owen, Govt. Printer, 140 pp. (1952). 24 cm.

Bartels, J., and J. Veldkamp. International data on magnetic disturbances, first quarter, 1953. J. Geophys. Res., **58**, No. 3, 408-410 (1953).

Bizette, H., R. Chevallier, et B. Tsaï. Propriétés thermomagnétiques de l'oxyde ferrique rhomboédrique. Paris, C.-R. Acad. sci., **236**, No. 21, 2043-2045 (1953).

Bodlé, Ralph R. Cheltenham three-hour-range indices *K* for April to June, 1953. J. Geophys. Res., **58**, No. 3, 311 (1953).

Burkhart, K. Zur Stromanalyse der magnetischen Variationen, insbesondere der Baistörungen. Beitr. Geophysik, **63**, Heft 2, 108-129 (1953).

Chapman, S. The morphology of geomagnetic storms: An extension of the analysis of $D_S$, the disturbance local-time inequality. Ann. Geofis., Roma, **5**, No. 4, 481-499 (1953).

Coimbra. Observacões de magnetismo terrestre no Instituto Geofisico da Universidade de Coimbra. Rev. Faculdade de Ciéncias da Universidade de Coimbra, Vol. XXII, 3-39 (1953).

Dehalu, M. Observations magnétiques à la frontière du Congo belge et de l'Ouganda entre les latitudes 1° 10′ Nord et Sud et en plusieurs points de l'Ouganda et du Kenya. Mém. Inst. R. Colonial Belge, **5**, Fasc. 4, 74 pp. (1953). 30 cm.

Denisse, J. F. Relations entre les phénomènes solaires et terrestres—Sur le contrôle de l'activité geomagnétique par les taches solaires. Paris, C.-R. Acad. sci., **236**, No. 19, 1856-1858 (1953).

Hurwitz, L. Reduction of airborne magnetometer results. Trans. Amer. Geophys. Union, **34**, No. 3, 360-362 (1953).

Istanbul-Kandilli Observatory. Annuaire magnétique, année 1951. Observatoire Astronomique et Géophysique d'Istanbul-Kandilli, Service Magnétique, 52 pp. (1952). 28 cm.

Kakioka Magnetic Observatory. Annual report of the Kakioka Magnetic Observatory. Geomagnetism 1938, 1939. Kakioka, No. 16, 115 pp. + 22 pls. (1953). 30 cm. [Contains magnetic results for the years 1938 and 1939.]

Laurie, P. S. Flamsteed's observations. Observatory, **73**, No. 874, 104-105 (1953). [A note with references to occasional observations of the variation of the compass made near London during 1680-1716.]

Lee, E. W. The influence of domain structure on the magnetization curves of single crystals. Proc. Phys. Soc., A, **66**, No. 403, 623-630 (1953).

McComb, H. E. Magnetic observatory manual. Washington, D.C., U.S. Dept. of Comm., Coast Geod. Surv., Spec. Pub. 283, 232 pp. (1952). 24 cm. [This is a long needed manual. It is for sale by the Superintendent of Documents, U.S. Government Printing Office, Washington 25, D.C.; price $1.50.]

Özdogan, İ. Variomètre électromagnétique pour la composante verticale. Ann. Géophys., **9**, No. 2, 161-163 (1953).

Paris, Institut de Physique du Globe. Annales de l'Institut de Physique du Globe de l'Université de Paris et du Bureau Central de Magnetisme Terrestre. Publiées par les soins de J. Coulomb. Paris, Imprimerie Nationale, Tome XXVI, 75 pp. + graphiques (1952). 31 cm.

[Contains magnetic results for Chambon-la-Forêt principally, 1949-1950; also for Nantes, Tananarive, and Ksara.]

SCHONSTEDT, E. O., AND H. R. IRONS. Airborne magnetometer for determining all magnetic components. Trans. Amer. Geophys. Union, **34**, No. 3, 363-378 (1953).

SLAUCITAJS, L. Resultados de las Investigaciones Geomagnéticas efectuadas en el año 1952 en Tierra del Fuego y parte S de Patagonia. Pub. Observatorio Astronómico de Eva Perón, Serie Geofísica, 7, 16 pp. (1952). 28 cm.

TEOLOYUCAN, OBSERVATORIO MAGNETICO DE. Valores magnéticos correspondientes al 1er semestre de 1952. Universidad Nacional de Mexico, Instituto de Geofísica, 27 pp. (1952). 26 cm.

TEOLOYUCAN, OBSERVATORIO MAGNETICO DE. Valores magnéticos correspondientes al 2° semestre de 1952. Universidad Nacional de Mexico, Instituto Geofísica, 20 pp. (1953). 26 cm.

TINO, Y. On a non-magnetic state found in irreversible Fe-Ni alloys. J. Sci. Res. Inst., Tokyo, **47**, Nos. 1301-1310, 7-11 (March 1953).

TOLEDO, OBSERVATORIO CENTRAL GEOFÍSICO. Geomagnetismo, año 1948. [Prepared by J. Sancho.] Madrid, Instituto Geografico y Catastral, 53 pp. + 15 graphs (1952). 24 cm.

TSUBOKAWA, I. Reduction of the results obtained by the magnetic survey of Japan (1948-51) to the epoch 1950.0 and deduction of the empirical formulae expressing the magnetic elements. Bull. Geog. Surv. Inst. Japan, **3**, Pt. 4, 1-29 + 3 pls. (June 1952).

WALKER, G. B., AND P. L. O'DEA. Geomagnetic secular-change impulses. Trans. Amer. Geophys. Union, **33**, No. 6, 797-800 (1952).

WIJK, A. M. VAN. Annual variation of the geomagnetic elements. J. Geophys. Res., 58, No. 3, 418-419 (1953). [Letter to Editor.]

## B—*Terrestrial Electricity*

CHAPMAN, S. Notes on auroral geometry and optics: I—To locate an elevated point viewed from two ground stations in the same diametral plane. J. Geophys. Res., 58, No. 3, 347-352 (1953).

CLAY, J. Ions and condensation nuclei in the atmosphere, balance of ions and value of cosmic radiation at sea level. J. Atmos. Terr. Phys., **3**, No. 3, 132-140 (1953).

FERRARO, V. C. A. The aurorae. Adv. Phys., **2**, No. 7, 265-320 (1953).

HESS, V. F., AND W. D. PARKINSON. Small ion balance over the ocean. Fordham University, Dept. of Physics, Sci. Rep. No. 2, 22 pp., min. (Dec. 1952).

MEINEL, A. B., AND D. H. SCHULTE. A note on auroral motions. Astroph. J., **117**, No. 3, 454-455 (1953).

PLUVINAGE, P., ET P. STAHL. La conductibilité électrique de l'air sur l'inlandsis groenlandais (Rapports scientifiques des Expeditions Polaires Françaises N IV 1). Ann. Géophys., **9**, No. 3, 34-43 (1953).

REYNOLDS, S. E. Thunderstorm-precipitation growth and electrical-charge generation. Bull. Amer. Met. Soc., **34**, No. 3, 117-123 (1953).

## C—*Cosmic Rays*

AMALDI, E., L. MEZZETTI, AND G. STOPPINI. On the longitudinal development of air showers according to Fermi's theory of meson production. Nuovo Cimento, **10**, No. 6, 803-816 (1953).

ASCOLI, G. Mass of cosmic-ray mesons at mountain altitudes. Phys. Rev., **90**, No. 6, 1079-1087 (1953).

DAWTON, D. I., AND H. ELLIOT. Day and night measurements of the total cosmic ray intensity at balloon altitudes. J. Atmos. Terr. Phys., **3**, No. 3, 217-222 (1953).

DE VOS, P. J. G., AND E. VAN A. G. VAN PITTIUS. Investigation on the low energy end of the cosmic protons and meson spectrum at sea-level by applying a differential absorption method. Physica, **19**, No. 4, 305-310 (1953).

FONGER, W. H. Cosmic radiation intensity-time variations and their origin. II. Energy dependence of 27-day variations. Phys. Rev., **91**, No. 2, 351-361 (1953).

HADDARA, S. R., AND D. JAKEMAN. The lateral structure of cosmic ray extensive air showers at sea level. Proc. Phys. Soc., A, **66**, 549-558 (1953).

Messel, H., and R. B. Potts. Longitudinal development of extensive air showers. Nuovo Cimento, **10**, No. 6, 754-778 (1953).

Neher, H. V., V. Z. Peterson, and E. A. Stern. Fluctuations and latitude effect of cosmic rays at high altitudes and latitudes. Phys. Rev., **90**, No. 4, 655-674 (1953).

Ray, E. C. Integrated cosmic ray intensity as a function of altitude. State University of Iowa, Dept. of Physics, 45 pp., mim. (June 1953). 28 cm.

Sarabhai, V., U. D. Desai, and R. P. Kane. Meteorological and extra-terrestrial causes of the daily variation of cosmic ray intensity. Proc. Indian Acad. Sci., **37**, No. 2, Sec. A, 287-303 (1953).

Thambyahpillai, T., and H. Elliot. World-wide changes in the phase of the cosmic-ray solar daily variation. Nature, **171**, 918-920 (May 23, 1953).

Trefall, H. Cosmic-ray intensity and the temperature of the upper atmosphere. Nature, **171**, 888-889 (May 16, 1953).

Van Allen, J. A. The cosmic ray intensity above the atmosphere near the geomagnetic pole. Nuovo Cimento, **10**, No. 5, 630-647 (1953).

## D—*Upper Air Research*

Appleton, E. Storm phenomena in the ionosphere. Archiv Elek. Uebertrag., 7, Heft 6, 271-273 (1953).

Bain, W. C. Observations on the propagation of very long radio waves reflected obliquely from the ionosphere during a solar flare. J. Atmos. Terr. Phys., **3**, No. 3, 141-152 (1953).

Bates, D. R., and G. Griffing. Scale height determinations and auroras. J. Atmos. Terr. Phys., **3**, No. 3, 212-216 (1953).

Bennington, T. W. Critical frequency variations, sunspot minimum to maximum in northern and southern hemispheres. Wireless Engineer, **30**, No. 7, 175-179 (1953).

Beynon, W. J. G., and G. M. Brown. Geophysical and meteorological changes in the period January-April 1949. Nature, **171**, 967-969 (May **30**, 1953). [Letter to Editor, with subsequent comments by R. P. W. Lewis and D. H. McIntosh.]

Budden, K. G. The propagation of very low frequency radio waves to great distances. Phil. Mag., **44**, No. 352, 504-513 (1953).

Cain, J. C. Auroral radio-echo table and diagram for a station in geomagnetic latitude 56°. J. Geophys. Res., 58, No. 3, 377-380 (1953).

Chapman, R. P., and B. W. Currie. Radio noise from aurora. J. Geophys. Res., 58, No. 3, 363-367 (1953).

Chatterjee, B. Some regularities of the ionospheric $F$ region. J. Geophys. Res., 58, No. 3, 353-362 (1953).

Christiansen, W. N. A high-resolution aerial for radio astronomy. Nature, **171**, 831-833 (May 9, 1953).

Clemmow, P. C. Radio propagation over a flat earth across a boundary separating two different media. Phil. Trans. R. Soc., A, **246**, No. 905, 1-55 (1953).

Covington, A. E. Three most intense solar noise bursts on a wave-length of 10.7 centimeters. J. R. Astr. Soc. Can., **47**, No. 402, 106-108 (1953).

Cutolo, M. Determinazione sperimentale dell'intensità totale del camp magnetico terrestre nella regione inferiore dell'alta atmosfera (strato $E$). Nuovo Cimento, **10**, No. 7, 915-925 (1953).

Davids, N. Optic axes and critical coupling in the ionosphere. J. Geophys. Res., 58 ,No. 3, 311-321 (1953).

Dungey, J. W. Conditions for the occurrence of electrical discharges in astrophysical systems. Phil. Mag., **44**, No. 354, 725-738 (1953).

Eriksen, G. Solar radio noise recording equipment built for the Solar Observatory at Harestua. Institute of Theoretical Astrophysics, Blindern, Oslo, Rep. No. 3, 17 pp. (May, 1953). 29 cm.

Gerjuoy, E., and M. A. Biondi. Dissociative recombination in the $E$-layer. J. Geophys. Res., 58, No. 3, 295-303 (1953).

Harang, L., and B. Landmark. Radio echoes observed during aurorae and terrestrial magnetic storms using 35 and 74 Mc/s waves simultaneously. Nature, **171**, 1017-1018 (June 6, 1953).

HINES, C. O. Wave hypothesis of moving irregularities in the ionosphere. Nature, **171**, 980 (May 30, 1953).

JANCEL, R., ET T. KAHAN. Propagation des ondes électromagnétiques planes dans l'ionosphère. Paris, C.-R. Acad. sci., **236**, No. 21, 2045-2047 (1953).

JONES, R. E. Instrumentation for measuring changes in phase of ionospheric echoes. Rev. Sci. Instr., **24**, No. 6, 433-436 (1953).

KAMIYAMA, H. Disturbances in the ionosphere during the geomagnetic bay. Sci. Rep. Tôhoku Univ., **4**, No. 3, 101-107 (1953).

KITAOKA, T. Nomenclature of the upper atmosphere. J. Aerological Observatory at Tateno, **5**, No. 2, 167-169 (1953).

LANDSBERG, H. E. The origin of the atmosphere. Sci. Amer., **189**, No. 2, 82-86 (1953).

LANGE-HESSE, G. 27tägige Variationen in der *D*-Schicht-Absorption der Ionosphäre über Singapore und Slough. J. Atmos. Terr. Phys., **3**, No. 3, 153-162 (1953).

LEWIS, R. P. W., AND D. H. MCINTOSH. Diurnal and storm-time variations of geomagnetic and ionospheric disturbances. J. Atmos. Terr. Phys., **3**, No. 3, 186-193 (1953).

MARTYN, D. F. The morphology of the ionospheric variations associated with magnetic disturbance. Proc. R. Soc., A, **218**, No. 1132, 1-18 (1953).

MITRA, S. K. Active nitrogen. Phys. Rev., **90**, No. 4, 516-521 (1953).

NAGATA, T., AND T. OGUTI. Ionospheric storms in the auroral zone. Rep. Ionosphere Res. Japan, **7**, No. 1, 21-28 (1953).

NAKATA, Y., M. KAN, AND H. UYEDA. Sweep-frequency *h't* measurement of the ionosphere. Rep. Ionosphere Res. Japan, **7**, No. 1, 1-6 (1953).

NICOLET, M. The collision frequency of electrons in the ionosphere. J. Atmos. Terr. Phys., **3**, No. 3, 200-211 (1953).

OLDENBERG, O. Active nitrogen, airglow. Phys. Rev., **90**, No. 5, 727-730 (1953).

PRICE, R. E. Travelling disturbances in the ionosphere. Nature, **172**, 115-116 (July 18, 1953).

RAWER, K., ET E. ARGENCE. Considérations critiques relatives à la formation de la région *E* de l'ionosphère. Ann. Géophys., **9**, No. 3, 1-25 (1953).

ROACH, F. E., D. R. WILLIAMS, AND HELEN PETTIT. Diurnal variation of [OI] 5577 in the nightglow. Astroph. J., **117**, No. 3, 456-460 (1953).

SEDDON, J. C. Propagation measurements in the ionosphere with the aid of rockets. J. Geophys. Res., **58**, No. 3, 323-335 (1953).

SHINN, D. H. Further remarks on Kelso's paper, "A procedure for the determination of the vertical distribution of the electron density in the ionosphere." J. Geophys. Res., 58, No. 3, 416-418 (1953). [Letter to Editor.]

SIEDENTOPF, H., A. BEHR, AND H. ELSÄSSER. Photoelectric observations of the zodiacal light. Nature, **171**, 1066-1067 (June 13, 1953).

SINNO, K. On the variation of the *F*2 layer accompanying geomagnetic storms. Rep. Ionosphere Res. Japan, **7**, No. 1, 7-14 (1953).

SOMAYAJULU, Y. V. Determination of the coefficient of recombination in the ionosphere. Science and Culture, 18, No. 10, 494-496 (1953). [Letter to Editor.]

VAN SABBEN, D. Relationship between radio-propagation disturbance, geomagnetic activity and solar noise. J. Atmos. Terr. Phys., **3**, No. 3, 194-199 (1953).

VASSY, E., ET A. VASSY. Temperature moyenne de l'ozone atmosphérique. Proc. Indian Acad. Sci., **37**, No. 2, Sec. A, 195-203 (1953).

VASSY, A., H. NORINDER, ET E. VASSY. Etude spectrophotométrique d'étincelles de grande longueur dans l'air. Ark. Fys., **6**, No. 42, 437-450 (1953).

YONEZAWA, T. A consideration of the mechanism of electron removal in the *F*2 layer of the ionosphere. Rep. Ionosphere Res. Japan, **7**, No. 1, 15-28 (1953).

## E—*Earth's Crust and Interior*

BÅTH, M. Comparison of microseisms in Greenland, Iceland, and Scandinavia. Tellus, 5, No. 2, 109-134 (1953).

BUCHHEIM, W., UND R. LAUTERBACH. Isanomalen-Richtungsstatistik als Hilfsmittel tektonischer. Beitr. Geophysik, **63**, Heft 2, 88-98 (1953).

Duvall, W. I. Strain-wave shapes in rock near explosions. Geophysics, **18**, No. 2, 310-323 (1953).

Honda, H., and K. Nakamura. On the reflection and refraction of the explosive sounds at the ocean bottom. Sci. Rep. Tôhóku Univ., **4**, No. 3, 125-133 (1953).

Imbert, B. Sondages séismiques en Terre Adélie (Rapports scientifiques des Expéditions Polaires Françaises S III 2). Ann. Géophys., **9**, No. 3, 85-92 (1953).

Jacobs, J. A. Temperatures of the interior of the earth. Nature, **171**, 835 (May 9, 1953). [Letter to Editor.]

Ramberg, H. Relationships between heats of reactions among solids and properties of the constituent ions, and some geochemical implications. J. Geology, **61**, No. 4, 318-352 (1953).

Toledo, Observatorio Central Geofísico. Corrientes telúricas, ano 1950. [Prepared by Luis de Miguel y González-Miranda.] Madrid, Instituto Geografico y Catastral, 48 pp. + 10 figs. (1952). 24 cm.

Uffen, R. J. A method of estimating the melting-point gradient in the earth's mantle. Trans. Amer. Geophys. Union, **33**, No. 6, 893-896 (1952).

Union Géodésique et Géophysique Internationale. Association de Seismologie et de Physique de l'Intérieur de la Terre, Conférence a Bruxelles, 20 août au 1$^{er}$ septembre 1951. Conseil International des Unions Scientifiques, Pub. Bureau Central Seismologique International, Ser. A, Travaux Scientifiques, Fasc. 18, 237 pp. (1952). 25 cm.

Verhoogen, J. Elasticity of olivine and constitution of the earth's mantle. J. Geophys. Res., **58**, No. 3, 337-346 (1953).

Vestine, E. H. Note on analytical tests for distinguishing types of seismic waves. J. Geophys. Res., **58**, No. 3, 401-404 (1953).

Vestine, E. H., and S. E. Forbush. Statistical study of waves from blasts recorded in the United States. J. Geophys. Res., **58**, No. 3, 381-400 (1953).

Wadsworth, G. P., E. A. Robinson, J. G. Bryan, and P. M. Hurley. Detection of reflections on seismic records by linear operators. Geophysics, **18**, No. 3, 539-586 (1953).

Wait, J. R. Propagation of radio waves over a stratified ground. Geophysics, **18**, No. 2, 416-422 (1953).

Weber, M. Theorie der Kombinationsseismographen. Zs. angew. Math. u. Phys., **4**, Fasc. 1, 57-81 (1953).

## F—*Miscellaneous*

Conseil International des Unions Scientifiques, Commission Mixte pour l'Etude des Relations entre les phénomènes solaire et terrestres. Réunion du 3 Septembre 1952 à Rome. Paris, V. and R. Sennac, 35 pp. (1953). 27 cm.

Holm, G. R. The physical basis of field phenomena. J. Geophys. Res., **58**, No. 3, 305-309 (1953).

International Council of Scientific Unions. The Sixth General Assembly of the International Council of Scientific Unions, held at Amsterdam, October 1st to 3rd, 1952. Reports of proceedings edited by F. J. M. Stratton, General Secretary. Cambridge, University Press, viii + 157 (1953). 25 cm.

Kiepenheuer, K. O. Photoelectric measurements of solar magnetic fields. Astroph. J., **117**, No. 3, 447-453 (1953).

Rense, W. A., J. M. Jackson, and B. Todd. Measurements of the inner zodiacal light during the total solar eclipse of February 25, 1952. J. Geophys. Res., **58**, No. 3, 369-376 (1953).

Waldmeier, M. Final relative sunspot-numbers for 1952. J. Geophys. Res., **58**, No. 3, 405-407 (1953).

Waldmeier, M. Provisional sunspot-numbers for April to June, 1953. J. Geophys. Res., **58**, No. 3, 411 (1953).

# *NOTICE*

When available, single unbound volumes can be supplied at $3.50 each and single numbers at $1 each, postpaid.

*Charges for reprints and covers*

Reprints can be supplied, but prices have increased considerably and costs depend on the number of articles per issue for which reprints are requested. It is no longer possible to publish a schedule of reprint charges, but if reprints are requested approximate estimates will be given when galley proofs are sent to authors. Reprints without covers are least expensive; standard covers (with title and author) can be supplied at an additional charge. Special printing on covers can also be supplied at further additional charge.

Fifty reprints, without covers, will be given to institutions paying the publication charge of $4.00 per page.

*Alterations*

Major alterations made by authors in proof will be charged at cost. Authors are requested, therefore, to make final revisions on their typewritten manuscripts.

*Orders for back issues and reprints should be sent to Editorial Office, 5241 Broad Branch Road, N.W., Washington 15, D.C., U.S.A.*

*Subscriptions are handled by The Editorial Office, 5241 Broad Branch Road, N.W., Washington 15, D.C., U.S.A.*

## *CONTENTS—Concluded*

# DATE DUE



| | | | |
|---|---|---|---|
| | | | |

PERIODICALS MUST BE RETURNED TO PERIODICALS DESK ONLY.